INSTITUTO DE BIOLOGÍA MOLECULAR Y CELULAR (IBMC)

UNIVERSIDAD MIGUEL HERNÁNDEZ DE ELCHE

BIOPHYSICAL CHARACTERIZATION OF MEMBRANE-ACTIVE REGIONS OF STRUCTURAL AND NON-STRUCTURAL PROTEINS FROM DENGUE VIRUS

CARACTERIZACIÓN BIOFÍSICA DE LAS REGIONES MEMBRANO-ACTIVAS DE PROTEÍNAS ESTRUCTURALES Y NO ESTRUCTURALES DEL VIRUS DEL DENGUE

Henrique de Castro Nemésio

PhD Thesis / Tesis Doctoral 2014

D. Antonio Ferrer Montiel, Catedrático de Bioquímica y Biología Molecular y Celular y Director del Instituto de Biología Molecular y Celular de la Universidad Miguel Hernández de Elche,

DA SU CONFORMIDAD a la lectura de tesis doctoral titulada:

"Biophysical characterization of membrane-active regions of structural and non-structural proteins from Dengue Virus" / " Caracterización biofísica de las regiones membrano-activas de proteínas estructurales y no estructurales del virus del Dengue", para optar al grado de Doctor en Ciencias presentada por D. Henrique de Castro Nemésio.

Para que conste y surta los efectos oportunos, firma el presente certificado en Elche, a 25 de Junio de 2014.

Fdo. Prof. Antonio Ferrer Montiel

Don José Villalaín Boullón, Doctor en Ciencias, Investigador del Instituto de Biología Molecular y Celular y Catedrático de Bioquímica y Biología Molecular de la Universidad Miguel Hernández de Elche,

CERTIFICA:

Que el trabajo de investigación que conduce a la obtención del grado de doctor titulado: "Biophysical characterization of membrane-active regions of structural and non-structural proteins from Dengue Virus" / " Caracterización biofísica de las regiones membrano-activas de proteínas estructurales y no estructurales del virus del Dengue", del que es autor D. Henrique de Castro Nemésio, ha sido realizado bajo su dirección en el Instituto de Biología Molecular y Celular de la Universidad Miguel Hernández de Elche.

Para que conste y surta los efectos oportunos, firma el presente certificado en Elche, a 25 de Junio de 2014

Fdo. Prof. Dr. José Villalaín Boullón

ACKNOWLEDGMENTS

One seldom has the opportunity to acknowledge the importance of someone or a group of people in our lives. I am about to finish an important stage and it wouldn't have been so without the help and support of many people of which I will name and thank in no particular order:

I would like to thank Professores Manuel Prieto and Miguel Castanho for having shown me the way to Profesor José Villalaín's laboratory, where I conducted the research required to produce this manuscript.

To Profesor José Villalaín, my tutor and advisor, it would be an understatement to say that this thesis would not exist without him. He trusted and took me under his protection in his laboratory, even knowing I had little to no laboratory experience. I knew I could count on him from day one when I arrived in the middle of "Semana Santa" in Spain and he picked me up from Alicante's train station and drove me to (an already arranged and booked for me) rented flat in Elche. I thank you for everything.

To Profesores Antonio Ferrer and José Manuel González Ros, directors of IBMC, the former as of today and the latter when I first arrived in Spain, for having given me the opportunity to be a part of this great IBMC family.

To Francis, I believe a thousand thanks would not suffice. She was my tutor in every aspect of the laboratory, much like a big sister that tells you how to do things the proper way and not mess up. She taught both the morose and often ineffective official techniques and their faster and effective unofficial counterparts. Owing to her, my Spanish was thrust forward at incommensurable speed and would never be the same from then on (no more OK's were heard in JVB lab). I will miss the coffee breaks, congresses, parties and everything that were part of our joint years.

To everyone at "Secretaria", especially to May and Javier for their never-ending help and knowledge of the ins and outs of the bureaucratic machinery.

To the first friends and companions I had in Elche, Cheo, Silvia and Sakthi. I owe you a lot ever since we first met in the institute. One might say that strangers in a strange land walk hand in hand.

To all the Cubans, Dani, Jenny, Regla, Raiselys and Yanelis, I thank you for your friendship and all that stemmed from it, stories, jokes, laughs, dinners and Salsa classes.

To Alicia and Pablo, a striking example of those cases where people that are right in front of you the whole time turn out to be really important. All the late night events, jokes, discussions and conversations will be sorely missed and always remembered.

To Estefanía, Lourdes, Marcela and Rocío for all the conversations and much needed work pauses and after-work events, from concerts to weekend excursions.

To all my friends in my country, they know who they are; I believe names are not required. Your friendship is invaluable.

To my parents Jorge and Maria Helena, how can you really thank your parents? All their support and trust all along the way has led me to this very point. All my decisions (provided they would be sort of good decisions) were always met with confidence and approval even if it meant leaving their roof (before any facial hair) was visible or meeting sporadically and for short periods of time. It is quite obvious you are essential in my life. The same goes to Clara, my sister. Both her frankness and honesty well beyond her years and her perseverance are qualities I admire and try to use them on a daily basis. I am lucky to call you my sister.

To Ana, your patience and unfaltering trust and love push me forward. I hope we can be side by side for quite some time; it is just a matter of synchronization.

I wholeheartedly thank you all for being a part of my life.

ABBREVIATIONS

(v) or (ds) RNA	(viral) or (double stranded) Ribonucleic acid
BMP	Bis (monomyristoyl) phosphate
BPI	L-α-Phosphatidylinositol-4-phosphate from bovine brain
BPS	Brain L-α-phosphatidylserine
CF	Carboxyfluorescein
Chol	Cholesterol
CL	Cardiolipin
CSF	Cerebrospinal fluid
DENV	Dengue virus
DENV1-4	Dengue virus serotype 1-4
DF	Dengue fever
DHF	Dengue haemorrhagic fever
DMPA	1, 2-dimyristoyl-*sn*-glycero-3-phosphate
DMPC	1, 2-dimyristoyl-*sn*-glycero-3-phosphocholine
DMPG	1, 2-dimyristoyl-*sn*-glycero-3-[Phospho-rac-(1-glycerol)]
DMPS	1, 2-dimyristoyl-*sn*-glycero-3-[Phospho-L-serine]
DMV	Double membrane vesicles
DOPC	1,2-dioleoyl-sn-glycero-3-phosphocholine
DPH	1, 6-diphenyl-1, 3, 5-hexatriene
DPPC	1,2-dipalmitoyl-sn-glycero-3-phosphocholine
DSC	Differential scanning calorimetry
DSPC	1,2-distearoyl-sn-glycero-3-phosphocholine
DSS	Dengue shock syndrome
EGF	Epidermal growth factor
EPA	Egg L-α-phosphatidic acid
EPC	Egg L-α-phosphatidylcholine
ER	Endoplasmic reticulum
ESM	Egg sphingomyelin
ESR	Electro spin resonance
FPE	Fluorescein phosphatidylethanolamine
FTIR/IR	Fourier transform infra-red
GUV	Giant unilamellar vesicles
HCV	Hepatitis C virus
H_I	Hexagonal normal phase
H_{II}	Hexagonal inverted phase
HIV	Human immunodeficiency virus
Hsp	Heat shock protein
HSV	Herpes simplex virus
HTS	High throughput screening
IFN	Interferon
KUNV	Kunjin virus
L_α	Lamellar liquid crystalline or disordered phase
L_β	Lamellar organized (gel) phase
L_β'	Lamellar organized (gel) phase with tilted chains
LEM	Late endosome membranes
LUV	Large unilamellar vesicles
MLV	Multi lamellar vesicles
NMR	Nuclear magnetic resonance
PA	Phosphatidic acid
P_β'	Ripple organized (gel) phase with tilted chains

PC	Phosphatidylcholine
PE	Phosphatidylethanolamine
PG	Phosphatidylglycerol
PMO	phosphorodiamidate morpholino oligomers
PS	Phosphatidylserine
PSM	N-stearoyl-D-erythro-sphingosylphosphorylcholine
SARS-CoV	Severe acute respiratory syndrome coronavirus
SFV	Simian foamy virus
SIV	Simian immunodeficiency virus
SM	Sphingomyelin
SNARE	Soluble N-ethylmaleimide sensitive Attachment protein Receptor
SNR	Signal-to-noise ratio
SUV	Small unilamellar vesicles
TBEV	Tick-borne encephalitis virus
TFE	2,2,2-trifluoroethanol
TGN	Trans-Golgi network
TLR	Toll-like receptors
T_m	Temperature of the main transition
TMA-DPH	1-(4-Trimethylammoniumphenyl)-6-Phenyl-1,3,5-Hexatriene
TPE	Egg L-α-phosphatidylethanolamine, transphosphatidylated
VSV	Vesicular stomatitis virus
WNV	West Nile virus
YFV	Yellow Fever virus

INDEX

PREFACIO

El presente trabajo doctoral se ha desarrollado en el Instituto de Biología Molecular y Celular de la Universidad Miguel Hernández de Elche, bajo la dirección del Profesor José Villalaín Boullón y con el apoyo de una beca para la formación de personal investigador en centros de investigación de la Comunitat Valenciana (programa Santiago Grisolía con identificación GRISOLIA/2010/072) asociada al proyecto BFU2008-02617-BMC (Ministerio de Ciencia y Tecnología, España) y una ayuda del Programa de Formación del Profesorado Universitario (FPU) del Ministerio de Educación, Cultura y Deporte (MECD) en el último año de contrato de práticas (con identificación FPU12/05580).

Siguiendo la normativa interna de la Universidad Miguel Hernández, la memoria correspondiente a la Tesis Doctoral titulada "Biophysical characterization of membrane--active regions of structural and non-structural proteins from Dengue Virus" ha sido redactada en lengua inglesa con apartados seleccionados en lengua española, que se presenta con un conjunto de publicaciones constando de los siguientes apartados:

1. Introducción general a la unidad temática y metodología de esta tesis y estado actual de las mismas.
2. Objetivos y plan de trabajo.
3. Anexo de publicaciones aceptadas y enviadas (listadas abajo) en lengua inglesa original.
4. Resumen de resultados obtenidos y discusión global.
5. Resumen de la tesis redactado en lengua española y lengua inglesa
6. Conclusiones redactadas en lengua española y lengua inglesa.

A continuación se detallan las publicaciones científicas que costan de esta tesis doctoral por orden de referencia en el texto.

Publicación 1. *The membrane-active regions of the dengue virus proteins C and E.* Henrique Nemésio, Francis Palomares-Jerez, José Villalaín. Biochimica et Biophysica Acta (BBA): Biomembranes, 1808:10 (2011), *pp.2390-2402*. **DOI**: 10.1016/j.bbamem.2011.06.019

Publicación 2. *Hydrophobic segment of dengue virus C protein. Interaction with model membranes.* Henrique Nemésio, M Francisca Palomares-Jerez, José Villalaín. Molecular Membrane Biology, 30:4 (2013), *pp.273-287*. **DOI**: 10.3109/09687688.2013.805835

Publicación 3. *NS4A and NS4B proteins from dengue virus: Membranotropic regions.* Henrique Nemésio, Francis Palomares-Jerez, José Villalaín. Biochimica et Biophysica Acta (BBA): Biomembranes, 1818:11 (2012), *pp.2818-2830*. **DOI**: 10.1016/j.bbamem.2012.06.022

Publicación 4. *Membranotropic regions of Dengue virus prM protein.* Henrique Nemésio, José Villalaín. Manuscrito enviado a la revista Biochemistry.

Publicación 5. *Membrane interacting regions of Dengue virus NS2A protein.* Henrique Nemésio, José Villalaín. Manuscrito enviado a la revista Journal of Physical Chemistry B.

En la sección de resumen de resultados y discusión global cada publicación será referenciada por su número listado en este apartado y cada figura hará referencia a su respectiva publicación. Un ejemplo sería hacer referencia a la figura 1 de la publicación 1 como Figure 1, P1.

CHAPTER 1. INTRODUCTION

CHAPTER 1. INTRODUCTION

1. BIOLOGICAL MEMBRANES AND THEIR LIPID CONSTITUENTS

1.1. RELEVANCE OF THE STUDY OF MEMBRANES

The single entity that forms every single type of organism, from unicellular to multicellular and from eukaryotic to prokaryotic is the cell. The diversity of cells is astonishing, yet they all share certain aspects, such as containing highly complex and often very specialized machinery responsible for essential functions of a cell such as providing the necessary energy for it to remain alive or arranging certain molecules that together provide the cell with its structural scaffolding. Cells are also alike in the sense that they are separated from its surroundings by one or more membranes. Apart from their function as a selective border between intracellular and extracellular spaces, these membranes also serve the purpose of isolating inner compartments of organelles from the intracellular medium in some types of cells. They can also serve as scaffolding for the cytoskeleton (in the sense that the latter is attached to the membrane through a myriad of proteins and molecules such as microtubules, actin or transmembrane proteins) [1], as insulators in myelin sheets or even the transduction of light in rods.

These membranes are highly specific and selective to the flow of a wide array of molecules with a plethora of properties (from relative charge to size or even hydrophobicity). This selective permeability to charged molecules is the basis for the maintenance of an electric potential across the membrane, essential to many different molecule exchanging processes, including those requiring ion channels. Furthermore, some proteins embedded in membranes are involved in molecular signalling for a wide range of pathways with distinct final objectives, whether for apoptosis signalling, activation of transcription (G-protein coupled receptors) or transport of molecules (different types of transporters).

Despite having major differences in overall composition, both prokaryotes and eukaryotes possess three major types of molecules in their membranes: lipids, proteins

and their variations with carbohydrate moieties. This fact can actually become a double-edged sword in what concerns the study of membrane interactions with its surroundings; if on the one hand, there is only a handful of possible physicochemical interactions between the different types of molecules (van der Waals force, hydrogen bonds, covalent bonds and electrostatic interactions), on the other hand the sheer amount of possible combinations available by combining those three types of molecules and the different properties they display, seriously hampers a thorough and rational examination of all the biological processes taking place in cells that are directly or indirectly related to membranes or their lipid composition. Yet, because lipid composition of membranes changes incessantly and the specific type of lipid is not as important as the overall physiochemical and structural properties it possesses, such as the polar head (in the case of phospholipids for instance) or the length of its hydrophobic chain, the study should focus more on supramolecular sets than on molecule by molecule.

1.2. SHORT HISTORICAL INTRODUCTION TO THE MEMBRANE MODEL

According to Benjamin Franklin, it was Pliny the Elder's first anecdotal evidence (in his *Natural History*) on the "soothing" effects oily substances had on the "rough element" that was water that led him to try and measure the thickness of an oily film, finding it to be around 2.5 nm [2]. In 1925, by measuring the capacitance of suspensions of "red corpuscles" or erythrocytes, Fricke concluded that the membrane had a thickness of 3.3 nm, but unknowingly, he found an approximate value for the thickness of the hydrophobic core rather than the whole membrane including polar heads (polar heads were fully hydrated, therefore, with his experimental settings, they would not be detected)[3].

Nowadays it is known that the thickness of membranes is highly dependent on its composition and as it will be seen later, it is not homogeneous all along the surface of membranes. For want of completion, the thickness measurement experiments were complemented with others where the geometry of the membrane was assessed. Using a method developed by Langmuir [4] and later optimized by Adam [5], Gorter and

Grendel determined that there was a ratio of 1:2 between the total surface area of erythrocytes and the area occupied by lipids extracted with acetone from those erythrocytes [6], suggesting a bilayered structure. It was only in 1935 that Davson and Danielli [7] tried to define certain functional aspects of the then called "lipoid film", especially as to what solubility was concerned. Considering the solubility of different molecules and the influence of charge on the relative permeability of protein ensembles to ions, they argued that membranes should be formed by a protein film adsorbed to a "lipoid" one and not by blocks of protein and lipoids interlaced that would have a frail stability. With the work of Bangham and Horne [8] in 1964 came another structural insight. In it, sonicated lecithin lipid suspensions were stained with phosphotungstate, analysed by electron microscopy and a bilayered structure was observed (Figure 1), proving at least that lipids could form bilayers.

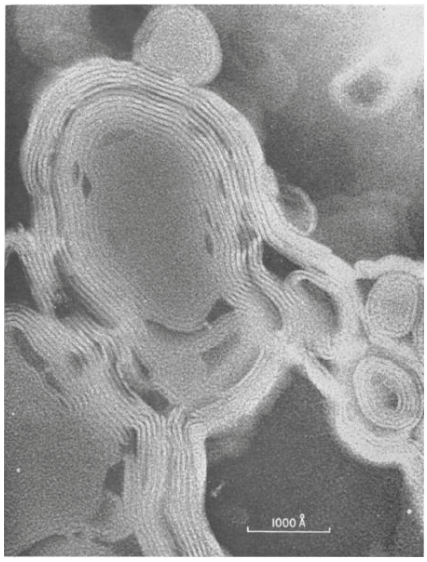

Figure 1 . Electron micrograph of ovolecithin treated by ultrasound and mixed with an equal volume of 2% potassium phosphotungstate. The multi-layered structure of lipid membranes is clearly seen in this figure, interspersed with patches of denser regions. Adapted from Bangham et al. 1964 [8]**.**

The Davson-Danielli model (Figure 2) suffered some slight modifications, yet it was not refuted for the best part of the three decades that followed. Despite not being able to explain membrane fluidity or the ability of certain proteins to permeate the membrane it was a pioneering work that provided two essential theories on the membrane model: the ubiquity (not exclusivity) of the bilayer structure and the asymmetry of lipid membranes.

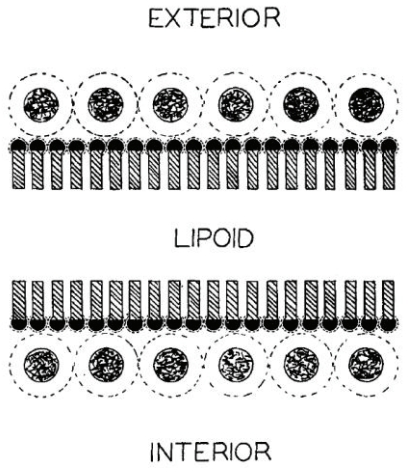

Figure 2 . Depiction of the Davson-Danielli model with the protein film in close contact with the polar heads of lipids. Adapted from [7].

Later on it was found that membranes cleaved in half by the plane parallel to the membrane (thus exposing its hydrophobic core) had small depressions that were then attributed (correctly) to proteins. This was the beginning of the downfall of the original assumptions of the Davson-Danielli model. With the work of Benson and later Greene, lipoprotein subunits were removed from mitochondrial membranes (resorting to freeze-fracture techniques) and later reconstituted to full functionality. This discovery prompted a re-evaluation of the Davson-Danielli model in the sense that it could not explain the bumps nor the existence of proteins associated with lipids. In 1972, Singer and Nicholson [9] proposed a model (Figure 3) trying to unify both thermodynamic theories and experimental data. In it, several considerations were made: (a) the hydrophobic acyl chains of lipids should be in contact with apolar or nonpolar molecules moieties, including acyl chains from other lipids, (b) their hydrophilic heads should be in contact with water and ions (these would not be found in the hydrophobic moiety), (c) since the major component of membranes by weight are proteins and their hydrophobic/hydrophilic character is defined by their amino acid composition, they would have regions in close association with membranes and others in polar moieties, (d) carbohydrates moieties and any other charged structure would always be the farthest away from hydrophobic regions, (e) there is a fine balance between hydrophobic and hydrophilic interactions to minimize the energy involved (in the previous Davson-Danielli model, films of protein surrounding films of lipid would not be stable mainly because this energy minimization would not be accomplished), (f) the long range

distribution of proteins in lipid membranes should be random and (g) membranes should be fluid (experiments by Frye and Edidin obtained a diffusion constant of 5.10^{-11} cm^2/s for some antigenic components of human and mouse cells [10]), otherwise large energies of activation would be needed in biological reactions that need protein rearrangement**.**

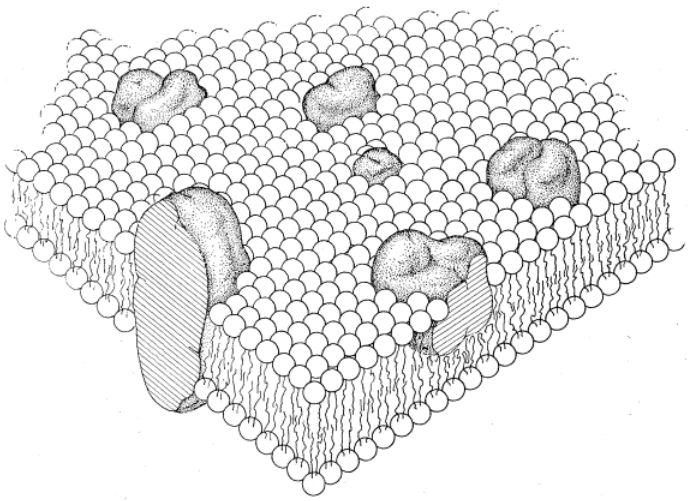

Figure 3 . Depiction of the Singer-Nicholson model with both amphipathic proteins and integral membrane proteins.

This model is still valid as a general idea being thus taught at every biochemistry and biology course nowadays and recent studies only add complexity to the model and are not a completely antithetical version of this one. It is now known that the lateral composition is highly heterogeneous and all molecules are densely packed, rendering the lateral movements of lipids less frequent and constrained by other molecules (summarized in [11]). With the crystallization of an ever-growing collection of membrane proteins and with the number of known protein-protein interactions (some transient) at the surface of membranes, we can undoubtedly refute the idea that the protein distribution in a membrane is random as postulated initially. The argument that the membrane should be symmetrical has also been proven incomplete with studies hinting at the existence of lipid rafts in membranes with specific composition [12], the knowledge that a large number of processes (including membrane fusion) require specific lipid compositions and also the assumption that the presence of lipid molecules with varying degrees of saturation, number of isomers and of different lengths in a single membrane are likely to result in an asymmetric structure. Therefore, the need to

address these inconsistencies in the original model resulted in the proposition of a more refined and complete model [13] in 2005 (Figure 4), where the membrane is highly crowded, heterogeneous and mainly asymmetrical, a highly complex mosaic and not a lipid sea where rafts and lateral diversity abound and the hydrophobic core of the membrane is relatively small compared to the two layers that surround it on both sides and where most of the biological processes occur.

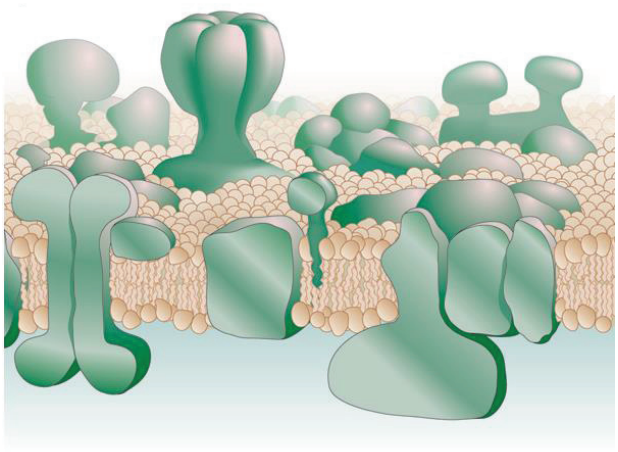

Figure 4 . Revised Singer-Nicholson model by Donald Engelman in 2005[13].

1.3. LIPID COMPLEXITY AND DISTRIBUTION IN CELLS

So far, no general description of lipid molecules has been put forward, therefore a presentation of the main types of lipids, their dynamics, possible supramolecular arrangements (structures) and distribution in the lipid bilayer structure (the most common type of lipid structure in cells) is required. To begin with, there are thousands of different lipid molecules while in cells this order of magnitude is only one unity smaller. All lipids share one property - their low solubility in water – despite most, if not all, being amphiphilic molecules. There are four main groups of lipids: glycerophospholipids, glycolipids (glycoglycerophospholipids and glycosphingolipids), sphingolipids and sterols. All but sterols contain at least one molecule of fatty acid covalently bonded to the polar head. The diversity starts with these fatty acids that surpass seven hundred in number and with their possible combinations in lipids (http://lipidbank.jp). Fatty acids are usually 10 to 24 carbon atoms long and this number is almost always even (except in plants and some marine animals). They are usually

referred to by common names, e.g. myristic acid or palmitoleic acid, or by their chain length and degree of saturation, e.g. C14:0 or C16:1(Δ9) that in turn provide part of the name of more complex lipids which are:

- **Glycerophospholipids** or simply **phospholipids** are the main constituent of membranes in nature, especially phosphatidylcholine. Phospholipids are composed of a molecule of glycerol to which a phosphate group has been added turning it into the chiral molecule *sn*-glycerol-3-phosphate. Esterification of C1 and C2 with fatty acids (usually a saturated is linked to C1 and an unsaturated to C2) turns these molecules into 1,2-diacylphosphoglycerides and finally the head group that is attached to the phosphate group gives the remainder of the name of phospholipid (Figure 5). This arrangement can become increasingly complex, e.g. phosphatidylglycerol can link to phosphatidic acid through its polar head group and give rise to cardiolipin (a major component of mitochondrial inner membrane or two molecules of myristic acid linked to C1 of a glycerol molecule can link to the same phosphate group by the C3 of their glycerol molecule and produce bis-(monomyristoyl)phosphate (BMP). Phosphatidylcholine (also called lecithin and abbreviated to PC) is by far the most abundant phospholipid in biomembranes. Molecules of PC are zwitterionic and do not form hydrogen bonds between them and therefore having a much lower transition temperature from the gel to liquid-crystalline phases when compared to other phospholipids. Phosphatidylethanolamine (also called cephalin and abbreviated to PE) is also zwitterionic but because it has no methyl groups attached to its amine, hydrogen bonds are formed resulting in, among other things, a higher gel to liquid crystalline transition temperature than PC. This phospholipid is not as abundant as the previous although it has a larger distribution in the brain. Furthermore, it is one of the most important lipids in the study of lipid polymorphism (described in a subsequent section). In eukaryotic cells, the most common type of phospholipid with a negative formal charge (one positive charge on the amine group and two negative charges on the phosphate and carboxyl groups) at neutral pH is phosphatidylserine (PS). This lipid is distributed asymmetrically in the membrane, being mostly found in the inner leaflet of the membrane (the exposure of PS on the outer leaflet signals apoptosis and induces phagocytosis and blood clotting). A significant amount of PS molecules localized to the same place confers a respectable electric potential to the membrane that is of the utmost importance for

several membrane processes that require the recruitment of cationic protein regions to membranes [14]. Like PE, PS is stabilized by hydrogen bonding, therefore their transition temperature is higher than that of PC. Another negatively charged phospholipid is phosphatidylglycerol (PG) with a transition temperature similar to that of PC. The simplest phospholipid, phosphatidic acid (PA) is also negatively charged and can from hydrogen bonds. Lipids without amines, such as PC are mostly found on the outer leaflet, while the others (PS and PE for example) are chiefly located on the inner leaflet.

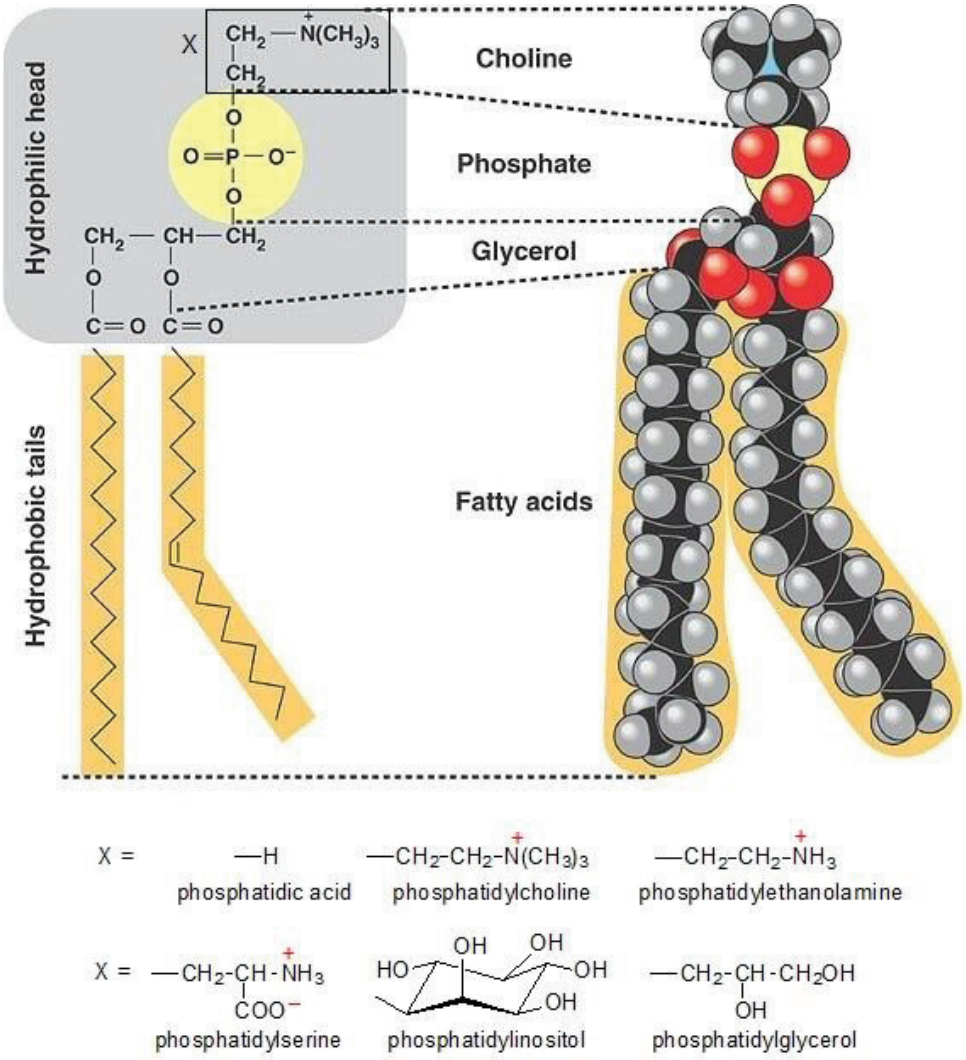

Figure 5 . Representation of a phosphatidylcholine molecule (top) and several polar head group substitutions (bottom) found in common lipids (adapted from [15] and http://kvhs.nbed.nb.ca/gallant/biology/phospholipid_structure.jpg).

- **Sphingolipids**: Structurally, this class of lipids is defined by a ceramide molecule (itself composed of sphingosine, an 18-carbon unsaturated aminoalcohol linked to a fatty acid) that has a polar head attached to its C1 carbon (Figure 6). Depending on the nature of this polar head they can have different denominations: cerebrosides have a simple sugar attached to C1, gangliosides have complex sugars attached to the same position and one specific and noteworthy modification is when a phosphorylcholine is linked to C1. This last lipid molecule is called sphingomyelin (SM), a very important component of eukaryotic cells both in relative proportions and in functionality. Apart from their structural role in membranes, sphingomyelin by-products such as ceramide or sphingosine are involved in cellular processes such as development and apoptosis [16]. Sphingomyelin accounts for 2-15% of the total phospholipid content of mammalian cell membranes [16] and, contrarily to PC, contains both hydrogen bond acceptors and donors in its interfacial region, increasing the number of possible interactions at that region. In sphingolipids, both these chains are larger and highly saturated; ergo they pack more tightly and present higher transition temperatures (T_m).

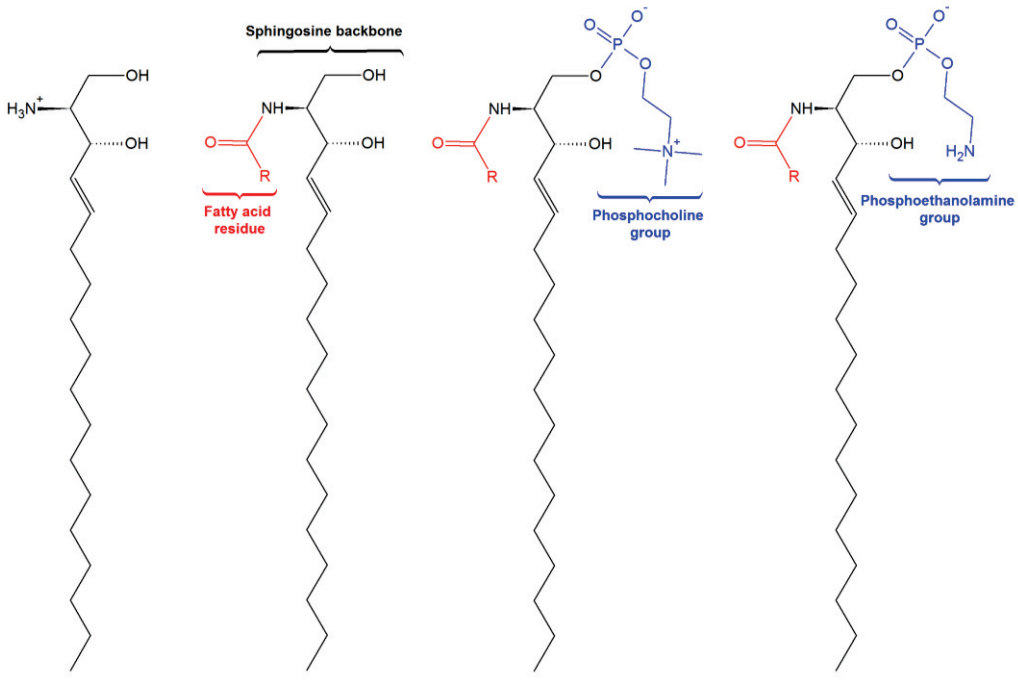

Figure 6 . Representation from left to right of sphingosine , ceramide (basic unit structure of sphingolipids) and two different sphingolipids, one with a phosphorylcholine head group, commonly called sphingomyelin and one with a phosphoethanolamine head group (taken from http://commons.wikimedia.org/wiki/File:Sphingolipids_general_structures.png).

These different physical properties explain the interplay between these two classes of lipids [17, 18].

- **Sterols**: These lipids are structurally dramatically different from all other classes of lipids described so far. They all contain one basic unit – sterol – a 17-carbon molecule. In eukaryotes, the predominant sterol is one of three (Figure 7): cholesterol (animal cells), ergosterol (fungi and yeast) or stigmasterol (plant cells), while prokaryotes contain little to no sterol molecules [2, 19]. In animal cells cholesterol accounts for 0 to 25 % of total lipid content [2] and it is essential to cell proliferation [20]. It is soluble in all membranes, yet less so in membranes with a significant amount of negatively charged lipids (PS, PG, PI and PA). Both the hydrophobic chain and the planar rings determine its orientation in the membrane while the 3-β-hydroxyl group affects the properties of the bilayer surface [21]. Cholesterol functions as a sort of membrane fluidity buffer in the sense that on the one hand it constrains unsaturated acyl chains, hence reducing the fluidity of highly fluid membranes and on the other hand it disrupts the tight packing of highly saturated acyl chains, thus increasing fluidity of membranes in a gel phase.

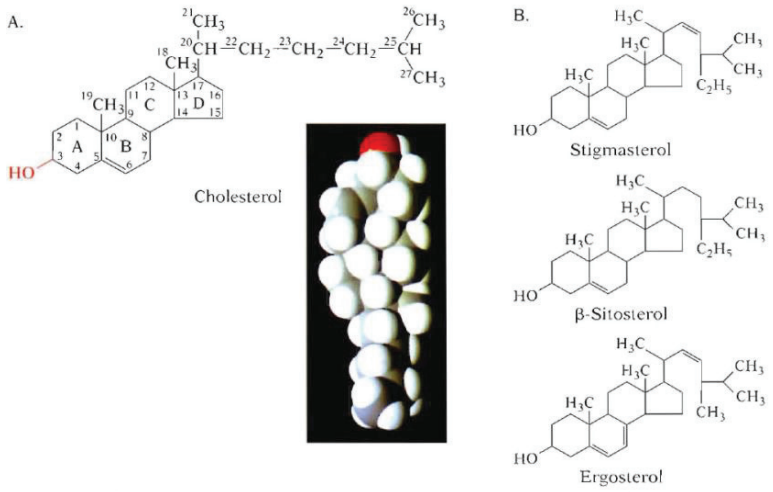

Figure 7 . Different types of sterols found in biological membranes. (A) Cholesterol is predominant in animal cells, (B) stigmasterol and β-sitosterol in plant cells and ergosterol in yeast and fungi. Adapted from [2].

- **Glycolipids**: In their most general form they differ from phospholipids in the sugar attached to *sn*3 of glycerol instead of the phosphate group, yet this general term is

also used to encompass other two types of glycolipids – glycoglycerophospholipids and glycosphingolipids – versions of the previously described classes where the polar heads are sugars. They are commonly found in plants, fungi and bacteria.

Bacterial plasmatic membranes usually contain one or two main phospholipids (in the case of *E.Coli* the two predominant lipids are PE and PG at 75 and 20% total lipid weight respectively with about 5% CL) and no cholesterol, archaea contain long prenyl chains instead of fatty acids [22] and eukaryotes display a dazzling diversity of lipids and each organelle has its own lipid composition [2]. While some types of membranes have a more or less consistent predominant lipid, there are some lipids (like PI) that despite being a minority are nonetheless essential in some functions like cellular trafficking and signalling. In Table 1, the composition of certain types of membranes is presented. There is clearly no unifying lipid composition in any given type of cell.

Table 1 . Lipid composition of selected biomembranes. Adapted from [23].

Lipid	Percentage of total lipid (by weight)					
	Hepatocyte plasma membrane	**Erythrocyte plasma membrane**	**Myelin**	**Mitochondrion (both membranes)**	**Endoplasmic reticulum**	***E. Coli***
Cholesterol	17	23	22	3	6	0
PE	7	18	15	28	17	70
PS	4	7	9	2	5	traces
PC	24	17	10	44	40	0
SM	19	18	8	0	5	0
Glycolipids	7	3	28	traces	traces	0
Others	22	14	8	23	27	30 (PG)

1.4. BILAYER STRUCTURE

The most common type of structure found in membranes by far is the bilayer structure, with a hydrophobic core composed of the acyl chains of lipids and planar rings of sterols, an interfacial region teeming with hydrogen bond acceptors and donors and the outer layers (both to the luminal side and to the external side) composed of lipid polar heads and proteins as described in a previous section. As seen before, the bilayer is both fluid and asymmetrical. One of the most accepted explanations for this phenomenon lies in the frequency difference between lateral movement ($\sim 10^7$ s^{-1}) and

flip-flop or transverse movement (~10^3 s^{-1}). This difference of four degrees of magnitude partially explains the fluidity and asymmetry of the membrane respectively. Lipid rotation along their main axis and entropic movements of acyl chains complete the four types of lipid movement. Details of lipid bilayer structure were obtained using a wide array of methodologies, from X-ray crystallography [24, 25] to molecular simulations based on experimental evidence and theory [26].

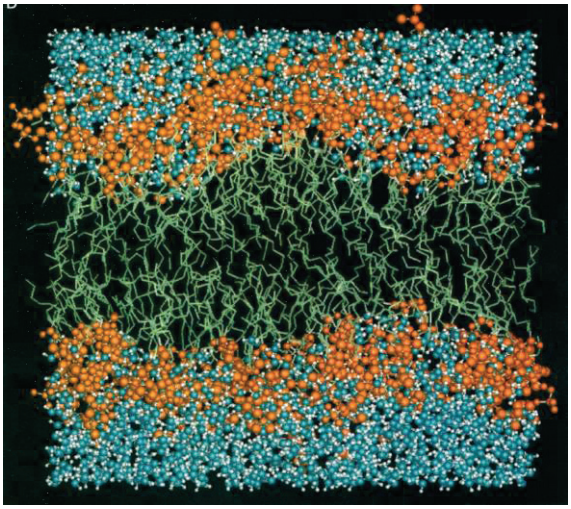

Figure 8 . Final frame of a molecular simulation of a lipid bilayer composed of 100 molecules of a certain saturated phosphatidylcholine (1, 2-dimyristoylphosphatidylcholine or DMPC) with 50 molecules per leaflet in water. Water molecules are depicted in blue and white, acyl chains in green and polar heads in orange. Adapted from [26].

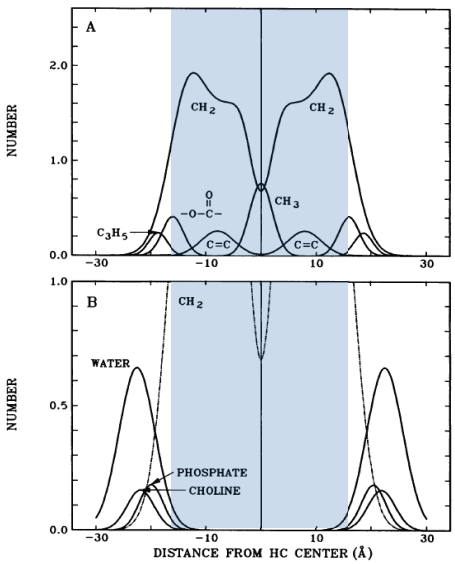

Figure 9 . Composition space structure obtained from X-ray experimental results of the structural determination of the liquid crystalline phase of 1, 2-dioleyl-*sn*-glycero-3-phosphocholine (DOPC). In (A) the structure without polar heads is shown and in (B) all the polar groups and water are shown, with methylene groups for scale. The hydrophobic core is shown in blue Adapted from [25].

It is clear from both Figures 8 and 9 that no charged particles are present in the hydrophobic core of the membrane (X-ray experiments show no charged molecules inside the region defined as hydrophobic and the simulation based on X-ray experiments predicts no polar molecules in said region). Furthermore, there is significant overlap of charged and uncharged groups at the interface. As said before, this region contains a large set of different molecules and groups, such as water, choline, glycerol, carbonyls (in both figures only one type of lipid was considered for sake of analytical simplicity) that have different interacting properties (some are hydrogen bond donors and others acceptors for example), therefore one should expect proteins and other molecules not directly bound to the membrane to localize, at least temporarily, to this region. The predicted thickness of the hydrophobic core is of some 30 Å (α helices have a diameter of ~10 Å, they could bind to the membrane in a parallel plane) and the molecular heterogeneity increases concomitantly with the distance to the centre of the hydrophobic core. This characteristic heterogeneity renders the interface the ideal place for all membrane interactions to occur [27].

1.5. LIPID POLYMORPHISM

There are a multitude of different structures lipid molecules adopt spontaneously in Nature. Lipids dispersed in an aqueous medium present three main types of structures (Figure 10): micelles (spheres where lipids have their polar heads at the surface and the hydrophobic chains pointing to the centre), liposomes (spheres like micelles yet the core of the sphere is hydrophilic in nature and lipids are arranged as bilayers) and bilayers (most common and heretofore referred).

Lipid bilayers can have different curvatures and shapes: from flat bilayers in fixed supports or in large liposomes (lipid molecules have a cylindrical shape in this case) to curved structures (lipid molecules are conical in overall shape with the apex opposed to the polar head), found in small liposomes or even complex structures like cubic phases. All of these structures are found in cells in specialized processes, for example, vesicles involved in protein trafficking inside the cell have an overall curved lipid bilayer and membrane fusion processes require membranes with a high curvature that can provide

part of the necessary energy for it to occur [28, 29]. The ability of lipid molecules to undergo morphological changes is termed lipid polymorphism.

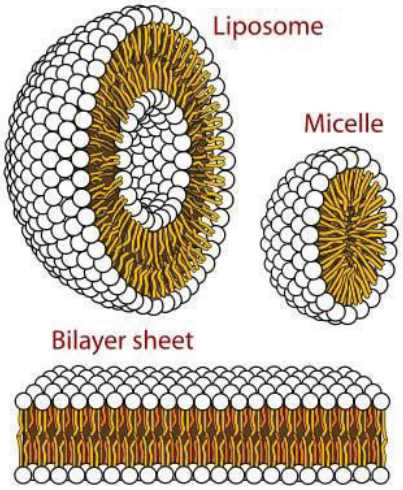

Figure 10 . Representation of the most common structures lipid molecules adopt in aqueous media.

The morphology of any given lipid supramolecular structure depends on the type of lipids involved (PE has a reduced polar head area and forms hydrogen bonds, it is mainly found in inverted phases); degree of hydration of the membrane (low hydration promotes inverted phases); temperature (some lipids have phase transitions between 0 and 100ºC – range of temperature for experiments using water as solvent – arising from the conversion of some *trans*- C-C single bonds – found at low temperature – to *gauche*- bonds as temperatures increases), pressure, pH and ionic force of the solvent [29, 30]. Some lipids possess a transition temperature (T_m), which is defined as the temperature needed to induce a change in the physical state of a lipid, from an ordered and tightly packed gel phase to a fluid or disordered liquid-crystalline phase. There are lipids with more transitions such as PE that has a liquid-crystalline to hexagonal phase II transition. The transition temperature (T_m) of lipids depends on the length and saturation of acyl chains, polar head charge and species. For example, as mentioned previously, SM usually has two saturated acyl chains and PC one saturated and one unsaturated and it has been found experimentally that SM has a higher T_m than PC (maintaining the hydrocarbon chain length).

Lipid molecules can be classified according to the packing parameter, p (ratio between the volume of the hydrocarbon chain and the product of the area occupied by the polar head and the length of the hydrocarbon chain) [31]. Should a lipid molecule has a $p < 1/3$, it has a conical shape with the base at the polar head, and it will tend to form spherical micelles, if $1/3 < p < 1/2$, it is still conical in shape with a truncated apex and these molecules tend to form non-spherical micelles. If $1/2 < p < 1$, the lipid molecule is cylindrical and forms lipid bilayers with equivalent molecules. Finally, lipids with $p > 1$ have a conical shape with a truncated apex at the polar head and tend to form inverted phases (Figure 11).

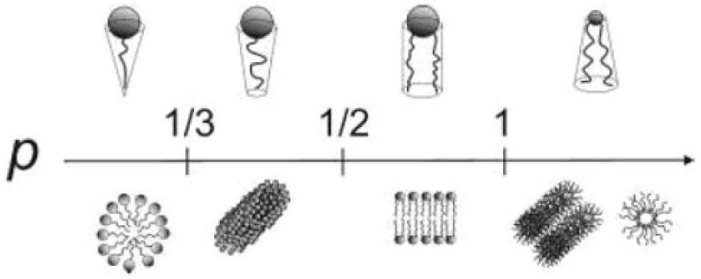

Figure 11 . Representation of the general shape of a lipid molecule (top) according to the packing parameter. The typical structural arrangement they adopt is shown below.

A lipid monolayer in equilibrium has a measurable lateral pressure profile; if that profile shows positive pressure on the polar region of the monolayer along with negative pressure on the hydrophobic region, the result is a phase arrangement called normal or of type I where the polar regions of lipids face the outer rim of the layer and the hydrophobic moiety makes up the core this lipid structure of type I (micelles are a good example of this type of lipid structure). Conversely, if the polar head region is subject to negative pressure and the hydrophobic region to positive pressure, the resulting phase arrangement is called inverted or of type II. Lipid phases can also be classified according to a multitude of parameters like long range order, organization of hydrocarbon chain, phase curvature and even according to the lateral pressure profile. As proposed by several studies [2, 32-34], long range order is expressed by a capitalized Latin letter: L for one-dimensional lamellar phase, H for bidimensional hexagonal phase, P for ripple bidimensional phase, Q for tridimensional cubic and the organization of the hydrocarbon chains is expressed by a Greek lowercase letter: α refers to

unordered (fluid) chains, β to organized (gel) chains and β' to organized (gel) tilted chains (Figure 12).

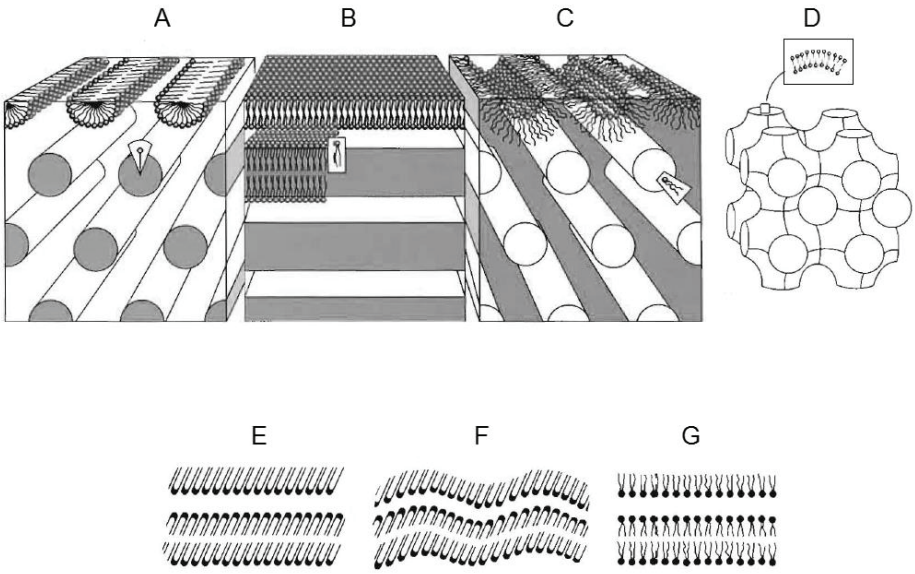

Figure 12 . Representation of some structures adopted by lipid molecules classified by long range order: (A) Hexagonal I (H_I) phase, (B) Lamellar liquid crystalline phase (L_α), (C) Hexagonal II (H_{II}) phase, (D) Cubic phase of bicontinuous type and hydrocarbon chain organization: (E) Lamellar organized (gel) tilted chains (L_β'), (F) Ripple organized (gel) tilted chains (P_β') and (G) Lamellar liquid crystalline or disordered (L_α). Adapted from [2].

Bilayers (also called lamellar) are ubiquitous and the predominant phases in biological membranes (cubic phases are also arranged as bilayers, hence the need to distinguish both by calling lamellar to the commonly depicted bidimensional lipid bilayer). The transition temperature (T_m) commonly found in literature refers to the transition from lamellar gel (L_β) phase to lamellar liquid crystalline phase (L_α). As it can be seen in Figure 12, hexagonal phases consist of periodic arrangements of long cylinders of lipids stacked on top of each other in an hexagonal arrangement. The length of these cylinders is so large compared to the diameter that they can be considered infinite without significant loss of accuracy. The inner region of the cylinder is either filled with the hydrophobic core of lipids in the case of the normal hexagonal phase H_I or with polar solvents (water in biological samples) in the case of the inverted phase H_{II}. Because lipids that spontaneously adopt hexagonal phases can affect membrane curvature (because of its high value of p, PE readily forms membranes with high

curvature), they are of utmost importance in processes that require membranes to be far from the zero value of curvature found in PC membranes, e.g. membrane fusion processes. Cubic phases are optically isotropic phases (contrarily to micellar phases) tridimensional arrangements (the number of possible structural permutations in three dimensions is far larger than in two dimensions) of rods with bilayers (type I and type II) that can be bicontinuous when both aqueous and lipid phases are continuous in space or discontinuous when there is exclusive continuity in the aqueous phase. These phases have been studied for their possible role as intermediates in fusion processes and as good protein crystallization environments [2, 34].

1.6. MEMBRANE FUSION PROCESSES AND VIRUS INDUCED FUSION

In eukaryotes, membrane fusion is an essential and ubiquitous process. A multitude of events require membrane reorganization and coalescence namely fertilization, mitochondrial fusion, cell-cell fusion, intercellular communication and even viral entry [35-39]. Cells possess different types of SNAREs (Soluble N-ethylmaleimide sensitive Attachment protein Receptors), a highly conserved set of proteins responsible for intracellular fusion regulation [35]. Fusion processes are classified into three types depending on its location and which structures are involved in it: (1) intracellular fusion of organelles and vesicles predominantly mediated by the SNARE family of proteins, (2) extracellular fusion of eukaryotic cells, such as the fusion between spermatozoid and oocyte during fecundation or the formation of syncytia in muscular cells, (3) extra and intracellular fusion of pathogens with host cells, for instance the fusion of viral membranes with cell membranes in the viral cycle of enveloped viruses. Such a process is enhanced by the action of fusion proteins [40].

Membranes do not undergo fusion spontaneously, requiring the aid of other molecules such as proteins through the whole process to overcome the otherwise unsurmountable energy barriers typical of fusion [41]. The conformational changes observed in some proteins seem to provide that energy to a multitude of processes [42-44]. Not only proteins but also lipids, with their characteristic polymorphism and their modulation of the overall physical properties of membranes, play an active role in

fusion [41, 45]. Non-lamellar lipids such as PE generally form inverted (type II) membranes, while lamellar lipids like PC form normal (type I) membranes. As referred in a previous section, the relative lipid composition of membranes modulates membrane curvature, an important parameter in membrane fusion processes. As a general trend, type I lipids inhibit fusion processes whilst type II lipids favour them. Changes in curvature result in increased tension of the overall membrane structure. This tension is stored as elastic energy that can be unleashed and used in membrane fusion [42, 46].

Taking into account theoretical and experimental evidence [28, 47-51], a model (stalk model) has been proposed to describe fusion processes (Figure 13). In it, the fusion process occurs in three steps: (1) soon to fuse membranes come into close contact and after overcoming hydration forces that prevent membrane lipid bilayers from getting any closer than 2-3 nm [42], (2) the outer leaflets of membranes with pronounced curvature fuse, forming a structure named hemi fusion stalk. In the vicinity of this hemi fusion stalk, either inverted [47, 52] or lamellar bicontinuous Q_{II} phases [51] might be present according to two different models (Figure 13A and 13B respectively). Finally, (3) the inner leaflets fuse and the aqueous compartments of both membranous structures merge.

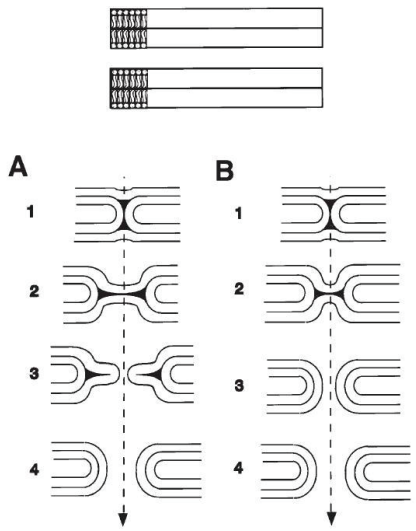

Figure 13 . Stalk mechanism of lipid bilayer fusion as initially proposed by (A) Kozlov in 1989 and (B) Siegel in 1993. In 1 the initial contacts between membrane leaflets occurs, followed by hemi fusion (2) and formation of the initial lipid fusion pore (3) and expansion of the same pore (4). The dark areas in schemes 1, 2 and 3 from the original stalk model and schemes 1 and 2 from the revised stalk model present highly unstable interstices. The hemi fusion zone in the original model is larger than the one from the revised model (Adapted from [42]).

There are various evidences supporting the most recent stalk model (Figure 13B), for it has been seen that fusion processes, both on viruses and cells, are enhanced by the existence of lipids in the membrane that have a spontaneous negative curvature (PE for example). The unstable fusion is apparently stabilized by the presence of large hydrophobic chains (lowering the energy levels in the voids created in the membrane) and on the other hand, lipids that induce the formation of spontaneous positively curved membranes would inhibit the fusion process [42]. The first observed evidence of the stalk structure has been resolved by electron tomography in thin sections of active regions in cortical synapsis of mice [53]. The intermediate structures in the fusion process have to be stabilized, that is, they need lower activation energies, or else the process will not occur. Bilayers can be destabilized by segments of fusion proteins, resulting in a lowering of the activation energy of the fusion process, allowing as such the existence of fusion intermediates. The relative distribution of type I and type II phase forming lipids is not the only important factor for fusion processes. Specific lipid structures called lipid rafts, with increased sphingomyelin and cholesterol content are used by certain viruses to their advantage, both during viral budding processes and during initial entry [54-58]. This higher cholesterol concentration acts as a fluidity buffer, possibly important to reduce the energy barrier of membrane fusion.

On another level, lipid rafts have higher concentrations of surface cell receptors used by many viruses. Several studies [59-67] have actually shown the importance of lipid rafts in the viral infection of some viruses: Japanese Encephalitis virus and Dengue virus (Flaviviruses), Ebola and Marburg viruses (Filoviruses), Variola virus (Orthopoxvirus), lymphocytic choriomeningitis virus (Arenavirus) and Herpes simplex virus (Herpesvirus). By reducing the cholesterol content of the membrane of target cells, the cell-to-cell fusion or the viral infection was diminished. For some viruses their membrane receptors are placed in regions with high cholesterol content so when cholesterol content is increased, the concentration of viral receptors on the membrane rises, favouring the fusion process. Despite these results, the existence of lipid rafts is not a *sine qua non* condition, though their positive influence in the concentration of receptors might be important to enhance the coupling of viruses to cells.

Viruses enter cells by a variety of pathways, for instance enveloped viruses resort to receptor-mediated endocytosis while other viruses rely on binding to specific receptors to reach the intracellular milieu. Despite different entry targets, their fusion proteins

often undergo conformational changes that expose their fusogenic regions, ultimately leading to membrane fusion. Viral fusion proteins can be classified into three different classes, based on structural considerations [40, 68] (Figure 14).

- Class I fusion proteins like influenza's hemagglutinin [69], HIV and SIV's gp41 [70, 71] or Ebola's gp2 [72] share a similar structure composed of a central triple-stranded coiled-coil region with outer C-terminal antiparallel α helical layers that form a trimer of helical hairpins [44, 73]. Following transition from a metastable state to a fusion trimeric induced in many cases by a decrease in pH, the transmembrane anchor, the glycine-rich fusion peptide and the now folded external domains synergistically achieve membrane fusion.

- Class II viral fusion proteins like SFV's E1 protein [74], DENV or WNV's E glycoproteins [75, 76] or HCV's E1 protein [77] have a mainly β-sheet secondary structure [78]. Their fusion mechanism is similar to that of class I fusion proteins in that a decrease in pH inside endosomes triggers a conformational change that exposes the fusion peptide. Both the transmembrane domains (domain III in flaviviruses) and the fusion peptide containing domain (domain II in flaviviruses) contribute to the fusion process. These conformational changes are produced by a hinge motion that joins transmembrane domains and the fusion peptide and it is this change that provides the energy to overcome the fusion energy barrier [75, 79-81]. A typical class II fusion process is shown in Figure 19 further ahead.

- Class III fusion proteins like Baculovirus's gp64 [82], VSV's G protein [83, 84] or HSV-1's gab protein [85] combine structural features of both class I and class II fusion proteins. On the one hand their fusion domain (composed of two fusion loops) is located at the tip of a mainly β-sheet domain like class II fusion proteins while on the other hand the post fusion state is arranged as an α-helical hairpin-like trimeric core like class I proteins [58, 73].

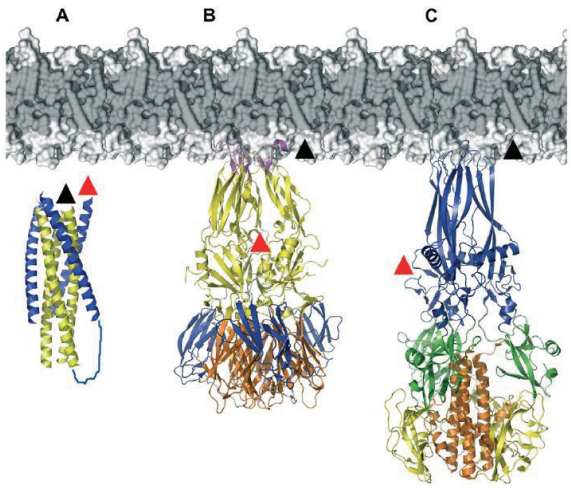

Figure 14 . Graphical simulation of structural motifs of three classes of viral fusion proteins in their post-fusion conformation. The lipid bilayer is coloured in grey, fusion peptides are indicated in black arrows and transmembrane domains in red arrows. (A) Class I is represented by the HIV-1 gp41 core structure, (B) class II by E protein of flaviviruses and (C) class III by VSV glycoprotein G (From [58]).

2. DENGUE VIRUS

2.1. TAXONOMY, DISTRIBUTION AND CLINICAL FEATURES

Dengue virus is classified into the Flavivirus genus, an integrant of the *Flaviviridae* family. This family is composed of three genera: *Hepacivirus* (HCV for example), *Pestivirus* (bovine viral diarrhoea) and *Flavivirus* (dengue virus, tick borne encephalitis virus, Japanese encephalitis virus). There are 56 species in the *Flavivirus* genus [86], of which yellow fever virus (one of the symptoms of the infection with this virus is jaundice, hence the name *Flaviviridae*; flavus is the Latin word for yellow), and Dengue virus are amongst the first agents shown to cause human diseases [87, 88]. Regarding vector association and antigenic relationships:

- Tick borne: Divided into mammalian (for example Kyasaunur Forest disease virus, Omsk haemorrhagic fever virus and tick-borne encephalitis virus) and seabird (for example Kadam virus or Suarez reef virus) virus groups;

- Mosquito-borne: Divided into two groups according to the vector involved. The two vectors are part of *Culex* spp. and *Aedes* spp.: the former transmit viruses like West Nile virus, Japanese encephalitis virus and St. Louis encephalitis virus, whereas the latter are responsible for the transmission of Dengue virus, yellow fever and Kedougou virus;

- Without a known vector: These viruses fall into three antigenically distinct groups and include Entebbe bat, Yokose and Sokoluk viruses.

DENV includes four distinct yet antigenically related serotypes (DENV1, DENV2, DENV3 and DENV4) in DENV antigenic complex [89]. DENV presents a restricted range of natural hosts, believed to consist exclusively of primates. Nowadays the four DENV serotypes can be found in all urban areas in the tropics, consistent with the widespread distribution of the main dengue virus vector *(Aedes aegypti)*.

Table 2 . Geographical distribution of representative genotypes from the four DENV serotypes.

Serotype	Genotype	Representative regions
DENV1	I	Southeast Asia, China and East Africa
	II	Thailand
	III	Malaysia
	IV	West Pacific and Australia
	V	Americas, West Africa and Asia
DENV2	Asian genotype I/II	Malaysia, Thailand (I) / Vietnam, China, Taiwan, Sri Lanka, Philippines (II)
	Cosmopolitan genotype	Australia, East and West Africa, Pacific and Indian Ocean's islands, Indian subcontinent and Middle East
	American genotype	Latin America, Caribbean, Indian subcontinent and Pacific
	Southeast Asian/ American genotype	Thailand, Vietnam and Americas
	Sylvatic genotype	West Africa and Southeast Asia
DENV3	I	Indonesia, Malaysia, Philippines and South Pacific islands
	II	Thailand, Vietnam and Bangladesh
	III	Sri Lanka, India, Samoa and Africa
	IV	Puerto Rico, Latin America
DENV4	I	Thailand, Philippines, Sri Lanka and Japan
	II	Indonesia, Malaysia, Tahiti, Caribbean and the Americas
	III	Thailand
	IV	Sylvatic strains

Classification was initially performed on the basis of T1 RNase fingerprinting [90-93] and later using nucleic acid sequencing, in which a genotype was defined as clusters of dengue viruses with nucleotide sequence divergence inferior or equal to 6% within a given genome region [94]. Using E/NS1 junction and E protein nucleotide sequences (partial and complete, respectively), DENV1 was grouped into five different genotypes: genotype I, with strains from Southeast Asia, China and East Africa, genotype II, strains from Thailand, genotype III, sylvatic strain collected in Malaysia, genotype IV, representing strains from West Pacific Islands and Australia and genotype V, with all the strains from the Americas and strains from West Africa and Asia [94-96]. DENV2 comprises five genotypes as well: Asian genotype, which consists of two genotypes

from Malaysia, Thailand (Asian genotype I), Vietnam, China, Taiwan, Sri Lanka and Philippines (Asian genotype II); cosmopolitan genotype, with strains from Australia, East and West Africa, the Pacific and Indian Ocean islands, the Indian subcontinent and Middle East; American genotype, representing strains from Latin America, Caribbean islands, Indian subcontinent and Pacific islands; southeast Asian/American genotype, with strains from Thailand, Vietnam and Americas; sylvatic genotype, including strains collected from humans, forest and sentinel monkeys in West Africa and Southeast Asia [97-102]. DENV3 is grouped into four genotypes: genotype I from Indonesia, Malaysia, Philippines and South Pacific Islands; genotype II, whose strains were collected in Thailand, Vietnam and Bangladesh; genotype III, with strains from Sri Lanka, India, Africa and Samoa; genotype IV, containing strains from Puerto Rico, Latin and central America [103]. To finish, DENV4 comprises four genotypes: genotype I, from Thailand, Philippines, Sri Lanka and Japan strains; genotype II, collected strains in Indonesia, Malaysia, Tahiti, Caribbean and the Americas; genotype III found in Thailand and genotype IV representing the sylvatic strains of this serotype. For ease of reading, all of these data can be found resumed in Table 2 above.

Dengue virus (DENV), the most common arthropod-borne virus (arbovirus) is endemic to over 100 countries, especially in the tropics and subtropics [104]. Initial predictions by the World Health Organization (WHO) and several authors [105-108] estimated somewhere between 50-100 million Dengue infections and half a million Dengue Haemorrhagic Fever (DHF) reported cases (a severe and potentially life threatening condition addressed subsequently) yearly and about 2.5 billion people at risk of contracting Dengue in the world. Using all available medical data and resorting to a formal modelling network taking into account local risk increasing variables (rainfall, temperature and level of urbanisation have been shown to positively correlate with higher infection risk), Bhatt and collaborators postulate that Dengue is ubiquitous in the tropics and that it is far more dispersed and serious than previously thought with a dismal prediction of about 400 million infections every year, of which about 96 million cases present any symptomatology [109] (Figure 15). It is noteworthy to refer that unapparent infections are worrying, considering infected individuals can be bitten by the mosquito virus and render it a vector.

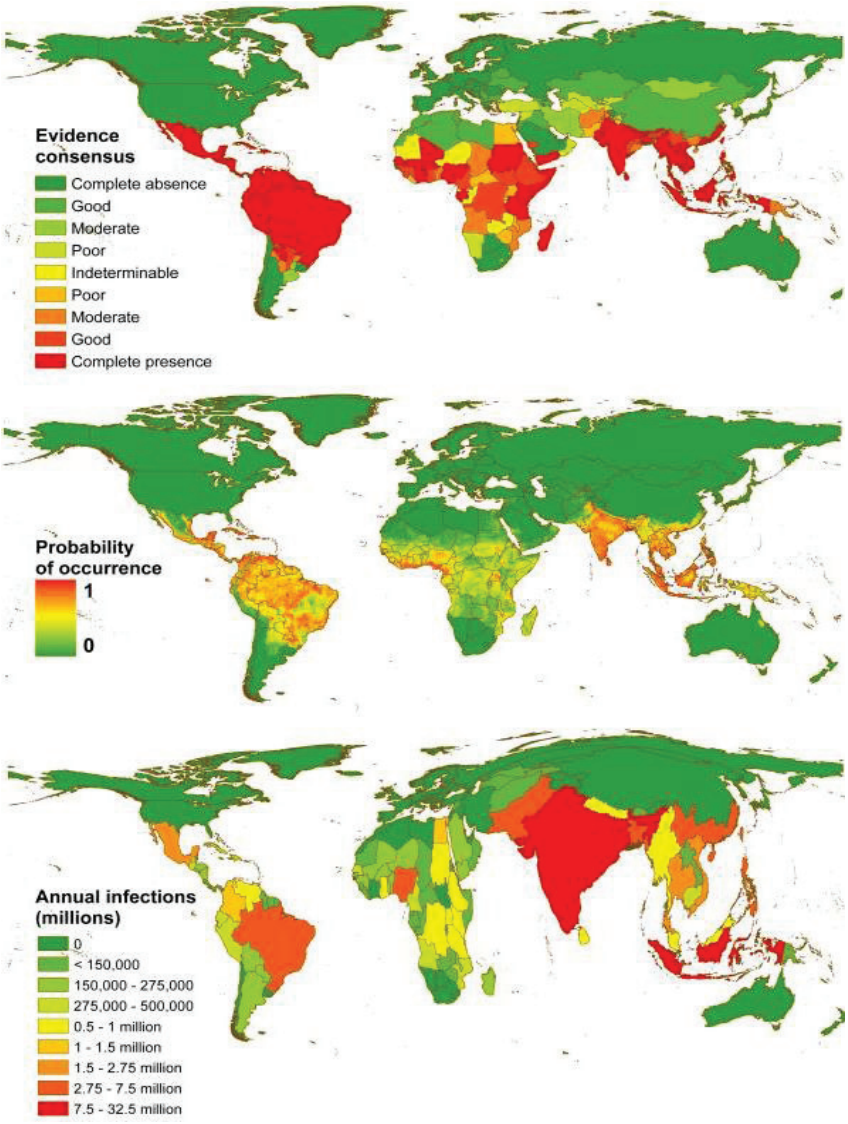

Figure 15 . Prevalence and risk of dengue infection in the world as of 2010. (A) Evidence of dengue infections at national and international levels, (B) Probability of dengue occurrence calculated in [109], Cartogram of total annual infections as a proportion of China's geographical area. Extracted and adapted from [109].

DENV is chiefly transmitted by mosquitoes of the *Aedes* genus (*Aedes* spp.), of which *Aedes albopictus* and *Aedes aegypti* account for the majority of infections, where the latter shows higher infection efficiency than the former [110-112]. Increased worldwide travelling has led to a widespread distribution of DENV to previously unaffected regions. There have been recent of Dengue cases in regions with previously existing *Aedes* spp. populations where Dengue infections were virtually non-existent: Madeira archipelago in Portugal [113], Pelješac peninsula in Croatia [114] and Nice in

France [115]. Furthermore, studies have shown that travellers have been bitten by an affected mosquito vector somewhere between 10.2 to 30 times per 1000 person-months, an important figure, higher than that found for other diseases [104, 105, 109]. This ever-increasing worldwide prevalence of DENV has motivated a renewed and frankly needed interest (from 238 hits for "dengue" as of 2000 to 1287 in 2013 and 536 as of May 2014) of the scientific community on the study, control and prevention of Dengue infections.Apart from the bite of an infected mosquito vector, DENV can be transmitted between humans (the natural reservoir of DENV) via blood (transfusions and maternal-foetal transmission) or organ and tissue transplantation [107, 116, 117]. Individuals infected by DENV can present one of four sets of clinical manifestations: asymptomatic, Dengue Fever (DF), Dengue Haemorrhagic Fever (DHF) or Dengue Shock Syndrome (DSS), i.e. from unimportant and often unnoticed infections to potentially life threatening situations (DHF and DSS). A typical Dengue Fever syndrome is characterized by fever, myalgia, fatigue and diarrhoea in the onset of infection, followed by a 2-7 day period of febrile state, haematuria and bradycardia. In more severe conditions (DHF and DSS), where individuals also present haemorrhaging and hypovolemia, infections start with a viraemia period of 5-8 days, concomitant with fever from 2 to 7 days, headaches, myalgia, bone and joint pain (these two symptoms are the reason for the attribution of the common name of break-bone fever to Dengue Haemorrhagic fever) rashes and less frequently leukopenia and haemorrhage [107, 116, 117]. WHO guidelines define DHF as an almost certain diagnosis for individuals presenting acute fever and at least two of the following signals and symptoms: headache, retro-orbital pain, myalgia, arthralgia, rash, haemorrhages and leukopenia [107, 117]. Furthermore, if an individual presents symptomatology consistent with DHF, hypotension and narrow pulse pressure (<= 20 mmHg) or significant shock/circulatory collapse, the diagnosis is DSS, the most severe syndrome of Dengue infection. The diagnosis of DF, DHF and DSS is usually confirmed using samples from cerebrospinal fluid (CSF), serum or tissue samples and subjecting them to the following methods of detection, dependent on the phase of the infection: (1) Detection of viral RNA in serum, (2) Detection of DENV antigens, usually performed during the acute febrile stage (less than 5 days after the onset of symptoms) using the NS1 protein as the antigen, (3) Detection of IgM anti-Dengue (usually performed after the initial acute febrile stage).

More than 70 viruses compose the Flavivirus genus e.g. Dengue virus (DENV), Japanese Encephalitis virus (JEV), tick-borne encephalitis virus (TBEV), West Nile virus (WNV). Flavivirus have many structural similarities (size of the virions, viral proteins, life cycle and parts of the viral genome structure). DENV virions (like all Flaviviruses) are quite small with about 60 nm in the immature state and 50 nm in the immature state (Figure 16, A and B respectively).

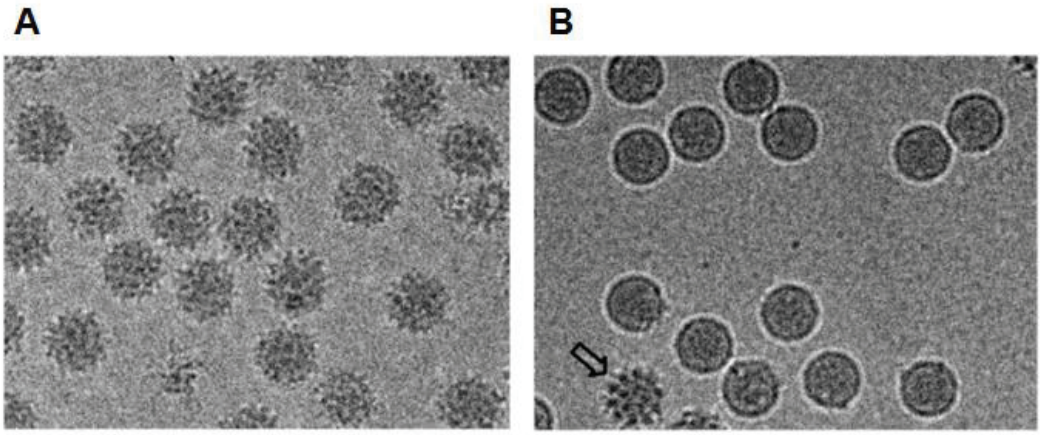

Figure 16 . Electron micrograph of DENV (A) immature and (B) mature virions. The mature virions were obtained by subjecting the immature virions to a decrease in pH and to furin action with a subsequent reversal of pH to the neutral pH of 7.5. Two distinct structural parameters can be easily discerned: the characteristic "spiky" conformation of DENV immature particles and the slightly larger diameter when compared to that of mature particles. Adapted from [118].

DENV consists of a nucleocapsid, composed of multiple copies of C protein bound to the viral genome, enveloped by a host derived lipid bilayer with host dependent lipid composition, where several arrangements of 180 copies of prM (immature virion)/M (mature virion) and E proteins are embedded. The immature virion has two possible pH dependent conformations: a characteristic spiky surface due to 60 trimeric spikes of prM and E heterodimers that protrude away from the viral membrane surface at neutral pH or a smoother surface conformation triggered by a decrease in pH (from 7.4 to 6.0). In the mature virion the pr peptide is no longer attached to the M moiety (furin cleaves the pr peptide and M protein during transit through the trans-Golgi network) and M and E

protein rearrange as 90 homodimers that lie flat against the viral surface, forming a herringbone pattern [79, 80, 119-121] (Figure 17).

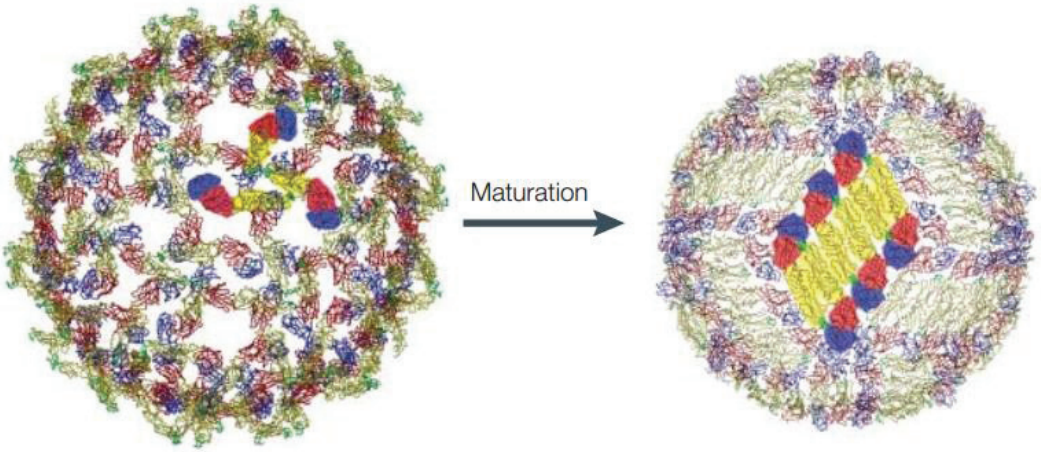

Figure 17 . Rearrangement of prM/E trimers as M/E dimers at the viral surface following maturation. Adapted from [119].

As for mature virions, the smooth surface conformation was thought to be the norm until Zhang and collaborators [122] found a surprising result. Immature particles had the same conformation at room temperature and at a human physiological temperature of 37 ºC, yet mature particles presented a smooth surface and a diameter of 50 nm as expected at the normal room temperature and a rough surface at 37ºC as well as a slightly larger diameter of 55 nm. Furthermore they found that mature particles incubated at 35/36ºC and then allowed to infect human cells, had significantly higher infectivity than mature particles that had remained at room temperature. They concluded that this different conformation depending on temperature and on the organism infected (mosquito at room temperature and human at 37 ºC) would imply a certain degree of evolutive adaptation.

DENV genome (as well as all flaviviruses) is a single positive sense strand of RNA with ~11 kb with a 5' type I cap [123] and a 3' end without a polyadenine tail. This genome encodes a single open reading frame (ORF) flanked by non-coding regions of 100 nucleotides (5' end) and 400-700 nucleotides (3' end) in length [124]. Translation of this ORF results in a polyprotein that after appropriate cleavage and maturation by viral and host proteases gives rise to three structural proteins: capsid or C (with ~11 kDa), membrane precursor or prM (with ~26 kDa), envelope or E (with ~53 kDa) and

seven non-structural (NS) proteins: NS1 (with ~46 kDa), NS2A (with ~22kDa), NS2B (with ~14 kDa), NS3 (with ~70 kDa), NS4A (with ~16 kDa), NS4B (with ~27 kDa) and NS5 (with ~103 kDa) [79, 80, 119, 125] (Figure 18).

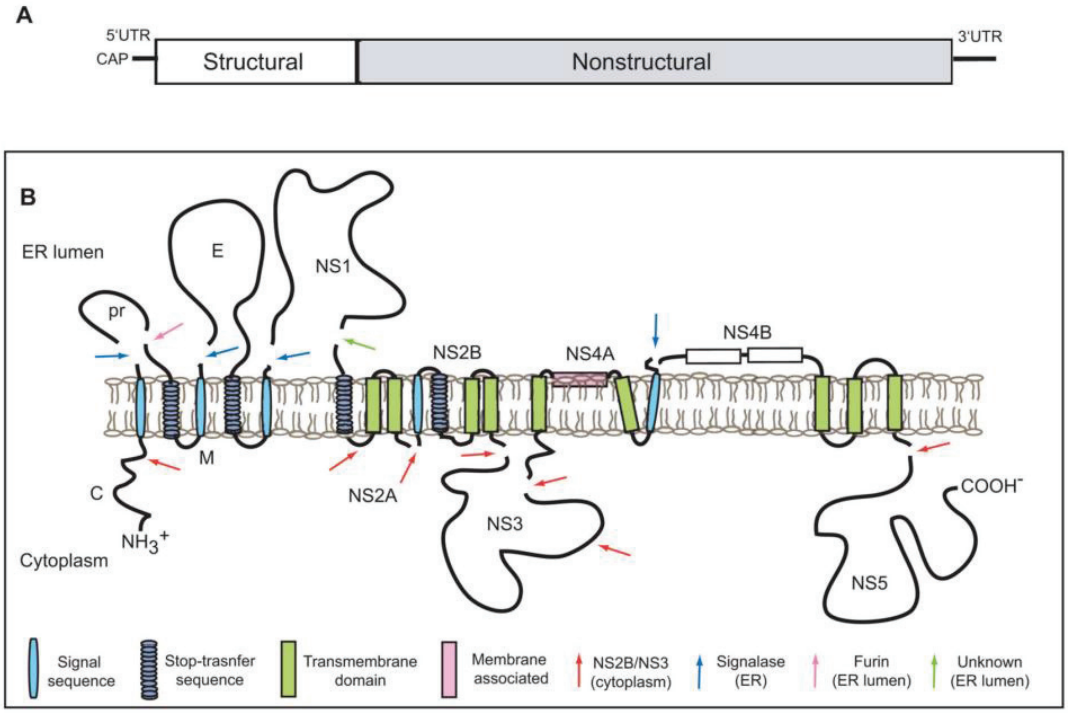

Figure 18 . Diagram of DENV (A) genome and (B) polyprotein with viral and host proteases cleavage sites. Adapted from [79].

2.3. DENGUE VIRUS LIFE CYCLE

Following a mosquito bite, DENV initially infects skin-resident Langerhans cells and dendritic cells (DC) [126, 127], spreading to monocytes [126, 128] and macrophages [126, 129] found on lymph nodes. Hepatocytes might function as natural reservoirs of DENV [130-132]. Infection by DENV does not seem to be cell type specific as corroborated by the large number of infectivity studies performed with a variety of cell lines from different organisms, from human (HEPG2, THP-1, U937, HUVEC, LoVo), mosquito (C6/36), monkey (Vero, CV-1 or LLC-Mk2), hamster (BHK), murine (Raw or J774) [130, 133-146]. It is therefore relatively safe to assume one of two possibilities, either DENV has a ubiquitous cell receptor or a myriad cell receptors. Experimental

data strongly favours the second option. A significant number of receptors associated with DENV have been hitherto found in mammalian cells: heparan sulphate [147-149], CD14 [150], heat shock protein (Hsp) 90 [151], GRP 78 (BiP) [152], a high affinity laminin receptor [153], and a handful of C-type lectin receptors in human myeloid cells like DC-SIGN [154], L-SIGN [155], CD206 [129] or CLEC5A/MDL-1 [135].

In a primary infection, DENV enters the cell by clathrin-mediated endocytosis, diffusing towards clathrin-coated pits upon membrane binding [156]. Following internalization, three factors influence DENV infectivity: maturation of the endosome, integrity of the cell's transportation machinery and the presence of specific lipids in endosomes. DENV is delivered to early endosomes containing Rab-5, which in turn mature into Rab-7 positive endosomes [156]. Many studies have found that DENV fuses mainly from late endosomes [156-158], yet Krishnan and colleagues have shown that it was Rab-5 and not Rab-7 that was essential for DENV infection, with about 70% DENV infection inhibition in Rab 5 knockout HeLa cells, meaning that DENV can fuse form both early and late endosomes [156, 159]. Monkey kidney cells BS-C-1 infected with DENV and treated (during infection) with nocodazole, an antineoplastic agent that inhibits microtubule polymerization [160], reduces infectivity by 30% suggesting that microtubule network integrity is a necessary yet not essential condition for efficient DENV infection [145]. The lipid composition of liposomes seems to affect DENV infection as well, specifically DENV might make use of anionic lipids, especially BMP, a PG analogue, found in late endosome membranes (LEM) as a cofactor for its fusion machinery [161]. In the low pH and anionic lipid rich environment of late endosomes, the E protein homodimers at the surface of DENV pass through an irreversible conformational change into E protein trimers. Firstly, E homodimers dissociate into E monomers [119, 162, 163] and secondly, E protein's domain II (out of three domains) extends away from the viral membrane and the fusion peptide located on its tip inserts into the host's lipid bilayer. At the same time, domain III (anchored parallel to the viral membrane) folds back to domain II and this conformational change along with membrane structural rearrangements provide the energy requirements for this class II fusion process described in a previous section (Figure 19) [54, 75].

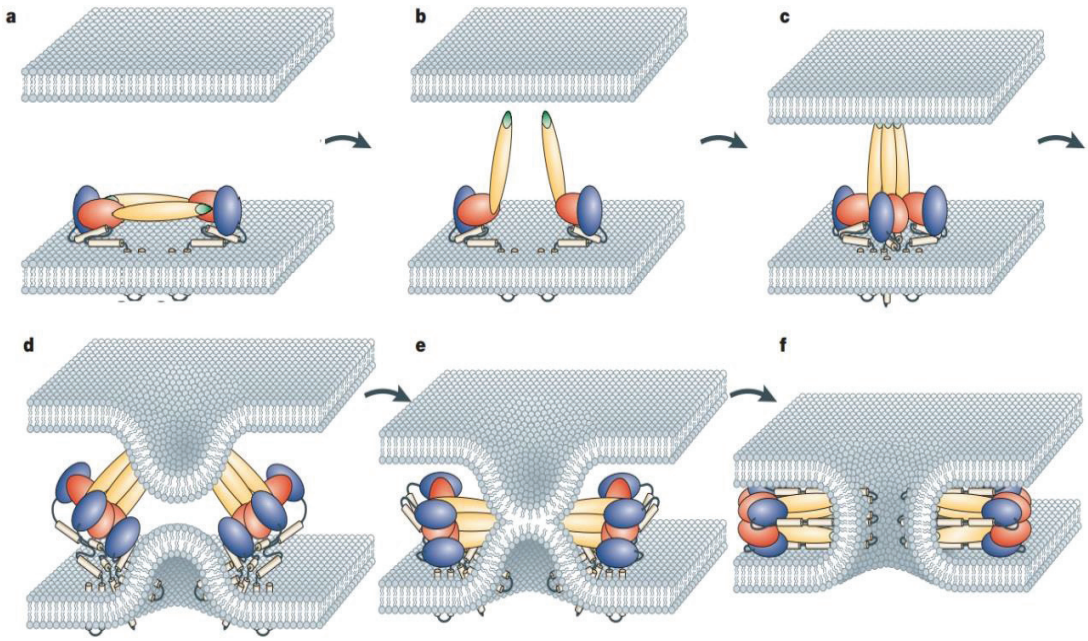

Figure 19 . Class II fusion. The dimeric E protein is on the virus surface with the fusion peptide (shown in green) buried in the dimer (a). The protein binds to a receptor and is internalized in the endosome. Under low-pH conditions, domain II swings outward towards the host cell membrane, presumably at the domain I–II hinge region (b). This conformational change allows the E proteins to rearrange laterally. The fusion peptide inserts itself into the outer leaflet of the host cell membrane, enabling trimerization of the E protein (c). Domain III of the E protein folds back onto itself, and in the process brings the viral membrane towards the fusion peptide and host cell membrane (d). As domain III moves towards domain II, hemi fusion of the lipid membranes occurs (e), and finally a trimer forms where the transmembrane regions and the fusion peptide are in close proximity and fusion takes place (f). Adapted from [119].

During translation structural proteins are anchored to the endoplasmic reticulum (ER) by signal sequences and membrane anchoring domains. Protein C remains associated to the ER during all the process, possibly required for its role in the specific encapsulation of the genome, while E and prM form stable dimers on the ER membrane [164, 165]. All the other non-structural proteins are involved in replication of the genome and in some flaviviruses, NS2A, NS3 and NS5 are involved in the assembly and maturation of the virion [166-168]. Association of flaviviruses' non-structural proteins in multi-protein complexes in lipid membranes and the ability of these complexes to modulate lipid bilayer structure, taking advantage of the polymorphic nature of lipids, have long been accepted [169, 170]. Membrane rearrangement and lipid sequestration are important if not essential processes in the life cycle of DENV. On the one hand membrane restructuring seems to be carried out by NS4A and NS4B in

concert with other non-structural proteins to form various types of membrane arrangements, e.g. large clusters of double membrane vesicles (DMV) of 50-400 nm in diameter (Figure 20), convoluted membranes and paracrystalline arrays. In Kunjin virus (another variant of West Nile virus), viral replication takes place in DMV whereas polyprotein processing occurs on convoluted membranes [170, 171]. On the other hand, DENV infection requires lipid raft domains with increased cholesterol content [172, 173], renewed cells lipid synthesis on the ER [174-176] and it modulates autophagy, an homeostatic process naturally triggered in cells by starvation or pathogen infection, in order to sequester and degrade lipid vesicles to obtain energy for its infectious processes [177, 178].

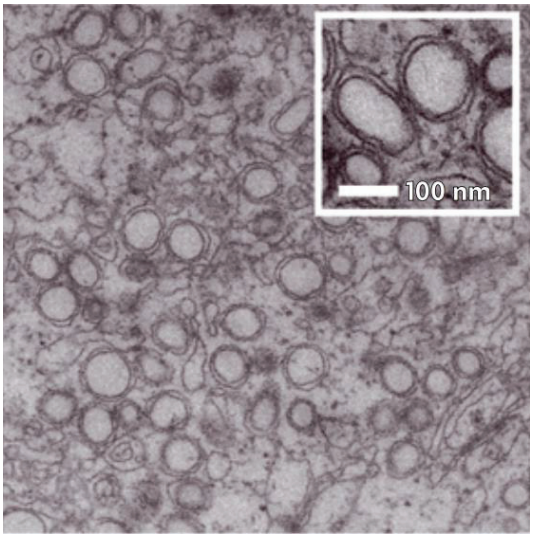

Figure 20 . Characteristic double membrane vesicles (DMV) found in DENV infected cells (Huh7 in this case fixed 24 hours post infection). Adapted from [170].

Autophagy inhibition and cholesterol reduction significantly inhibit DENV infection. Interestingly, infection of cells treated beforehand with cholesterol is significantly reduced, suggesting that precise cholesterol proportions in membranes are required for DENV to properly infect cells, at least in the early steps of its life cycle [59, 173]. Welsch and colleagues [171] found that ER-derived membranes with viral replication complexes had a direct connection to the cytosol, possibly an exit route for the vRNA, replicated by that same replication complex. Other authors postulate that C proteins embedded in the ER membrane could bind to the vRNA exiting through that structure, forming the nucleocapsid that would in turn bud with an ER membrane containing E and prM heterodimers and form the immature virion [179]. This viral budding process

is not very efficient in DENV, considering that sub-viral particles lacking the nucleocapsid are often detected in the extracellular medium [180, 181]. Following viral budding, immature virions (complete particles) are transported to the Golgi complex where their transit through the trans-Golgi network begins. It is during this transit that a decrease in pH inside vesicles favours the cleavage of the pr peptide from prM by furin. During the secretory pathway the cleaved pr peptide is released exposing the fusion peptide (already outside the cellular environment). This marks the full maturation the virus. A sketch adapted from [182] illustrating the main processes described is shown in Figure 21.

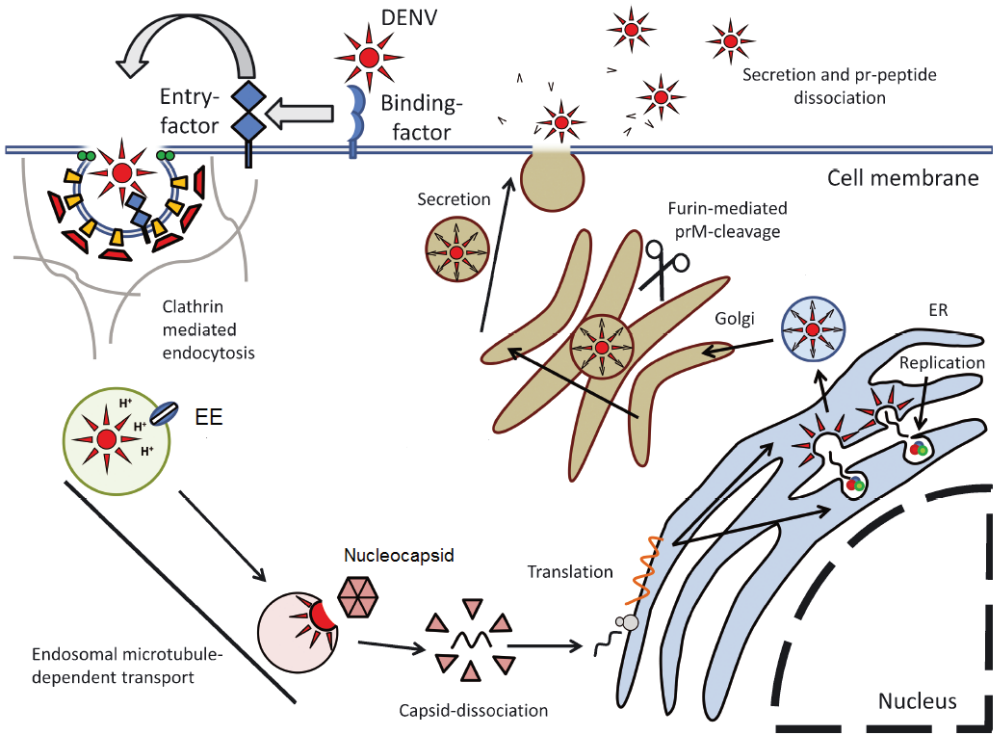

Figure 21 . Life cycle of Dengue virus (adapted from [182]). DENV particles bind to a variety of receptors at the cell surface and diffuse to clathrin-coated pits. It then enters the cell via receptor-mediated endocytosis and fuses either with early endosomes (EE) or late endosomes (LE). In the second case, specific lipid composition and the acidic pH in LE triggers a conformational change of the E glycoprotein that ultimately results in membrane fusion and release of the nucleocapsid (NC) into the cytosol. NC dissociates into C proteins and viral RNA (vRNA) genome and translation occurs on the ER membrane. C and E-prM heterodimers remain attached to ER-derived membranes. At the same time, several non-structural proteins modulate ER-derived membranes and form the replication complex. C proteins bind to newly formed vRNA strands and the viral budding process is terminated with the formation of a host derived lipid bilayer with embedded E-prM heterodimers. This immature virion starts its transit through the TGN, where furin cleaves the pr peptide. Following the secretory pathway the virion is released into the extracellular medium and the pr peptide is fully removed, resulting in a mature viral particle.

2.4. HOST IMMUNE RESPONSE AND ANTIBODY-DEPENDENT ENHANCEMENT OF DENV

Following DENV internalization, there are two possible immune responses. In a primary infection, a normal immune response occurs, with DENV endocyted particles triggering IFN production in many cell types, including interstitial dendritic cells (DC) [183-186]. DENV particle recognition is mainly accomplished by TLR 3 and TLR 7 [135, 187, 188] in endosomes and the cytoplasmic viral genome is recognized by RIG-I and MDA-5 [189]. IFN binding to the cell surface triggers a cytokine storm using STAT1 dependent and independent pathways. Humoral immunity is only attained 6 days after the initial mosquito bite. This response occurs at two levels, either through the inhibition of DENV interaction with cell surface receptors [190, 191] or through antibody binding to several DENV antigens: E protein's domain III (putative receptor binding site) [192-194], fusion loop [193, 195] and domain II [196], the pr peptide in prM [197] and NS1, expressed on the surface of infected cells [198]. In a secondary heterologous infection, antibodies against the previous serotype are produced. Most of them will bind to the new serotype yet they will not be neutralizing [199, 200]. Furthermore, these antibodies seem to increase infectivity by antibody-dependent enhancement (ADE) [201]. The current model postulates that virus-antibody complexes bind to Fcγ receptors at the cell surface of monocytes, macrophages and DC, just as in the primary infection [202-204]. Opsonized antibodies enter infected cells by phagocytosis [203-205] and in a closely related flavivirus (WNV), they also enter the cell by receptor-mediated endocytosis (as seen in a primary infection). Interestingly, antibodies against E and prM proteins seem to enhance the infectivity of immature particles [202, 206, 207]. It is not yet clear but immatures particles might be delivered to endosomes after phagocytosis and the acidic environment in phagolysosomes might trigger a maturation process similar to the one found in the secretory pathway [120, 207-209]. DENV ADE seems to reduce IFN β expression [210, 211], debilitating the antiviral state and decreasing nitric oxide production [134], thus allowing infected cells to survive longer, increasing total virus output [134, 202, 212, 213].

2.5. STRUCTURAL PROTEINS

2.5.1. CAPSID (C) PROTEIN

The capsid protein (C) of DENV is found in association with the viral RNA (vRNA) genome in mature virions, forming the nucleocapsid (NC). This protein has several functions including assembly of the viral particles, attested by its distribution in ER membranes up until the viral budding process [214, 215] and the specific encapsulation of the genome occur, evidenced by the existence of sub viral particles lacking both C protein and vRNA [166, 181]. Additionally it has been found that C proteins localize to the nucleus in some cell lines [216] and bind to histones in hepatocytes, preventing nucleosome formation, what suggests that DENV C protein might specifically target histones to sequester the host's replication machinery in its own favour [217]. Furthermore it accumulates in lipid droplets, proving its interaction with membranes [218]. This 114-mer protein becomes fully mature after appropriate cleavage of its C-terminal signal sequence by the NS2B-NS3 serine protease complex. Ma and collaborators [219] found that C proteins readily form dimers in solution and that these dimers present a region with an abnormally large charge concentration (+46). Recurring to NMR spectroscopy, these authors have obtained the structure of an incomplete C protein (from residues 21-100), lacking both the N-terminal conformationally labile region and the signal sequence, from residues 1 to 20 and 101 to 114 respectively.

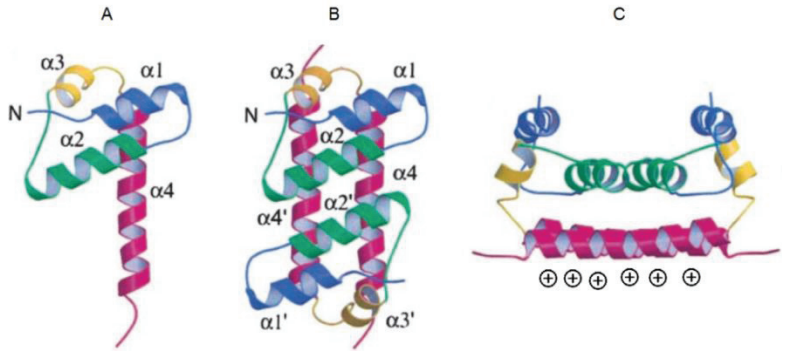

Figure 22 . Structure of C protein as resolved by NMR spectroscopy: (A) monomer with colour-coded helices displayed, (B) dimer in a top down perspective and (C) dimer in a transversal perspective where both the concave and highly hydrophobic α2-α2' region (green) and the α4-α4' region (magenta) with a large concentration of positive charges are visible. Adapted from [219].

Each monomer is composed of four α-helices interconnected by short loops and the dimer presents a highly hydrophobic region encompassing the α2 helices of both monomers and a significantly charged region made up by both α4 helices as seen in Figure 22. On the one hand, the α2-α2' region (the prime distinguishes monomers) forms a concave groove that might interact with lipid membranes and on the other hand, the α4-α4' region, with its charge of +46 might interact with negative vRNA (Figure 23).

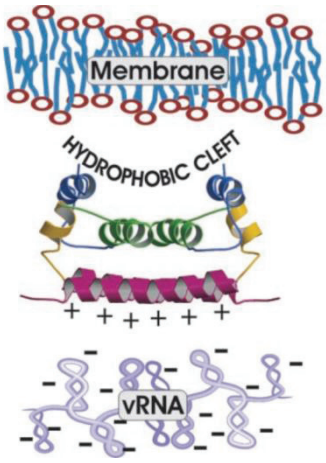

Figure 23 . Dimer of protein C as resolved by NMR spectroscopy and possible interactions it might have with viral RNA on one side and membranes on the other [219].

2.5.2.PRM/M PROTEIN

The full length prM protein of some 26 kDa is composed of two sections, pr peptide and M protein [125]. The former is located at the N-terminal region from residues 1 to 91 and the latter from residues 91 to 166. They are separated by a furin cleavage site from residues 86 to 89 with a canonical sequence R-X-K/R-R, a target sequence of furin, commonly found in many viral proteins that require furin cleavage in their maturation process [220-222]. The pr peptide has a mainly β sheet secondary structure and its chief function is to prevent an early fusion of the immature virion with host membranes in the secretory pathway by covering the fusion loop of the envelope protein as seen by X-ray crystallography [208]. As for the M protein, it consists of an α helical stem region followed by two transmembrane helices [208, 209, 223]. Apart from the

fusion preventive function, a few other have been unravelled recently: a region of the M protein triggered apoptosis in mouse and human tumour cells [224, 225], prM/M interacts with host proteins involved in endosomal pH regulation like vATP and transportation machinery like dynein and claudin-1 [226-228]. It has been postulated that prM and E remain anchored to ER-derived membranes during the viral replication [164, 165]. Wang and collaborators not only reconfirmed this but also found that the M protein forms oligomers and might restructure ER membranes [229].

2.5.3. E (GLYCO)PROTEIN

The envelope protein (E) has at least two different conformations in a mature virion, a pre-fusion conformation with 90 E homodimers lying flat against the surface and a post-fusion conformation with 60 E trimers protruding from the viral membrane surface with the fusion loop exposed and ready to partake in membrane fusion. Homodimers in the pre-fusion conformation have three mainly β-strand domains [75, 120, 121, 209, 230]. Domain I contains the N-terminal region flanked on one side by domain III, where the putative receptor binding sites are located [119], and on the other by domain II, with the fusion peptide at its tip (Figure 24).

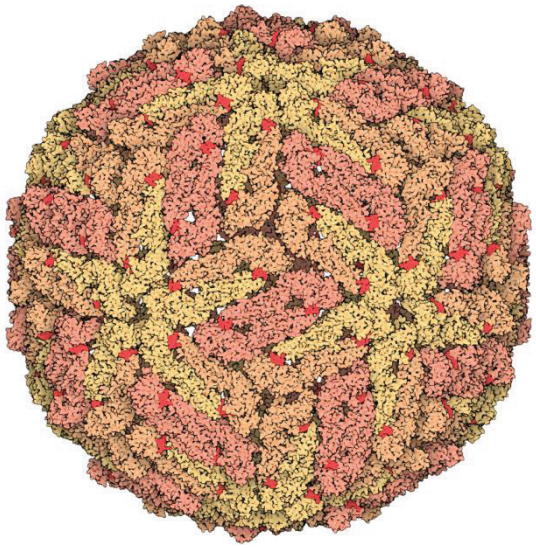

Figure 24 . Structure of a flavivirus obtained by fitting the known structure of a flavivirus E protein into the cryo EM electron density map of mature viral particles. Dimers are clearly visible and the fusion loop is highlighted in red. PDB ID: 1K4R [120].

Domains I and II are linked by four polypeptide chains, whereas domains I and III are connected by a single polypeptide linker, a more flexible connection important in the conformational rearrangements associated with the transition from a homodimeric pre- to a trimeric post-fusion conformation of E protein. Within a dimer, the fusion peptide of one monomer is placed between domains I and III of the other monomer. Two potentially N-linked carbohydrate sites are glycosylated as found in dengue virions produced in cell culture [230]. Allied to the flexibility of the bond between domains I and III, differences in the angle between domains I and II of several crystal structures suggest a possible hinge motion that would be required in the conformational changes that direct the fusion peptide to the host membrane during fusion [231] (Figure 25).

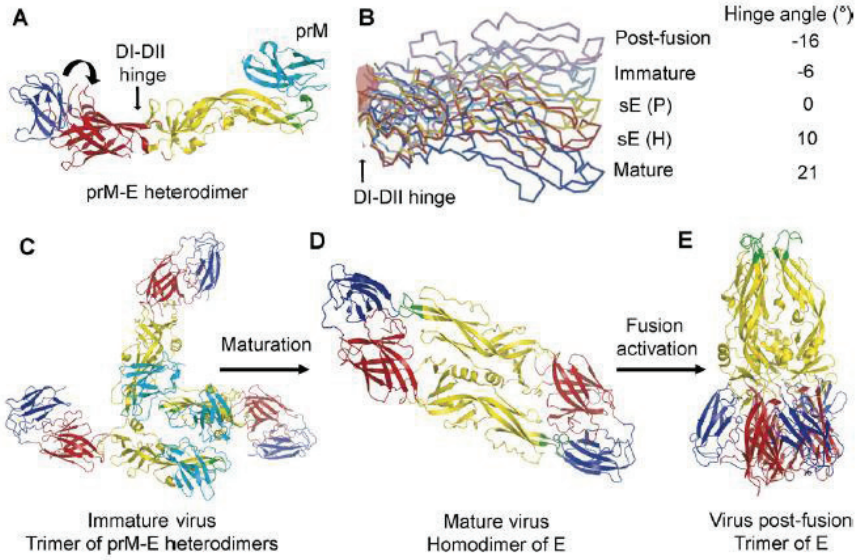

Figure 25 . Structure and conformational changes of the prM/E complex during the fusion process: (A) Structure of a prM-E heterodimer with E protein domains I (red), II (yellow) and III (dark blue) and prM protein (cyan) visible, (B) variations of the angle between domains I and II that give rise to conformational changes required for appropriate fusion and the three-step conformational changes associated with all fusion stages from virus formation in one cell to fusion with another cell, (C) Trimer of prM/E heterodimers in immature virions at low pH, (D) Structure of an E homodimer with the fusion loop highlighted in green at the tip of domain II (yellow) and (E) post-fusion trimer conformation of E protein in a mature virus at low pH [231].

Another study has shown that the region corresponding to the fusion peptide of protein E interacts strongly with membrane model systems, thus it might be of some importance for proper viral activation and fusion [232]. Interactions between domains I and III explain why the amplitude of the movement between those domains is lower

than expected in domains with a similar flexible connection at neutral pH [54]. Decrease in pH disrupts those interactions and domain III adopts a different conformation conducing to a post-fusion trimer conformation [230]. Following the insertion of the fusion loop into the host membrane, the tree domains of protein E retain most of their folded structures, yet their relative positions are altered: domain II rotates approximately 30 º with respect to domain I about a hinge close to residue 191 and the kI hairpin from residues 270 to 279, while domain III rotates 70º in the direction of the fusion loop, bringing its C-terminal closer to the fusion loop [75]. This C-terminal region (from residues 400 to 496) was resolved by cryo-EM [223]. It consists of a stem region composed of two amphipathic helices EH1 and EH2, followed by two transmembrane helices TM1 and TM2 [223]. While the former are involved in the viral assembly with EH1 affecting prM-E heterodimerization and EH2 the interaction of this stem region with lipid membranes, the latter are poorly conserved sequences (in flaviviruses in general), where TM1 is required in the early steps of membrane fusion and contains a stop transfer sequence for E and TM2 is involved in the later fusion stages, required for trimer stability and acting as a signal sequence for NS1 translocation into the luminal side of ER [125, 233, 234].

2.6. NON-STRUCTURAL (NS) PROTEINS

In the context of this thesis, only the less characterized and highly hydrophobic NS2A, NS4A and NS4B were subjected to biophysical studies. The remainder will be addressed shortly in sequential order.

Non-structural protein 1 (NS1) is a 46 kDa (55 kDa in its glycosylated state) glycoprotein found in a multitude of oligomeric arrangements in a variety of cell compartments e.g. as a soluble secreted hexameric lipoprotein complex sNS1 [235] or as membrane associated complexes, both in the intracellular space associated with replication complexes or at the cell surface [125]. Both soluble and membrane-associated complexes are highly immunogenic and are implicated in DENV pathogenesis and host immune response [236-239]. Intracellular NS1 co-localizes with replication complexes and dsRNA, suggesting a role in viral replication [240, 241].

NS2B is a rather small (14 kDa) protein that serves as a cofactor in the protease function of NS3 (NS3pro) [242, 243], intercalating itself within the serine protease domain of that protein. It also binds to membranes, possibly anchoring the NS2B-NS3pro complex during the viral cycle.

NS3 is one of the largest DENV proteins (70 kDa) with functions related to viral replication and polyprotein processing. A serine protease complex formed by NS3's N-terminal region and NS2B is responsible for most of the cleavages performed on the polyprotein at NS2A/NS2B, NS2B/NS3, NS3/NS4A and NS4B/NS5 junctions and for generating the C-termini of the mature C protein and NS4A [125, 244, 245]. Its C-terminal region has at least three assigned functions: RNA-stimulated nucleoside triphosphatase (NTPase), RNA helicase and an RNA-5'-triphosphatase (RTPase), all vital functions for viral replication [246-249].

NS5 is the largest and most conserved of all flavivirus' proteins with some 103 kDa. At least two functions related to viral propagation [250, 251] have been assigned to this protein, namely an N-terminal S-adenosyl-methionine.dependent methyltransferase (MTase) responsible for capping and methylation of the capped positive strand of vRNA [252], and a C-terminal RNA-dependent RNA polymerase (RdRp), required in the synthesis of an intermediate RNA template [253, 254]. Furthermore, it has been shown that NS5 forms a complex with NS3, stimulating both its NTPase and RTPase functions [255-257] and that it might play a role both in immune evasion [258] and in viral propagation (it recruits inflammatory cells through IL8 [259]).

2.6.1.NS2A PROTEIN

NS2A is a 22 kDa [125] highly hydrophobic protein. According to a recently published topology model it contains at least five transmembrane segments and two membrane interacting domains [260] (Figure 26). Its precise functions in the viral cycle are far from fully defined. It co-localizes with dsRNA, NS1, NS3 and NS5 in the replication complex [261] what suggests a possible role in the viral replication. Moreover when the following mutations were performed on different flaviviral NS2A proteins the viral output was significantly diminished: R84(A/S) in DENV2 [260], I59N

in KUNV [262] and K190S in YFV [166]. These mutations seem to specifically target the viral assembly and not the viral replication functions. It is also required for the proper processing of NS1 and possesses recognition sites for some proteases. Furthermore, in concert with NS4A and NS4B it effects the IFN antagonism and host immune response evasion [237, 262, 263]. The mechanism(s) by which NS2A influences viral assembly is (are) not yet clear yet, considering its hydrophobicity, the number of predicted transmembrane segments and its association with membrane-bound replication complexes, it is clear that membranes are essential for its proper function and it should not be ruled out that it could modulate lipid polymorphism and rearrange membrane structure.

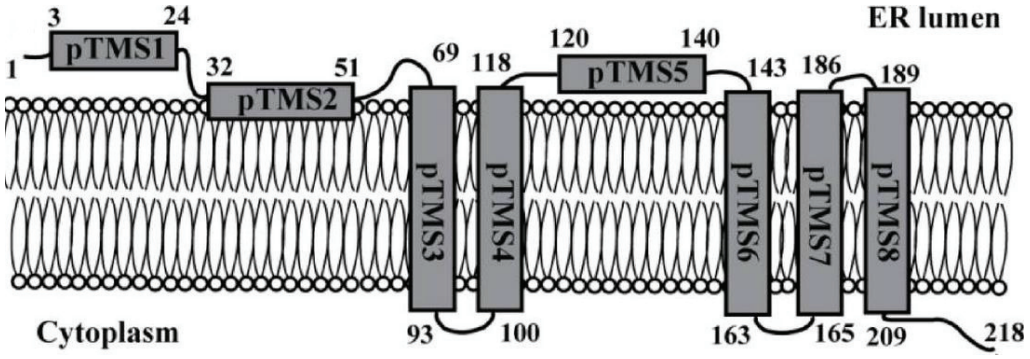

Figure 26 . Membrane topology of NS2A as proposed by Xie and collaborators [260]. The first segment pTMS1 would not associate with membranes, while both pTMS2 and pTMS5 would be in close association with it and pTMS3, pTMS4 and pTMS6-8 would be responsible for NS2A anchoring.

2.6.2.NS4A PROTEIN

NS4A is a small hydrophobic protein with about 16 kDa [125], which according to a recent topology model [264] (Figure 27) is composed of two transmembrane segments, another intimately associated with membranes and a fourth C-terminal fragment 2k (due to its 2 kDa size) that serves as a signal sequence for NS4B translocation into the ER [245]. Knowledge of NS4A and its functions in the viral cycle remains sparse. Its N-terminal region seems to influence the ATPase function of NS3 [265]. Evidence has shown that NS4A co-localizes with dsRNA and other non-structural proteins in the replication complex thus it might be involved in viral replication [261, 264, 266].

Furthermore this protein was found in ER-derived membranes with structural features characteristic of flaviviral infections and it could modulate membrane curvature [264, 267], suggesting a possible role in membrane rearrangements necessary to establish specific sites of replication.

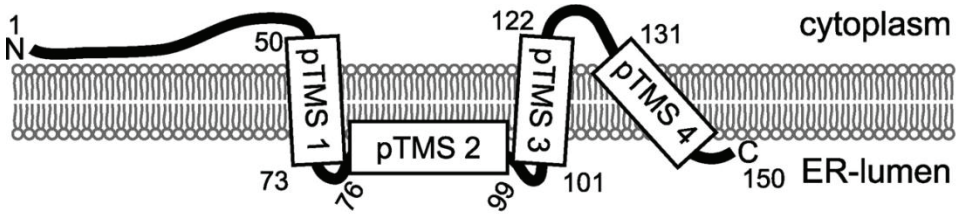

Figure 27 . Membrane topology model of NS4A proposed by Miller and colleagues [264]. The N-terminal region from residues 1 to 50 would not interact with membranes, pTMS1, pTMS3 and pTMS4 (2k fragment) would traverse membranes and pTMS2 would be in close association with the membrane without traversing it.

This protein, in concert with NS2A and NS4B is required for IFN antagonism [263]. DENV infects a wide range of cells, yet only some (epithelial cells and fibroblasts are examples) are not killed in the infection process. In these cells, PI3K dependent autophagy, which in turn up-regulates pro-survival signalling, was found up-regulated when DENV was allowed to infect them [268-270]. In the same line of thought, a study found that NS4A alone would up-regulate this process thereby protecting cells from death and aiding viral propagation [271].

2.6.3.NS4B PROTEIN

Like NS2A and NS4A, NS4B (~27 kDa) is also highly hydrophobic [125] and poorly characterized, mainly owing to its lack of enzymatic activities (like the other two) and because it is hard to obtain whole proteins. According to a recently published topology model this protein has at least three transmembrane domains, pTMD3 from residues 101 to 129, pTMD4 from residues 165 to 190 and pTMD5 from residues 217 to 244 and two hydrophobic segments from residues 1 to 56 and 56 to 93 that do not traverse membranes [272] (Figure 28). This protein is the chief antagonist of the IFN signalling and does it by inhibiting the phosphorylation of STAT1 in that pathway [263, 273], it

also inhibits the host RNAi response [274], modulates the NS3 helicase function in a conformational dependent fashion [272]. On top of that it co-localizes with dsRNA, NS3 and NS5 in a complex that holds the strands as the helicase moves along the duplex [272, 275]. In a recent study it was also found that NS4B dimerizes when expressed by itself *in vitro*, much like WNV's NS4B. The region between pTMD3 and pTMD4, also called a cytosolic loop, is possibly the region of contact between monomers during dimerization [276].

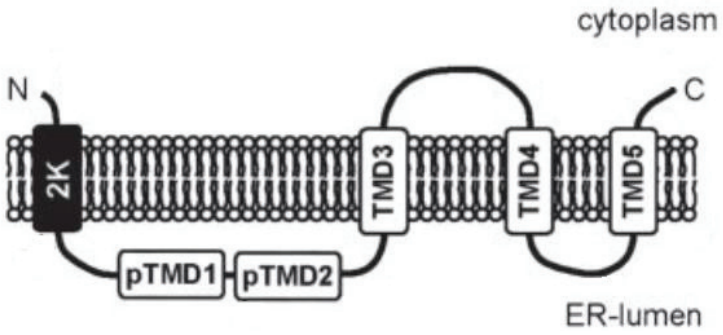

Figure 28 . Membrane topology model of NS4B according to Miller and colleagues. Three transmembrane domains would compose the C-terminal domains and two N-terminal membranes would not be in contact with the membrane.

2.7. DENGUE VIRUS THERAPEUTICS

Control and management of DENV infections is mainly of a prophylactic nature and is carried out by employing three main strategies: control and/or extermination of mosquito populations, clinical management of DENV infection symptoms and the specific targeting of the virus, either through the use of antiviral drugs or relying on vaccination [277]. Nowadays, the most developed, cost-effective and widely applied of those three strategies is the control of mosquito populations [55, 278]. This is achieved by a multitude of actions: eliminating stagnant water reservoirs and avoiding rivers and lakes (known mosquito breeding grounds), use of protective clothing and mosquito nettings, use of mosquito repellents and insecticides [279]. Other ideas have come to light in recent years such as the use of flightless mosquito females that are easy targets for predators and cannot take part in the normal courting processes [280], release of sterile males into the environment [281] and introduction of *Wolbachia Pipientis*, a

parasite that reduces the lifespan of fruit flies and can also affect mosquitoes [282]. Clinical management of DHF and DSS is highly dependent on the quality of medical facilities that is subpar in many Dengue endemic countries in the tropics and subtropics. Treatment of DENV infections is of course a last resort and is certainly not a preventive measure; therefore other strategies have to be envisaged to counter this pathogen and its infection [277, 279, 283].

Antiviral drugs and vaccines are being developed to target several steps of the viral cycle by specifically inhibiting the function of structural and non-structural proteins. Some groups have made significant advances in the development of antiviral drugs addressing structural proteins. At the entry level three candidate regions for inhibitor development have been described for the E protein: a β-OG binding pocket buried in the hinge between domains I and II that has to be free if the hinge motion associated with the fusion process is to be achieved [284, 285], two pockets accessible when E homodimers lie flat against the surface of the viral particle [283] and critical regions in the fusion active trimer E that have been targeted with peptides and monoclonal antibodies like HM14c10 [286] which bind specifically to those regions, thus thwarting its conformational changes of vital importance for a proper viral infection [231, 287, 288]. Other strategies to prevent viral binding to cell receptors are being developed although, considering the inexistence of a specific DENV receptor, the complexity of this approach is considerable. Peptides derived from membrane active regions and the stem region of the E protein [288, 289] have been used to inhibit DENV and in the former case, when that peptide was ministered to cells previous to DENV infection, viral particles lacking the genome were produced [290, 291]. RNA interference strategies have been used with mild effects, possibly due to the inaccessibility of the replication complex, safely hidden in ER-derived membranous structures [283]. The majority of antiviral drugs have been engineered against the viral exclusive enzymes NS3 and NS5, a strategy that has proven fruitful in other viruses like HIV-1 [292] or HCV [293]. Both high throughput screening (HTS) of antiviral compounds and the development of peptidomimetic compounds have been employed to discover novel inhibitors of the NS2B/NS3 protease active site [294, 295]. Nucleoside (tide) inhibitors like NITD008 (an adenosine analogue) have been shown to inhibit DENV *in vitro et vivo* [296]. Pockets found on NS5 are candidate regions for HTS of compound libraries [297]. Ribavirin, a broad spectrum antiviral used to counter HCV infection had a

cytostatic effect on DENV infected cells and proved ineffective in animal models [283]. Short anti-sense peptide conjugated oligomers called phosphorodiamidate morpholino oligomers (P-PMOs) that form short duplexes that bind to RNA have been used with success to inhibit translation and consequently reduce viral output of DENV2 by 95% [298-300]. Xie and collaborators have found an inhibitor that possibly targets the interaction between NS4B and NS3 and specifically inhibits DENV infection of all four serotypes [260, 275]. It is known that the glycosylation of several DENV proteins is crucial for the viral infection and production [79, 301]. Celgosivir, a clinically approved drug that prevents glycosylation of several proteins, has been used to prevent NS1 glycosylation, resulting in the improvement of the survival rate DENV infected mice [302]. Both HTS of compound libraries and peptidomimetic compounds are proving invaluable in the discovery of novel antiviral compounds [303].

Finally, vaccine development for DENV is not as straightforward as initially thought when vaccines for YFV and JEV were developed. This is mainly due to the fact that although YFV and JEV vaccines merely required monovalent formulations, a safe and effective DENV vaccine requires tetravalent formulations due to cross reactivity and ADE of DENV infection [304]. The first approach to vaccine development relied on classical live attenuated vaccines (one licensed to Sanofi Pasteur [305] and the other to GlaxoSmithKline [306]) that induced high seroconversion rates when monovalent formulations were used yet, unfortunately, were not so effective with tetravalent formulations, owing to the aforementioned interference between serotypes. These vaccines were put on hold. Chimeric vaccines are also being studied, of which the following are examples: one composed of a YFV-17D backbone with its prM/E genes substituted by those of DENV (ChimeriVax [307]) that has reached phase III clinical trials, another made up of a DENV2-strain backbone with prM/E genes of other serotypes (DENVax [308]) or vaccines with nucleotide deletions [309] induce high levels of seroconversion that are maintained in tetravalent formulations. These vaccines are still undergoing clinical trials. Other types of vaccines like protein vaccines e.g. one with a subunit of prM and 80% of E protein [310], and DNA vaccines with plasmids encoding prM/E genes of all four serotypes are promising candidates having completed phase I clinical trials [311].

CHAPTER 2 . METHODOLOGY

CHAPTER 2. METHODOLOGY

1. MEMBRANE MODEL SYSTEMS

Lipid amphyphilic molecules dispersed in aqueous medium arrange spontaneously in a multitude of structures, one of which is the enclosed lipid bilayer or liposome. These liposomes are generally acknowledged as important simple models of membranes that can be used to transport and deliver drugs or other compounds and they can be formed using a customized mixture of lipids in order to study specific interactions between lipids or between a given lipid and proteins. Bangham and his collaborators [8, 312, 313] found that liposomes were enclosed membrane systems, using electron microscopy. This discovery marked the beginning of the general use of liposomes in basic and applied science, from permeability studies of membranes with different lipid composition and substances to characterization of physic and chemical properties of lipids and interactions between these and other molecules such as proteins. Techniques such as electron-spin resonance (ESR), nuclear magnetic resonance (NMR), differential scanning calorimetry (DSC), infrared spectroscopy (IR spectroscopy) or fluorescence spectroscopy studies have been employed to attest the aforementioned properties. Liposomes can be grouped according to their size and morphology [314, 315].

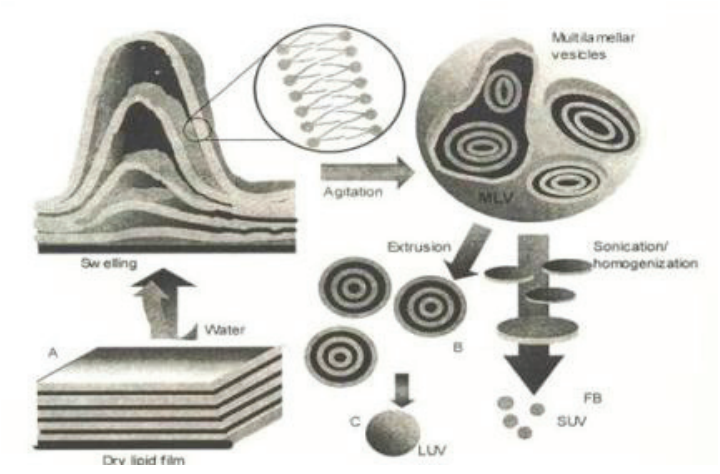

Figure 29 . Different types of liposomes, with methods for obtaining them (Adapted from[316]).

There are several types of liposomes (Figure 29):

- Multilamellar Large Vesicles or MLV: These are the easiest structures to obtain, requiring only agitation following hydration. Organized in concentric lipid bilayers, with diameter ranging from 100 to 5000 nm and 7 to 10 internal concentric lamellae (lipid bilayers);
- Small Unilamellar Vesicles or SUV: Composed of a single lipid bilayer, with diameter between 20 and 50 nm. Ultrasonication of MLV originates SUV;
- Large Unilamellar Vesicles or LUV: Composed of a single lipid bilayer, with a diameter range of 50-500 nm. Detergent dialysis, extrusion with French press or polycarbonate filters, Ca^{2+} induced SUV fusion or reverse evaporation of organic solvent are methods applied to obtain LUV;
- Giant Unilamellar Vesicles or GUV: The largest of all unilamellar vesicles, with diameter as large as 300 μm;

MLV's are used for industrial applications such as drug delivery. Its application as model for lipid interaction with external agents is limited, since only a small percentage (10-15%) of all phospholipids are in the outermost bilayer. Both SUV's and LUV's are well characterized and widely applied membrane model systems [317]. Apart from size, the lipid distribution in both monolayers (external and internal) of LUVs and SUVs is quite different. In LUV's with approximately 95 nm in diameter, the lipid distribution is quasi-symmetric according to the study by Mayer and collaborators [29] and according to Butko and co-workers [318], approximately 54% of lipids are localized in the external membrane and 46% in the internal membrane. In the other hand, the small curvature radius of SUV's confers a different lipid distribution, with about 60-70% of lipid molecules on the external membrane [319]. The different lipid distribution in the bilayer confers specific properties to liposomes: the lipid packing in external and internal monolayer is different; if the temperature is maintained below their transition temperature (T_m), lipid molecules are more organized in MLV's and LUV's than in SUV's; the lowering of the lateral mobility and miscibility of lipids contributes to the formation of lipid rafts with different composition on the same membrane, even above the transition temperature [320]. LUVs present more advantages than SUVs for application in biophysical studies.

The hydrophobic moments measure the periodicity of residue distribution along a secondary-structure element [321] and were calculated according to Eisenberg *et al.* [322, 323]. Hydrophobicity scales (experimentally determined transfer free-energies of amino acids) are important to infer the energetics of protein-bilayer interactions. Two practical scales, considering peptide bonds contribution, are used: one related to the transfer of unfolded chains from water to bilayer interface – interfaciality values – and one for the transfer of folded chains into the hydrocarbon interior – hydrophobicity values. These values were obtained from [27, 324]. The bidimensional charts of all these values (hydrophobic moments, hydrophobicity and interfaciality) were disposed in a seven amino acid frame, accounting for the spatial arrangement of amino acids assuming a α-helix secondary structure [321, 325, 326] as depicted in Figure 30.

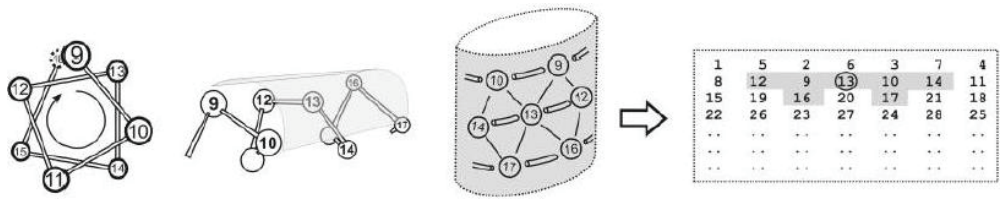

Figure 30 . Depiction of the arrangement of the amino acid sequence into an α-helix secondary structure. To the left lies the actual organization of the amino acids into a bidimensional map. Each number represents one amino acid (Adapted from [321]).

Each position on the bidimensional chart that is not associated to an amino acid value (hydrophobicity moment, hydrophobicity or interfaciality value) represents the average value of the neighbouring values. A positive value represents a positive transfer free-energy and the larger it is, the higher is the probability for an interaction between protein or peptide and interface or hydrophobic core of the bilayer to occur [327, 328].

3. FLUORESCENCE SPECTROSCOPY

Following excitation to higher energy levels, a molecule has a tendency to return to its fundamental, with the lowest energy state. The energy involved in such phenomenon can be dissipated in many forms, being one of them through the emission of light. At low temperatures, this light emission is called luminescence and if it occurs at high temperatures it is called incandescence. Photoluminescence is a type of luminescence caused by re-radiation of photons following previous photon absorption. It can be divided into two categories: fluorescence, when the re-radiated photons present lower energy than those absorbed and phosphorescence when light emission persists after removal of excitation source. Molecules present different main energy levels for electrons, defined by quantum mechanics. In each main level there are different vibrational and rotational levels. In the case of fluorescence, upon absorbing a photon, the molecule can be excited, that is, electrons of the molecule reach higher energy levels. On returning to the fundamental energy level, electrons can occupy different vibrational levels, producing photons with different energies (Figure 31). Therefore, if a set of molecules is excited with a radiation of constant frequency (therefore energy), they all emit photons at different frequencies. These frequencies arrange to form the fluorescence emission spectra. If only one type of molecule is present in the medium to be excited, the obtained spectrum is an excitation spectrum. For a molecule to absorb a photon, it has to have a chromophore, a certain region capable of absorbing the energy correspondent to the photon, for instance the resonance system formed by successive, alternate, simple and double bonds in certain molecules. Moreover, the same molecule must present a region responsible for the emission of a photon (called fluorophore), for instance, certain amino acids in proteins (tryptophan, tyrosine or phenylalanine). Fluorophores can be extrinsic or intrinsic whether they are not part of the molecule (molecular probes for example) or part of it (as said before, amino acids of molecules). For the fluorescence study of proteins, lipids, their interactions and biophysical properties, both extrinsic and intrinsic fluorophores are important: fluorescent probes such as (5) – carboxyfluorescein (CF) are an example of those and protein amino acids like tryptophan are an example of these. There are several methods for the biophysical characterization of lipids, proteins and their interactions that employ fluorescence, such as membrane leakage, hemi fusion and fusion studies. In membrane leakage, a probe is

encapsulated into a liposome and the interactions between a protein (or peptide) and liposomes is evaluated through the variation in fluorescence of the sample; if it rises, the concentration of probe outside the liposome is higher, being a direct measure of membrane leakage of vesicle contents.

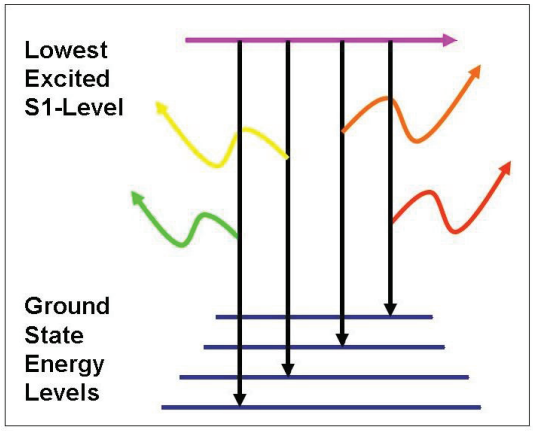

Figure 31 . A fluorescent process. Depending on the ground level that the previously excited electron reaches, the emitted photon has different frequencies. In the figure, the frequencies of the emitted photons are all on the visible region of the spectra.

Based on this phenomenon, a wide array of techniques has been used to study different biomolecular interactions and processes, of which the ones used in the context of this thesis, will be addressed.

3.1. STEADY-STATE FLUORESCENCE ANISOTROPY

Fluorophores absorb preferentially photons with an electric vector parallel to their dipole transition moment and emit fluorescence polarized along that same dipole transition moment. Any given fluorophore population can be photoselectively excited and the speed of rotation of a fluorophore while in an excited state determines its polarization or anisotropy. This measure has been extensively used to determine viscoelastic properties of lipid membranes, protein volumes, peptide insertion into bilayers and many other important variables. In this thesis, this technique was used to assess the effect of selected peptides on the thermotropic properties of membranes. A fluorescent probe 1,6-diphenyl-1,3,5-hexatriene (DPH) and its derivative 1-(4-

trimethylammoniumphenyl)-6-fenil-1, 3, 5-hexatriene (TMA-DPH) were considered. This molecule has properties that render it very interesting for studies of peptide location in the lipid palisade: (a) it is a highly hydrophobic molecule therefore it is expected to be confined to the depths of the hydrophobic core, (b) it has about 14 Å in length, less than half the average membrane length of 30 Å, (c) it has a rod-like shape, ideal for a tight packaging in the lipid palisade. Furthermore, its derivative TMA-DPH is less hydrophobic and locates closer to the interphase (DPH is 8 to 11 Å away from the hydrophobic core and TMA-DPH about 19 Å), therefore the localization of a peptide in the membrane can be further resolved [329, 330].

3.2. MEASUREMENTS OF SURFACE ELECTROSTATIC POTENTIAL

There are three types of electrostatic potentials in membranes: surface electrostatic potential (Ψ_S), dipole potential (Φ_d) and transmembrane potential ($\Delta\Psi$) (Figure 32). Surface electrostatic potential is the result of the lipid water interphase, rich in charged molecules, e.g. water, the polar head groups of negatively charged lipids (PS, PG, PI, PA) their counter-ions and molecules with carbohydrate moieties. These charges at the surface of the membrane can also be the result of inhomogeneous adsorption of water molecules at the membrane surface. This charged layer that goes from the surface of the membrane to the water moiety is about 20 nm thick [331].Ψ_S affects ionic distribution in the aqueous phase mainly because of the attraction between counter-ions and charged molecules and repulsion of co-ions. The Gouy-Chapman model is valid and has provided theoretical support to predict membrane electrostatic potential [331-333]. It assumes four conditions: (a) charges are uniformly distributed at the membrane surface, therefore there is a surface charge density (membrane charges cannot be considered points), (b) ions in solution are zero dimension particles, (c) repulsion between mobile ions is not considered, (d) the dielectric constant of the aqueous phase is the same up until the membrane surface. Combining the Bolzmann equation in logarithm form and the Henderson-Hasselbach equation, the following equation is obtained: $pK_S = pK_B + \Psi_S$. This equation shows the relationship between the electrostatic surface potential and the acidity of the medium around the surface of the membrane. It also shows that the

proton concentration at the surface of the membrane is different than that of the aqueous medium. There are pH sensitive fluorescent probes, such as fluorescein-phosphatidylethanolamine (FPE) that can be used to detect variations in the electrostatic surface potential if the aqueous medium is maintained at a constant pH (changes in its protonation state result in changes to its fluorescence emission properties). These changes in fluorescence can be used as an indirect measure of the binding of charged particles to the membrane surface [334, 335].

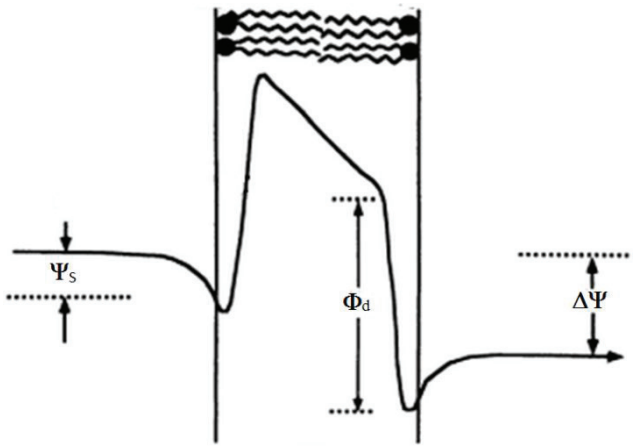

Figure 32 . Energy profile of the interaction of a particle with the membrane. Inhomogeneous distribution of charge at the surface of the membrane (due to proteins, lipids and other charged molecules) produces a surface electrostatic potential (Ψ_S). The bilayer produces a high internal dipole potential (Φ_d), responsible for the positive potential of the hydrophobic core with respect to the aqueous medium. Charge separation between leaflets produces a transmembrane electrostatic potential ($\Delta\Psi$). Adapted from [336].

4. DIFFERENTIAL SCANNING CALORIMETRY

One of the most used and trustworthy techniques to analyse thermotropic behaviour of macromolecules [337-341] is differential scanning calorimetry (DSC). It relies on the fact that different samples and molecules have characteristic thermotropic behaviour when heated/cooled. Registering the deviations in apparent heat capacity (C_p) with varying temperature will yield the thermograms for a given sample. Nowadays, differential (because they measure the difference of heat capacity between a sample and a reference cell) scanning calorimeters are commonplace. Both cells are contained in an adiabatic container (Figure 33) and connected to a highly sensitive thermocouple that

measures the temperature difference between them. Each cell is connected to a resistor. Because the sample and its corresponding reference (usually the buffer in which the sample is prepared) have different heat capacities, thermal power is provided to the resistor of the coldest cell to adjust for different temperatures. If the experiment is performed at a constant rate of temperature change, the communicated thermal power (variable measured by the instrument) is proportional to the difference in heat capacity of both cells [342].

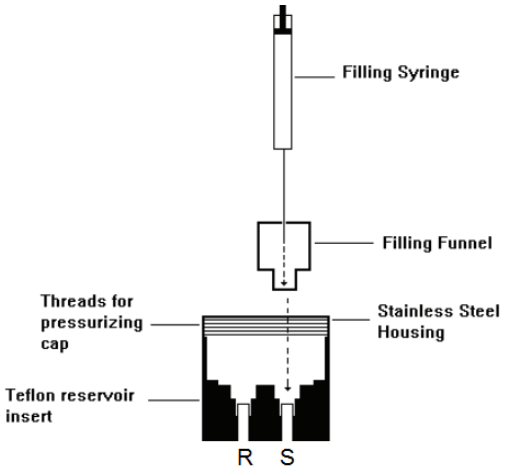

Figure 33 . Typical arrangement of the reference and sample cells in a differential scanning calorimeter.

In a well-defined system, all the thermodynamic quantities (ΔH, ΔS, ΔG and ΔCp and T_m) associated to a temperature induced transition can be derived from a thermogram and thermodynamic equations (Figure 34). As it was said in a previous section, lipid phases depend on a variety of factors, including temperature. In the specific case of lipids, each phase transition in a pure lipid will have an associated peak in the thermogram, directly related to the change in hydrocarbon chain order. Of all lipid phase transitions studied in aqueous medium (temperatures range from 0 to 100 ºC), the gel to liquid-crystalline phase transition has the largest entropy change, hence the most intense peak in the thermogram [343]. By comparing pure lipid samples with and without other molecules such as peptides it is possible to infer the effect the latter might have on the former.

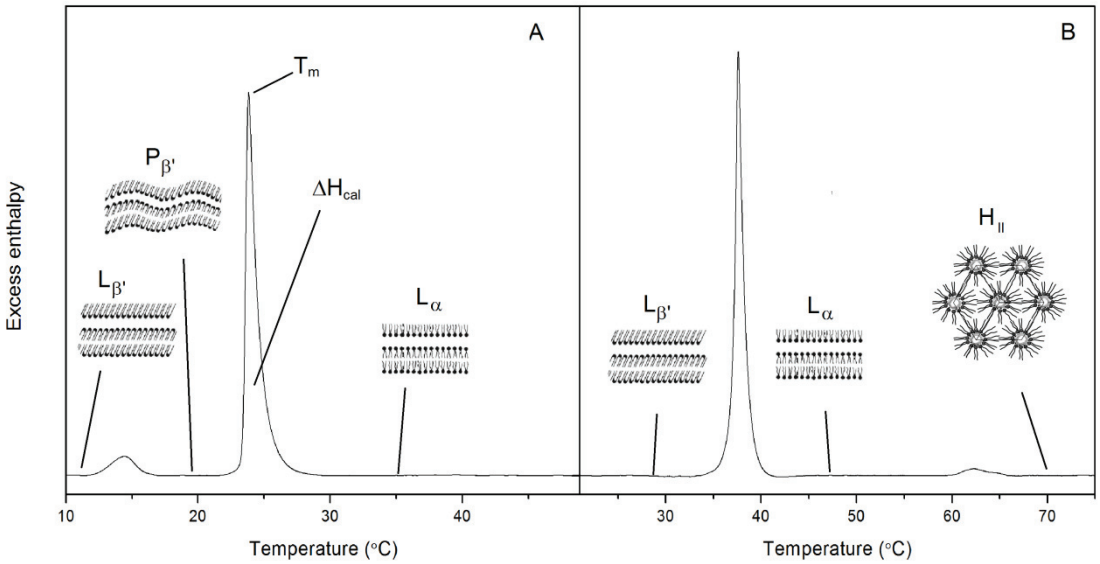

Figure 34 . Thermograms of (A) DMPC and (B) DEPE. Two thermodynamic parameters are shown in graphic A, ΔHcal of the main transition (the area below that section) and T_m (the temperature of the maximum excess enthalpy). Furthermore, typical transitions of these lipids are clearly visible and illustrated by insets.

5. FOURIER TRANSFORM INFRARED (FTIR) SPECTROSCOPY

Infrared spectroscopy measures the transitions between vibrational states in the same electronic energy level resulting from absorption of infrared radiation. These vibrational levels correspond to certain intra-molecular movements, e.g. symmetrical and antisymmetrical stretching, scissoring, rocking, wagging and twisting of functional groups. These movements occur in an ultra-fast timescale (~$10^{13}s^{-1}$). In the study of proteins and peptides in membranes it has advantages over the other techniques. For example, unlike X-ray crystallography, it does not require crystals that are extremely difficult to obtain with protein lipid complexes, samples with high turbidity (important when dealing with optically abstruse lipid suspensions) can be analysed with IR spectroscopy without loss of signal to noise ratio (SNR) and minute quantities (when compared to X-ray crystallography and NMR) are needed (~150 μg) [344, 345] to account for an acceptable SNR.

Infrared spectroscopy provides important information with respect to peptide/protein-lipid interaction:

- Minute quantities (~150 μg) of sample are required to obtain a good SNR;
- No probes (that could affect the system) are required to obtain IR spectra;
- There is no molecular size limit (NMR techniques are useful to study proteins with only a few kDa);
- Samples can be in virtually any physical state;
- In a single IR experiment, structural information for both proteins and lipids can be obtained.

This technique has been used since 1952 [346] to study protein structure, yet only with the advent of instrumentation based on the Michelson interferometer and data analysis based on the Fourier transform (both enhanced the signal to noise ratio of the technique and most importantly, improved the subtraction of H_2O signal) did it become, along with X-ray crystallography and nuclear magnetic resonance (NMR), a major experimental technique for structural studies. The transmission intensity for every position of the reflecting components (mirrors) is measured and the Fourier transform is applied (fast Fourier transform or FFT is the algorithm used) to that set of data. After appropriate phase correction and data apodization, a spectrum of intensity versus wavenumber (cm^{-1}) is obtained. The low resolution of this technique means that in the frequency (or the equivalent wavenumber) spectrum of IR, functional groups of both lipids and proteins appear as bands rather than sharp and easily distinguishable peaks. There are several transformations that can be applied to every set of IR data in order to enhance resolution: taking derivatives, applying a Fourier self-deconvolution and fine-structure enhancement, of which the two initial ones are the most commonly used [347-349]. In protein IR spectra, the functional group that has the most useful set of bands, from which the most interesting information can be extracted, is the amide group of the peptide bond. The amide bands visible in the spectrum are assigned to several of the previously described vibrational movements [350, 351] described and are summarized in Table 3.

Table 3 . Characteristic amide bands associated to the peptide bond [352].

Symmetry	Designation of the band		Wavenumber (cm^{-1})
Planar	Amide	A	3300
		B	3100
		I	1650
		II	1550
		III	1300
Off-plane		IV	625
		V	725
		VI	600
		VII	200

Amide I and Amide II are the most commonly used bands in literature, especially the former, owing to its higher intensity and conformational stability and relative immunity to interference from lateral chains. Amide I vibrational modes are a result of the coupling of C=O stretching and the flexion of both N-H and C-N bonds. All together, these modes are visible in the region between 1600 and 1700 cm^{-1}. These three groups form hydrogen bonds and are thus affected by protein conformation changes and the coupling of transitory dipoles (dependent on the orientation and distance between them) induces changes in the Amide I band. This means the relative spatial orientation of peptide groups can be discerned (up to a certain degree) with IR spectroscopy). Each secondary structure component contributes with a peak to the overall Amide I band, yet the width of each peak is usually larger than the distance between each peak's maximum. This would otherwise hinder any further extraction of information were it not for the aforementioned mathematical techniques developed by several groups [347, 349, 351]. In FTIR experiments, it is important to highlight that H_2O strongly absorbs infrared radiation of some 1650 cm^{-1}, exactly in the Amide I band. This requires the use of D_2O that absorbs at some 2500 cm^{-1}, leaving the Amide I region unscathed. Using theoretical calculations [353] and IR experiments with homopeptides [354, 355], several secondary structures have been assigned to specific regions in the IR spectra (Table 4). Amide modes in H_2O are referred to as Amide I, II, III and so forth whereas Amide modes in D_2O have a prime attached to it: Amide I', II', III' and so on.

Table 4 . Representative secondary structure assignments in Amide I and I' bands.

Secondary structure	Amide I/I' wavenumber (cm^{-1})
α helix	1648/1660
3_{10} helix	1660/1668
Unordered structures	1640/1648
β loops	1660/1685
Intramolecular β sheet	1680/1690 1630/1640
Intermolecular β sheet	1670/1695 1610/1625

As for lipids (especially phospholipids), there are three important vibrational modes discernible by FTIR spectroscopy; those corresponding to acyl chains, interfacial region and polar heads [352]. The first are a result of CH, CH_2 and CH_3's stretching modes, which give rise to one band for CH at 3012 cm^{-1} and two bands per each of the other functional groups, one symmetrical and one antisymmetrical, centred respectively at 2850 cm^{-1} and 2929 cm^{-1} for CH_2, at 2870 cm^{-1} and 2956 cm^{-1} for CH_3. These groups are highly sensitive to the ratio of trans- and gauche-isomers and therefore are of marked importance when studying phase transitions of lipids. Additionally if these groups are deuterated, these bands shift to the 2000-2300 cm^{-1} region, meaning that deuterated and undeuterated lipids can be used simultaneously and their phase behaviour in the presence of other molecules (such as peptides) assessed independently. The stretching band of C=O at 1700-1750 cm^{-1} is also commonly used, since C=O forms hydrogen bonds and is therefore a good probe of intermolecular interactions at the interface of a membrane. This band is composed of two bands at 1728 cm^{-1} and 1742 cm^{-1} (lipids that take part in hydrogen bonding and lipids that are not forming hydrogen bonds) that usually vary in intensity (not frequency/wavenumber) according to the environment it is inserted in, altering the frequency of the overall band (sum of the two). The phosphate group bands, located at 1220 cm^{-1} and 1240 cm^{-1} are also frequently used to assess electrostatic interactions and hydration (the former corresponds to hydrated phosphate groups and the latter to dehydrated phosphate groups).

CHAPTER 3 . WORK PLAN AND OBJECTIVES

CHAPTER 3. WORK PLAN AND OBJECTIVES

1. Biophysical characterization of membrane active regions of structural proteins C, prM and E and non-structural proteins NS2A, NS4A and NS4B.

In order to better understand the mechanisms by which these proteins interact and affect membranes and modulate their polymorphism we sought to characterize which regions of these proteins would affect membranes resorting to peptide libraries encompassing the full length of these proteins and model membrane systems with different compositions. For this topic we followed the under described steps:

- Highlighting possible interfacial or transmembrane segments by using published values of free energies of water-to-bilayer and water to interface transfer of amino acid residues and resorting to our own methodology in order to highlight hydrophobic and interfacial regions.
- Effect of those peptides on the rupture of membrane model systems by using fluorescence spectroscopy.
- Study of the effect those peptides have on the thermotropic and structural properties of membranes recurring to differential scanning calorimetry (DSC) and Fourier-transform infrared spectroscopy (FTIR).
- Characterization of the relative location of peptides in membranes recurring to steady state fluorescence anisotropy measurements of DPH and its derivatives.
- Elucidation of the secondary structure of peptides in the absence and presence of lipid membranes using Fourier-transform infrared spectroscopy (FTIR).

These studies were performed with a battery of different lipid compositions and gave rise to four different publications, of which two have been accepted (P1 and P2) while the other two (P4 and P5) have been sent to scientific journals (they are designated by their order in the Prefacio section).

P1. *The membrane-active regions of the dengue virus proteins C and E.* Henrique Nemésio, Francis Palomares-Jerez, José Villalaín. Biochimica et Biophysica Acta (BBA): Biomembranes, 1808:10 (2011), *pp.2390-2402*. **DOI:** 10.1016/j.bbamem.2011.06.019

P3. *NS4A and NS4B from dengue virus: Membranotropic regions.* Henrique Nemésio, Francis Palomares-Jerez, José Villalaín. Biochimica et Biophysica Acta (BBA): Biomembranes, 1818:11 (2012), *pp. 2818-2830*. **DOI:** 10.1016/j.bbamem.2012.06.022

P4. *Membranotropic regions of dengue virus prM protein.* Henrique Nemésio, José Villalaín. Sent to Biochemistry

P5. *Membrane interacting regions of dengue virus NS2A protein.* Henrique Nemésio, José Villalaín. Sent to the Journal of Physical Chemistry B.

2. **Biophysical characterization of DENV2$_{C6}$, a peptide derived from the capsid protein of Dengue virus**

From the first set of experiments, a membrane active segment from protein C had dramatic effects on membranes, especially on membrane rupture, independent of lipid composition. This peptide was thus selected to be subjected to thorough biophysical characterization (techniques are in parenthesis), from its effect on membrane rupture (fluorescence spectroscopy with measurements of encapsulated CF and dextrans), thermotropic properties of membranes (differential scanning calorimetry and infrared spectroscopy), as well as its partition and localization in membranes (fluorescence spectroscopy measurements of FPE-labelled membranes and DPH derivatives) and its secondary structure in membranes. This study resulted in the publication of a scientific article:

P2. *Hydrophobic segment of dengue virus C protein. Interaction with model membranes*. Henrique Nemésio, M. Francisca Palomares-Jerez, José Villalaín. Molecular Membrane Biology, 30:4 (2013), *pp. 273-287*. **DOI:** 10.3109/09687688.2013.805835

CHAPTER 4 . ANNEX OF PUBLICATIONS

1. FIRST PUBLICATION (ACCEPTED)

The membrane-active regions of the dengue virus proteins C and E.

Henrique Nemésio, Francis Palomares-Jerez, José Villalaín

Instituto de Biología Molecular y Celular, Universidad Miguel Hernández, E-03202 Elche (Alicante), Spain

Biochimica et Biophysica Acta 1808:10 (2011) 2390-2402

DOI: 10.1016/j.bbamem.2011.06.019

Biochimica et Biophysica Acta 1808 (2011) 2390–2402

Contents lists available at ScienceDirect

Biochimica et Biophysica Acta

journal homepage: www.elsevier.com/locate/bbamem

The membrane-active regions of the dengue virus proteins C and E

Henrique Nemésio, Francis Palomares-Jerez, José Villalaín *

Instituto de Biología Molecular y Celular, Universidad "Miguel Hernández", E-03202 Elche-Alicante, Spain

ARTICLE INFO

Article history:
Received 4 May 2011
Received in revised form 23 June 2011
Accepted 28 June 2011
Available online xxxx

Keywords:
C/E dengue proteins
Dengue
Virus–cell entry
Membrane fusion
DENV

ABSTRACT

We have identified the membranotropic regions of proteins C and E of DENV virus by performing an exhaustive study of membrane rupture induced by two C and E-derived peptide libraries on model membranes having different phospholipid compositions as well as its ability to modulate the DEPE L_β–L_α and L_α–H_{II} phospholipid phase transitions. Protein C presents one hydrophobic leakage-prone region coincidental with a proposed membrane interacting domain, whereas protein E presents five membrane-rupture zones coincidental with different significant zones of the protein, i.e., the fusion peptide, a proline-rich sequence, a sequence containing a hydrophobic pocket as well as the stem and transmembrane domains of the protein. The identification of these membrane-active segments supports their role in viral membrane fusion, formation of the replication complex and morphogenesis and therefore attractive targets for development of new anti-viral compounds.

1. Introduction

Dengue virus (DENV) is a member of the family *Flaviviridae* in the genus *Flavivirus*. DENV is the leading cause of arboviral diseases in the tropical and subtropical regions, affecting more than 70 million people each year [1]. DENV comprises four serologically and genetically related viruses, DENV viruses 1–4, which possess 69–78% identity at the amino acid level [2]. DENV infections might be either asymptomatic or result in what is known as dengue fever; some individuals develop a severe and potentially life-threatening disease known as dengue hemorrhagic fever or dengue shock syndrome, leading to more than 25,000 deaths per year. Despite the urgent medical need and considerable efforts, no antivirals or vaccines against DENV virus are currently available, so that more than 2 billion people, mainly in poor countries, are at risk in the world [3]. DENV is a positive-sense, single-stranded RNA virus with a single open reading frame encoding a polyprotein, which is subsequently cleaved by cellular and viral proteases into three structural proteins, C, prM and E, and seven nonstructural (NS) proteins, NS1, NS2A, NS2B, NS3, NS4A, NS4B and NS5 [4] (Fig. 1A). Similarly to other enveloped viruses, the DENV virus enters the cells through receptor mediated endocytosis [4–7] and rearranges cell internal membranes to establish specific sites of replication [8–10]. Details about DENV replication process remain largely unclear, but most, if not all of the DENV proteins, are involved and function in a complex web of protein–protein interactions. The mature DENV virus has a capsid (C) protein core complexed with the RNA genome, surrounded by a host-derived lipid bilayer in which multiple copies of the viral envelope (E) and membrane (M) proteins are embedded.

The C proteins of *Flaviviridae* are dimeric, basic, have an overall helical fold and are responsible for genome packaging. Protein C seems also to associate with intracellular membranes through a conserved hydrophobic domain [11]. Recently, it has been found that protein C accumulates around endoplasmic reticulum (ER) derived lipid droplets [12]. Similarly to other enveloped viruses, DENV replicates its genome in a membrane-associated replication complex, and morphogenesis and virion budding has been suggested to take place in the ER or modified ER membranes. These modified membranes could provide a platform for capsid formation during viral assembly [12]. Although *Flaviviridae* C proteins are shorter than the *Hepacivirus* core proteins, their roles should be similar as well as their capacity to bind to phospholipid membranes [13–15].

The DENV E protein is a class II fusion protein, essential for attachment, membrane fusion, and assembly. The three-dimensional structure of class I and class II membrane fusion proteins is different but their function is identical, so they must share structural and functional characteristics in specific domains which interact with and disrupt biological membranes [6,16]. A series of conformational changes occurring in the DENV E protein driven by the endosomal

Abbreviations: BMP, S,R-bis(monooleoylglycero)phosphate; BPI, Bovine brain L-α-phosphadidylinositol; BPS, Bovine brain L-α-phosphatidylserine; CF, 5-Carboxyfluorescein; CHOL, Cholesterol; CL, 1′,3′-bis[1,2-dimyristoyl-*sn*-glycero-3-phospho]-*sn*-glycerol; DENV, Dengue virus; DEPE, 1,2-Dielaidoyl-sn-glycero-3-phosphatidylethanolamine; DSC, Differential Scanning Calorimetry; EPA, Egg L-α-phosphatidic acid; EPC, Egg L-α-phosphatidylcholine; ER, Endoplasmic reticulum; ESM, Egg sphingomyelin; LUV, Large unilamellar vesicles; MLV, Multilamellar vesicles; NS, Non-structural protein; TFE, Trifluoroethanol; T_m, Temperature of the gel-to–liquid crystalline phase transition; TM, Transmembrane domain; TPE, Egg trans-esterified L-α-phosphatidylethanolamine

* Corresponding author. Tel.: +34 966 658 762; fax: +34 966 658 758.
E-mail address: jvillalain@umh.es (J. Villalaín).

0005-2736/$ – see front matter © 2011 Elsevier B.V. All rights reserved.
doi:10.1016/j.bbamem.2011.06.019

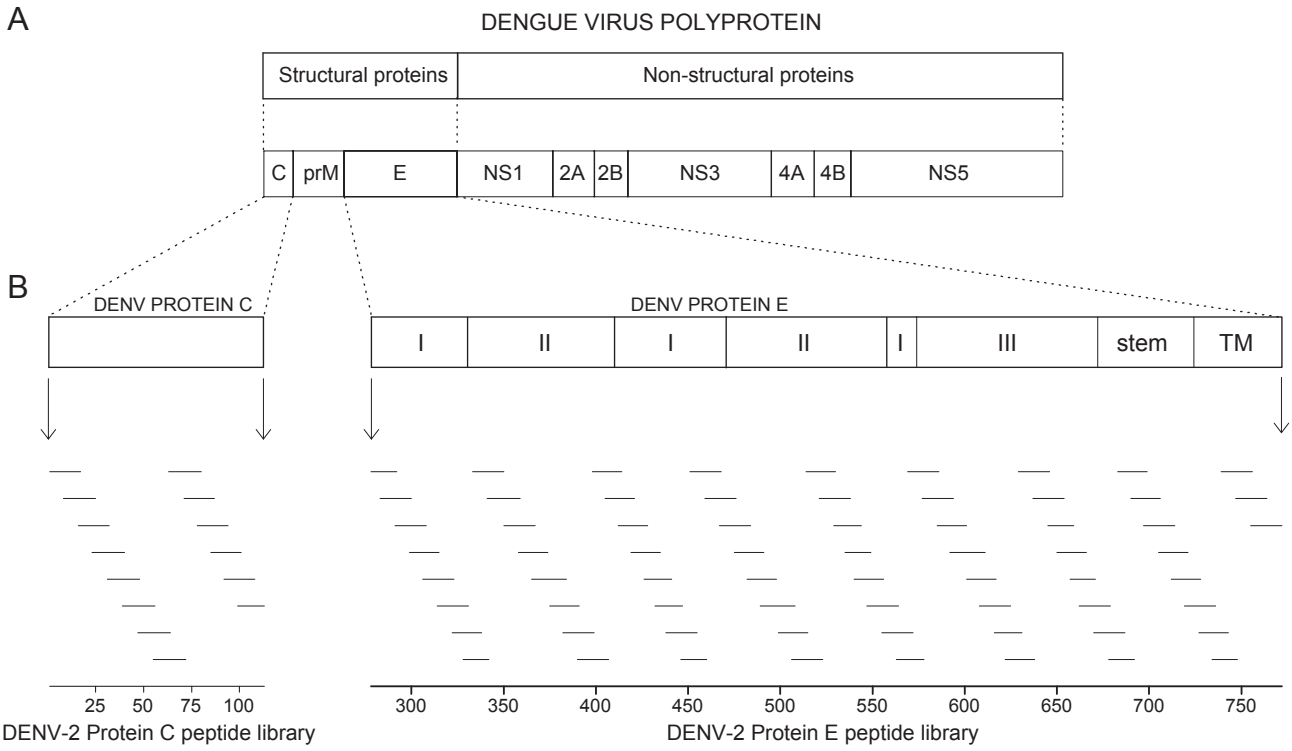

Fig. 1. (A) Scheme of the structure of the DENV virus structural (C, prM and E) and non-structural proteins (NS1, NS2A, NS2B, NS3, NS4A, NS4B and NS5), according to literature consensus. The approximate segments of domains I, II, III, the stem and the transmembrane anchor of E protein are depicted (see text for details). (B) The sequence and relative location of the peptide libraries derived from the Dengue Virus Type 2 NGC C (14 peptides) and E proteins (67 peptides) are shown with respect to the full sequence of both proteins. Peptide line length is related to the number of amino acids in the peptide. Maximum overlap between adjacent peptides is 11 amino acids.

low-pH gives place to the fusion of the viral and endosomal membranes [4,7]. The DENV E protein, being the first point of contact between the virus and the host cell, is a determinant of tropism and virulence, as well as the major target of DENV neutralizing and enhancing antibodies [7]. The N-terminal ectodomain of the protein presents three domains consisting predominantly of β-strands (amino acids 1 to 395, DENV2 numbering) [5,7]. The fusion loop of the E protein is located between amino acids 98 and 112 [17]. Two α-helices that link the soluble ectodomain and the two transmembrane domains of the E protein form a stem (amino acids 396 to 447) which contribute to the flexibility required for the conformational change [18]. Based on tick-borne encephalitis virus E protein, DENV E protein would have two transmembrane (TM) domains (amino acids 448 to 491) and both of them are required for assembly of E protein into particles; similarly, the two α-helices are implicated either in homo and/or in hetero protein–protein interaction or membrane interaction or both [19,20]. Interestingly, E protein might interact with other proteins through a conserved Pro-rich motif [21]. Significantly, the stem region of the E protein has been proposed to be engaged in the fusion process but the critical regions of the stem region involved are not known with certainty [4–6,22].

We have recently identified the membrane-active regions of a number of viral proteins by observing the effect of glycoprotein-derived peptide libraries on model membrane integrity [15,23–26]. These results allowed us to propose the location of different segments in these proteins that are implicated in either protein–lipid or protein–protein interactions and helped us to understand the mechanisms underlying the interaction between viral proteins and membranes. There are still many questions to be answered regarding the C and E mode of action in membrane fusion, assembly, replication and/or release during the DENV viral cycle. Segments of both C and E proteins have been used as vaccine candidates for DENV [27]. For example, domain III of the E protein can block the entry of the virus as well as peptides derived from the fusion loop can interfere with infectivity [28]. Additionally, DENV membrane interaction is an attractive target for anti-DENV therapy. To investigate the structural basis of the interaction of proteins C and D from DENV virus and identify new targets for searching new DENV inhibitors, we have carried out the analysis of the different regions of DENV C and E proteins which might interact with phospholipid membranes using a similar approach to that used before [26,29,30]. By monitoring the effect of these peptide libraries on membrane integrity we have identified different regions on DENV C and E proteins with membrane-interacting capabilities, suggesting the location of different segments implicated in oligomerization (protein–protein binding) and membrane interaction and destabilization. These results should help in our understanding of the molecular mechanism of viral fusion and morphogenesis as well as making possible the future development of DENV entry inhibitors which may lead to new vaccine strategies.

2. Materials and methods

2.1. Materials and reagents

Two sets of 14 (Table 1) and 67 (Table 2) peptides derived from Dengue Virus Type 2 NGC C and E proteins were obtained through BEI Resources, National Institute of Allergy and Infectious Diseases, Manassas, VA, USA. Peptides were solubilized in water/TFE at 70:30 ratios (v/v). Bovine brain phosphatidylserine (BPS), S,R-bis(monooleoylglycero)phosphate ammonium salt (BMP), bovine liver L-α-phosphatidylinositol (BPI), cholesterol (CHOL), egg phosphatidic acid (EPA), egg L-α-phosphatidylcholine (EPC), egg sphingomyelin (ESM), egg trans-esterified L-α-phosphatidylethanolamine (TPE), 1′,3′-bis[1,2-dimyristoyl-*sn*-glycero-3-phospho]-*sn*-glycerol (cardiolipin, CL), dielaidoyl-sn-glycero-3-

Table 1
Sequences of the peptides pertaining to the DENV C protein derived peptide library.

Order	No. aa	Sequence
1	17	NNQRKKARNTPFNMLKR
2	18	RNTPFNMLKRERNRVSTV
3	17	KRERNRVSTVQQLTKRF
4	18	STVQQLTKRFSLGMLQGR
5	18	RFSLGMLQGRGPLKLFMA
6	18	GRGPLKLFMALVAFLRFL
7	18	MALVAFLRFLTIPPTAGI
8	18	FLTIPPTAGILKRWGTIK
9	18	GILKRWGTIKKSKAINVL
10	17	IKKSKAINVLRGFRKEI
11	17	NVLRGFRKEIGRMLNIL
12	17	KEIGRMLNILNRRRRTA
13	17	NILNRRRRTAGMIIMLI
14	15	RTAGMIIMLIPTVMA

Table 2
Sequences of the peptides pertaining to the DENV E protein derived peptide library.

Order	No. aa	Sequence
1	15	MRCIGISNRDFVEGV
2	18	ISNRDFVEGVSGGSWVDI
3	18	GVSGGSWVDIVLEHGSCV
4	17	DIVLEHGSCVTTMAKNK
5	18	SCVTTMAKNKPTLDFELI
6	18	NKPTLDFELIKTEAKQPA
7	17	LIKTEAKQPATLRKYCI
8	15	KQPATLRKYCIEAKL
9	18	LRKYCIEAKLTNTTTDSR
10	19	KLTNTTTDSRCPTQGEPTL
11	18	RCPTQGEPTLNEEQDKRF
12	17	TLNEEQDKRFVCKHSMV
13	20	KRFVCKHSMVDRGWGNGCGL
14	17	DRGWGNGCGLFGKGGIV
15	18	CGLFGKGGIVTCAMFTCK
16	18	IVTCAMFTCKKNMEGKIV
17	17	CKKNMEGKIVQPENLEY
18	17	KIVQPENLEYTVVITPH
19	17	LEYTVVITPHSGEEHAV
20	17	TPHSGEEHAVGNDTGKH
21	16	HAVGNDTGKHGKEVKI
22	16	TGKHGKEVKITPQSSI
23	18	EVKITPQSSITEAELTGY
24	15	SITEAELTGYGTVTM
25	18	ELTGYGTVTMECSPRTGL
26	18	TMECSPRTGLDFNEMVLL
27	18	GLDFNEMVLLQMKDKAWL
28	17	LLQMKDKAWLVHRQWFL
29	17	AWLVHRQWFLDLPLPWL
30	20	WFLDLPLPWLPGADTQGSNW
31	17	PGADTQGSNWIQKETLV
32	18	SNWIQKETLVTFKNPHAK
33	17	LVTFKNPHAKKQDVVVL
34	18	HAKKQDVVVLGSQEGAMH
35	16	VLGSQEGAMHTALTGA
36	15	GAMHTALTGATEIQM
37	17	ALTGATEIQMSSGNLLF
38	18	IQMSSGNLLFTGHLKCRL
39	18	LFTGHLKCRLRMDKLQLK
40	16	RLRMDKLQLKGMSYSM
41	18	LQLKGMSYSMCTGKFKVV
42	18	SMCTGKFKVVKEIAETQH
43	17	VVKEIAETQHGTIVIRV
44	20	TQHGTIVIRVQYEGDGSPCK
45	17	VQYEGDGSPCKTPFEIM
46	18	SPCKTPFEIMDLEKRHVL
47	16	IMDLEKRHVLGRLTTV
48	17	RHVLGRLTTVNPIVTEK
49	18	TTVNPIVTEKDSPVNIEA
50	18	EKDSPVNIEAEPPFGDSY
51	15	EAEPPFGDSYIIIGV
52	17	FGDSYIIIGVEPGQLKL
53	15	IGVEPGQLKLDWFKK
54	18	GQLKLDWFKKGSSIGQMF
55	18	KKGSSIGQMFETTMRGAK
56	15	MFETTMRGAKRMAIL
57	17	MRGAKRMAILGDTAWDF
58	17	AILGDTAWDFGSLGGVF
59	18	WDFGSLGGVFTSIGKALH
60	17	VFTSIGKALHQVFGAIY
61	17	ALHQVFGAIYGAAFSGV
62	18	AIYGAAFSGVSWTMKILI
63	17	GVSWTMKILIGVIITWI
64	15	ILIGVIITWIGMNSR
65	18	IITWIGMNSRSTSLSVSL
66	18	SRSTSLSVSLVLVGIVTL
67	18	SLVLVGIVTLYLGVMVQA

phosphatidylethanolamine (DEPE) and liver lipid extract were obtained from Avanti Polar Lipids (Alabaster, AL, USA). The lipid composition of the synthetic endoplasmic reticulum was EPC/CL/BPI/TPE/BPS/EPA/SM/CHOL at a molar ratio of 59:0.37:7.7:18:3.1:1.2:3.4:7.8 [31,32]. 5-Carboxyfluorescein (CF, >95% by HPLC), Triton X-100, EDTA and HEPES were purchased from Sigma-Aldrich (Madrid, ES). All other chemicals were commercial samples of the highest purity available (Sigma-Aldrich, Madrid, ES). Water was deionized, twice-distilled and passed through a Milli-Q equipment (Millipore Ibérica, Madrid, ES) to a resistivity higher than 18 MΩ cm.

2.2. Vesicle preparation

Aliquots containing the appropriate amount of lipid in chloroform-methanol (2:1 vol/vol) were placed in a test tube, the solvents were removed by evaporation under a stream of O_2-free nitrogen, and finally, traces of solvents were eliminated under vacuum in the dark for >3 h. The lipid films were resuspended in an appropriate buffer and incubated either at 25 °C or 10 °C above the phase transition temperature (T_m) with intermittent vortexing for 30 min to hydrate the samples and obtain multilamellar vesicles (MLV). The samples were frozen and thawed five times to ensure complete homogenization and maximization of peptide/lipid contacts with occasional vortexing. Large unilamellar vesicles (LUV) with a mean diameter of 0.1 μm were prepared from MLV by the extrusion method [33] using polycarbonate filters with a pore size of 0.1 (Nuclepore Corp., Cambridge, CA, USA). Breakdown of the vesicle membrane leads to contents leakage, i.e., CF fluorescence. Non-encapsulated CF was separated from the vesicle suspension through a Sephadex G-75 filtration column (Pharmacia, Uppsala, SW, EU) eluted with buffer containing either 10 mM Tris, 100 mM NaCl, 0.1 mM EDTA, pH 7.4. Phospholipid and peptide concentration were measured by methods described previously [34,35].

2.3. Membrane leakage measurement

Leakage of intraliposomal CF was assayed by treating the probe-loaded liposomes (final lipid concentration, 0.125 mM) with the appropriate amounts of peptides on microtiter plates stabilized at 25 °C using a microplate reader (FLUOstar, BMG Labtech, GER, EU), each well containing a final volume of 170 μl. The medium in the microtiter plates was continuously stirred to allow the rapid mixing of peptide and vesicles. Leakage was measured at an approximate peptide-to-lipid molar ratio of 1:25. Changes in fluorescence intensity were recorded with excitation and emission wavelengths set at 492 and 517 nm, respectively. One hundred percent release was achieved by adding Triton X-100 to a final concentration of 0.5% (w/w) to the microtiter plates. Fluorescence measurements were made initially with probe-loaded liposomes, afterwards by adding peptide solution and finally adding Triton X-100 to obtain 100%

leakage. Leakage was quantified on a percentage basis according to the equation,

$$\% \text{ Release} = \frac{F_f - F_0}{F_{100} - F_0} \cdot 100$$

F_f being the equilibrium value of fluorescence after peptide addition, F_0 the initial fluorescence of the vesicle suspension and F_{100} the fluorescence value after addition of Triton X-100. For details see refs [36,37].

2.4. Differential scanning calorimetry

MLVs were formed as stated above in 20 mM HEPES, 100 mM NaCl, 0.1 mM EDTA, pH 7.4. The peptides were added to obtain a peptide/lipid molar ratio of 1:15 and incubated 10 °C above the T_m of DEPE for 30 min with occasional vortexing and then centrifuged. Samples containing 1.5 mg of total phospholipid were transferred to 50 μl DSC aluminum and hermetically sealed pans and subjected to DSC analysis in a differential scanning calorimeter Pyris 6 DSC (Perkin-Elmer Instruments, Shelton, U.S.A.) under a constant external pressure of 30 psi in order to avoid bubble formation. Thermograms were recorded at a constant rate of 4 °C/min. After data acquisition, the pans were opened and the phospholipid content was determined. To avoid artifacts due to the thermal history of the sample, the first scan was never considered; second and further scans were carried out until a reproducible and reversible pattern was obtained. Data acquisition was performed using the Pyris Software for Thermal Analysis, version 4.0 (Perkin-Elmer Instruments LLC) and Microcal Origin software (Microcal Software Inc., Northampton, MA, U.S.A.) was used for data analysis. The thermograms were defined by the onset and completion temperatures of the transition peaks obtained from heating scans. The phase transition temperature was defined as the temperature at the peak maximum.

2.5. Hydrophobic moments, hydrophobicity and interfaciality

In order to detect membrane partitioning and/or membrane interacting surfaces along the DENV C and E proteins, two-dimensional plots of the hydrophobic moments, hydrophobicity and interfaciality have been obtained taking into consideration the arrangement of the amino acids in the space and assuming an α-helical structure [23]. The scale for calculating hydrophobic moments was taken from Engelman [38,39], whereas the hydrophobicity and interfacial values, i.e., whole residue scales for the transfer of an amino acid of an unfolded chain into the membrane hydrocarbon palisade and the membrane interface respectively, were obtained from Wimley and White [40,41]. Positive values represent positive bilayer-to water transfer free energy values and therefore the higher the value, the greater the probability to interact with the membrane surface and/or hydrophobic core.

3. Results

As we have commented above, DENV E protein is a class II fusion protein, essential for attachment, membrane fusion, and virus assembly, whereas DENV C protein is responsible for genome packaging and by associating with and modifying intracellular membranes it forms the replication complex, RC [2]. In a similar way to other enveloped viruses, DENV virus modifies cell internal membranes to establish specific sites of replication designed as the membranous web, i.e., the RC, fundamental for the viral life cycle [8,9]. In order to detect surfaces along the C and E sequences which might be identified as membrane partitioning and/or membrane interacting zones related to either tertiary or quaternary structures or both, we have plotted the average surface hydrophobic moment, hydrophobicity and interfaciality versus the amino-acid sequence of the C and E protein sequences of DENV 2 New Guinea C strain supposing they adopt an α-helical structure along the whole sequence (Figs. 2 and 3, respectively) [29]. Whereas DENV virus C protein has a majority of α-helical structure [42,43], DENV virus E protein has a much lower α-helix content than that of Class I membrane fusion proteins; in fact, its three ectodomains consist predominantly of β-strands [44]. However, the methodology we use gives us a depiction of the potential surface zones that are possibly implicated in a membranotropic action as it has been previously demonstrated [23,29].

As observed in Figs. 2 and 3, it is readily evident the existence of different regions with large hydrophobic moment values along both DENV C and E proteins. These sequences should show comparable capability to partition and/or interaction with membranes and should be biologically functional in their roles. Using these two-dimensional plots, it would be possible to distinguish two types of hydrophobic moment, hydrophobicity and/or interfaciality patches, those which do not comprise the length of the helix and those which embrace the full length [29]. The first type, located along limited zones of the protein surface, could favor the interaction with other similar patches along the same or other proteins as well as with the surface of the membrane. The second one, having large positive values covering the full horizontal length of the plot, would encompass two subtypes: patches containing about 15 or less amino acids which could represent membrane interacting domains and patches containing more than 15 amino acids which could represent transmembrane domains [15,24,29,45]. However there is not a clear separation between these two subtypes in all cases.

By observing the C protein data (Fig. 2A–C), it is possible to detect one localized highly positive hydrophobic moment, hydrophobicity and interfaciality region comprised by amino acid residues 40 to 59 (Region C1). Significantly, this region is surrounded by two regions displaying a highly ionic character, from amino acids residues 3 to 32 and from amino acids residues 67 to 100 (Fig. 2D). This results are in accordance with previous data, since it was previously proposed the presence of a highly hydrophobic patch comprising residues 46 to 66 [11] whereas the first thirty-two residues in the N-terminal region and the last twenty-six residues in the C-terminal region of the protein would interact with the viral RNA through its basic amino acids [46]. Significantly, specific residues within this hydrophobic patch have been identified as crucial determinants for lipid droplet localization and DENV replication [12].

The two-dimensional plots corresponding to DENV protein E are presented in Fig. 3A–C, where it is possible to distinguish different highly positive hydrophobic moment zones presenting diverse characteristics. Seven patches located along limited zones of the protein surface can be described, i.e., zones encompassing residues, but not all in between, located from amino acids 20 to 31 (Region E1), from amino acids 179 to 185 (Region E2), from amino acids 213 to 222 (Region E3), from amino acids 255 to 266 (Region E4), from amino acids 277 to 287 (Region E5), from amino acids 376 to 382 (Region E6) and from amino acids 397 to 409 (Region E7). On the other hand, five regions of large positive values covering the full horizontal length of the plot are found, i.e., zones encompassing amino acids 101 to 118 (Region E8), from amino acids 420 to 436 (Region E9), from amino acids 439 to 453 (Region E10), from amino acids 457 to 469 (Region E11) and from amino acids 476 to 493 (Region E12). Regions E1 through E6 belong to one of the three ectodomains of E protein, whereas region E7 belongs to the EH1 α-helical domain of the stem region of the protein. These regions could show a tendency to partition into membranes and/or interact with the membrane surface; however, it should not be ruled out that some areas could also be responsible for the interaction with other proteins as it has been suggested previously [21]. Region E3 coincides with a conserved proline-rich motif which might be engaged in monomer–monomer interaction [21] whereas regions E4 and E5 coincide with the β-hairpin which opens/closes a previously described hydrophobic pocket [47]. Significantly, zones E1, E3, E6 and E7 present both highly hydrophobic moment and interfaciality values (Fig. 3A and C). Region E8 coincides with the described fusion loop of E protein,

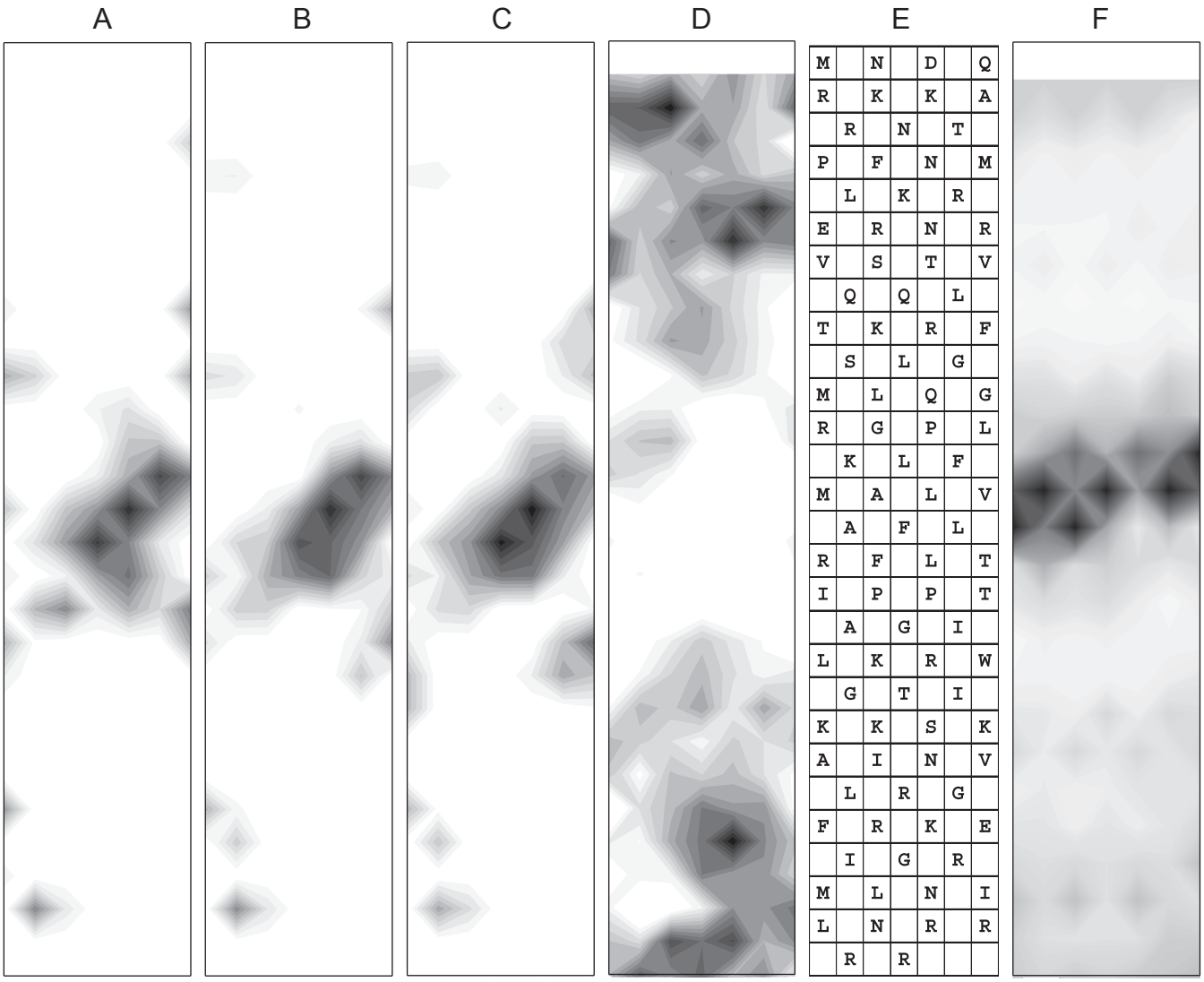

Fig. 2. Two-dimensional plot of (A) hydrophobic moment, (B) hydrophobicity, (C) interfacial hydrophobicity, (D) charge distribution, (E) the sequence of DENV protein C and (F) average experimental leakage for all tested liposome compositions [23]. The hydrophobic moment, hydrophobicity, and interfaciality plots show only positive bilayer-to water transfer free energy values.

regions E9 and E10 would encompass the second α-helical domain, EH2, of the stem region, and regions E11–E12 would belong to the proposed two transmembrane domains of the protein [5,7,18,44]. It is interesting to note that this description of DENV E protein hydrophobic-rich surfaces matches very well with some of the previously described regions of the protein, highlighting the specific roles they might have for the proper biological functioning of the protein and emphasizing that the actual distribution of hydrophobicity and interfaciality, i.e., structure-related factors, along DENV E protein (as well as C protein) would affect the biological function of these sequences (see below).

The two peptide libraries we have used in this study and their correlation with the DENV C and E envelope protein sequences are shown in Tables 1 and 2 and in Fig. 1B. It can be observed in the figure that the peptide libraries include the whole sequence of both proteins. Since two and three consecutive peptides in the library have an overlap of approximately 11 and 4 amino acids respectively, it seems reasonably thinking on peptide-defined regions as we will present below. We have studied the effect of these two peptide libraries on membrane rupture by monitoring leakage from different liposome compositions. Figs. 4 and 5 present the membrane leakage results for both C and E protein derived libraries, respectively, whereas Table 3 shows the peptides and their sequences which display the most significant leakage values. We have tested different lipid compositions, from simple to complex. The simple compositions contained EPC/Chol at a phospholipid molar ratio of 5:1, EPC/Chol at a phospholipid molar ratio of 5:2, EPC/Chol at a phospholipid molar ratio of 5:3, EPC/SM/Chol at a phospholipid molar ratio of 5:2:1, and EPC/BMP at a phospholipid molar ratio of 5:2. The presence of both SM and Chol has been related to the occurrence of laterally segregated membrane microdomains or "lipid rafts", and, for several viruses, it has been found a strong relationship between viral interaction with membranes and their content of Chol and SM [48]. BMP is an anionic phospholipid present in relatively high concentrations in late endosomes, i.e., where the fusion of the DENV virus envelope takes place, and therefore possibly engaged in the fusion process through specific interactions [49]. Since DENV virus is also associated with membranes of the ER or an ER-derived modified compartment, we have studied the effect of both C and E proteins on membrane rupture using a complex lipid composition resembling the ER membrane (containing EPC, CL, BPI, TPE, BPS, EPA, ESM and CHOL at a molar ratio of 59:0.37:7.4:18:3.1:1.2:3.4:7.8 [31]). In order to check the effect of each lipid in this complex composition we have designed an ER synthetic membrane composed of EPC/CL/BPI/TPE/BPS/EPA/ESM/CHOL at a molar ratio of 58:6:6:6.6:6:6:6 ($ER^{58:6}$) and tested this mixture as well as seven

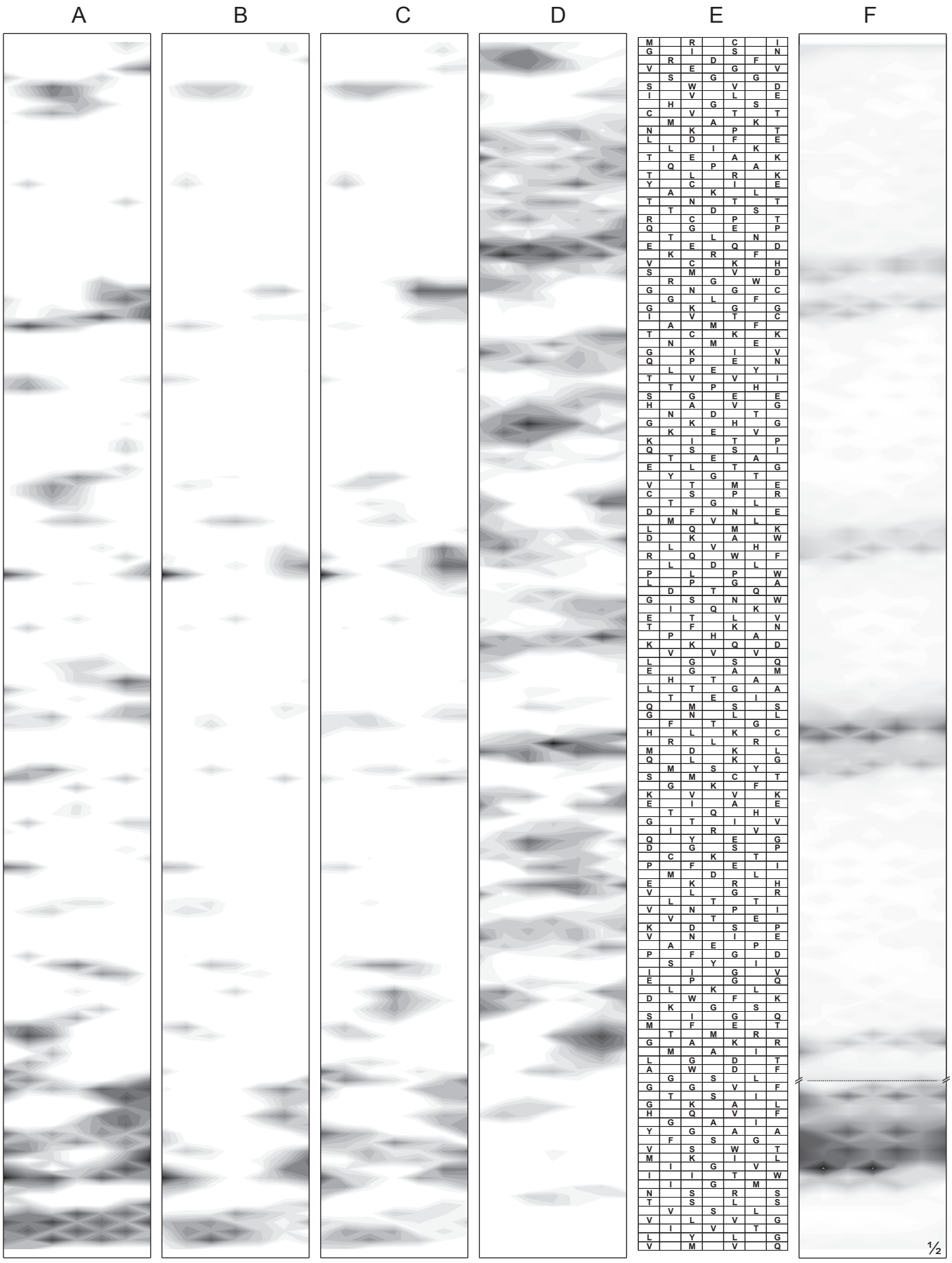

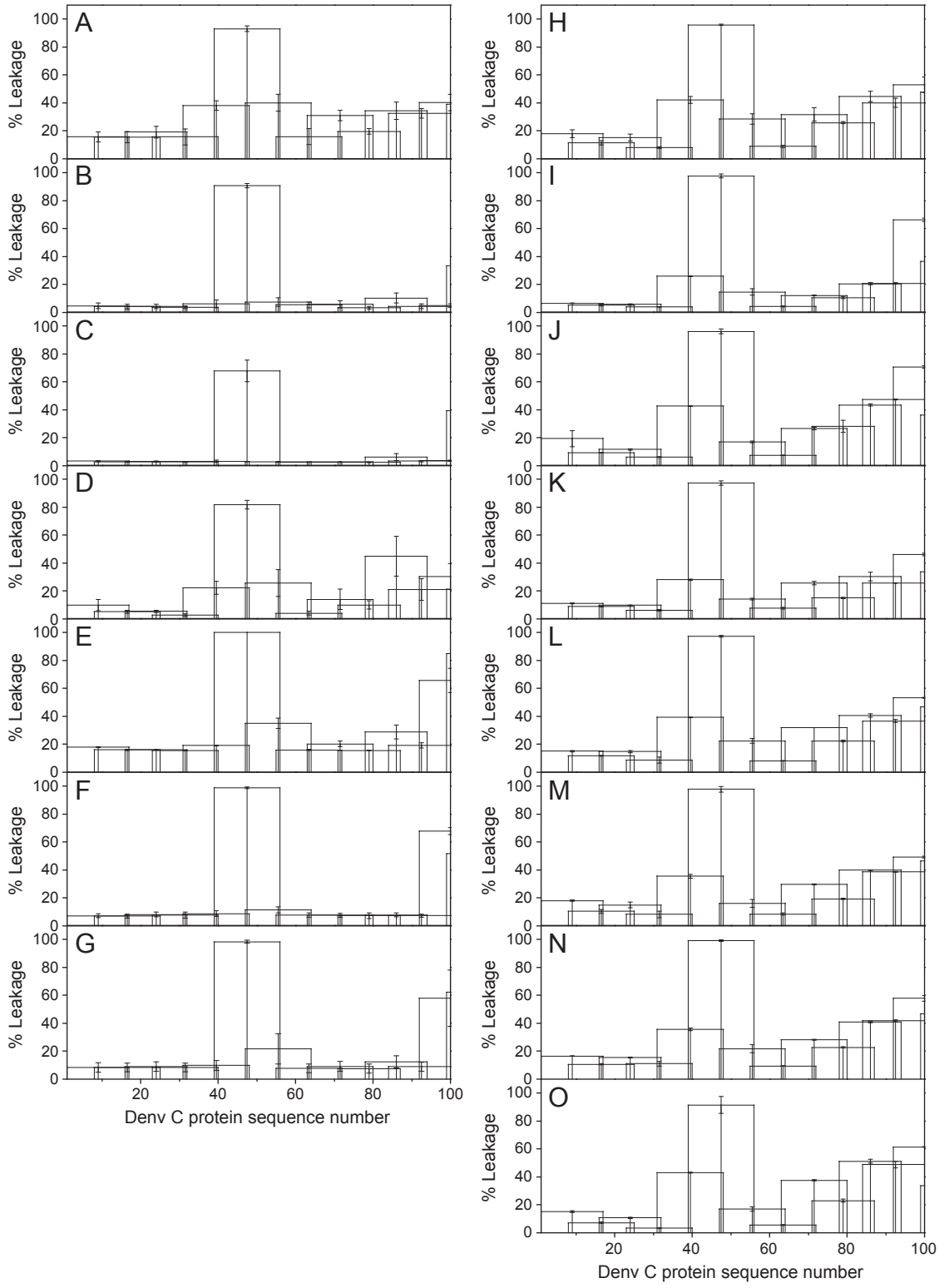

Fig. 4. Effect of the peptide library derived from the DENV C protein on the release of LUV contents for different lipid compositions. Leakage data (membrane rupture) for LUVs composed of (A) EPC/Chol at a phospholipid molar ratio of 5:1, (B) EPC/Chol at a phospholipid molar ratio of 5:2,(C) EPC/Chol at a phospholipid molar ratio of 5:3,(D) EPC/SM/Chol at a phospholipid molar ratio of 5:2:1, (E) EPC/BMP at a phospholipid molar ratio of 5:2, (F) lipid extract of liver membranes, (G) ER complex synthetic lipid mixture (EPC/CL/BPI/TPE/BPS/EPA/SM/Chol at a molar ratio of 59:0.37:7.7:18:3.1:1.2:3.4:7.8), (H) $ER^{58:6}$ complex lipid mixture (EPC/CL/BPI/TPE/BPS/EPA/ESM/CHOL at a molar ratio of 58:6:6:6.6:6:6:6), (I) $ER^{58:6}$ minus ESM, (J) $ER^{58:6}$ minus CHOL, (K) $ER^{58:6}$ minus EPA, (L) $ER^{58:6}$ minus BPI, (M) $ER^{58:6}$ minus BPS, (N) $ER^{58:6}$ minus TPE and (O) $ER^{58:6}$ minus CL. Vertical bars indicate standard deviations of the mean of quintuplicate samples. See text for details.

Fig. 3. Two-dimensional plot of (A) hydrophobic moment, (B) hydrophobicity, (C) interfacial hydrophobicity, (D) charge distribution, (E) the sequence of DENV protein C and (F) average experimental leakage for all tested liposome compositions [23]. The hydrophobic moment, hydrophobicity, and interfaciality plots show only positive bilayer-to water transfer free energy values. Note the different scales in (F).

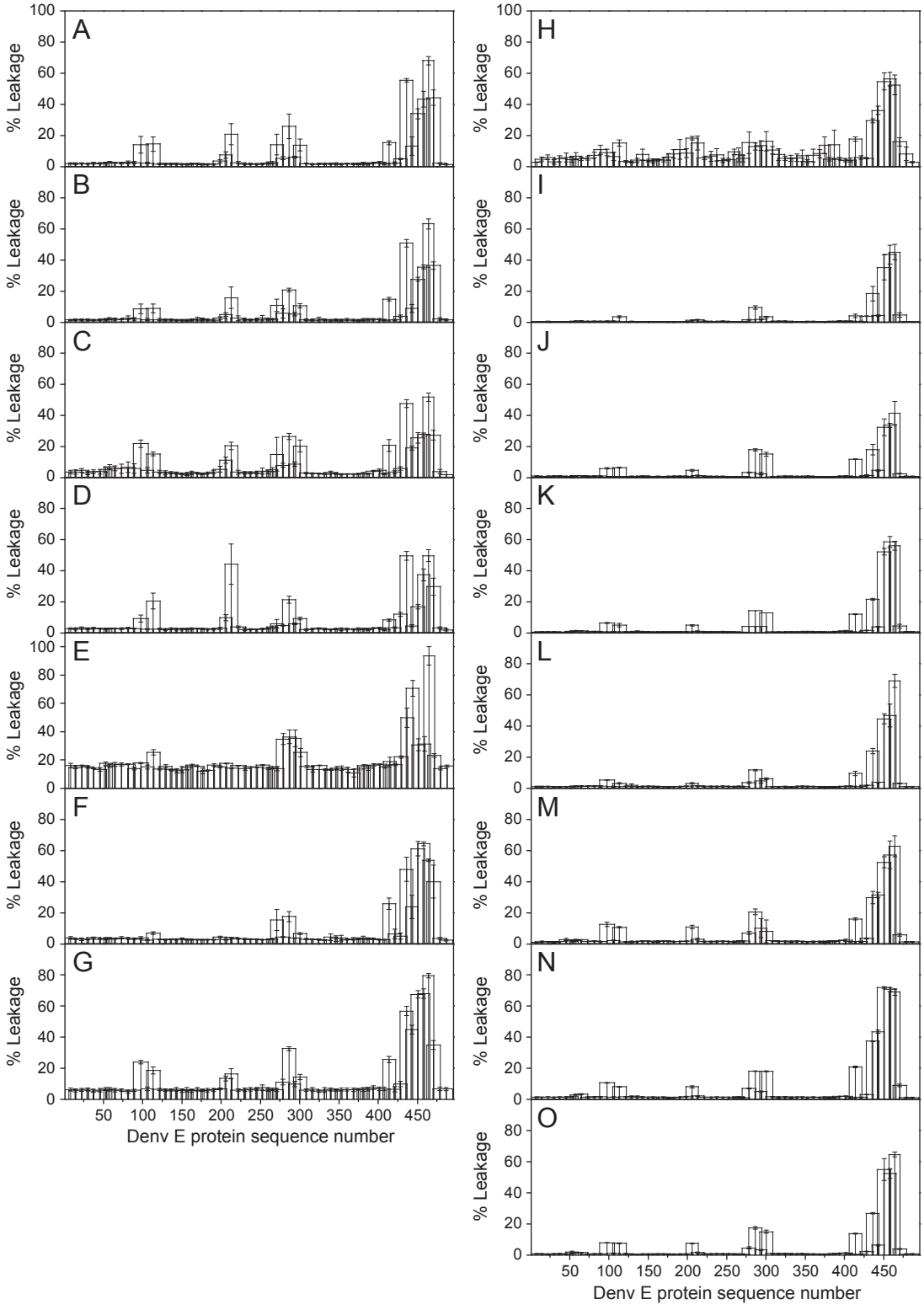

Fig. 5. Effect of the peptide library derived from the DENV E protein on the release of LUV contents for different lipid compositions. Leakage data (membrane rupture) for LUVs composed of (A) EPC/Chol at a phospholipid molar ratio of 5:1, (B) EPC/Chol at a phospholipid molar ratio of 5:2,(C) EPC/Chol at a phospholipid molar ratio of 5:3,(D) EPC/SM/Chol at a phospholipid molar ratio of 5:2:1, (E) EPC/BMP at a phospholipid molar ratio of 5:2, (F) lipid extract of liver membranes, (G) ER complex synthetic lipid mixture (EPC/CL/BPI/TPE/BPS/EPA/SM/Chol at a molar ratio of 59:0.37:7.7:18:3.1:1.2:3.4:7.8), (H) $ER^{58:6}$ complex lipid mixture (EPC/CL/BPI/TPE/BPS/EPA/ESM/CHOL at a molar ratio of 58:6:6:6.6:6:6:6), (I) $ER^{58:6}$ minus BPI, (J) $ER^{58:6}$ minus BPS, (K) $ER^{58:6}$ minus CHOL, (L) $ER^{58:6}$ minus CL, (M) $ER^{58:6}$ minus EPA, (N) $ER^{58:6}$ minus ESM, and (O) $ER^{58:6}$ minus TPE. Vertical bars indicate standard deviations of the mean of quintuplicate samples. See text for details.

different lipid mixtures lacking one and only one of those lipids in the mixture (except EPC). This complex mixture could be very useful in order to study the effect of each lipid component on the interaction of each peptide of the peptide library with the membrane. We have also studied liposomes containing a lipid liver extract (42%, PC, 22% PE, 7% Chol, 8% PI, 1% LPC, and 21% neutral lipids as stated by the manufacturer).

Table 3
Membrane leakage values (%) for representative membrane compositions. All numbers have been rounded to the nearest integer.

Peptide number	EPC/CHOL 5:1	EPC/CHOL 5:2	EPC/CHOL 5:3	EPC/SM/CHOL 5:2:1	Liver	ER	ER$^{59:6}$
Protein C, Peptide 6 GRGPLKLFMALVAFLRFL	93 ± 2	91 ± 1.5	68 ± 8	82 ± 3	99 ± 1	98 ± 1	96 ± 1
Protein E, Peptide 29 AWLVHRQWFLDLPLPWL	21 ± 7	15.8 ± 7	21 ± 2	44 ± 13	4 ± 0	16 ± 3	15 ± 4
Protein E, Peptide 39 LFTGHLKCRLRMDKLQLK	26 ± 8	21 ± 1	26 ± 2	21 ± 2	18 ± 3	32 ± 1	13 ± 2
Protein E, Peptide 60 VFTSIGKALHQVFGAIY	55 ± 1	51 ± 2	47 ± 2	49 ± 3	48 ± 8	57 ± 3	29 ± 1
Protein E, Peptide 64 ILIGVIITWIGMNSR	68 ± 3	63 ± 3	52 ± 3	50 ± 4	54 ± 1	79 ± 1	52 ± 6

In addition, it seems reasonably to think on the combined effect of peptide groups or segments rather than on the effect of isolated peptides so that leakage data would define protein segments or zones as we will see below.

The leakage data corresponding to the C protein derived peptide library is shown in Fig. 4. The most remarkable effect was observed for peptide comprising residues 39–56, which produced leakage values between 75 and 95%, depending on the specific lipid composition of the liposomes (Fig. 4). This peptide would define a leakage zone, CL1, which coincides with region C1 shown above. Peptide corresponding to residues 39–56, i.e., zones C1 and CL1, matches with C protein highly hydrophobic region commented

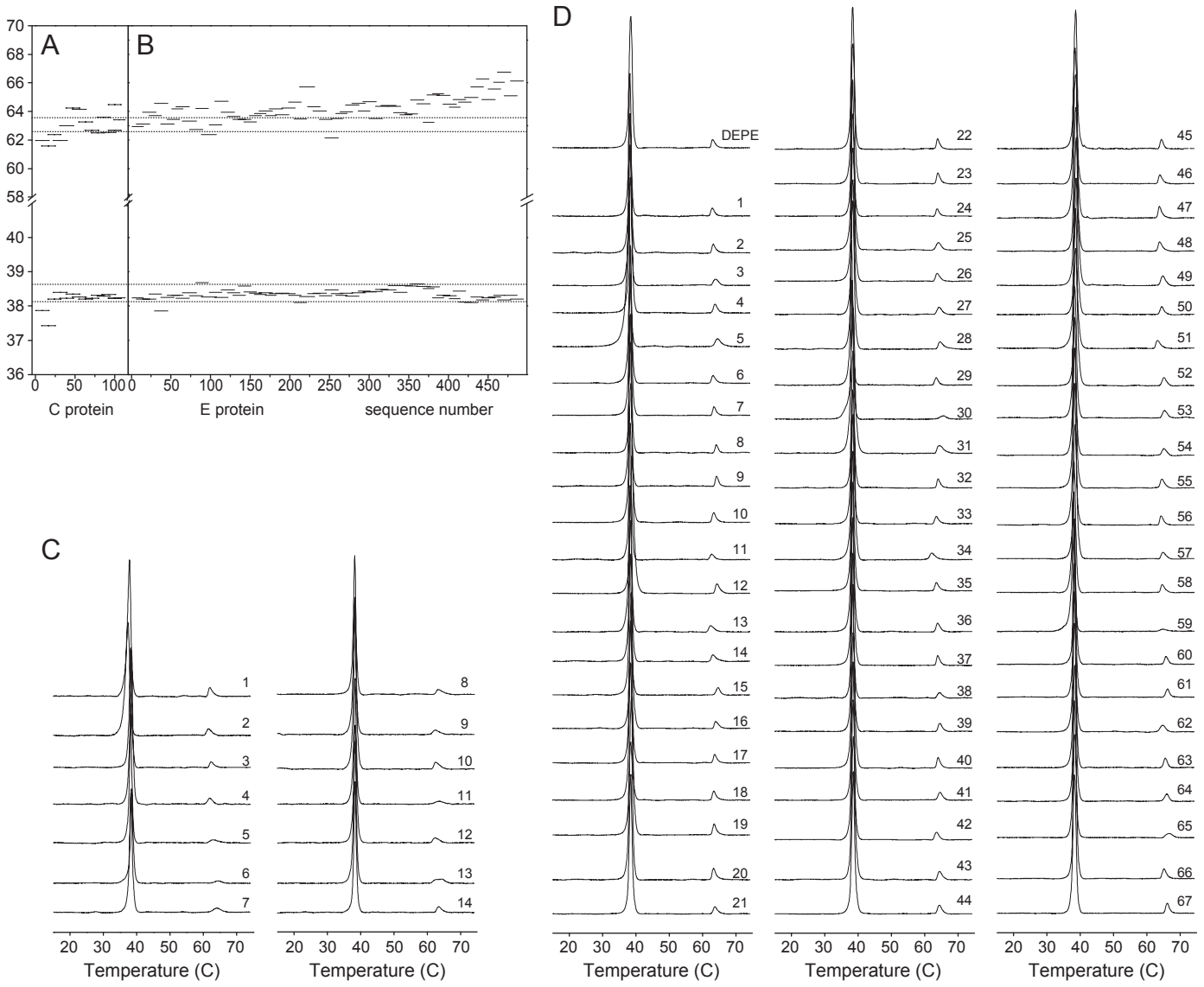

Fig. 6. Temperature of the gel-to-liquid crystalline and lamellar-hexagonal phase transitions of DEPE in the presence of the peptide libraries belonging to the (A) C and (B) E DENV proteins, respectively. Dotted lines define $T_m \pm 0.25$ °C and $H_{II} \pm 0.5$ °C zones of pure DEPE. Note the extended temperature scale. The DSC heating thermograms of DEPE in the presence of the peptides belonging to C and E protein libraries at a phospholipid/peptide molar ratio of 15:1 are shown in (C) and (D), respectively. Numbers represent their peptide number in the library (see Fig. 1). All the thermograms were normalized to the same amount of lipid.

previously. Other peptides that elicited some leakage were those comprising residues 31–47, 47–64, 78–94 and 92–108. The small leakage values observed for peptides 31–47 and 47–64 might be due to their overlapping with peptides 39–56. Peptide comprising residues 78–94 elicited a relative significant leakage in liposomes composed of EPC/ESM/CHOL whereas peptide comprising residues 92–108 elicited significant leakage in liposomes composed of EPC/BMP, the liver extract and the ER-like membranes (Fig. 4). For liposomes containing the $ER^{58:6}$ complex mixture and its variations (Fig. 4H to O) the most remarkable effect was observed for peptide comprising residues 39–56 similarly to the other membrane compositions tested, which produced leakage values between 90 and 100%, depending on the specific composition of the liposomes. Significantly, this peptide induced membrane leakage for all lipid compositions so that neither of the lipids tested have a specific interaction with the peptide, the peptide rupturing all types of membrane model systems. Other peptides that showed leakage were those comprising residues 31–47, 63–80, 78–94, 84–101 and 92–108 (Fig. 4H to O). There were no significant differences between the $ER^{58:6}$ mixture and those with one of the lipids removed. Fig. 2F presents the average leakage of all liposomes compositions tested, where it can be observed the significant relationship between hydrophobic moments, hydrophobicity, and interfaciality with membrane leakage (Fig. 2A–C). The conservation of this pattern across different strains of DENV as well as its significant effect on all liposome compositions indicates that this sequence is an essential membrane interacting region in this protein [11].

When the peptides corresponding to the E peptide library were assayed on liposomes containing EPC and either CHOL, SM or BMP some exerted a significant leakage effect (Fig. 5A to E). A quick bird's eye view of the leakage data presented in the figures shows the presence of five different leakage zones: the first one, EL1, would be comprised by two peptides defined by residues 88–107 and 105–122, the second one, EL2, by two peptides defined by residues 198–214 and 205–221, the third one, EL3, by three peptides defined by residues 270–287, 278–295 and 292–309, the fourth one, EL4, by one peptide defined by residues 406–422, whereas the fifth and last group, EL5, would be defined by six peptides comprising residues 428–444, 435–451, 442–459, 450–466, 457–471, and 462–479. Following the same reasoning commented above, we have also tested liposomes containing lipid complex compositions, i.e., lipid liver extract and ER synthetic membranes (Fig. 5F and G). These two liposome compositions showed the same leakage zones observed above for the simpler ones, although they were less defined for the case of the lipid liver extract. We have also tested the $ER^{58:6}$ lipid complex composition and its variations (Fig. 5I–O). Although all the zones commented above were defined, there were subtle differences depending on lipid composition. The four zones were clearly marked for liposomes composed of EPC/CHOL, EPC/ESM/CHOL, ER lipids as well as the $ER^{58:6}$ and derived compositions (Fig. 5A–D, G, H–O). Whereas the first, third and fourth zones were discerned to a different extent on all liposome compositions tested, the second zone was not clearly defined in membranes composed of EPC/BMP and the liver lipid extract (Fig. 5E and F). Similarly to the data obtained for the C protein derived library, Fig. 3F presents the average leakage of all liposomes compositions tested for the E protein derived library. It can be observed that there is a relationship between membrane leakage with hydrophobic moments, hydrophobicity, and interfaciality for some but not for all leakage zones (Figs. 2A–C). The first leakage zone, EL1, coincides with region E8, where the described fusion peptide of E protein resides. This zone presents high positive values of hydrophobic moment and interfaciality and it is a very low charged region (Figs. 5A, 3C and D). Whereas the second leakage zone, EL2, coincides with region E3, a conserved proline-rich motif engaged in protein–protein interaction, the third leakage zone, EL3, coincides with zone E5, where a previously described hydrophobic pocket is located (see above). It is worthwhile to comment that this hydrophobic pocket, represented by zones EL3/E5, shows itself as a relatively charged zone surrounded by two hydrophobic patches (compare Fig. 3A and D). Leakage region EL4 coincides with part of the stem domain of the E protein, region E7, and specifically with the so called EH1 helix [18]. The last leakage region EL5 is comprised by six peptides defining a long stretch of approximately fifty amino acids, from residue 428 to residue 479, which coincides with the previously defined zones E9 through E11 (see above). This leakage region would be comprised by helix EH2 from the stem as well as by one of the proposed TM domains of the protein, TM1. Interestingly, peptides corresponding to the proposed TM2 domain do not show any significant leakage (Fig. 3A and F). Among all leakage zones, region EL5 is the one which shows the highest leakage values (Fig. 5). As it was commented above, the exact function of the stem region of the E protein is not known with certainty but these results would be in accordance with its proposed interaction with the membrane and possibly with the fusion process [4–6,22]. Recently it has been described that region EL5 has a high membrane interacting capacity and derived peptides inhibit DENV infectivity [50], highlighting that this region should be engaged in fusion. The fact that the region comprising the proposed TM1 domain also presents a high leakage activity would suggest that this region could interact with the membrane before, at or after the fusion process, possibly in concerted action with the stem region of the protein and most probably with segment EH2, acting likely the pre-transmembrane segment of other class I and II membrane fusion proteins (see below). The coincidental results obtained through both the theoretical and experimental data, would point out that these sequences should be important regions of this protein and would be engaged in membrane interaction.

Since both C and E proteins interact with membranes and might modify and/or modulate its structure, we have used differential scanning calorimetry (DSC) to examine the effect of each of these two peptide libraries on the phase transitions of DEPE (Fig. 6). In this way we can obtain information on the structural organization of the DEPE/peptide systems and their capacity to modify and/or modulate the polymorphic behavior of phospholipid membranes [51]. Aqueous dispersions of pure DEPE undergo a gel to liquid-crystalline ($L_\beta \rightarrow L_\alpha$) phase transition T_m in the lamellar phase at 38.4 °C and in addition a lamellar liquid-crystalline to hexagonal-H_{II} ($L_\alpha \rightarrow H_{II}$) phase transition at about 63.1 °C [52]. As observed in Fig. 6, both gel to liquid-crystalline and lamellar liquid-crystalline to hexagonal-H_{II} transitions were present in all samples, no peptide induced any significant change in the enthalpy of the main transition but some transition temperatures were different to the pure lipid. In the case of the peptides pertaining to the C protein peptide library, peptides 1 and 2 were the only ones that slightly lowered the T_m from 38.4 °C to 37.8 °C and 37.4 °C, respectively. All the other peptides did not modify the T_m of DEPE (see Fig. 6A and C). More differences were observed for the H_{II} transition, since this transition is much more sensitive than the lamellar one to molecular interaction [52]. Some peptides shifted the H_{II} transition to lower temperatures, peptides 1–4, whereas other ones shifted it to higher ones, peptides 6, 7 and 13. Interestingly, peptides 6 and 7 overlap leakage zone CL1 (see above) and peptide 13 gave place to two discernible H_{II} transitions which appeared at 62.7 °C and 64.5 °C (Fig. 6C). In the case of the peptides pertaining to the E protein peptide library, all peptides except peptide no. 5, which slightly lowered the T_m to 37.9 °C, did not induce changes in the T_m temperatures of DEPE (Fig. 6B and D). Similarly to what was observed for the C derived peptide library, some differences were observed for the H_{II} transition. There were only two peptides that shifted the H_{II} transition to lower temperatures, peptides 13 and 34 (Fig. 6D). Of those peptides which shifted significantly the H_{II} transition to higher temperatures, peptide 15 (to 64.7 °C) overlapped with zone EL1, peptide 34 (to 65.7 °C) overlapped with zone EL2 and peptides 59–67 (64.6 °C-66.75 °C) overlapped with zone EL5. The coincidence of these relatively high-effect peptides with high leakage zones demonstrates their specific interaction with the membrane as well as their modulatory effect.

4. Discussion

The virus family *Flaviviridae* includes Dengue virus (DENV) as well as other viruses such as Japanese encephalitis, Yellow fever, West Nile and tick-borne encephalitis viruses. Similarly to other enveloped viruses, they enter the cell through receptor mediated endocytosis and rearrange internal cell membranes to form the replication complex, an essential step for viral replication [4–10]. The mature DENV virus has a capsid (C) protein core complexed with the RNA, surrounded by a lipid bilayer in which the viral envelope (E) protein is embedded. Whereas the C protein, a dimeric basic helical protein, is responsible for RNA packaging and membrane interaction, the E protein, composed of three ectodomains with β-strand structure plus a stem and a transmembrane domain, is a class II membrane fusion protein [4,7,11–15]. The E protein of DENV apparently possess two transmembrane spanning sequences, whereas class I, alphavirus class II and class III membrane fusion proteins possess a single transmembrane spanning sequence [53]. In general, fusion implies the insertion of specific regions that disrupt the membrane, leading to the formation of an initial local lipid connection (lipid stalk) [54,55]. This lipid stalk is then believed to expand into a hemifusion diaphragm whose rupture would finally generate a fusion pore [54,55]. Membrane fusion does not necessarily occur at the plasma membrane level; viral entry can also involve endocytosis and vesicular trafficking, as it happens in the case of DENV. There are still many questions to be answered regarding the C and E mode of action in membrane fusion, assembly, replication and/or release during the DENV viral cycle. Additionally, DENV membrane interaction is an attractive target for anti-DENV therapy. Therefore, we have carried an exhaustive analysis of the different regions of DENV C and E proteins which might interact with phospholipid membranes using a similar approach to that used before [26] and have identified different regions on these proteins with membrane-interacting capabilities.

We are aware that the use of peptide fragments might not mimic the properties of the intact protein, as well as it is not obvious that peptide–membrane interaction is directly related to membrane rupture [26,29,30]. However, these data give us an indication of the relative propensity of the different domains to bind to and interact with membranes in relation to each other, i.e., help us to classify the different regions and segments of the C and E envelope proteins according to their effect in an ample representation of membrane systems.

When all the leakage values were taken into account for all lipid compositions assayed using the C protein derived peptide library, one peptide displayed a significant membrane rupture activity (region CL1), coincidental with a localized highly positive hydrophobic moment, hydrophobicity and interfaciality region (region C1), namely the region encompassing amino acid residues 39 to 56. Remarkably, peptides pertaining to this zone affected the H_{II} transition temperature of DEPE but they did not make it to disappear. This highly hydrophobic region is surrounded by two regions with a highly ionic character, confirming previous data which proposed the presence of a membrane interacting domain surrounded by two RNA interacting domains [11,12,46]. The highly hydrophobic character of this region is remarkable, since it is completely independent of the phospholipid composition and caused leakage of all membrane compositions tested, simple and complex. Its significant effect on all liposome compositions emphasizes that the region of protein C where this sequence resides should be an essential membrane interacting region [11]. There were subtle leakage differences for peptides comprising residues 78–94 and 92–108, which pertain to a highly charged region of the protein; these subtle effects possibly result from the interaction of these peptides with the charged phospholipid headgroups. These data would point out to two essential functions of DENV protein C, binding to RNA and interaction with the membrane, either viral or cellular or both [43]. The high hydrophobicity and membrane interacting capacity of region CL1/C1, which could be accompanied by different conformations of the C protein, would suggest that it has an important but unknown function in morphogenesis and/or budding.

When the peptides corresponding to the E protein derived peptide library were assayed on membrane vesicles some exerted a significant leakage effect, giving place to five leakage different regions, i.e., EL1 (peptides 88–107 and 105–122), EL2 (peptides 198–214 and 205–221), EL3 (peptides 270–287, 278–295 and 292–309), EL4 (peptides 406–422) and EL5 (peptides 428–444, 435–451, 442–459, 450–466, 457–471, and 462–479). These regions could partition into membranes and/or interact with the membrane surface but could also interact with other proteins [21]. Significantly, these zones match previously described regions of the E protein, highlighting their specific roles necessary for the proper biological functioning of the protein and emphasizing that the actual distribution of hydrophobicity and interfaciality along the surface of the protein, i.e., structure-related factors, would affect the biological function of these sequences. The average leakage of all liposomes compositions tested for the E protein derived library show that some of them are indeed related with the hydrophobic moment, hydrophobicity, and interfaciality zones but others do not. Region EL1 (E8) overlaps with the proposed fusion peptide of DENV E protein, region EL2 (E3) coincides with a conserved proline-rich motif engaged in protein–protein interaction, region EL3 (E5) matches with a previously described hydrophobic pocket and interestingly region EL4 (E7) corresponds with part of the E protein stem domain and specifically with the EH1 helix. Region EL5 (E9/E11) is comprised by a long stretch of amino acids which coincides in part with the stem domain, specifically with the EH2 helix, as well as with the first proposed TM domain, TM1. This region, EL5, is the one which shows the highest leakage values. Interestingly, some peptides pertaining to regions EL1, EL2 and EL5 showed some effect on the H_{II} transition temperature of DEPE (see above). Although the precise function of the stem region of the E protein is not known with certainty, these data would suggest that both EH1 and EH2 segments would interact with the membrane and possibly necessary for the fusion process [4–6,18,22]. It could be also suggested that its biological role should be similar to the pre-transmembrane or membrane-proximal external domains of other class I and class II membrane fusion proteins [25,56–58]. These pre-transmembrane segments show high leakage values on different membrane compositions, similarly to what has been found here for the E protein, and all of them have essential roles in membrane fusion. It should be therefore easy to suggest that the stem region of DENV E protein should be essential for viral entry, its function should be comparable to similar pre-transmembrane regions of class I and class II membrane fusion proteins and therefore a target for its inhibition. This is in fact what has been found very recently [59]. The high leakage activity of the proposed TM1 domain, in contrast with the lack of activity of other TM domains pertaining to other proteins, would suggest that it would be engaged in a direct membrane interaction; TM2 region of protein E should be the real counterpart to other TM domains of other membrane fusion proteins [53]. The analogous results we have obtained in this work through both the theoretical and experimental data would corroborate these data. Therefore, not only the fusion domain but also the stem and TM1 regions of protein E should be essential for DENV membrane fusion and therefore viral entry. Both TM domains of protein E should play an important role in membrane fusion and/or budding [60] and therefore molecules interacting with them should therefore be conceived as DENV entry inhibitors [61].

Understanding the factors that determine the specificity and stability of the metastable and stable conformations of membrane-interacting viral proteins are required to know the mechanism of viral entry, replication and morphogenesis. The change in conformation and the possible formation of oligomeric forms in the presence of membranes could indicate the propensity of the proteins to self-

assemble and suggests that these changes might be part of the structural transition that transform them from the inactive to the active state; they are probably driven by the interaction of different segments, such as those described in this work. The inhibition of membrane interaction by direct action on either C or E or both proteins is an additional approach to combat against DENV infection or prevent its spread. An understanding of the structural features of these processes, directly related to membrane interaction, is essential because they are attractive drug targets.

Acknowledgements

This work was partially supported by grant BFU2008-02617-BMC (Ministerio de Ciencia y Tecnología, Spain) to J.V. We are especially grateful to BEI Resources, National Institute of Allergy and Infectious Diseases, Manassas, VA, USA, for the peptides used in this work. H.N. is supported by a Santiago Grisolía fellowship from Generalitat Valenciana.

References

[1] M.G. Guzman, G. Kouri, Dengue: an update, Lancet Infect. Dis. 2 (2002) 33–42.
[2] S. Urcuqui-Inchima, C. Patino, S. Torres, A.L. Haenni, F.J. Diaz, Recent developments in understanding dengue virus replication, Adv. Virus Res. 77 (2010) 1–39.
[3] B. Pastorino, A. Nougairede, N. Wurtz, E. Gould, X. de Lamballerie, Role of host cell factors in flavivirus infection: implications for pathogenesis and development of antiviral drugs, Antiviral Res. 87 (2010) 281–294.
[4] R. Perera, R.J. Kuhn, Structural proteomics of dengue virus, Curr. Opin. Microbiol. 11 (2008) 369–377.
[5] S. Bressanelli, K. Stiasny, S.L. Allison, E.A. Stura, S. Duquerroy, J. Lescar, F.X. Heinz, F.A. Rey, Structure of a flavivirus envelope glycoprotein in its low-pH-induced membrane fusion conformation, EMBO J. 23 (2004) 728–738.
[6] M. Kielian, F.A. Rey, Virus membrane-fusion proteins: more than one way to make a hairpin, Nat. Rev. Microbiol. 4 (2006) 67–76.
[7] S. Mukhopadhyay, R.J. Kuhn, M.G. Rossmann, A structural perspective of the flavivirus life cycle, Nat. Rev. Microbiol. 3 (2005) 13–22.
[8] S. Miller, S. Kastner, J. Krijnse-Locker, S. Buhler, R. Bartenschlager, The non-structural protein 4A of dengue virus is an integral membrane protein inducing membrane alterations in a 2K-regulated manner, J. Biol. Chem. 282 (2007) 8873–8882.
[9] S. Miller, J. Krijnse-Locker, Modification of intracellular membrane structures for virus replication, Nat. Rev. Microbiol. 6 (2008) 363–374.
[10] S. Welsch, S. Miller, I. Romero-Brey, A. Merz, C.K. Bleck, P. Walther, S.D. Fuller, C. Antony, J. Krijnse-Locker, R. Bartenschlager, Composition and three-dimensional architecture of the dengue virus replication and assembly sites, Cell Host Microbe 5 (2009) 365–375.
[11] L. Markoff, B. Falgout, A. Chang, A conserved internal hydrophobic domain mediates the stable membrane integration of the dengue virus capsid protein, Virology 233 (1997) 105–117.
[12] M.M. Samsa, J.A. Mondotte, N.G. Iglesias, I. Assuncao-Miranda, G. Barbosa-Lima, A.T. Da Poian, P.T. Bozza, A.V. Gamarnik, Dengue virus capsid protein usurps lipid droplets for viral particle formation, PLoS Pathog. 5 (2009) e1000632.
[13] S. Boulant, C. Vanbelle, C. Ebel, F. Penin, J.P. Lavergne, Hepatitis C virus core protein is a dimeric alpha-helical protein exhibiting membrane protein features, J. Virol. 79 (2005) 11353–11365.
[14] R. Ivanyi-Nagy, J.L. Darlix, Intrinsic disorder in the core proteins of flaviviruses, Protein Pept. Lett. 17 (2010) 1019–1025.
[15] A.J. Perez-Berna, A.S. Veiga, M.A. Castanho, J. Villalain, Hepatitis C virus core protein binding to lipid membranes: the role of domains 1 and 2, J. Viral Hepat. 15 (2008) 346–356.
[16] D.J. Schibli, W. Weissenhorn, Class I and class II viral fusion protein structures reveal similar principles in membrane fusion, Mol. Membr. Biol. 21 (2004) 361–371.
[17] S.L. Allison, J. Schalich, K. Stiasny, C.W. Mandl, F.X. Heinz, Mutational evidence for an internal fusion peptide in flavivirus envelope protein E, J. Virol. 75 (2001) 4268–4275.
[18] W. Zhang, P.R. Chipman, J. Corver, P.R. Johnson, Y. Zhang, S. Mukhopadhyay, T.S. Baker, J.H. Strauss, M.G. Rossmann, R.J. Kuhn, Visualization of membrane protein domains by cryo-electron microscopy of dengue virus, Nat. Struct. Biol. 10 (2003) 907–912.
[19] S.L. Allison, K. Stiasny, K. Stadler, C.W. Mandl, F.X. Heinz, Mapping of functional elements in the stem-anchor region of tick-borne encephalitis virus envelope protein E, J. Virol. 73 (1999) 5605–5612.
[20] K.K. Orlinger, V.M. Hoenninger, R.M. Kofler, C.W. Mandl, Construction and mutagenesis of an artificial bicistronic tick-borne encephalitis virus genome reveals an essential function of the second transmembrane region of protein e in flavivirus assembly, J. Virol. 80 (2006) 12197–12208.
[21] R.A. Gadkari, N. Srinivasan, Prediction of protein–protein interactions in dengue virus coat proteins guided by low resolution cryoEM structures, BMC Struct. Biol. 10 (2010) 17.
[22] S.C. Hsieh, G. Zou, W.Y. Tsai, M. Qing, G.J. Chang, P.Y. Shi, W.K. Wang, The C-terminal helical domain of dengue virus precursor membrane protein is involved in virus assembly and entry, Virology 410 (2011) 170–180.
[23] J. Guillen, A.J. Perez-Berna, M.R. Moreno, J. Villalain, Identification of the membrane-active regions of the severe acute respiratory syndrome coronavirus spike membrane glycoprotein using a 16/18-mer peptide scan: implications for the viral fusion mechanism, J. Virol. 79 (2005) 1743–1752.
[24] A.J. Perez-Berna, M.R. Moreno, J. Guillen, A. Bernabeu, J. Villalain, The membrane-active regions of the hepatitis C virus E1 and E2 envelope glycoproteins, Biochemistry 45 (2006) 3755–3768.
[25] M.R. Moreno, M. Giudici, J. Villalain, The membranotropic regions of the endo and ecto domains of HIV gp41 envelope glycoprotein, Biochim. Biophys. Acta 1758 (2006) 111–123.
[26] A.J. Perez-Berna, J. Guillen, M.R. Moreno, A. Bernabeu, G. Pabst, P. Laggner, J. Villalain, Identification of the membrane-active regions of hepatitis C virus p7 protein: biophysical characterization of the loop region, J. Biol. Chem. 283 (2008) 8089–8101.
[27] I. Valdes, L. Gil, Y. Romero, J. Castro, P. Puente, L. Lazo, E. Marcos, M.G. Guzman, G. Guillen, L. Hermida, The chimeric protein domain III-capsid of dengue virus serotype 2 (DEN-2) successfully boosts neutralizing antibodies generated in monkeys upon infection with DEN-2, Clin. Vaccine Immunol. 18 (2011) 455–459.
[28] C.G. Noble, Y.L. Chen, H. Dong, F. Gu, S.P. Lim, W. Schul, Q.Y. Wang, P.Y. Shi, Strategies for development of dengue virus inhibitors, Antiviral Res. 85 (2010) 450–462.
[29] J. Guillen, A. Gonzalez-Alvarez, J. Villalain, A membranotropic region in the C-terminal domain of hepatitis C virus protein NS4B interaction with membranes, Biochim. Biophys. Acta 1798 (2010) 327–337.
[30] A.J. Perez-Berna, G. Pabst, P. Laggner, J. Villalain, Biophysical characterization of the fusogenic region of HCV envelope glycoprotein E1, Biochim. Biophys. Acta 1788 (2009) 2183–2193.
[31] A.G. Krainev, D.A. Ferrington, T.D. Williams, T.C. Squier, D.J. Bigelow, Adaptive changes in lipid composition of skeletal sarcoplasmic reticulum membranes associated with aging, Biochim. Biophys. Acta 1235 (1995) 406–418.
[32] T.W. Keenan, D.J. Morre, Phospholipid class and fatty acid composition of golgi apparatus isolated from rat liver and comparison with other cell fractions, Biochemistry 9 (1970) 19–25.
[33] L.D. Mayer, M.J. Hope, P.R. Cullis, Vesicles of variable sizes produced by a rapid extrusion procedure, Biochim. Biophys. Acta 858 (1986) 161–168.
[34] C.S.F. Böttcher, C.M. Van Gent, C. Fries, A rapid and sensitive sub-micro phosphorus determination, Anal. Chim. Acta 1061 (1961) 203–204.
[35] H. Edelhoch, Spectroscopic determination of tryptophan and tyrosine in proteins, Biochemistry 6 (1967) 1948–1954.
[36] A. Bernabeu, J. Guillen, A.J. Perez-Berna, M.R. Moreno, J. Villalain, Structure of the C-terminal domain of the pro-apoptotic protein Hrk and its interaction with model membranes, Biochim. Biophys. Acta 1768 (2007) 1659–1670.
[37] M.R. Moreno, J. Guillen, A.J. Perez-Berna, D. Amoros, A.I. Gomez, A. Bernabeu, J. Villalain, Characterization of the interaction of two peptides from the N terminus of the NHR domain of HIV-1 gp41 with phospholipid membranes, Biochemistry 46 (2007) 10572–10584.
[38] D. Eisenberg, E. Schwarz, M. Komaromy, R. Wall, Analysis of membrane and surface protein sequences with the hydrophobic moment plot, J. Mol. Biol. 179 (1984) 125–142.
[39] D.M. Engelman, T.A. Steitz, A. Goldman, Identifying nonpolar transbilayer helices in amino acid sequences of membrane proteins, Annu. Rev. Biophys. Biophys. Chem. 15 (1986) 321–353.
[40] W.C. Wimley, S.H. White, Experimentally determined hydrophobicity scale for proteins at membrane interfaces, Nat. Struct. Biol. 3 (1996) 842–848.
[41] W.C. Wimley, T.P. Creamer, S.H. White, Solvation energies of amino acid side chains and backbone in a family of host-guest pentapeptides, Biochemistry 35 (1996) 5109–5124.
[42] C.T. Jones, L. Ma, J.W. Burgner, T.D. Groesch, C.B. Post, R.J. Kuhn, Flavivirus capsid is a dimeric alpha-helical protein, J. Virol. 77 (2003) 7143–7149.
[43] L. Ma, C.T. Jones, T.D. Groesch, R.J. Kuhn, C.B. Post, Solution structure of dengue virus capsid protein reveals another fold, Proc. Natl. Acad. Sci. U.S.A. 101 (2004) 3414–3419.
[44] Y. Modis, S. Ogata, D. Clements, S.C. Harrison, Structure of the dengue virus envelope protein after membrane fusion, Nature 427 (2004) 313–319.
[45] M.F. Palomares-Jerez, J. Villalain, Membrane interaction of segment H1 (NS4B(H1)) from hepatitis C virus non-structural protein 4B, Biochim. Biophys. Acta 1808 (2011) 1219–1229.
[46] A.A. Khromykh, E.G. Westaway, RNA binding properties of core protein of the flavivirus Kunjin, Arch. Virol. 141 (1996) 685–699.
[47] Y. Modis, S. Ogata, D. Clements, S.C. Harrison, A ligand-binding pocket in the dengue virus envelope glycoprotein, Proc. Natl. Acad. Sci. U.S.A. 100 (2003) 6986–6991.
[48] A. Ahn, D.L. Gibbons, M. Kielian, The fusion peptide of Semliki Forest virus associates with sterol-rich membrane domains, J. Virol. 76 (2002) 3267–3275.
[49] S.T. Yang, E. Zaitseva, L.V. Chernomordik, K. Melikov, Cell-penetrating peptide induces leaky fusion of liposomes containing late endosome-specific anionic lipid, Biophys. J. 99 (2010) 2525–2533.
[50] A.G. Schmidt, P.L. Yang, S.C. Harrison, Peptide inhibitors of flavivirus entry derived from the E protein stem, J. Virol. 84 (2010) 12549–12554.
[51] A.J. Perez-Berna, G. Pabst, P. Laggner, J. Villalain, Screening a peptide library by DSC and SAXD: comparison with the biological function of the parent proteins, PLoS One 4 (2009) e4356.
[52] R.M. Epand, Lipid polymorphism and protein–lipid interactions, Biochim. Biophys. Acta 1376 (1998) 353–368.

[53] J.M. White, S.E. Delos, M. Brecher, K. Schornberg, Structures and mechanisms of viral membrane fusion proteins: multiple variations on a common theme, Crit. Rev. Biochem. Mol. Biol. 43 (2008) 189–219.
[54] L.V. Chernomordik, M.M. Kozlov, Protein–lipid interplay in fusion and fission of biological membranes, Annu. Rev. Biochem. 72 (2003) 175–207.
[55] L.V. Chernomordik, J. Zimmerberg, M.M. Kozlov, Membranes of the world unite! J. Cell Biol. 175 (2006) 201–207.
[56] A.J. Perez-Berna, A. Bernabeu, M.R. Moreno, J. Guillen, J. Villalain, The pre-transmembrane region of the HCV E1 envelope glycoprotein: interaction with model membranes, Biochim. Biophys. Acta 1778 (2008) 2069–2080.
[57] M.R. Moreno, A.J. Perez-Berna, J. Guillen, J. Villalain, Biophysical characterization and membrane interaction of the most membranotropic region of the HIV-1 gp41 endodomain, Biochim. Biophys. Acta 1778 (2008) 1298–1307.
[58] J. Guillen, M.R. Moreno, A.J. Perez-Berna, A. Bernabeu, J. Villalain, Interaction of a peptide from the pre-transmembrane domain of the severe acute respiratory syndrome coronavirus spike protein with phospholipid membranes, J. Phys. Chem. B 111 (2007) 13714–13725.
[59] S.R. Lin, G. Zou, S.C. Hsieh, M. Qing, W.Y. Tsai, P.Y. Shi, W.K. Wang, The helical domains of the stem region of dengue virus envelope protein are involved in both virus assembly and entry, J. Virol. 85 (2011) 5159–5171.
[60] R. Fritz, J. Blazevic, C. Taucher, K. Pangerl, F.X. Heinz, K. Stiasny, The unique transmembrane hairpin of the flavivirus fusion protein E is essential for membrane fusion, J. Virol. 85 (2011) 4377–4385.
[61] M. Porotto, C.C. Yokoyama, L.M. Palermo, B. Mungall, M. Aljofan, R. Cortese, A. Pessi, A. Moscona, Viral entry inhibitors targeted to the membrane site of action, J. Virol. 84 (2010) 6760–6768.

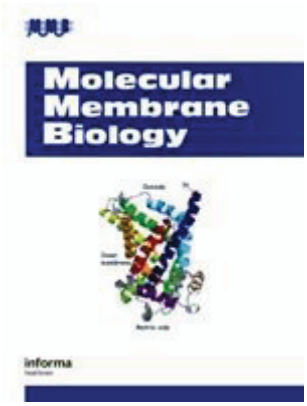

Hydrophobic segment of dengue virus C protein.

Interaction with model membranes.

Henrique Nemésio, M. Francisca Palomares-Jerez, José Villalaín

Instituto de Biología Molecular y Celular, Universidad Miguel Hernández, E-03202 Elche (Alicante), Spain

Molecular Membrane Biology 30:4 (2013) 273-287

DOI: 10.3109/09687688.2013.805835

Molecular Membrane Biology, 2013; Early Online, 1–15

informa
healthcare

Hydrophobic segment of dengue virus C protein. Interaction with model membranes

HENRIQUE NEMÉSIO, M. FRANCISCA PALOMARES-JEREZ & JOSÉ VILLALAÍN

Instituto de Biología Molecular y Celular, Universidad Miguel Hernández, Elche-Alicante, Spain

(Received 8 March 2013; and in revised form 25 April 2013)

Abstract

Dengue virus (DENV) C protein is essential for viral assembly. DENV C protein associates with intracellular membranes through a conserved hydrophobic domain and accumulates around endoplasmic reticulum-derived lipid droplets which could provide a platform for capsid formation during assembly. In a previous work we described a region in DENV C protein which induced a nearly complete membrane rupture of several membrane model systems, which was coincident with the theoretically predicted highly hydrophobic region of the protein. In this work we have carried out a study of the binding to and interaction with model biomembranes of a peptide corresponding to this DENV C region, $DENV2_{C6}$. We show that $DENV2_{C6}$ partitions into phospholipid membranes, is capable of rupturing membranes even at very low peptide-to-lipid ratios and its membrane-activity is modulated by lipid composition. These results identify an important region in the DENV C protein which might be directly implicated in the DENV life cycle through the modulation of membrane structure.

Keywords: *Membrane protein, viral protein, viral peptide*

Introduction

There are three genera in the *Flaviviridae* family: *Flavivirus*, *Hepacivirus and Pestivirus*. Dengue virus (DENV) is sorted into the *Flavivirus* genus and it is the leading cause of arboviral diseases in the tropical and subtropical regions, with an estimation of 390 million dengue infections per year (Bhatt et al. 2013). DENV comprises four serologically and genetically related viruses, DENV viruses 1–4, which possess 69–78% identity at the amino acid level (Urcuqui-Inchima et al. 2010). DENV infections might be either asymptomatic or result in what is known as dengue fever; some individuals develop a severe and potentially life-threatening disease known as dengue haemorrhagic fever or dengue shock syndrome, leading to more than 25,000 deaths per annum. Despite the urgent medical need and considerable efforts, no antivirals or vaccines against DENV virus are currently available, so that more than 2 billion people, mainly in less developed countries, are at risk in the world (Pastorino et al. 2010). Furthermore, due to the increased global temperature and travelling, there is a real risk of dispersion of the mosquito vector to previously unaffected zones. Although several compounds have been identified to inhibit DENV replication (Noble et al. 2010), there is actually no clinical treatment for DENV infection.

DENV is a positive-sense, single-stranded RNA virus with approximately 10.7 kb. It contains untranslated regions both at the 5′ and 3′ ends, flanking a single open reading frame (ORF) encoding a polyprotein of over 3000 amino acids, which is subsequently cleaved by cellular and viral proteases into three structural proteins, C, prM and E, and seven non-structural proteins, NS1, NS2A, NS2B, NS3, NS4A, NS4B and NS5 (Perera and Kuhn 2008). Similarly to other enveloped viruses, the DENV virus enters the cells through receptor mediated endocytosis (Bressanelli et al. 2004, Mukhopadhyay et al. 2005, Kielian and Rey 2006, Perera and Kuhn 2008) and rearranges internal cell membranes to establish specific sites of replication (Miller et al. 2007, Miller and Krijnse-Locker 2008, Welsch et al. 2009). Details about DENV replication process remain largely unclear, but most if not all of the DENV proteins are involved and function in a complex web of protein-protein and protein-lipid interactions. The mature DENV virus has a capsid (C) protein core complexed with the RNA genome (forming the

Correspondence: Dr José Villalaín, Instituto de Biología Molecular y Celular, Universidad 'Miguel Hernández', E-03202 Elche-Alicante, Spain. Tel: +34 966658762. Fax: +34 966658762. E-mail: jvillalain@umh.es

ISSN 0968-7688 print/ISSN 1464-5203 online © 2013 Informa UK, Ltd.
DOI: 10.3109/09687688.2013.805835

nucleocapsid), surrounded by a host-derived lipid bilayer in which multiple copies of the viral envelope (E) and membrane (M) proteins are embedded.

The C proteins of *Flaviviridae* are dimeric, basic, have an overall helical fold and are responsible for genome packaging. These proteins are essential for viral assembly in order to ensure specific encapsidation of the viral genome. Nonetheless, little is known about the recognition of the viral RNA by protein C or RNA packaging. Furthermore, protein C seems to associate with intracellular membranes through a conserved hydrophobic domain (Markoff et al. 1997). Recently, it has been found that protein C accumulates around endoplasmic reticulum (ER) derived lipid droplets (Samsa et al. 2009). Similarly to other enveloped viruses, DENV replicates its genome in a membrane-associated replication complex, and morphogenesis and virion budding has been suggested to take place in the ER or modified ER membranes. These modified membranes could provide a platform for capsid formation during viral assembly (Samsa et al. 2009). Although *Flaviviridae* C proteins are shorter than the *Hepacivirus* core proteins, their roles should be similar as well as their capacity to bind to phospholipid membranes (Boulant et al. 2005, Perez-Berna et al. 2008, Ivanyi-Nagy and Darlix 2010). From the analysis of structural parameters (Boulant et al. 2005), dimers of protein C contain a highly hydrophobic region comprising the α2 helices of each of the monomers. This region also forms a concave groove which would be the responsible of binding to the viral membrane. On the other hand, this region could be also involved in lipid droplet association (Martins et al. 2012). Since no specific treatment is currently available for treating DENV infection, it is therefore essential to understand the DENV life cycle as well as protein/protein and protein/membrane interactions.

In a previous work (Nemesio et al. 2011), we described a region that induced a nearly complete membrane rupture of several membrane model systems, which was coincident with a theoretically predicted highly hydrophobic region of protein C. The main objective of this work has been the characterization of this region in the presence of different membrane model systems, in short $DENV2_{C6}$ (Figure 1A), using fluorescence spectroscopy techniques to assess membrane rupture, alteration of the fluorescence signal of FPE-labelled membranes in the presence of this peptide as well as steady state-fluorescence anisotropy. Calorimetric studies using differential scanning calorimetry (DSC) and Fourier transform infrared spectroscopy (FTIR) were also performed, using several model membrane systems. This characterization was motivated by the fundamental role this protein might play in the viral infection and the importance of this specific region for the interaction with biological membranes, an essential step of enveloped viruses' infection. Moreover, an understanding of protein-membrane molecular interactions during the DENV replication cycle might allow the identification of new targets for the treatment of Dengue virus infection (Table I).

Materials and methods

Materials and reagents

The peptide $DENV2_{C6}$ corresponding to the sequence ^{39}GRGPLKLFMALVAFLRFL^{56} from Dengue Virus Type 2 NGC (New Guinea C) C protein (with N-terminal acetylation and C-terminal acetylation) was obtained from Genemed Synthesis (San Antonio, TX, USA). This peptide was purified by reverse-phase HPLC (Kromasil C18, 250 × 4.6 mm, with a flow rate of 1 ml/min, solvent A, 0.1% trifluoroacetic acid, solvent B, 99.9% acetonitrile and 0.1% trifluoroacetic acid) to > 95% purity and its composition and molecular mass were confirmed by amino acid analysis and mass spectroscopy. Considering that trifluoroacetate has a strong infrared absorbance at approximately 1673 cm^{-1}, that can interfere significantly with the peptide Amide I band (Surewicz et al. 1993), residual trifluoroacetic acid, used both in peptide synthesis and in the HPLC mobile phase, was removed after several lyophilization/solubilization cycles in 10 mM HCl (Zhang et al. 1992). Bovine brain phosphatidylserine (BPS), bovine liver L-α-phosphatidylinositol (BPI), cholesterol (Chol), egg phosphatidic acid (EPA), egg L-α-phosphatidylcholine (EPC), egg sphingomyelin (ESM), egg trans-phosphatidylated L-α-phosphatidylethanolamine (TPE), tetramyristoyl cardiolipin (CL), bovine liver lipid extract, bis(monomyristoylglycero) phosphate (14BMP), bis(monooleoylglycero)phosphate (18BMP), 1,2-dimyristoilphosphatidylcholine (DMPC), 1,2-dimyristoylphosphatidylglycerol (DMPG), 1,2-dimyristoylphosphatidylserine (DMPS), 1,2-dimyristoylphosphatidic acid (DMPA), N-palmitoyl-D-erythro-sphingosylphosphorylcholine (PSM) and 1,2-dielaidoyl-sn-glycero-3-phosphatidylethanolamine (DEPE) were obtained from Avanti Polar Lipids (Alabaster, AL, USA). The lipid composition of the synthetic ER membrane was EPC/CL/BPI/TPE/BPS/EPA/ESM/Chol at a molar ratio of 59:0.37:7.4:18:3.1:1.2:3.4:7.8 (Krainev et al. 1995). 5-Carboxyfluorescein (CF, > 95% by HPLC), fluorescein isothiocyanate-labeled dextrans FD20 and FD70 (with respective average molecular weights of 20,000 and 70,000), deuterium oxide (99.9% by atom),

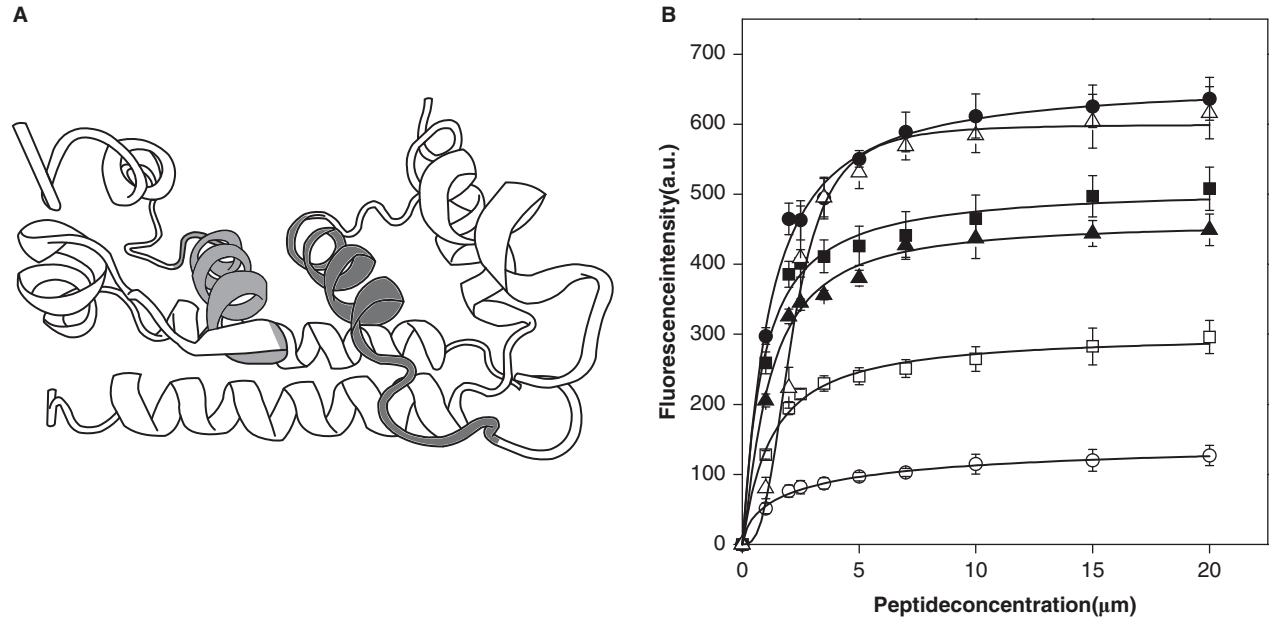

Figure 1. (A) Scheme indicating the position of the domain corresponding to $DENV2_{C6}$ peptide on the DENVC structure (grey shading). The dimer of DENVC has been represented (Ma et al. 2004). (B) Fluorescence signal amplitude of FPE versus peptide concentration in μM to determine $DENV2_{C6}$ peptide binding to membrane model systems with different lipid compositions. The lipid compositions used were EPC (■), EPC/CHOL at a molar ratio of 5:1 (○), EPC/ESM/CHOL at a molar ratio of 5:2:1 (□), EPC/EPA at a molar ratio of 5:2 (●), EPC/BPS at a molar ratio of 5:2 (▲) and synthetic ER membranes (Δ).The lipid concentration was 200 μM. Vertical bars indicate standard deviations of the mean of triplicate samples.

Triton X-100, EDTA and HEPES were purchased from Sigma-Aldrich (Madrid, ES). 1,6-diphenyl-1,3,5-hexatriene (DPH) and 1-(4-trimethylammoniumphenyl)-6-phenyl-1,3,5-hexatriene (TMA-DPH) and *N*-(Fluorescein-5-thiocarbamyl)-1,2-dihexadecanoyl-*sn*-glycero-3-phosphoethanolamine (FPE) were obtained from Molecular Probes (Eugene, OR, USA). All other chemicals were commercial samples of the highest purity available (Sigma-Aldrich, Madrid, Spain). Water was deionized, twice-distilled and passed through a Milli-Q equipment (Millipore Ibérica, Madrid, Spain) to a resistivity higher than 18 MΩ·cm.

Vesicle preparation

Aliquots containing the appropriate amount of lipid in chloroform/methanol (2:1 vol/vol) were placed in a test tube, the solvents were removed by evaporation under a stream of O_2-free N_2, and finally, traces of solvents were eliminated under vacuum in the dark for > 3 h. The lipid films were re-suspended in an appropriate buffer and incubated either at 25°C or 10°C above the phase transition temperature (T_m) with intermittent vortexing for 30 min to hydrate the samples and obtain multilamellar vesicles (MLV). The samples were frozen and thawed five times to ensure complete homogenization and maximization of peptide/lipid contacts with occasional vortexing. Large unilamellar vesicles (LUV) with mean diameters of 0.1 μm and 0.2 μm were prepared from MLV by the extrusion method (Mayer et al. 1986) using polycarbonate filters with a pore size of 0.1 μm and 0.2 μm (Nuclepore Corp., Cambridge, CA, USA). For infrared spectroscopy, aliquots containing the appropriate amount of lipid in chloroform/methanol (2:1, v/v) were placed in a test tube containing 200 μg of dried lyophilized peptide. After vortexing, the solvents were removed by evaporation under a stream of O_2-free N_2, and finally, traces of solvents were eliminated under vacuum in the dark for more than three hours. The samples were hydrated in 100 μl of D_2O buffer containing 20 mM HEPES, 100 mM NaCl, 0.1 mM EDTA, pH 7.4 and incubated at 10°C above the T_m of the phospholipid mixture with intermittent vortexing for 45 min to hydrate the samples and obtain MLV. The samples were frozen and thawed as above. Finally the suspensions were centrifuged at 14,000 rpm at 25°C for 10 min to remove the peptide unbound to the membranes. The pellet was re-suspended in 25 μl of D_2O buffer and incubated for 45 min at 10°C above the T_m of the lipid mixture, unless stated otherwise. The phospholipid and peptide concentration were measured by methods described previously (Böttcher et al 1961, Edelhoch 1967).

Table I. Alignment (ClustalW2) of $DENV2_{C6}$ peptide from reference strains representing the major genotypes of Dengue virus. The $DENV2_{C6}$ and consensus sequences are shown beneath the alignment.

DENV	Strain	Sequence	DENV	Strain	Sequence
Type 2	MD917	GRGPLKLFMALVAFLRFL	Type 3	C036094-C	GQGPMKLVMAFIAFLRFL
	BIDV687	GRGPLKLFMALVAFLRFL		ThD31283_98-C	GQGPMKLVMAFIAFLRFL
	MD903	GRGPLKLFMALVTFLRFL		BIDV1831VN2007-C	GQGPMKLVMAFIAFLRFL
	BIDV633	GHGPLKLFMALVAFLRFL		07CHLS001-C	GQGPMKLVMAFIAFLRFL
	CSF381-C	GRGPLKLFMALVAFLRFL		BIDV1874VN2007-C	GQGPMKLVMAFIAFLRFL
	MD1504	GRGPLKLFMALVAFLRFL		05K797DK1-C	GQGPMKLVMAFIAFLRFL
	CSF63-C	GRGPLKLFMALVAFLRFL		98TWmosq-C	GQGPMKLVMAFIAFLRFL
	DakArD20761	GRGPLKLFMALVAFLRFL		BR29002-C	GQGPMKLVMAFIAFLRFL
	DF755-C	GRGPLKLFMALVAFLRFL		98-C	GQGPMKLVMAFIAFLRFL
	DF707	GRGPLKLFMALVAFLRFL		TB55i-C	GQGPMKLVMAFIAFLRFL
Type 1	02_20-C	GQGPMKLVMAFIAFLRFL	Type 4	2A-C	GKGPLRMVLAFITFLRVL
	ThD1004901-C	GQGPMKLVMAFIAFLRFL		BIDV2165VE1998-C	GKGPLRMVLAFITFLRVL
	BIDV1841-C	GQGPMKLVMAFIAFLRFL		BIDV2170VE1999-C	GKGPLRMVLAFITFLRVL
	BIDV1926VN2008	GQGPMKLVMAFIAFLRFL		Vp4-C	GKGPLRMVLAFITFLRVL
	BIDV1800	GQGPMKLVMAFIAFLRFL		Yama-C	GKGPLRMVLAFITFLRVL
	BIDV1323	GQGPMKLVMAFIAFLRFL		Sin897695-C	GKGPLRMVLAFITFLRVL
	BIDV2243VE2007	GQGPMKLVMAFIAFLRFL		rDEN4del30-C	GKGPLRMVLAFITFLRVL
	05K4147DK1	GQGPMKLVMAFIAFLRFL		H241-C	GKGPLRMVLAFITFLRVL
	297arg00	GQGPMKLVMAFIAFLRFL		ThD4048501-C	GKGPLRMVLAFITFLRVL
	BIDV2143-C	GQGPMKLVMAFIAFLRFL		ThD4047697-C	GKGPLRMVLAFITFLRVL
	Consensus sequence	*:**::::.*:::***.*			
	PEPTIDE $DENV2_{C6}$	GRGPLKLFMALVAFLRFL			

Membrane leakage measurement

LUVs with a mean diameter of 0.1 μm (for CF) and 0.2 μm (for FD20/FD70) were prepared as indicated above in buffer containing 10 mM Tris, 20 mM NaCl, pH 7.4 (at 25°C), and either CF at a concentration of 40 mM or FD20/FD70 at a concentration of 100 mg/ml. Non-encapsulated CF or FD20/FD70 were separated from the vesicle suspension through a filtration column containing Sephadex G-50 or Sephadex S500HR Sephacryl, respectively (GE Healthcare), eluted with buffer containing 10 mM Tris, 10 mM NaCl and 0.1 mM EDTA at pH 7.4. Membrane rupture (leakage) of intraliposomal CF was assayed by treating the probe-loaded liposomes (final lipid concentration, 0.125 mM) with the appropriate amount of peptide (peptide-to-lipid molar ratio of 1:25) on microtiter plates using a microplate reader (FLUOstar; BMG Labtech, Offenburg, Germany), stabilized at 25°C, each well containing 170 μl. The medium in the microtiter plates was continuously stirred to allow the rapid mixing of peptide and vesicles. Membrane leakage of intraliposomal FD20 or FD70 was carried out using 5 × 5 mm quartz cuvettes stabilized at 25°C in a final volume of 400 μl (100 μM lipid concentration). Leakage was assayed until no more change in fluorescence was obtained. The fluorescence was measured using a Varian Cary Eclipse spectrofluorimeter. Changes in fluorescence intensity were recorded with excitation and emission wavelengths set at 492 and 517 nm, respectively. Excitation and emission slits were set at 5 nm. One hundred per cent release was achieved by adding Triton X-100 to either the microtiter plate or the cuvette to a final concentration of 0.5% (w/w). Fluorescence measurements were made initially with probe-loaded liposomes, afterwards by adding peptide solution and finally adding Triton X-100 to obtain 100% leakage. Leakage was quantified on a percentage basis according to the equation, % Release = $100(F_f\text{-}F_0)/ (F_{100}\text{-}F_0)$, F_f being the equilibrium value of fluorescence after peptide addition, F_0 the initial fluorescence of the vesicle suspension and F_{100} the fluorescence value after addition of Triton X-100.

Steady-state fluorescence anisotropy

DPH and its derivatives represent popular membrane fluorescent probes for monitoring the organization and dynamics of membranes; whereas DPH is known to partition mainly into the hydrophobic core of the membrane, TMA-DPH is oriented at the membrane bilayer with its charge localized at the lipid-water interface (Lentz 1993). MLVs were formed in a buffer composed of 20 mM HEPES, 100 mM NaCl and 0.1 mM EDTA at pH 7.4 (at 25°C). Aliquots of TMA-DPH or DPH in N, N′-dimethylformamide (0.2 mM) were directly added to the lipid dispersion to obtain a probe/lipid molar ratio of 1:500. Samples were incubated for 15 and 60 min, respectively, when

TMA-DPH and DPH were used, 10°C above the T_m of each lipid for 1 h, with occasional vortexing. All fluorescence studies were carried out using 5 × 5 mm quartz cuvettes in a final volume of 400 µl (315 µM lipid concentration). All the data were corrected for background intensities and progressive dilution. The steady state fluorescence anisotropy, <r>, was measured with an automated polarization accessory using a Varian Cary Eclipse fluorescence spectrometer, coupled to a Peltier device (Varian) for automatic temperature change. The vertically and horizontally polarized emission intensities, elicited by vertically polarized excitation, were corrected for background scattering by subtracting the corresponding polarized intensities of a phospholipid preparation lacking probes. The G-factor, accounting for differential polarization sensitivity, was determined by measuring the polarized components of the fluorescence of the probe with horizontally polarized excitation ($G = I_{HV}/I_{HH}$). Samples were excited at 360 nm and emission was recorded at 430 nm, with excitation and emission slits of 5 nm. Anisotropy values were calculated using the formula $<r> = (I_{VV}-GI_{VH})/(I_{VV}+2GI_{VH})$, where I_{VV} and I_{VH} are the measured fluorescence intensities (after appropriate background subtraction) with the excitation polarizer vertically oriented and the emission polarizer vertically and horizontally oriented, respectively.

Fluorescence measurements using FPE-labelled membranes

LUVs with a mean diameter of 0.1 µM were prepared in buffer containing 10 mM Tris-HCl at pH 7.4 (at 25°C). The vesicles were labelled exclusively in the outer bilayer leaflet with FPE as described previously (Wall et al. 1995). LUVs were incubated with 0.1 mol% FPE dissolved in ethanol (never more than 0.1% of the total aqueous volume) at 37°C for 1 h in the dark. Any remaining unincorporated FPE was removed by gel filtration on Sephadex G-25 column equilibrated with the appropriate buffer. FPE-vesicles were stored at 4°C until use in an O_2-free atmosphere. Fluorescence time courses of FPE-labelled vesicles were measured after the desired amount of peptide was added into 400 µl of lipid suspensions (200 µM lipid) using a Varian Cary Eclipse fluorescence spectrometer. Excitation and emission wavelengths were set at 490 and 520 nm, respectively, using excitation and emission slits set at 5 nm. Temperature was controlled with a thermostatic bath at 25°C. The contribution of light scattering to the fluorescence signals was measured in experiments without the dye and was subtracted from the fluorescence traces. Data were fitted to a hyperbolic binding model (Golding et al. 1996) using the equations $F = F_{max}[P]/(K_d+[P])$ or $F = F_{max}[P]^n/(K_d+[P]^n)$, where F is the fluorescence variation, F_{max} the maximum fluorescence variation, $[P]$ the peptide concentration, K_d the dissociation constant of the membrane binding process and n, the Hill coefficient.

Differential scanning calorimetry

MLVs were formed as stated above in 20 mM HEPES, 100 mM NaCl, 0.1 mM EDTA, pH 7.4. The peptide was added to obtain a peptide/lipid molar ratio of 1:15. The final volume was 0.8 ml (0.6 mM lipid concentration), and incubated 10°C above the T_m of each phospholipid for 1 h with occasional vortexing. Differential scanning calorimetry (DSC) experiments were performed in a VP-DSC differential scanning calorimeter (MicroCal LLC, MA, USA) under a constant external pressure of 30 psi in order to avoid bubble formation and samples were heated at a constant scan rate of 60°C/h. Experimental data were corrected from small mismatches between the two cells by subtracting a buffer baseline prior to data analysis. The excess heat capacity functions were analysed using Origin 7.0 (Microcal Software). The thermograms were defined by the onset and completion temperatures of the transition peaks obtained from heating scans. In order to avoid artefacts due to the thermal history of the sample, the first scan was never considered; second and further scans were carried out until a reproducible and reversible pattern was obtained.

Infrared spectroscopy

Approximately 25 µl of a pelleted sample in D_2O were placed between two CaF_2 windows separated by 56-µm thick Teflon spacers in a liquid demountable cell (Harrick, Ossining, NY, USA). The spectra were obtained in a Bruker IF66S spectrometer using a deuterated triglycine sulphate detector. Each spectrum was obtained by collecting 250 interferograms with a nominal resolution of 2 cm^{-1}, transformed using triangular apodization and, in order to average background spectra between sample spectra over the same time period, a sample shuttle accessory was used to obtain sample and background spectra. The spectrometer was continuously purged with dry air at a dew point of −40°C in order to remove atmospheric water vapour from the bands of interest. All samples were equilibrated at the lowest temperature for 20 min before acquisition. An external bath circulator, connected to the infrared spectrometer, controlled the sample temperature. For temperature studies, samples were scanned using 2°C intervals

and a 2-min delay between each consecutive scan. The data were analyzed as previously described (Guillen et al. 2010, Palomares-Jerez and Villalain 2011).

Results

Since peptide $DENV2_{C6}$ lacks a Trp residue and therefore intrinsic fluorescence, we have used the electrostatic surface potential probe FPE (Moreno et al. 2007) to monitor its ability to bind to model membranes composed of different lipid compositions at different lipid/peptide ratios (Figure 1B). $DENV2_{C6}$ had a higher affinity for model membranes composed of zwitterionic, i.e., EPC, and negatively charged phospholipids, i.e., EPC/EPA and EPC/BPS, as well as the complex membrane simulating ER membranes. Interestingly, lower affinity was observed for liposomes composed of EPC/Chol and EPC/SM/Chol (Figure 1B). Except for $DENV2_{C6}$ in the presence of ER-like model membranes, all data could be adjusted to a binding profile having either a sigmoidal (Hill coefficient of approximately 1) or a hyperbolic dependence, which might suggest that the interaction of the peptide with the membrane was monomeric. For $DENV2_{C6}$ in the presence of ER-like membranes, a sigmoidal dependence with a Hill coefficient of approximately 2.9 could be observed, suggesting that the interaction of the peptide with this complex membrane could be through a trimeric form of the peptide.

The effect of the $DENV2_{C6}$ peptide on the release of encapsulated fluorophores trapped inside model membranes was studied to explore the interaction of the peptide with phospholipid membranes (Palomares-Jerez and Villalain 2011). $DENV2_{C6}$ was able to induce the release of encapsulated CF in a dose-dependent manner and the effect was significantly different for different lipid compositions (Figure 2A). Liposomes composed of EPC elicited significant leakage effects, since $DENV2_{C6}$ induced leakage values of about 83% at a very high lipid/peptide ratio of 800:1. Since it is known that late endosome membranes are the place where membrane fusion entry takes place and have high concentrations of negatively charged phospholipids, namely PS and BMP (Zaitseva et al. 2010), we have tested membranes containing different contents of negatively-charged phospholipids. However, liposomes composed of negatively-charged phospholipids presented lower leakage values than zwitterionic membranes. At the lipid/peptide ratio of 800:1, liposomes composed of EPC/EPA and EPC/BPS at molar ratios of 5:2 as well as the ER-like complex mixture presented leakage values of 30–20% (Figure 2A). Liposomes composed of EPC/BMP at a molar ratio of 5:2 presented similar leakage values at similar lipid/peptide ratios (Figure 2A).

Significantly lower values were found for liposomes composed of liver lipid extract where leakage values of about 10% were observed at a lipid/peptide ratio of 300:1 (Figure 2A). Since Chol seems to be required in the fusion process (Carro and Damonte 2013), we have tested the presence of Chol in negatively-charged membranes. However, addition of Chol to negatively charged lipid compositions, i.e., EPC/EPA/Chol and EPC/BPS/Chol at a molar ratio of 5:2.1, did not change significantly the leakage values, since at a lipid/peptide ratio of 800:1 leakage values of 10 and 35% were observed, respectively (Figure 2B). In the same way, Chol did not change leakage values when it was added to EPC liposomes at diverse molar ratios: EPC/Chol at molar ratios of 5:1, 5:2 and 5:3 presented leakage values of about 83%, 89% and 93%, respectively (Figure 2B). We have also used membranes containing both SM and Chol lipids, since their presence has been related to the occurrence of laterally segregated membrane microdomains or 'lipid rafts'. Interestingly, it has been shown that viral active replication complexes and/or non-structural proteins can be associated to lipid rafts (Noisakran et al. 2008). Different EPC, ESM and Chol compositions were studied to observe any specific interaction between the peptide and the phospholipids (Figure 2C). $DENV2_{C6}$ elicited a leakage value of about 85% for liposomes containing EPC/ESM at a molar ratio of 5:2, similar to the leakage values found for EPC/ESM/Chol at a molar ratio of 5:2:1 (Figure 2C). Likewise, EPC/ESM/Chol at molar ratios of 5:1:1, 5:2:1 and 5:3:1 presented leakage values of about 95%. From all these data it could be concluded that neither Chol nor ESM affect significantly the interaction of $DENV2_{C6}$ with lipid membranes, yet leakage was noticeably lower when negatively charged phospholipids were used.

We have studied the effect of the $DENV2_{C6}$ peptide on membrane rupture using a complex lipid composition resembling the ER-like membrane to assess the effect of each component of the complex mixture (Figure 2D). The synthetic ER complex membrane used above was composed of EPC, CL, BPI, TPE, BPS, EPA, ESM and Chol at a molar ratio of 59:0.37:7.4:18:3.1:1.2:3.4:7.8 (Krainev et al. 1995). Therefore we have designed an additional ER synthetic membrane composed of the same types of lipids, i.e., EPC/CL/BPI/TPE/BPS/EPA/ESM/Chol, but at a molar ratio of 58:6:6:6.6:6:6:6 ($ER^{58:6}$).

As shown in Figure 2D, $DENV2_{C6}$ was capable of rupturing the $ER^{58:6}$ complex membrane effectively: at a lipid/peptide ratio of 800:1, about 87% leakage

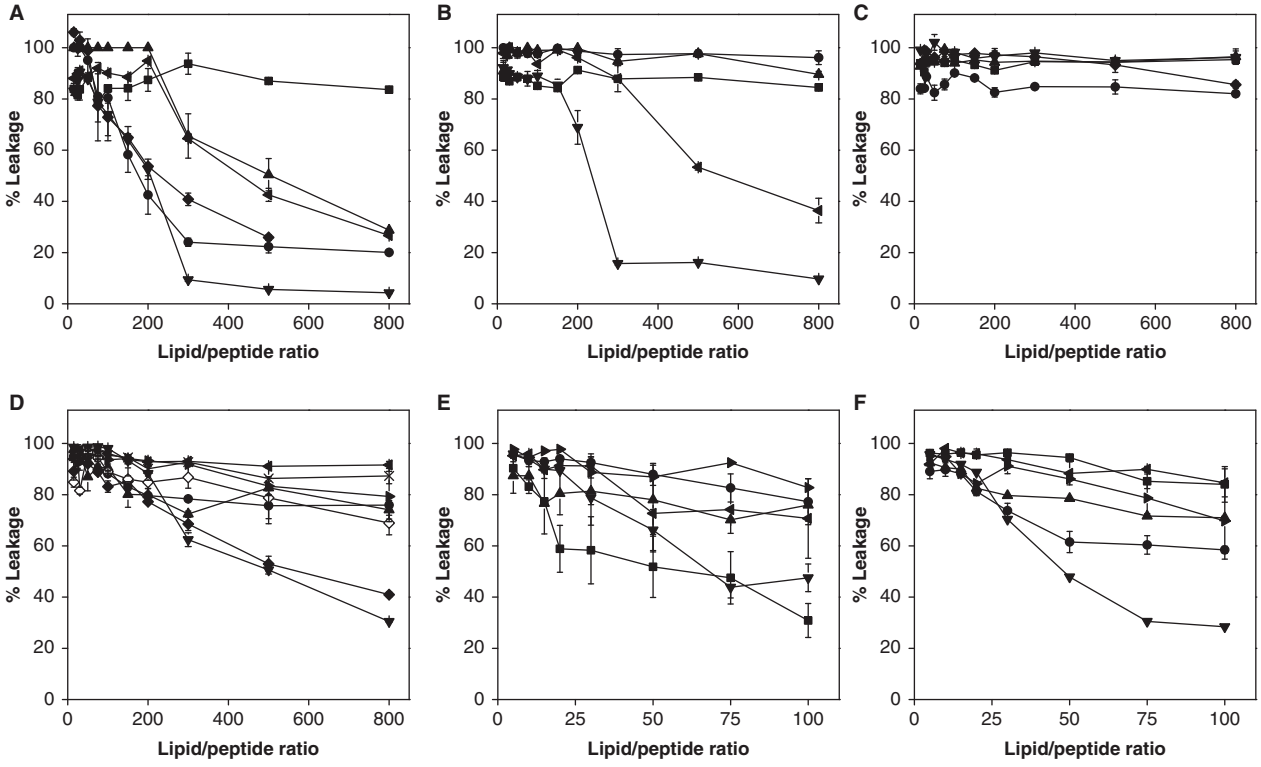

Figure 2. Effect of the $DENV2_{C6}$ peptide on the release (membrane rupture) of CF (A, B, C and D), FD20 (E) and FD70 (F) for general different lipid compositions (A, B, E and F), lipid compositions containing different molar ratios of EPC, ESM and Chol (C) and the $ER^{58:6}$ complex lipid mixture and its variations (D). In (A), model membranes with the following lipid compositions are shown: EPC (■), EPC/EPA in a molar proportion of 5:2 (●), EPC BPS at a molar ratio of 5:2 (▲), total lipid liver extract (▼), ER-like membranes (◀), and EPC/BMP at a molar ratio of 5:2 (◆). In (B), the following model membranes are shown: EPC/CHOL at a molar ratio of 5:1 (■), EPC/CHOL at a molar ratio of 5:2 (▲), EPC/CHOL at a molar ratio of 5:3 (▲), EPC/EPA/CHOL at a molar ratio of 5:2:1 (▼) and EPC/BPS/CHOL at a molar ratio of 5:2:1 (◀). In (C), the following model membranes are shown: EPC/ESM/CHOL at a molar ratio of 5:1:1 (■), EPC/ESM/CHOL at a molar ratio of 5:2:1 (▲), EPC/ESM/CHOL at a molar ratio of 5:3:1 (▲), EPC/ESM/CHOL at a molar ratio of 5:2:2 (▼) and EPC/ESM at a molar ratio of 5:2 (◇). In (D), the following model membranes are shown: ER $^{58:6}$ (x), $ER^{58:6}$ minus Chol (▲), $ER^{58:6}$ minus BPI (▼), $ER^{58:6}$ minus TPE (◇), $ER^{58:6}$ minus ESM (▲), $ER^{58:6}$ minus BPS (◀), $ER^{58:6}$ minus EPA (◇) and $ER^{58:6}$ minus CL (▶). The lipid compositions of the model membranes used to study the release of FD20 (E) and FD70 (F) were: EPC (■), EPC/CHOL in a molar proportion 5:1 (▲), EPC/ESM/CHOL in a molar proportion 5:2:1 (▲), EPC/EPA in a molar proportion 5:2 (▼), EPC/BPS in a molar proportion 5:2 (◀) and ER-like membranes (▶). Vertical bars indicate standard deviations of the mean of triplicate samples.

was observed. In contrast, a leakage value of about 28% was obtained for the ER-like complex mixture at a lipid/peptide ratio of 800:1 (Figure 2A). When BPS was removed, leakage values slightly increased, whereas when either one of the other lipid molecules was removed, i.e., CL, EPA, ESM or Chol, leakage values decreased to a lesser extent. However, a significant decrease in leakage was observed when either TPE or BPI were removed from the membrane (Figure 2D). Since CF is a relatively small molecule (Stokes radius about 6 Å) we have studied the release of membrane-encapsulated molecules with a larger size (FITC-dextrans FD20 and FD70 having a Stokes radius of about 33 Å and 60 Å, respectively) (Laurent and Granath 1967, Fisher and Cash-Clark 2000). As observed in Figures 2E and 2F, $DENV2_{C6}$ was capable of inducing a significant percentage of leakage for both FD20 and FD70 fluorophores, although at slightly slower different values than CF at comparable lipid/peptide ratios. The capacity of the $DENV2_{C6}$ peptide to induce leakage of FITC-dextrans although to a lower extent than the small CF molecule demonstrates that $DENV2_{C6}$ is capable of forming relatively large pores in the membrane (Yang et al. 2001).

Phospholipids can undergo a cooperative melting reaction linked to the loss of conformational order of the lipid chains; this melting process can be influenced by many types of molecules including peptides and proteins. The effect of $DENV2_{C6}$ on the structural and thermotropic properties of phospholipid membranes was investigated by measuring the steady-state fluorescence anisotropy of the fluorescent probes DPH and TMA-DPH incorporated into model membranes as a function of temperature (Figure 3).

DMPC, in the presence of the peptide, presented a slight decrease in the cooperativity of the thermal

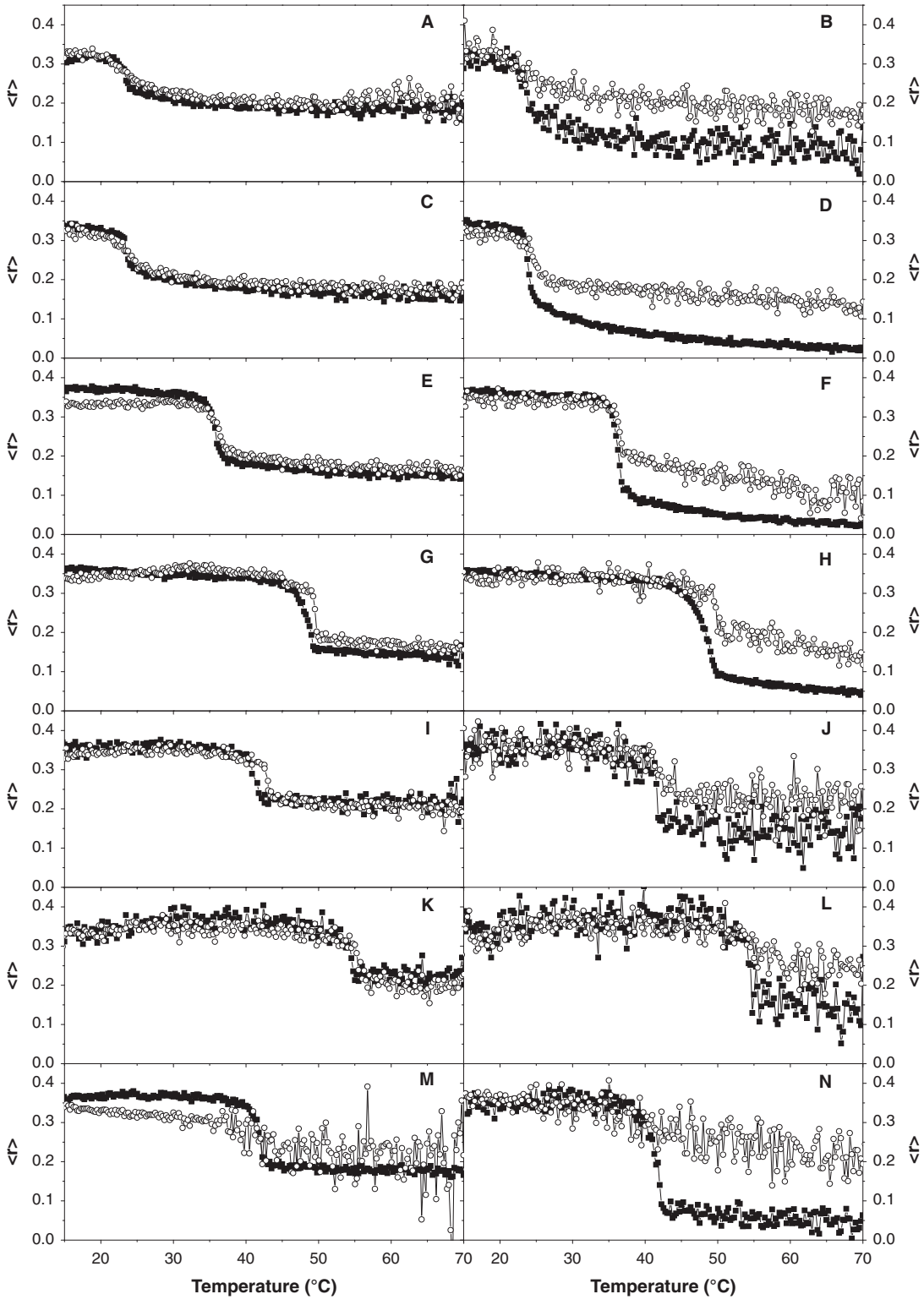

Figure 3. Steady-state anisotropy, <*r*>, of TMA-DPH and DPH (left and right columns, respectively) incorporated into MLVs composed of DMPC (A and B), DMPG (C and D), DMPS (E and F), DMPA (G and H), DPPC (I and J), DSPC (K and L), and 14BMP (M and N) model membranes as a function of temperature. Data correspond to vesicles in the absence (■) and presence of the DENV2$_{C6}$ peptide (○). The peptide to phospholipid molar ratio was 1:15.

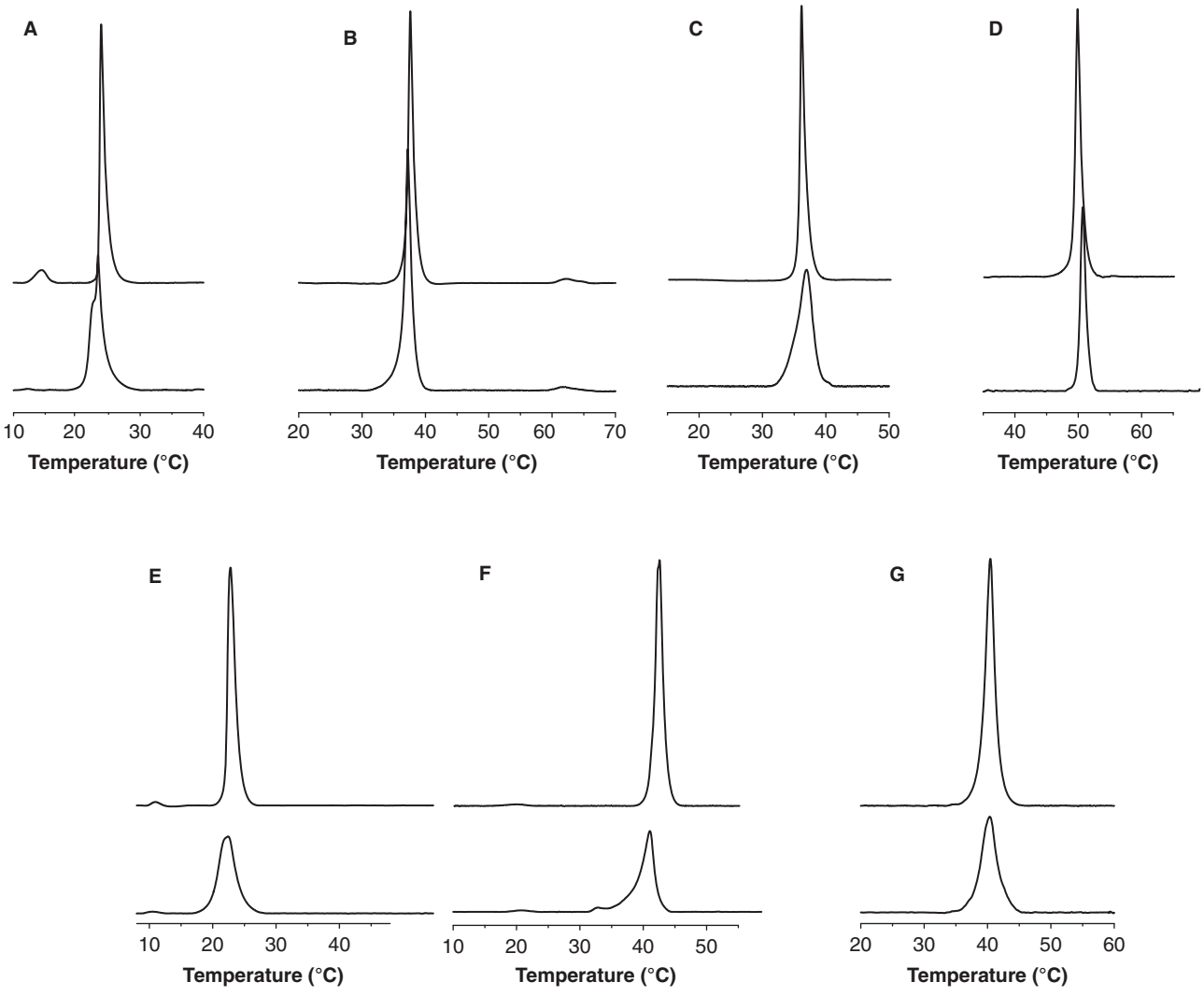

Figure 4. Differential scanning calorimetry heating thermograms corresponding to model membranes composed of (A) DMPC, (B) DEPE, (C) DMPS, (D) DMPA, (E) DMPG, (F) 14BMP and (G) PSM in the absence (top curves) and presence of $DENV2_{C6}$ peptide (bottom curves) at a phospholipid/peptide molar ratio of 15:1. All the thermograms were normalized to the same amount of lipid.

transition, but no change in the T_m of the phospholipid was observed when compared to the pure lipid; additionally, the anisotropy of DPH but not TMA-DPH was increased above the T_m (Figures 3A and B). When the negatively charged phospholipids DMPG and DMPS were studied, $DENV2_{C6}$ induced a similar behavior to that found for DMPC, i.e., a slight decrease in the cooperativity of the thermal transition, no change in the T_m of the phospholipid and the anisotropy of DPH but not TMA-DPH was increased above the T_m (Figures 3C and 3F). The case of DMPA was different, since an increase in T_m of about 2°C was found in the presence of $DENV2_{C6}$ (Figures 3G and 3H). However, the anisotropy of DPH was increased above the T_m but no significant change in cooperativity was found. We also studied the phospholipids DPPC and DSPC to compare with DMPC, since DPPC is longer that DMPC by two methylene groups whereas DSPC is larger by four. Additionally, the T_m of DPPC and DSPC appear at about 43°C and 54°C, whereas the T_m of DMPC appears at about 23°C. As observed in Figures 3I and 3L, $DENV2_{C6}$ induces in both phospholipid a similar behavior as DMPA, since it induces an increase of about 1–2°C in the T_m of both phospholipids as well as an increase in anisotropy above T_m. However, a decrease in cooperativity was observed for DPH but not for TMA-DPH (Figures 3I and 3L). The effect of $DENV2_{C6}$ on another phospholipid, namely 14BMP, was also studied (Figures 4M and 4N). $DENV2_{C6}$ induced a significant decrease in cooperativity in both DPH and TMA-DPH probes, as well as an increase in anisotropy above the T_m for DPH and below the T_m for TMA-DPH. $DENV2_{C6}$ is therefore capable

of affecting the thermal transition T_m of these phospholipids; moreover, the peptide changed the anisotropy of DPH to a greater extent than TMA-DPH, so it should be located slightly deeper in the membrane, influencing the fluidity of the phospholipids (Contreras et al. 2001).

The effect of $DENV2_{C6}$ on the thermotropic phase behavior of phospholipid multilamellar vesicles was also studied using differential scanning calorimetry, DSC (Figure 4). Incorporation of $DENV2_{C6}$ in DMPC at a lipid/peptide ratio of 15:1 significantly altered the thermotropic behavior of the phospholipid, since the peptide completely abolished the pre-transition, and decreased the T_m of the lipid concomitantly with a significant broadening of the main transition (Figure 5A). The main transition of DMPC in the presence of $DENV2_{C6}$ is apparently composed of at least two different peaks, which should be due to mixed phases. In the case of DEPE, $DENV2_{C6}$ induced a slight decrease in the T_m of the phospholipid but no significant broadening was observed, neither on the gel to liquid-crystalline phase transition nor on the lamellar liquid-crystalline to hexagonal-H_{II} phase transition (Figure 4B). For both DMPS and DMPA, $DENV2_{C6}$ slightly decreased the cooperativity of the transitions but no change in T_m was apparent (Figures 4C and 4D). Incorporation of $DENV2_{C6}$ into DMPG membranes at a lipid/peptide ratio of 15:1 (Figure 4E) did not significantly alter the thermotropic behavior of the phospholipid, since the peptide did not completely abolish the pre-transition; however, the main transition of the phospholipid was broadened and shifted to lower temperatures than the T_m. The incorporation of $DENV2_{C6}$ into 14BMP membranes did not alter the thermotropic behavior of the lower temperature endothermic peak (L_{c1}-L_{c2}) but broadened and shifted to lower temperatures the higher temperature peak (L_{c2}-L_{α}) (Figure 4F). Interestingly, a small relatively broad peak appeared at slightly lower temperatures than that of the main transition (Figure 4F).The incorporation of $DENV2_{C6}$ into PSM membranes altered the thermotropic behavior of the phospholipid, inducing a broadening of the main transition peak without altering T_m (Figure 4G). These results are in accordance with those commented above, since $DENV2_{C6}$ is capable of affecting the thermal transition T_m of all phospholipids studied here; furthermore, in some cases, it is capable of inducing the presence of mixed phases.

The infrared Amide I' region of fully hydrated $DENV2_{C6}$ in buffer is shown in Figure 5A. The Amide I' band presented different bands with varying intensities depending on temperature. At low temperatures, two narrow bands at about 1624 and 1693 cm^{-1}, the former with higher intensity that the later, were apparent as well as a broad one with a maximum at about 1651 cm^{-1} (Figure 5A). At higher temperatures, the band at 1624 cm^{-1} shifted to about 1621 cm^{-1} whereas the band at about 1693 cm^{-1} diminished steadily in intensity. Increasing the temperature, a new band at 1683 cm^{-1} appeared and increased gradually in intensity; however, the broad band at about 1651 cm^{-1} did not change significantly in frequency upon increasing the temperature although its intensity decreased. The band at about 1624–1621 cm^{-1} would indicate the existence of aggregated β structures, whereas the broad band with the intensity maxima at about 1651 cm^{-1} would correspond to a mixture of unordered and helical structures (Byler and Susi 1986, Arrondo and Goni 1999). The conjoint appearance of bands at about 1693 cm^{-1} and narrow intense bands at about 1624 cm^{-1} would correspond to aggregated β structures. The band at about 1683 cm^{-1} would correspond to β-turn structures. The global spectrum envelope would suggest that, although helical and unordered structures might be present, the main secondary structure component of $DENV2_{C6}$ consists of aggregated structures (Figure 5A). In the presence of DMPC, the Amide I' envelope of the $DENV2_{C6}$ peptide presented a broad band with a maximum at about 1650 cm^{-1} and a shoulder at about 1625 cm^{-1} at all temperatures (Figure 5B). When $DENV2_{C6}$ was combined with either DMPG (Figure 5C) or 14BMP (Figure 5D), the Amide I' band was reasonably similar to the peptide in solution (Figure 5A), except that the intensity of the different peaks varied. These data would suggest that the main secondary structure component of the peptide should be aggregated structures with some helical and disordered structures in the presence of all lipids, except DMPC. In the presence of DMPC, the main secondary structure component of the peptide should be composed of helical and disordered structures and a minor content of aggregated structures.

We have also analyzed the hydrocarbon CH_2 and ester C = O stretching bands of the phospholipids in the presence of $DENV2_{C6}$ (Figure 6). The frequency maximum of the ester C = O band of pure DMPC displayed two transitions, one at about 12°C, coincident with the pre-transition, and another one at about 24°C, coincident with the main gel to liquid crystalline phase transition (Figure 6A). The hydrocarbon CH_2 frequency displayed only one transition coincident with the main gel to liquid crystalline phase transition at about 24°C (Figure 6D). In the presence of $DENV2_{C6}$, the frequencies of the hydrocarbon CH_2 and ester C = O stretching bands of DMPC displayed only one transition at about 20°C, in accordance with the DSC data (Figure 6A). The absolute

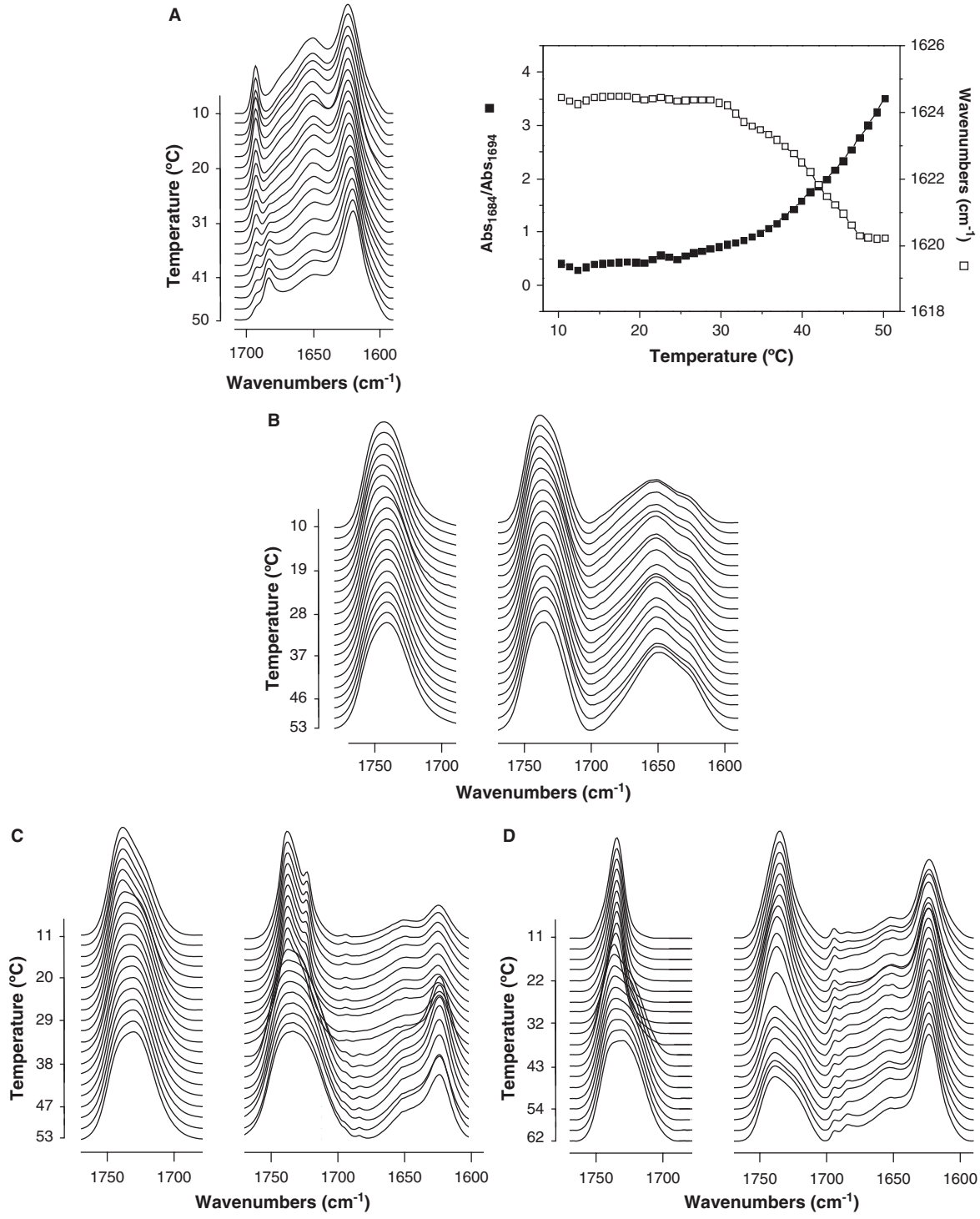

Figure 5. Stacked infrared spectra of the C = O and Amide I' regions of $DENV2_{C6}$ (A) in solution and in the presence of (B) DMPC, (C) DMPG, (D) DMPG and (E) 14BMP at different temperatures as indicated. The pure phospholipid is shown on the left whereas the phospholipid/peptide mixture is shown on the right. The temperature dependence of the frequency at the maximum of the Amide I' region of $DENV2_{C6}$ in solution (□) and the intensity ratio of the 1684 cm^{-1} and 1694 cm^{-1} bands (■) are shown in the upper right figure. The phospholipid/peptide molar ratio was 15:1.

frequency of the C = O band was higher in the presence of the peptide than in its absence, suggesting that the peptide increased the intensity of the 1743 cm^{-1} component relative to the 1727 cm^{-1} one, i.e., the amount of non-hydrogen bonded C = O ester bands increased in the presence of the

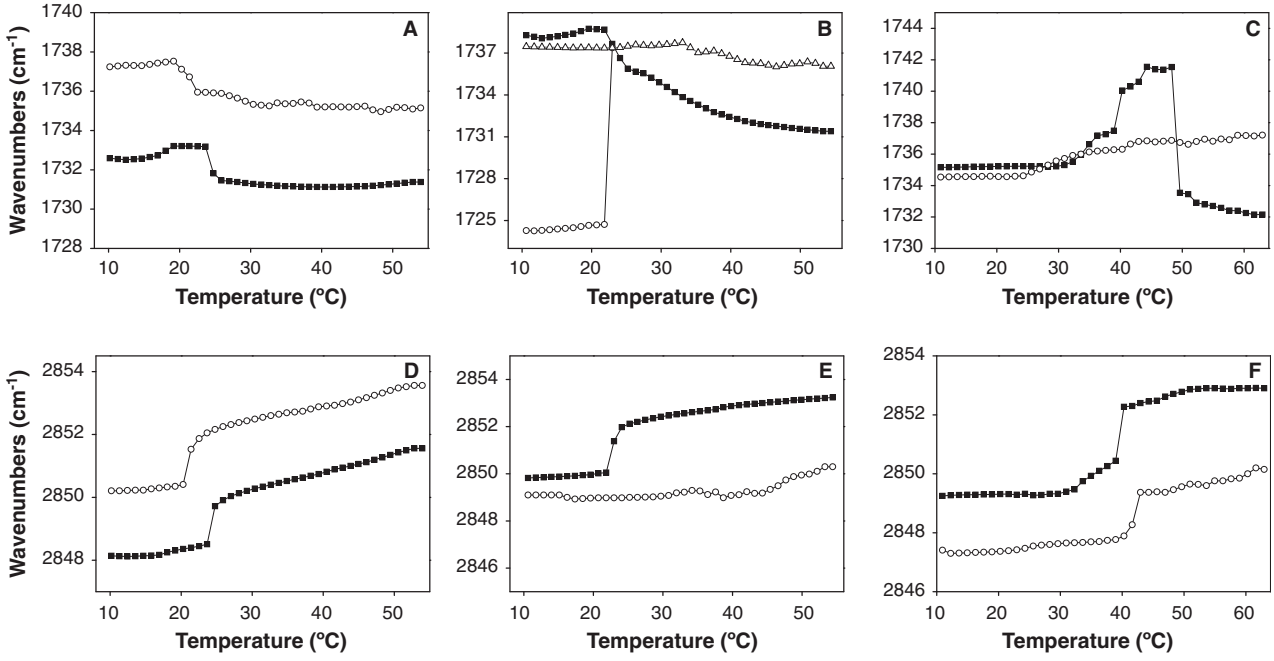

Figure 6. Temperature dependence of the frequencies of the (A, B, C) C = O carbonyl and (D, E, F) CH_2 symmetric stretching bands for samples of (A, D) DMPC, (B, E) DMPG and (C, F) 14BMP in the pure form (■) and in the presence of the $DENV2_{C6}$ peptide (○). The phospholipid/peptide molar ratio was 15:1.

peptide (Blume et al. 1988, Lewis et al. 1994). The same behavior was observed for the CH_2 symmetric stretching band, but in this case the increase in frequency indicates that the peptide increased the mobility of the hydrocarbon chains at all studied temperatures (Figure 6D). The pattern of the thermotropic phase behavior exhibited by pure DMPG was similar to that of pure DMPC, since a transition at about 24°C was observed; however, no change in the frequency of the C = O band of the phospholipid coincidental with the pre-transition of the lipid was observed (Figures 6B and 6E). However, in the presence of the peptide and at low temperatures, the C = O carbonyl band of DMPG presented a main peak and a shoulder, which could suggest the formation of a quasi-crystalline lamellar phase (Figures 6B and 5C) (Epand et al. 1992, Garidel et al. 2000). At higher temperatures the two peaks coalesced into a broad C = O band similar in appearance to the one observed for pure DMPG, suggesting the formation of a normal liquid crystalline phase (Figures 6B and 5D). The ester C = O bands of pure 14BMP displayed a sharp band at low temperatures, with a maximum at about 1735 cm^{-1}, and a broad one at high temperatures, with a maximum at about 1732 cm^{-1} (Figure 5D). The frequency of both CH_2 and ester C = O bands defined two transition temperatures in accordance with the DSC results commented above (Figures 6G and 6H). In the presence of $DENV2_{C6}$, 14BMP displayed two transitions, a broad one at approx. 25°C observed through the ester C = O band frequency (Figure 6C) and a cooperative one at approx. 41°C, observed through the hydrocarbon CH_2 frequency (Figure 6F).

Discussion

DENV C protein is a very basic protein which is essential for virus assembly since it is responsible for genome packaging. DENV C protein has a hydrophobic segment, approximately spanning residues 45–60, which seems to be required for maturation, lipid droplet binding and assembly of the viral particles (Markoff et al. 1997, Samsa et al. 2009). In a previous work (Nemesio et al. 2011), we found a region in DENV C protein that induced membrane rupture of several membrane model systems, which was coincident with the predicted highly hydrophobic region of the protein. Since the biological role/roles of DENV C protein is/are intrinsically related to its interaction with the RNA and the membrane, we have extended our previous work to investigate the binding and interaction of this highly conserved membranotropic region of DENV C, i.e., peptide $DENV2_{C6}$, with different membrane model systems. We have carried out an in-depth biophysical study aimed at the elucidation of the capacity of this region to interact and disrupt membranes, as well as to study the structural and dynamic features which might be relevant for that disruption.

Peptide $DENV2_{C6}$ binds with high affinity to phospholipid model membranes, as it has been previously found for other peptides (Pascual et al. 2005). We have also shown that the $DENV2_{C6}$ peptide is capable of affecting the steady state fluorescence anisotropy of fluorescent probes located in the palisade structure of the membrane. Calorimetry experiments further corroborated these results, and additionally indicated that the $DENV2_{C6}$ peptide induced the formation of mixed lipid phases, enriched and impoverished in peptide. Similar results were obtained by studying the hydrocarbon CH_2 and ester C = O stretching bands of the phospholipids in the presence of $DENV2_{C6}$. The $DENV2_{C6}$ peptide was capable of altering membrane stability causing the release of fluorescent probes, this effect being dependent on the lipid/peptide molar ratio and on lipid composition. The highest CF release was observed for liposomes containing the phospholipid EPC, although lower yet still significant leakage values were observed for liposomes containing negatively-charged phospholipids. It should be recalled that leakage was observed even at a very high lipid/peptide ratio as 800:1. Interestingly, Chol addition did not lower the leakage elicited by the peptide, since its addition to different membrane compositions induced neither higher nor lower leakage values. Apart from that, $DENV2_{C6}$ was able to form relatively large pores in the membrane as demonstrated by the release of relatively large size molecules such as FITC-dextrans. Since $DENV2_{C6}$ affected more significantly membranes containing BMP, which is known to be enriched in the late endosome membrane (Zaitseva et al. 2010), a concerted action of DENV C and E proteins and late endosome lipids should not be ruled out to be essential for viral fusion. Taking into account all these data, the specific disrupting effect elicited by $DENV2_{C6}$ should be primarily due to hydrophobic interactions within the bilayer, although the specific charge of the phospholipid head-groups would influence the extent of membrane leakage. The infrared spectra of the Amide I' region of the fully hydrated $DENV2_{C6}$ peptide in solution displayed a coexistence of mainly aggregated structures although unordered and helical structures were also present. This overall structure did not change in the presence of either DMPG or 14BMP; however, in the presence of DMPC the main components were helical and disordered structures with a minor content of aggregated structures. These results imply that the secondary structure of the $DENV2_{C6}$ peptide was affected by its binding to specific lipid in the membrane, so that membrane binding modulates the secondary structure of the peptide as it has been suggested for other peptides (Guillen et al. 2010, Palomares-Jerez et al. 2010).

Recently, Carvalho et al. (2012) have found that DENVC is capable of binding to several proteins on the surface of intracellular lipid droplets. It could be envisaged that DENVC, specifically interacting with lipid droplet proteins, would initiate a conformational arrangement of the proteins; this conformational changes would allow the direct interaction of the hydrophobic segment where the $DENV2_{C6}$ resides with lipid droplet lipids. The binding of $DENV2_{C6}$ to the membrane and the modulation of the phospholipid biophysical properties that takes place as its consequence could be related to the conformational changes that might occur during the biological activity of the DENV C protein. The conservation of its sequence and hence its structure and physico-chemical properties among different DENV strains should be essential to its function. Our results provide new insight as to how this segment can contribute to the interaction with the membrane. Although the peptide is not deeply buried in the membrane, its interaction with the membrane depends on its composition and it is able to affect the lipid milieu from the membrane surface down to the hydrophobic core. These results identify an important region in the DENV C protein which might be directly implicated in the DENV life cycle. Moreover, an understanding of $DENV2_{C6}$ membrane molecular interactions during the DENV replication cycle might allow the identification of new targets for the treatment of Dengue virus infection.

Acknowledgements

This work was partially supported by grant BFU2008-02617-BMC (Ministerio de Ciencia y Tecnología, Spain) to J.V. H.N. is supported by a "Santiago Grisolía" fellowship from Generalitat Valenciana Autonomous Government.

***Declaration of interest*:** The authors report no conflicts of interest. The authors alone are responsible for the content and writing of the paper.

References

Arrondo JL, Goni FM. 1999. Structure and dynamics of membrane proteins as studied by infrared spectroscopy. Prog Biophys Mol Biol 72:367–405.

Bhatt S, Gething PW, Brady OJ, Messina JP, Farlow AW, Moyes CL, et al. 2013. The global distribution and burden of dengue. Nature 496:504–507.

Blume A, Hubner W, Messner G. 1988. Fourier transform infrared spectroscopy of 13C = O-labeled phospholipids hydrogen bonding to carbonyl groups. Biochemistry 27:8239–8249.

Böttcher CSF, Van Gent CM, Fries C. 1961. A rapid and sensitive sub-micro phosphorus determination. Anal Chim Acta 1061:203–204.

Boulant S, Vanbelle C, Ebel C, Penin F, Lavergne JP. 2005. Hepatitis C virus core protein is a dimeric alpha-helical protein exhibiting membrane protein features. J Virol 79:11353–11365.

Bressanelli S, Stiasny K, Allison SL, Stura EA, Duquerroy S, Lescar J, et al. 2004. Structure of a flavivirus envelope glycoprotein in its low-pH-induced membrane fusion conformation. Embo J 23:728–738.

Byler DM, Susi H. 1986. Examination of the secondary structure of proteins by deconvolved FTIR spectra. Biopolymers 25:469–487.

Carro AC, Damonte EB. 2013. Requirement of cholesterol in the viral envelope for dengue virus infection. Virus Res 174:78–87.

Carvalho FA, Carneiro FA, Martins IC, Assuncao-Miranda I, Faustino AF, Pereira RM, et al. 2012. Dengue virus capsid protein binding to hepatic lipid droplets (LD) is potassium ion dependent and is mediated by LD surface proteins. J Virol 86:2096–2108.

Contreras LM, Aranda FJ, Gavilanes F, Gonzalez-Ros JM, Villalain J. 2001. Structure and interaction with membrane model systems of a peptide derived from the major epitope region of HIV protein gp41: Implications on viral fusion mechanism. Biochemistry 40:3196–3207.

Edelhoch H. 1967. Spectroscopic determination of tryptophan and tyrosine in proteins. Biochemistry 6:1948–1954.

Epand RM, Gabel B, Epand RF, Sen A, Hui SW, Muga A, et al. 1992. Formation of a new stable phase of phosphatidylglycerols. Biophys J 63:327–332.

Fisher DB, Cash-Clark CE. 2000. Sieve tube unloading and post-phloem transport of fluorescent tracers and proteins injected into sieve tubes via severed aphid stylets. Plant Physiol 123:125–138.

Garidel P, Blume A, Hubner W. 2000. A Fourier transform infrared spectroscopic study of the interaction of alkaline earth cations with the negatively charged phospholipid 1, 2-dimyristoyl-sn-glycero-3-phosphoglycerol. Biochim Biophys Acta 1466:245–259.

Golding C, Senior S, Wilson MT, O'Shea P. 1996. Time resolution of binding and membrane insertion of a mitochondrial signal peptide: Correlation with structural changes and evidence for cooperativity. Biochemistry 35:10931–10937.

Guillen J, Gonzalez-Alvarez A, Villalain J. 2010. A membranotropic region in the C-terminal domain of Hepatitis C virus protein NS4B Interaction with membranes. Biochim Biophys Acta 1798:327–337.

Ivanyi-Nagy R, Darlix JL. 2010. Intrinsic disorder in the core proteins of flaviviruses. Protein Pept Lett 17:1019–1025.

Kielian M, Rey FA. 2006. Virus membrane-fusion proteins: More than one way to make a hairpin. Nat Rev Microbiol 4:67–76.

Krainev AG, Ferrington DA, Williams TD, Squier TC, Bigelow DJ. 1995. Adaptive changes in lipid composition of skeletal sarcoplasmic reticulum membranes associated with aging. Biochim Biophys Acta 1235:406–418.

Laurent TC, Granath KA. 1967. Fractionation of dextran and Ficoll by chromatography on Sephadex G-200. Biochim Biophys Acta 136:191–198.

Lentz BR. 1993. Use of fluorescent probes to monitor molecular order and motions within liposome bilayers. Chem Phys Lipids 64:99–116.

Lewis RN, McElhaney RN, Pohle W, Mantsch HH. 1994. Components of the carbonyl stretching band in the infrared spectra of hydrated 1,2-diacylglycerolipid bilayers: A re-evaluation. Biophys J 67:2367–2375.

Ma L, Jones CT, Groesch TD, Kuhn RJ, Post CB. 2004. Solution structure of dengue virus capsid protein reveals another fold. Proc Natl Acad Sci USA 101:3414–3419.

Markoff L, Falgout B, Chang A. 1997. A conserved internal hydrophobic domain mediates the stable membrane integration of the dengue virus capsid protein. Virology 233:105–117.

Martins IC, Gomes-Neto F, Faustino AF, Carvalho FA, Carneiro FA, Bozza PT, et al. 2012. The disordered N-terminal region of dengue virus capsid protein contains a lipid-droplet-binding motif. Biochem J 444:405–415.

Mayer LD, Hope MJ, Cullis PR. 1986. Vesicles of variable sizes produced by a rapid extrusion procedure. Biochim Biophys Acta 858:161–168.

Miller S, Kastner S, Krijnse-Locker J, Buhler S, Bartenschlager R. 2007. The non-structural protein 4A of dengue virus is an integral membrane protein inducing membrane alterations in a 2K-regulated manner. J Biol Chem 282:8873–8882.

Miller S, Krijnse-Locker J. 2008. Modification of intracellular membrane structures for virus replication. Nat Rev Microbiol 6:363–374.

Moreno MR, Guillen J, Perez-Berna AJ, Amoros D, Gomez AI, Bernabeu A, et al. 2007. Characterization of the interaction of two peptides from the N terminus of the NHR domain of HIV-1 gp41 with phospholipid membranes. Biochemistry 46:10572–10584.

Mukhopadhyay S, Kuhn RJ, Rossmann MG. 2005. A structural perspective of the flavivirus life cycle. Nat Rev Microbiol 3:13–22.

Nemesio H, Palomares-Jerez F, Villalain J. 2011. The membrane-active regions of the dengue virus proteins C and E. Biochim Biophys Acta 1808:2390–2402.

Noble CG, Chen YL, Dong H, Gu F, Lim SP, Schul W, et al. 2010. Strategies for development of Dengue virus inhibitors. Antiviral Res 85:450–462.

Noisakran S, Dechtawewat T, Avirutnan P, Kinoshita T, Siripanyaphinyo U, Puttikhunt C, et al. 2008. Association of dengue virus NS1 protein with lipid rafts. J Gen Virol 89:2492–2500.

Palomares-Jerez MF, Guillen J, Villalain J. 2010. Interaction of the N-terminal segment of HCV protein NS5A with model membranes. Biochim Biophys Acta 1798:1212–1224.

Palomares-Jerez MF, Villalain J. 2011. Membrane interaction of segment H1 (NS4B(H1)) from hepatitis C virus non-structural protein 4B. Biochim Biophys Acta 1808:1219–1229.

Pascual R, Contreras M, Fedorov A, Prieto M, Villalain J. 2005. Interaction of a peptide derived from the N-heptad repeat region of gp41 Env ectodomain with model membranes. Modulation of phospholipid phase behavior. Biochemistry 44:14275–14288.

Pastorino B, Nougairede A, Wurtz N, Gould E, de Lamballerie X. 2010. Role of host cell factors in flavivirus infection: Implications for pathogenesis and development of antiviral drugs. Antiviral Res 87:281–294.

Perera R, Kuhn RJ. 2008. Structural proteomics of dengue virus. Curr Opin Microbiol 11:369–377.

Perez-Berna AJ, Veiga AS, Castanho MA, Villalain J. 2008. Hepatitis C virus core protein binding to lipid membranes: The role of domains 1 and 2. J Viral Hepat 15:346–356.

Samsa MM, Mondotte JA, Iglesias NG, Assuncao-Miranda I, Barbosa-Lima G, Da Poian AT, et al. 2009. Dengue virus

capsid protein usurps lipid droplets for viral particle formation. PLoS Pathog 5:e1000632.

Surewicz WK, Mantsch HH, Chapman D. 1993. Determination of protein secondary structure by Fourier transform infrared spectroscopy: A critical assessment. Biochemistry 32:389–394.

Urcuqui-Inchima S, Patino C, Torres S, Haenni AL, Diaz FJ. 2010. Recent developments in understanding dengue virus replication. Adv Virus Res 77:1–39.

Wall J, Ayoub F, O'Shea P. 1995. Interactions of macromolecules with the mammalian cell surface. J Cell Sci 108 (Pt 7):2673–2682.

Welsch S, Miller S, Romero-Brey I, Merz A, Bleck CK, Walther P, et al. 2009. Composition and three-dimensional architecture of the dengue virus replication and assembly sites. Cell Host Microbe 5:365–375.

Yang L, Harroun TA, Weiss TM, Ding L, Huang HW. 2001. Barrel-stave model or toroidal model? A case study on melittin pores. Biophys J 81:1475–1485.

Zaitseva E, Yang ST, Melikov K, Pourmal S, Chernomordik LV. 2010. Dengue virus ensures its fusion in late endosomes using compartment-specific lipids. PLoS Pathog 6.

Zhang YP, Lewis RN, Hodges RS, McElhaney RN. 1992. FTIR spectroscopic studies of the conformation and amide hydrogen exchange of a peptide model of the hydrophobic transmembrane alpha-helices of membrane proteins. Biochemistry 31:11572–11578.

NS4A and NS4B proteins from dengue virus: Membranotropic regions.

Henrique Nemésio, Francis Palomares-Jerez, José Villalaín

Instituto de Biología Molecular y Celular, Universidad Miguel Hernández, E-03202 Elche (Alicante), Spain

Biochimica et Biophysica Acta 1818:11 (2012) 2818-2830

DOI: 10.1016/j.bbamem.2012.06.022

Biochimica et Biophysica Acta 1818 (2012) 2818–2830

Contents lists available at SciVerse ScienceDirect

Biochimica et Biophysica Acta

journal homepage: www.elsevier.com/locate/bbamem

NS4A and NS4B proteins from dengue virus: Membranotropic regions

Henrique Nemésio, Francis Palomares-Jerez, José Villalaín *

Instituto de Biología Molecular y Celular, Universidad "Miguel Hernández", E-03202 Elche-Alicante, Spain

ARTICLE INFO

Article history:
Received 9 May 2012
Received in revised form 26 June 2012
Accepted 27 June 2012
Available online 05 July 2012

Keywords:
DENV replication
DENV
Lipid–peptide interaction
Membranous web
Replication complex

ABSTRACT

Proteins NS4A and NS4B from Dengue Virus (DENV) are highly hydrophobic transmembrane proteins which are responsible, at least in part, for the membrane arrangements leading to the formation of the viral replication complex, essential for the viral life cycle. In this work we have identified the membranotropic regions of DENV NS4A and NS4B proteins by performing an exhaustive study of membrane rupture induced by NS4A and NS4B peptide libraries on simple and complex model membranes as well as their ability to modulate the phospholipid phase transitions $P_{\beta'}$–L_α of DMPC and L_β–L_α/L_α–H_{II} of DEPE. Protein NS4A presents three membrane active regions coincident with putative transmembrane segments, whereas NS4B presented up to nine membrane active regions, four of them presumably putative transmembrane segments. These data recognize the existence of different membrane-active segments on these proteins and support their role in the formation of the replication complex and therefore directly implicated in the DENV life cycle.

1. Introduction

The *Flaviviridae* family contains three genera, *Flavivirus, Hepacivirus and Pestivirus.* Dengue virus (DENV), a member of the genus *Flavivirus*, is the leading cause of arboviral diseases in the tropical and subtropical regions, affecting 70 to 100 million people every year of dengue fever and dengue hemorrhagic fever [1,2]. DENV comprises four serologically and genetically related viruses which possess 69–78% identity at the amino acid level [3]. Despite the urgent medical need and considerable efforts to treat DENV derived infections, no antivirals or vaccines against DENV virus are currently available, so that more than 2 billion people, mainly in poor countries, are at risk in the world [4]. Furthermore, due to the increasing world global temperature as well as travelling, there is a real risk of mosquito vector spreading to previously unaffected zones.

DENV is a positive-sense, single-stranded RNA virus with a single open reading frame encoding a polyprotein, which is subsequently cleaved by cellular and viral proteases into three structural and seven non-structural (NS) proteins [5]. Similarly to other enveloped viruses, DENV enters the cells through receptor mediated endocytosis [5–8] and rearranges cell internal membranes to establish specific sites of replication [9–11]. DENV replicates its genome in a membrane-associated replication complex, and morphogenesis and virion budding have been suggested to take place in the endoplasmic reticulum (ER) or modified ER membranes. These modified membranes could provide a platform for capsid formation during viral assembly [12]. Details about DENV replication process remain largely unclear, but most, if not all of the DENV proteins, are involved and function in a complex web of protein–protein interactions [5,8]. The majority of the NS proteins are thought to be responsible for both polyprotein processing and viral RNA replication, the latter taking place in the membrane-associated replication complexes (RC) of the virus [13]. The exact function of each of the NS proteins is far from explained, yet some studies have unveiled some information. It has been reported that NS1, in association with NS4A, might be determinant in the early steps of viral RNA replication and mutations in NS1 affected the start of the minus RNA strand synthesis [14,15]. NS3 is a multifunctional protein with RNA helicase, 5′-terminal RNA triphosphatase and serine protease functions [16]. NS5, the most conserved protein in DENV has RNA-dependent RNA polymerase activity at its C-terminal domain and methyltransferase activity at its N-terminal domains, essential functions for capping of the mRNA [17].

As for the remaining small hydrophobic DENV proteins, i.e., NS2A, NS4A and NS4B, little is known hitherto about their function in the viral cycle of dengue virus and remain the most poorly characterized proteins [18]. NS4A, a highly hydrophobic protein, contains an initial sequence (residues 1 to 49) that apparently does not interact with membranes and appears to function as a cofactor of NS3 [19], three hydrophobic regions (residues 50 to 73, residues 76 to 89, and residues 101 to 127) which are tightly associated to membranes, a small loop

Abbreviations: BMP, S,R-bis(monooleoylglycero)phosphate; BPI, bovine liver L-α-phosphadidylinositol; BPS, bovine brain L-α-phosphatidylserine; CF, 5-carboxyfluorescein; CHOL, cholesterol; CL, bovine heart cardiolipin; DENV, dengue virus; DEPE, 1,2-Dielaidoyl-sn-glycero-3-phosphatidylethanolamine; DMPC, 1,2-dimyristoyl-*sn*-glycero-3-phosphatidylcholine; DPH, 1,6-diphenyl-1,3,5-hexatriene; DSC, differential scanning calorimetry; EPA, egg L-α-phosphatidic acid; EPC, egg L-α-phosphatidylcholine; EPG, egg L-α-phosphatidylglycerol; ER, endoplasmic reticulum; ESM, egg sphingomyelin; HCV, hepatitis C virus; LEM, late endosome membrane; LUV, large unilamellar vesicles; MLV, multilamellar vesicles; NS, non-structural protein; TFE, 2,2,2-Trifluoroethanol; T_m, temperature of the gel-to-liquid crystalline phase transition; TM, transmembrane domain; TPE, egg transphosphatidylated L-α-phosphatidylethanolamine

* Corresponding author. Tel.: +34 966 658 762; fax: +34 966 658 758.
E-mail address: jvillalain@umh.es (J. Villalaín).

0005-2736/$ – see front matter © 2012 Elsevier B.V. All rights reserved.
doi:10.1016/j.bbamem.2012.06.022

that exposes the NS4A-2k cleavage site (residues 123 to 130) and a C-terminal fragment called 2k that acts as the signal sequence for translocation of the NS4B protein into the ER lumen [9]. NS4A, in concert with other viral and host proteins, promotes the membrane rearrangements essential for viral replication [9,20,21]. Another evidence of the role of NS4A in viral RNA replication of DENV is given by the fact that this protein was found in reticular structures and cytoplasmic foci (derived from or associated to the ER) [9,18,22,23]. Interestingly, it has been recently shown that NS4A induces autophagy in epithelial cells, protecting the host cell against death [21]. NS4B is another highly hydrophobic membrane protein which appears to have two hydrophobic segments (residues 1 to 56 and residues 56–93) which are probably associated to the ER lumen side of the membrane and supposedly three C-terminal TM segments (residues 93 to 146, residues 146 to 190 and residues 190 to 248) [18]. NS4B is capable of interfering with phosphorylation of STAT1 blocking the IFN-α/β induced signal transduction cascade [24]. NS4B is also a negative modulator of the NS3 helicase function, being this modulation dependent on the conformation of NS4B. This model is supported, among other evidences, by the fact that a single point mutation disrupts the interaction between NS3 and NS4B; furthermore, NS3, NS4B and NS5 might form a complex that holds the separated strands apart as the helicase moves along the duplex [18,25]. Lastly, NS4A and NS4B might function cooperatively in viral replication and the anti-host response [9,26].

We have recently identified the membrane-active regions of a number of viral proteins by observing the effect of protein-derived peptide libraries on model membrane integrity [27–32]. These results allowed us to propose the location of different protein segments implicated in either protein–lipid or protein–protein interactions and help us to understand the mechanisms underlying the interaction between viral proteins and membranes. Motivated by the need to understand the interaction between the highly hydrophobic DENV NS4A and NS4B proteins with membranes, considering that they are fundamental in the viral RNA replication process, and additionally, that DENV protein/membrane interaction is an attractive target for antiviral drug development, we have characterized the membranotropic regions of DENV proteins NS4A and NS4B. By using peptide libraries encompassing the full length of both proteins, by observing their effect on membrane integrity as well as their effect on model biomembranes, we have identified different regions on DENV proteins NS4A and NS4B with membrane-interacting capabilities. These data will help us to understand the molecular mechanism of viral fusion and morphogenesis as well as making possible the future development of DENV entry inhibitors which may lead to new vaccine strategies.

2. Materials and methods

2.1. Materials and reagents

The peptide library, consisting of 66 peptides (Table 1), was derived from Dengue Virus Type 2 NGC NS4A, 2k and NS4B proteins and was obtained from BEI Resources, National Institute of Allergy and Infectious Diseases, Manassas, VA, USA. The peptides had a purity of about 80%. Peptides were solubilized in water/TFE/DMSO at 50:20:30 ratios (v/v/v). Bovine brain phosphatidylserine (BPS), bovine liver L-α-phosphatidylinositol (BPI), cholesterol (Chol), egg L-α-phosphatidic acid (EPA), egg L-α-phosphatidylcholine (EPC), egg sphingomyelin (ESM), egg transphosphatidylated L-α-phosphatidylethanolamine (TPE), bovine heart cardiolipin (CL), 1,2-dimyristoyl-sn-glycero-3-phosphatidylcholine (DMPC), 1,2-dielaidoyl-sn-glycero-3-phosphatidylethanolamine (DEPE) and liver lipid extract were obtained from Avanti Polar Lipids (Alabaster, AL, USA). The lipid composition of the synthetic endoplasmic reticulum was EPC/CL/BPI/

Table 1
Sequence and residue position of all peptides contained in the DENV NS4A/2k/NS4B libraries. The amino acid position in the protein sequence is relative to each protein. Residues in cursive constitute the 2k fragment.

Protein	Peptide number	Amino acid sequence	Amino acid position	Protein	Peptide number	Amino acid sequence	Amino acid position
NS4A	1	SLTLNLITEMGRLPTFM	1–17	NS4B	9	YAVATTFVTPMLRHSIE	40–57
NS4A	2	ITEMGRLPTFMTQKARD	7–23	NS4B	10	FVTPMLRHSIENSSVNV	46–63
NS4A	3	LPTFMTQKARDALDNLA	13–29	NS4B	11	RHSIENSSVNVSLTAIA	52–69
NS4A	4	TQKARDALDNLAVLHTA	18–34	NS4B	12	SSVNVSLTAIANQATVL	58–75
NS4A	5	ALDNLAVLHTAEAGGRA	24–40	NS4B	13	LTAIANQATVLMGLGKG	64–81
NS4A	6	VLHTAEAGGRAYNHAL	30–45	NS4B	14	NQATVLMGLGKGWPLSK	69–86
NS4A	7	AEAGGRAYNHALSELPE	34–50	NS4B	15	MGLGKGWPLSKMDIGV	75–91
NS4A	8	AYNHALSELPETLETLL	40–56	NS4B	16	GWPLSKMDIGVPLLAIG	80–97
NS4A	9	SELPETLETLLLLTLLA	46–62	NS4B	17	MDIGVPLLAIGCYSQVN	86–103
NS4A	10	LETLLLLTLLATVTGGI	52–68	NS4B	18	LLAIGCYSQVNPITLTA	92–109
NS4A	11	LTLLATVTGGIFLFLM	58–73	NS4B	19	YSQVNPITLTAALFLLV	98–115
NS4A	12	TVTGGIFLFLMSGRGIG	63–79	NS4B	20	ITLTAALFLLVAHYAII	104–121
NS4A	13	FLFLMSGRGIGKMTLGM	69–85	NS4B	21	LFLLVAHYAIIGPGLQA	110–127
NS4A	14	GRGIGKMTLGMCCIITA	75–91	NS4B	22	HYAIIGPGLQAKATREA	116–133
NS4A	15	MTLGMCCIITASILLWY	81–97	NS4B	23	PGLQAKATREAQKR	122–136
NS4A	16	CIITASILLWYAQIQPH	87–103	NS4B	24	AAAGIMKNPTVDGITVI	136–153
NS4A	17	ILLWYAQIQPHWIAASI	93–109	NS4B	25	KNPTVDGITVIDLDPI	142–158
NS4A	18	AQIQPHWIAASIILEFF	98–114	NS4B	26	DGITVIDLDPIPYDPKF	147–164
NS4A	19	WIAASIILEFFLIVLLI	104–120	NS4B	27	DLDPIPYDPKFEKQLGQ	153–170
NS4A	20	ILEFFLIVLLIPEPEKQ	110–126	NS4B	28	YDPKFEKQLGQVMLLVL	159–176
NS4A	21	IVLLIPEPEKQRTPQDN	116–132	NS4B	29	KQLGQVMLLVLCVTQVL	165–182
NS4A/2k	22	PEPEKQR*TPQDNQLTYV*	121–137	NS4B	30	MLLVLCVTQVLMMRTTW	171–188
NS4A/2k	23	R*TPQDNQLTYVVIAILT*	127–143	NS4B	31	VTQVLMMRTTWALCEAL	177–194
2k	24	*NQLTYVVIAILTVVAAT*	132–148	NS4B	32	MRTTWALCEALTLATG	183–199
2k/NS4B	25	*VIAILTVVAATMA*NEMG	138–150	NS4B	33	ALCEALTLATGPISTLW	188–205
2k/NS4B	1	VVAATMANEMGFLEKTK	−7–10	NS4B	34	TLATGPISTLWEGNPGR	194–211
2k/NS4B	2	ANEMGFLEKTKKDLGLG	−1–16	NS4B	35	ISTLWEGNPGRFWNTTI	200–217
NS4B	3	LEKTKKDLGLGSITTQQ	5–22	NS4B	36	GNPGRFWNTTIAVSMAN	206–223
NS4B	4	DLGLGSITTQQPESNIL	11–28	NS4B	37	WNTTIAVSMANIFRGSY	212–229
NS4B	5	ITTQQPESNILDIDLR	17–33	NS4B	38	VSMANIFRGSYLAGAGL	218–235
NS4B	6	PESNILDIDLRPASAWT	22–39	NS4B	39	FRGSYLAGAGLLFSIMK	224–241
NS4B	7	DIDLRPASAWTLYAVAT	28–45	NS4B	40	AGAGLLFSIMKNTTNTR	230–247
NS4B	8	ASAWTLYAVATTFVTPM	34–51	NS4B	41	FSIMKNTTNTRR	236–248

TPE/BPS/EPA/ESM/Chol at a molar ratio of 59:0.37:7.7:18:3.1:1.2:3.4:7.8 [33,34]. 1,6-Diphenyl-1,3,5-hexatriene (DPH) was obtained from Molecular Probes (Eugene, OR). 5-Carboxyfluorescein (CF, >95% by HPLC), Triton X-100, EDTA and HEPES were purchased from Sigma-Aldrich (Madrid, ES). All other chemicals were commercial samples of the highest purity available (Sigma-Aldrich, Madrid, ES). Water was deionized, twice-distilled and passed through a Milli-Q equipment (Millipore Ibérica, Madrid, ES) to a resistivity higher than 18 MΩ cm.

2.2. Vesicle preparation

Aliquots containing the appropriate amount of lipid in chloroform-methanol (2:1 vol/vol) were placed in a test tube, the solvents were removed by evaporation under a stream of O_2-free nitrogen, and finally, traces of solvents were eliminated under vacuum in the dark for >3 h. The lipid films were resuspended in an appropriate buffer and incubated either at 25 °C or 10 °C above the phase transition temperature (T_m) with intermittent vortexing for 30 min to hydrate the samples and obtain multilamellar vesicles (MLV). The samples were frozen and thawed five times to ensure complete homogenization and maximization of peptide/lipid contacts with occasional vortexing. Large unilamellar vesicles (LUV) with a mean diameter of 0.1 μm were prepared from MLV by the extrusion method [35] using polycarbonate filters with a pore size of 0.1 μm (Nuclepore Corp., Cambridge, CA, USA). Breakdown of the vesicle membrane leads to contents leakage, i.e., CF fluorescence. Non-encapsulated CF was separated from the vesicle suspension through a Sephadex G-75 filtration column (Pharmacia, Uppsala, SW, EU) eluted with buffer containing either 10 mM Tris, 100 mM NaCl, 0.1 mM EDTA, pH 7.4. Phospholipid and peptide concentration were measured by methods described previously [36,37].

2.3. Membrane leakage measurement

Leakage of intraliposomal CF was assayed by treating the probe-loaded liposomes (final lipid concentration, 0.125 mM) with the appropriate amounts of peptides on microtiter plates stabilized at 25 °C using a microplate reader (FLUOstar, BMG Labtech, GER, EU), each well containing a final volume of 170 μl. The medium in the microtiter plates was continuously stirred to allow the rapid mixing of peptide and vesicles. Leakage was measured at an approximate peptide-to-lipid molar ratio of 1:25. Changes in fluorescence intensity were recorded with excitation and emission wavelengths set at 492 and 517 nm, respectively. One hundred percent release was achieved by adding Triton X-100 to a final concentration of 0.5% (w/w) to the microtiter plates. Fluorescence measurements were made initially with probe-loaded liposomes, afterwards by adding peptide solution and finally adding Triton X-100 to obtain 100% leakage. Leakage was quantified on a percentage basis according to the equation, % Release = $[(F_f - F_0)/(F_{100} - F_0)]$ 100, F_f being the equilibrium value of fluorescence after peptide addition, F_0 the initial fluorescence of the vesicle suspension and F_{100} the fluorescence value after addition of Triton X-100. For details see refs. [38,39].

2.4. Differential scanning calorimetry

MLVs were formed as stated above in 20 mM HEPES, 100 mM NaCl, 0.1 mM EDTA, pH 7.4. The peptides were added to obtain a peptide/lipid molar ratio of 1:15 and incubated 10 °C above the T_m of DEPE for 30 min with occasional vortexing and then centrifuged. Samples containing 1.5 mg of total phospholipid were transferred to 50 μl DSC aluminum and hermetically sealed pans and subjected to DSC analysis in a differential scanning calorimeter Pyris 6 DSC (Perkin-Elmer Instruments, Shelton, U.S.A.) under a constant external pressure of 30 psi in order to avoid bubble formation. Thermograms were recorded at a constant rate of 4 °C/min. After data acquisition, the pans were opened and the phospholipid content was determined. To avoid artefacts due to the thermal history of the sample, the first scan was never considered; second and further scans were carried out until a reproducible and reversible pattern was obtained. Data acquisition was performed using the Pyris Software for Thermal Analysis, version 4.0 (Perkin-Elmer Instruments LLC) and Microcal Origin software (Microcal Software Inc., Northampton, MA, U.S.A.) was used for data analysis. The thermograms were defined by the onset and completion temperatures of the transition peaks obtained from heating scans. The phase transition temperature was defined as the temperature at the peak maximum.

2.5. Steady-state fluorescence anisotropy

MLVs were formed in a buffer composed of 100 mM NaCl, 0.1 mM EDTA, 20 mM HEPES at pH 7.4 (at 25 °C). Aliquots of DPH in N,N′-dimethylformamide (0.2 mM) were directly added to the lipid suspension to obtain a probe/lipid molar ratio of 1:500. DPH, a popular membrane fluorescent probe for monitoring the organization and dynamics of membranes, is known to partition mainly into the hydrophobic core of the membrane [40]. Samples were incubated for 60 min at 10 °C above the gel to liquid-crystalline phase transition temperature T_m of the phospholipid mixture. Afterwards, the peptides were added to obtain a peptide/lipid molar ratio of 1:15 and incubated 10 °C above the T_m of each lipid for 1 h, with occasional vortexing. All fluorescence studies were carried using 5 mm x 5 mm quartz cuvettes in a final volume of 400 μl (315 μM lipid concentration). The steady state fluorescence anisotropy was measured with an automated polarization accessory using a Varian Cary Eclipse fluorescence spectrometer, coupled to a Peltier for automatic temperature change. The vertically and horizontally polarized emission intensities, elicited by vertically polarized excitation, were corrected for background scattering by subtracting the corresponding polarized intensities of a phospholipid preparation lacking probes. The G-factor, accounting for differential polarization sensitivity, was determined by measuring the polarized components of the fluorescence of the probe with horizontally polarized excitation ($G = I_{HV}/I_{HH}$). Samples were excited at 360 nm and emission was recorded at 430 nm, with excitation and emission slits of 5 nm. Anisotropy values were calculated using the formula $\langle r \rangle = (I_{VV} - GI_{VH})/(I_{VV} + 2GI_{VH})$, where I_{VV} and I_{VH} are the measured fluorescence intensities (after appropriate background subtraction) with the excitation polarizer vertically oriented and the emission polarizer vertically and horizontally oriented, respectively.

3. Results

In a similar way to other enveloped viruses, DENV virus modifies cell internal membranes to establish specific sites of replication described as the membranous web or replication complex (RC), fundamental for the viral life cycle [9,10]. The small, hydrophobic and poorly characterized DENV NS4A and NS4B proteins are responsible for the membrane rearrangements essential for viral replication and they are engaged in a plethora of other functions [9,18,20,21,25,26]. In order to detect surfaces along the NS4A and NS4B proteins which might be identified as membrane partitioning and/or membrane interacting zones, two-dimensional plots of hydrophobicity, obtained taking into consideration the arrangement of the amino acids in the space assuming they adopt an α-helical structure along the whole sequence [28,41], are shown in Fig. 1. It is readily evident the existence of different regions with large hydrophobic moment values along the NS4A and NS4B proteins. As it has been noted before, using these two-dimensional plots, it would be possible to distinguish two types of patches, those which do not comprise the perimeter of the helix and those which embrace the full perimeter [41]. The first type could favor the interaction with other similar patches along the same or other proteins as well as with the membrane surface. The second one would encompass patches containing more than 15 amino acids which could represent TM

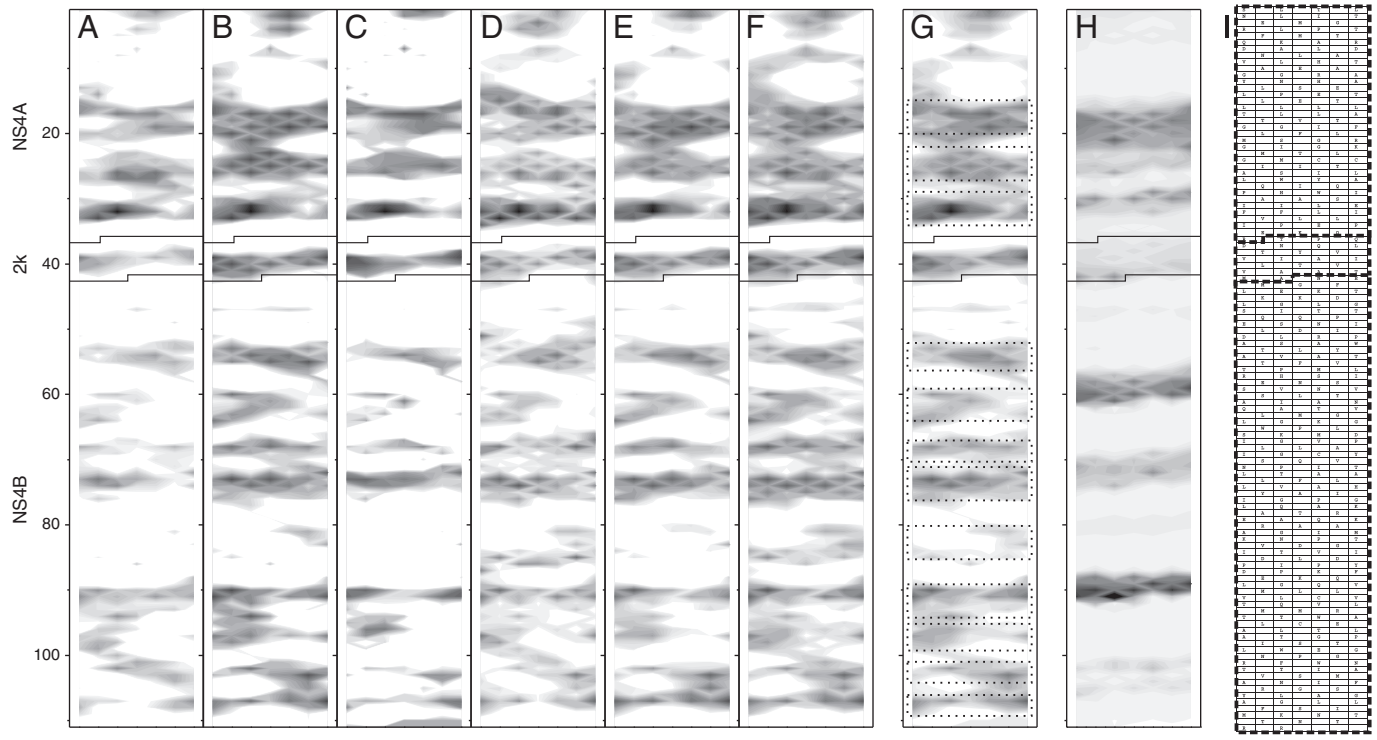

Fig. 1. Two-dimensional plots of the values of the water–membrane transfer free energy scales in kcal/mol for DENV NS4A, 2k and NS4B proteins according to (A) Wimley and White [50], (B) Engelman et al. [51], (C) Hessa et al. [52], (D) Moon and Fleming [53], (E) Meiler et al. [54] and (F) Eisenberg et al. [55]. Positive values represent positive bilayer-to-water transfer free energy values and therefore the higher (darker) the value, the greater the probability to interact with the membrane surface and/or hydrophobic core. The average of scales (A)–(F) is shown in (G), the average experimental leakage values are shown in (H) and the sequences of the NS4A, 2k and NS4B proteins in relation to the two-dimensional plots are shown in (I). The hydrophobic regions discussed in the text are boxed in (G).

domains and patches containing 15 or less amino acids which could represent membrane interacting domains [27,29,41,42].

By observing the NS4A protein data, it is possible to detect three localized highly positive hydrophobic regions covering the full horizontal length of the plot. These regions would be comprised approximately from amino acid residues 51 to 72, residues 78 to 98 and residues 103 to 120 (Fig. 1). These results are in accordance with former data, since it was previously proposed the presence of highly hydrophobic patches from residues 50 to 73, residues 76 to 89, and residues 101 to 127 [9]. These patches contain about 22, 21 and 18 amino acids so that they could match (and represent) TM domains [27,29,41,42]. Two patches located along limited zones of the protein surface can be described from residues 2 to 11 and from 21 to 31 approximately. Whereas the previous three hydrophobic regions supposedly traverse the palisade structure of the membrane, these last two regions could show a tendency to interact with the membrane surface; however, it should not be ruled out that these areas could also be responsible for the interaction with other proteins [43]. The 2k fragment, which functions as a signal sequence [9], presents as expected a highly positive hydrophobic region (from residues 7 to 20, 2k numbering, Fig. 1). The two-dimensional plot corresponding to protein NS4B, shown in Fig. 1, displays different highly positive hydrophobic moment zones presenting diverse characteristics along the full sequence of the protein. Nine patches can be described for NS4B, i.e., from residues 35 to 52 (21 amino acids in length), from residues 60 to 78 (19 amino acids), from residues 89 to 100 (12 amino acids), from residues 103 to 122 (20 amino acids), from residues 137 to 155 (19 amino acids), from residues 168 to 188 (21 amino acids), from residues 190 to 205 (16 amino acids), from residues 212 to 225 (14 amino acids), and from residues 229 to 240 (12 amino acids). As it was commented above, there is not a clear separation between patches corresponding to either membrane interacting or TM domains. However, it is very clear from Fig. 1 that NS4B is a highly hydrophobic protein with the capacity of traversing the membrane several times [18]. It is interesting to note that this description of NS4B hydrophobic-rich surfaces fits very well with some of the previously described regions of the protein, highlighting the specific roles they might have for the proper biological functioning of the protein. In this way, the distribution of hydrophobicity and interfaciality, i.e., structure-related factors, along NS4A and NS4B proteins would affect their biological function.

The peptide libraries we have used in this study, composed by a total of 66 peptides, and their correlation with the NS4A, 2k, and NS4B protein sequences are shown in Fig. 2; it can be observed in the figure that the peptide libraries include the whole sequence of the proteins. Since two and three consecutive peptides in the library have an overlap of approximately 11 and 4 amino acids respectively, it seems reasonably to think on the combined effect of peptide groups or segments rather than on the effect of isolated peptides, so that leakage data elicited by each peptide would define protein segments or zones as commented below. It is also observed in Fig. 2 that the sequences of the four DENV strains are very well conserved, so that the information gathered studying DENV strain 2 should be essentially similar to the other DENV strains. We have studied the effect of these peptide libraries on membrane rupture by monitoring leakage from different liposome compositions and the results are presented in Figs. 3 and 4 [42]. We have tested different lipid compositions, from simple to complex (Fig. 3). The set of simple compositions contained EPC/Chol at a phospholipid molar ratio of 5:1 and EPC/SM/Chol at a phospholipid molar ratio of 5:2:1. Two complex lipid compositions were used, a lipid extract of liver membranes (42%, PC, 22% PE, 7% Chol, 8% PI, 1% LPC, and 21% neutral lipids as stated by the manufacturer) and a synthetic lipid mixture resembling the ER membrane (EPC/CL/BPI/TPE/BPS/EPA/ESM/Chol at a molar ratio of 59:0.37:7.7:18:3.1:1.2:3.4:7.8 [33,34]). It should be recalled that DENV virus is associated with membranes of the ER or an ER-derived modified compartment. In order to check the effect of each lipid in

Strain		NS4A (residues 1-62)
Nauru/West Pac/1974	(DENV-1)	SVSGDLILEIGKLPQHLTQRAQNALDNLVMLHNSEQGGKAYRHAMEELPDTIETLMLLALIA
Thailand/NGS-C/1944	(DENV-2)	SLTLNLITEMGRLPTFMTQKARDALDNLAVLHTAEAGGRAYNHALSELPETLETLLLLTLLA
Philippines/H87/1956	(DENV-3)	SIALDLVTEIGRVPSHLAHRTRNALDNLVMLHTSEHGGRAYRHAVEELPETMETLLLLGLMI
Thailand/0476/1997	(DENV-4)	SITLDILTEIASLPTYLSSRAKLALDNIVMLHTTERGGRAYQHALNELPESLETLMLVALLG
Alignment (Clustalw)		*:: ::: *:. :* .:: ::: ****:.:**.:* **:**.**:.***:::***:*: *:

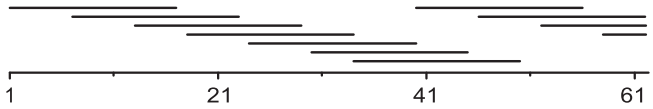

Strain		NS4A (residues 63 -127)
Nauru/West Pac/1974	(DENV-1)	VLTGGVTLFFLSGRGLGKTSIGLLCVIASSALLWMASVEPHWIAASIILEFFLMVLLIPEPDRQR
Thailand/NGS-C/1944	(DENV-2)	TVTGGIFLFLMSGRGIGKMTLGMCCIITASILLWYAQIQPHWIAASIILEFFLIVLLIPEPEKQR
Philippines/H87/1956	(DENV-3)	LLTGGAMLFLISGKGIGKTSIGLICVIASSGMLWMADVPLQWIASAIVLEFFMMVLLIPEPEKQR
Thailand/0476/1997	(DENV-4)	AMTAGIFLFFMQGKGIGKLSVGLIAIAVASGLLWVAEIQPQWIAASIILEFFLMVLLIPEPEKQR
Alignment (Clustalw)		:*.* **::.*:*:** ::*: .: .:* :** *.: :***::*:****::*******::**

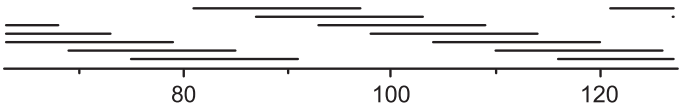

Strain		2k fragment (1-23)
Nauru/West Pac/1974	(DENV-1)	TPQDNQLAYVVIGLLFMILTAAA
Thailand/NGS-C/1944	(DENV-2)	TPQDNQLAYVVIGLLFMILTAAA
Philippines/H87/1956	(DENV-3)	TPQDNQLAYVVIGILTLAAIVAA
Thailand/0476/1997	(DENV-4)	TPQDNQLIYVILAILTIIGLVAA
Alignment (Clustalw)		******* **:::.:* : .**

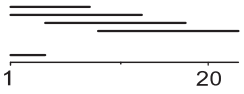

Strain		NS4B (residues 1 – 82)
Nauru/West Pac/1974	(DENV-1)	NEMGLLETTKKDLGIGHAAAENHHHAAMLDVDLHPASAWTLYAVATTIITPMMRHTIENTTANISLTAIANQAAILMGLDKG
Thailand/NGS-C/1944	(DENV-2)	NEMGFLEKTKKDLGLG-SITTQQPESNILDIDLRPASAWTLYAVATTFVTPMLRHSIENSSVNVSLTAIANQATVLMGLGKG
Philippines/H87/1956	(DENV-3)	NEMGLLETTKRDLGMSKEPGVVSP-TSYLDVDLHPASAWTLYAVATTVITPMLRHTIENSTANVSLAAIANQAVVLMGLDKG
Thailand/0476/1997	(DENV-4)	NEMGLIEKTKADFGFY-QVKT---ETTILDVDLRPASAWTLYAVATTILTPMLRHTIENTSANLSLAAIANQAAVLMGLGKG
Alignment (Clustalw)		*: :**:******:******** ** *::.:*:.:********************:************ .***:*: **.**

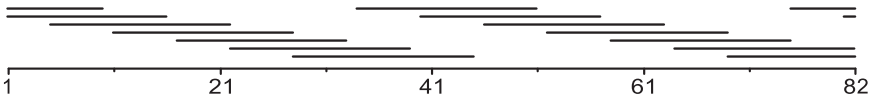

Strain		NS4B (residues 83 – 165)
Nauru/West Pac/1974	(DENV-1)	WPISKMDIGVPLLALGCYSQVNPLTLTAAVFMLVAHYAIIGPGLQAKATREAQKRTAAGIMKNPTVDGIVAIDLDPVVYDAKF
Thailand/NGS-C/1944	(DENV-2)	WPLSKMDIGVPLLAIGCYSQVNPITLTAALFLLVAHYAIIGPGLQAKATREAQKRAAAGIMKNPTVDGITVIDLDPIPYDPKF
Philippines/H87/1956	(DENV-3)	WPISKMDLGVPLLALGCYSQVNPLTLIAAVLLLVTHYAIIGPGLQAKATREAQKRTAAGIMKNPTVDGIMTIDLDPVIYDSKF
Thailand/0476/1997	(DENV-4)	WPLHRMDLGVPLLAMGCYSQVNPTTLTASLVMLLVHYAIIGPGLQAKATREAQKRTAAGIMKNPTVDGITVIDLEPISYDPKF
Alignment (Clustalw)		**: :**:******:******** ** *::.:*:.:********************:************ .***:*: **.**

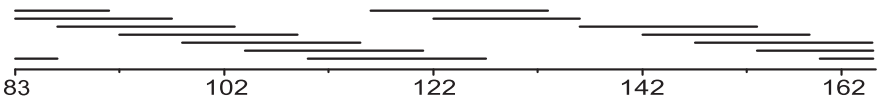

Strain		NS4B (residues 166 – 249)
Nauru/West Pac/1974	(DENV-1)	EKQLGQIMLLILCTSQILLMRTTWALCESITLATGPLTTLWEGSPGKFWNTTIAVSMANIFRGSYLAGAGLAFSLMKSLGGGRR
Thailand/NGS-C/1944	(DENV-2)	EKQLGQVMLLVLCVTQVLMMRTTWALCEALTLATGPISTLWEGNPGRFWNTTIAVSMANIFRGSYLAGAGLLFSIMKNTTNTRR
Philippines/H87/1956	(DENV-3)	EKQLGQVMLLVLCAVQLLLMRTSWALCEVLTLATGPITTLWEGSPGKFWNTTIAVSMANIFRGSYLAGAGLALSIMKSVGTGKR
Thailand/0476/1997	(DENV-4)	EKQLGQVMLLVLCAGQLLLMRTTWAFCEVLTLATGPVLTLWEGNPGRFWNTTIAVSTANIFRGSYLAGAGLAFSLIKNAQTPRR
Alignment (Clustalw)		******:***:**. *:*:***:**:** :******: *****.**:********** ********** :*::*. :*

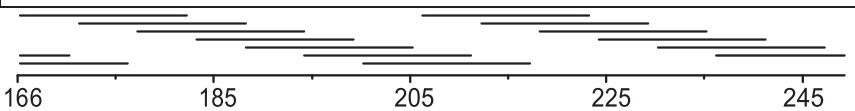

Fig. 2. Sequences of the NS4A (first and second tables from the top), 2k (third table from the top) and NS4B (fourth, fifth and sixth tables from the top) proteins for the four different dengue virus serotypes according to literature. The sequences were split for better visualization. For each protein, a global alignment was computed using Clustalw. Below each table there is a graphic showing the relative location of each peptide in the peptide library. Peptide line length is related to the number of amino acids in the peptide. Maximum overlap between adjacent peptides is 11 amino acids. It should be noted that the 2k fragment is composed of peptides included in the NS4A peptide library.

this complex composition we have designed an ER synthetic membrane composed of EPC/CL/BPI/TPE/BPS/EPA/ESM/CHOL at a molar ratio of 58:6:6:6.6:6:6:6 ($ER^{58:6}$) and tested this mixture as well as seven different lipid mixtures lacking one and only one of the lipids in the mixture (except EPC) (Fig. 4). These lipid compositions could be very useful to study the effect of each lipid component on the interaction of each peptide of the peptide library with the membrane.

The leakage data corresponding to the NS4A protein derived peptide library (Fig. 3) show that some peptides exerted a significant leakage effect. A quick bird's eye view of the leakage data shows the presence

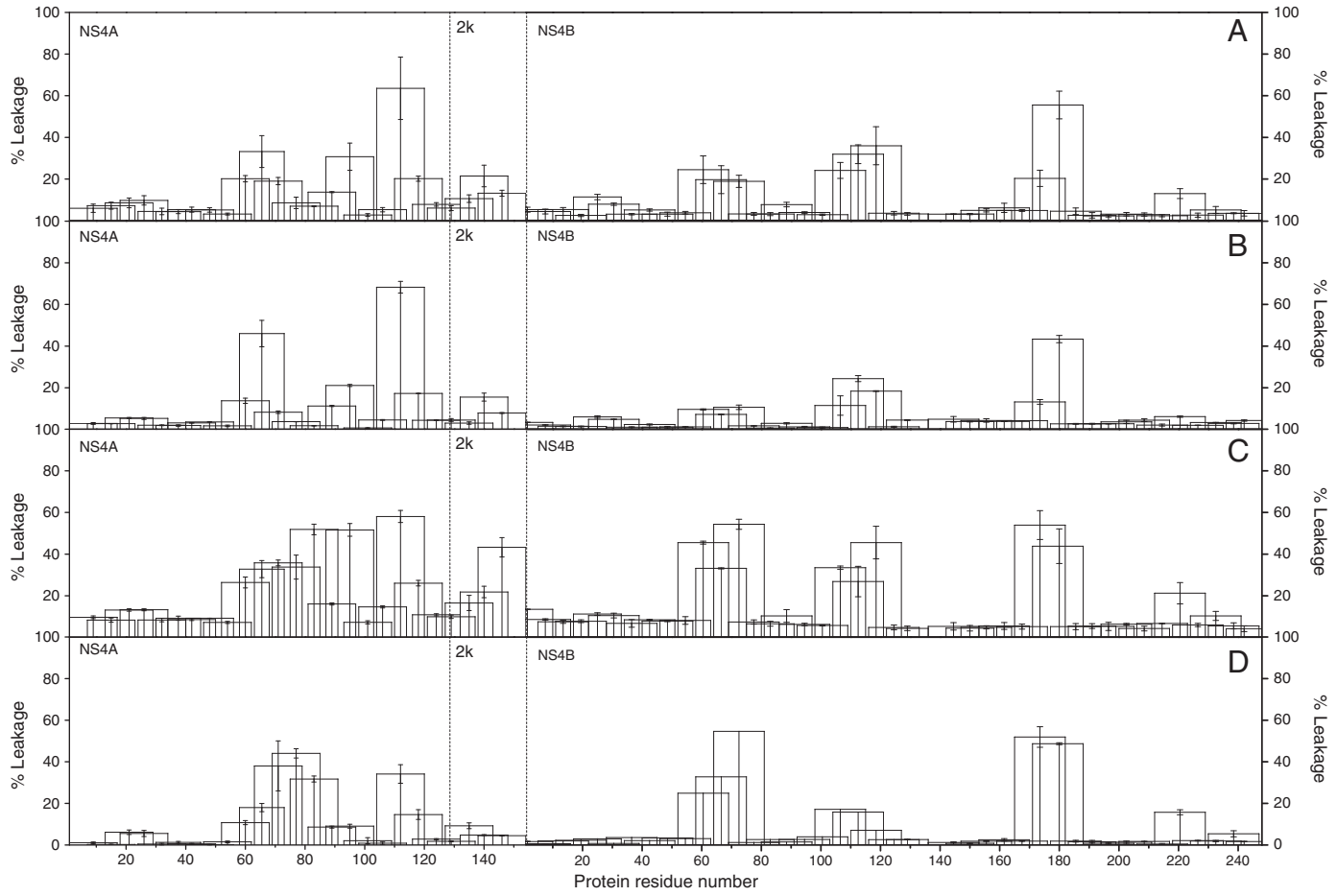

Fig. 3. Effect of the peptide library derived from the NS4A, 2k, and NS4B proteins on the release of LUV contents for different lipid compositions. Leakage data (membrane rupture) for LUVs composed of (A) EPC/Chol at a molar proportion of 5:1, (B) EPC/ESM/Chol at a molar proportion of 5:2:1, (C) lipid extract of liver membranes, and (D) ER complex synthetic lipid mixture (EPC/CL/BPI/TPE/BPS/EPA/ESM/Chol at a molar proportion of 59:0.37:7.7:18:3.1:1.2:3.4:7.8). Vertical bars indicate standard deviations of the mean of quadruplicate samples.

of two broad segments from residues 52 to 90 and residues 90 to 125, approximately. Although there were some differences depending on liposome composition, they were not significant to infer any specific relationship between lipid composition and leakage. Interestingly, leakage values were significant, since for segment 52–90 it oscillated between 30 and 50% whereas for segment 90–125 it fluctuated between 40 and 60%. For liposomes containing the $ER^{58:6}$ complex mixture and its variations (Fig. 4), results were similar; however, although the segment comprised by residues 55 to 90 elicited significant leakage values, the segment comprising residues 90 to 127 induced smaller leakage values. The average leakage of all liposome compositions tested for the NS4A protein, presented in Fig. 1H as a two-dimensional plot, shows the relationship between membrane leakage and hydrophobicity. As displayed in the figure, these two leakage zones, i.e., 52–90 and 90–125, fit perfectly well with the hydrophobic regions detected in the two dimensional plots, i.e., 51–72, 78–98 and 103–120 (Fig. 1A–F).

The leakage data corresponding to the NS4B protein derived peptide library (Fig. 3) defined in this case four broad segments, i.e., from residues 50 to 80, from residues 94 to 127, from residues 163 to 190 and from residues 210 to 240, approximately. Similarly to NS4A, differences on leakage were not significant to infer any specific relationship between leakage and lipid composition. There were also variations in the extent of leakage for the different segments, since leakage values between 20–50%, 10–40%, 40–50% and 30–50% approximately were observed for those four segments commented above. When liposomes containing the $ER^{58:6}$ complex mixture and its variations were tested, similar results were obtained (Fig. 4). The same four segments commented above, i.e., segments comprising residues 50 to 80, 94 to 127, 163 to 190 and 210 to 240, produced a significant leakage effect, i.e., 20–30%, 10–15%, 30–40% and 10–15% for all membranes tested (Fig. 4). The total average leakage, presented in Fig. 1H, shows the relationship between membrane leakage and hydrophobicity for the NS4B protein. In this representation the four leakage regions are well defined. As observed in the figure, leakage zones from residues 50 to 80, from residues 94 to 127, from residues 163 to 190 and from residues 210 to 240, fit with the hydrophobic regions detected in the two dimensional plots, i.e., from residues 60 to 78, from residues 89 to 100 and 103 to 122, from residues 168 to 188 and from residues 212 to 225 and 229 to 240 (Fig. 1A–F). The first leakage zone comprises the proposed hydrophobic segment from residues 56 to 93, whereas the other three leakage zones comprise the proposed TM segments from residues 93 to 146, from residues 146 to 190 and from residues 190 to 248. In

Fig. 4. Effect of the peptide library derived from the NS4A, 2k, and NS4B proteins on the release of LUV contents for different lipid compositions. Leakage data (membrane rupture) for LUVs composed of (A) ER59:6 complex lipid mixture (EPC/CL/BPI/TPE/BPS/EPA/ESM/CHOL at a molar proportion of 59:6:6:6.6:6:6:6), (B) ER59:6 minus BPI, (C) ER59:6 minus CHOL, (D) ER59:6 minus EPA, (E) ER59:6 minus ESM, (F) ER59:6 minus TPE, (G) ER59:6 minus BPS and (H) ER59:6 minus CL. Vertical bars indicate standard deviations of the mean of quadruplicate samples.

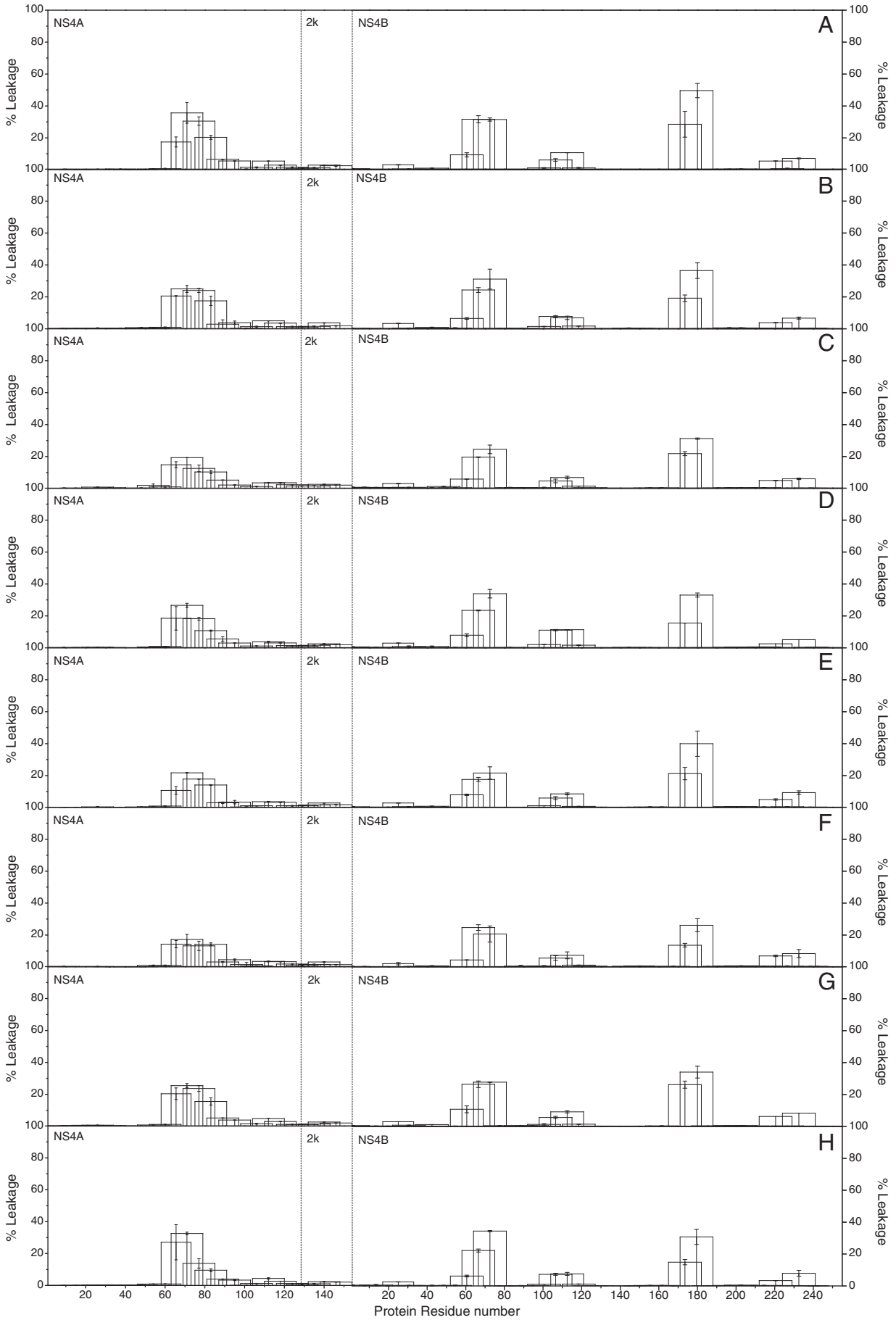
NS4A
2k
NS4B
A
B
C
D
E
F
G
H
% Leakage
Protein Residue number

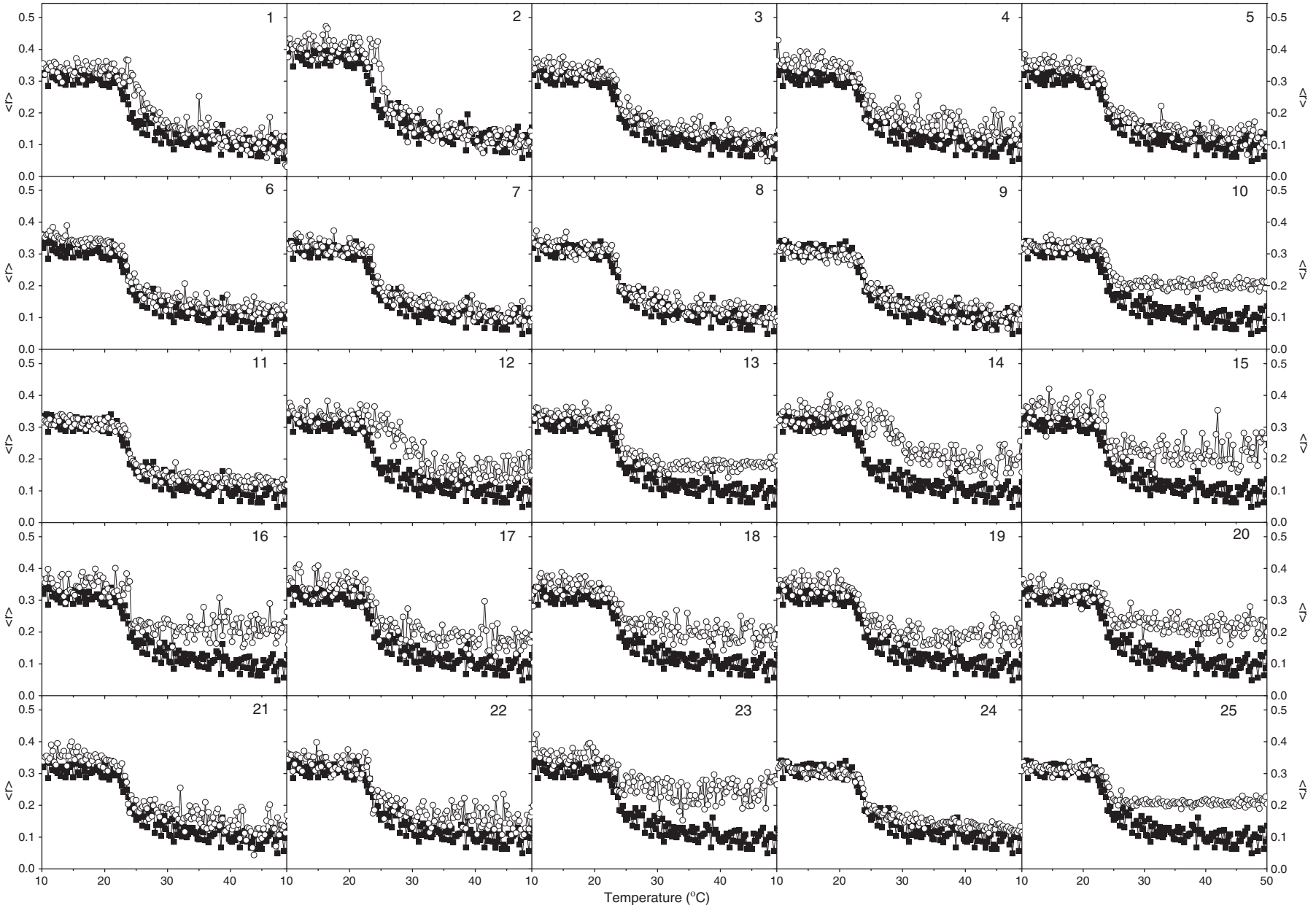

Fig. 5. Steady-state anisotropy, <r>, of DPH incorporated into DMPC model membranes as a function of temperature in the presence of the peptide library corresponding to NS4A/2k. Each peptide is identified by its corresponding number. Data correspond to vesicles containing pure phospholipids (●) and phospholipids plus peptides (○).The peptide to phospholipid molar ratio was 1:15.

summary, peptides from both NS4A and NS4B, capable of inducing membrane leakage, did not have any specific interaction with any specific lipid, as they elicited membrane rupture on all types of membrane model systems independently of phospholipid head group, charge and structure. The coincidental results obtained through both the theoretical and experimental data, would point out that these sequences should be important regions of this protein and would be engaged in membrane interaction.

Membrane lipids undergo a cooperative melting reaction, linked to the loss of conformational order of the lipid chains and influenced by many types of molecules including peptides and proteins. To examine the interaction of the NS4A and NS4B peptide libraries on the phase transitions of DMPC and DEPE as a function of temperature, we have used the steady-state fluorescence anisotropy of the fluorescent probe DPH incorporated into model membranes composed of DMPC (Figs. 5 and 6 for the NS4A and NS4B peptide libraries, respectively) and differential scanning calorimetry (DSC) for model membranes composed of DEPE (Fig. 7). When DMPC was studied in the presence of each one of the peptides corresponding to the NS4A derived peptide library, some of them elicited a significant effect both on the $P_{\beta'}$–L_α transition temperature and the anisotropy (Fig. 5). Peptides 1, 2, 12 and 14 significantly changed the T_m of DMPC whereas peptides 10, 13-20, 23 and 25 increased the anisotropy above but not below the T_m of the phospholipid. When the peptides corresponding to the NS4B derived peptide library were studied, some of them elicited a significant effect both on the transition temperature and on the anisotropy (Fig. 6). Peptides 1, 8–11, 13–16, 18–21 and 41 significantly changed the T_m of DMPC whereas peptides 1, 7, 9–11, 13–23, 28–32, and 34–35 changed the anisotropy either above, below or both the T_m of the phospholipid. Therefore, some peptides pertaining to the NS4A and NS4B derived libraries were capable of affecting the thermal transition T_m of DMPC, hence the conclusion that their effect should be primarily due to their location at the lipid–water interface influencing the fluidity of the phospholipids [44].

Aqueous dispersions of pure DEPE undergo a gel to liquid-crystalline phase transition (L_β–L_α) T_m in the lamellar phase at about 38 °C and in addition a lamellar liquid-crystalline to hexagonal-H_{II} (L_α–H_{II}) phase transition at about 63 °C [45]. As observed in Fig. 7, both gel to liquid-crystalline and lamellar liquid-crystalline to hexagonal-H_{II} transitions were present in all samples, independently of the peptide tested. No peptide induced any significant change on the main transition but some of them did change both the transition temperature and the enthalpy of the lamellar liquid-crystalline to hexagonal-H_{II} transition of DEPE, since this transition is much more sensitive than the lamellar one to molecular interactions [45]. When the peptides corresponding to the NS4A derived peptide library were mixed with DEPE, peptide 18 was the only one that elicited a significant effect, since the L_α–H_{II} transition decreased about 5 °C and the L_β–L_α transition about 0.2 °C (Fig. 7). When the NS4B derived peptides were assayed, the ones which elicited some effect on the L_α–H_{II} phase transition were peptides 5, 18, 26, 29, 35 and 41 (Fig. 7). However, the differences were not significant ($\pm$0.2 °C for the L_β–L_α transition and $\pm$1°C for the L_α–H_{II} transition). The coincidence of these relatively high-effect peptides with high leakage zones demonstrates their specific interaction with the membrane as well as their modulatory effect.

4. Discussion

The virus family Flaviviridae includes Dengue virus (DENV) as well as other viruses such as Japanese encephalitis, Yellow fever, West Nile and tick-borne encephalitis viruses. Similarly to other enveloped viruses, they enter the cell through receptor mediated endocytosis and rearrange internal cell membranes to form the RC, an essential step for viral replication [5–11]. DENV NS4A and NS4B proteins are responsible of the membrane rearrangements which lead to the formation of the RC but its high hydrophobicity precludes the gathering of useful information in a straightforward manner. There are still many questions to be answered regarding the effect both NS4A and NS4B have on membranes. Adding to that and considering the stated previously on this text, they are highly attractive targets for anti-DENV therapy. Therefore, we have carried an exhaustive analysis of the different regions of DENV NS4A and NS4B proteins which might interact with phospholipid membranes using a similar approach to that used before [31,32] and have identified different membranotropic regions on these proteins with the capacity to interact and disrupt membranes.

For NS4A, in accordance with previously obtained data [9], three localized highly positive hydrophobic regions covering the full horizontal length of the two-dimensional plot were observed, segments 51–72, 78–98 and 103–120. These three segments would have therefore the possibility to transverse the membrane as a TM segment. Additionally, in the N-terminal region of the protein we localized two patches along limited zones of the protein surface, i.e., which are characterized by having one polar and one hydrophobic side, segments 2–11 and 21–31, which would represent membrane- and/or protein-interacting zones [43]. In the case of protein NS4B, a total of nine hydrophobic zones were observed, i.e., 35–52, 60–78, 89–100, 103–122, 137–55, 168–188, 190–205, 212–225, and 229–240. Of these, zone 35–52 has 21 amino acids in length, zone 60–78 19 amino acids, zone 103–122 20 amino acids, zone 137–155 19 amino acids and zone 168–188 21 amino acids, so that these five zones could be candidates to transverse the membrane, i.e., constitute TM domains. The other shorter zones could represent membrane- and/or protein-interacting zones. From this picture, it is clear that the distribution of hydrophobicity and interfaciality along the surface of these proteins determine its biological function and membrane interaction.

In this work, we have made an exhaustive study of the effect on membrane integrity of DENV NS4A and NS4B peptide libraries by monitoring leakage from simple and complex liposome compositions. We are aware that a) the use of peptides might not mimic the properties of the intact protein and b) it is not obvious that peptide–membrane interaction is directly related to membrane rupture [31,41,46]. However, two and three consecutive peptides in the library have an overlap of approximately 11 and 4 amino acids respectively, so it seems reasonably to think on the combined effect of peptide groups, i.e., segments, rather than on the effect of isolated peptides. These segments would define therefore membrane interacting domains.

For NS4A, the three hydrophobic regions detected in the two dimensional plots, i.e., 51–72, 78–98 and 103–120, coincided pretty well with the observed leakage zones, i.e., 52–90 and 90–125, though no specificity on liposome composition was observed. Interestingly, peptide no. 18 pertaining to the NS4A peptide library and comprising amino acids 98 to 114 affected significantly the polymorphic phase of DEPE, so that the NS4A region this peptide belongs to could be engaged in changing the membrane phase of lipids, which would lead to the formation of the RC complex by rearrangement of membranes. The highly hydrophobic character of NS4A is remarkable, implying that this protein should be the most important one to be engaged in membrane interaction and structure modulation. The NS4A topology model described previously by Bartensschlager et al. suggests the existence of two transmembrane domains and a tightly membrane associated one [9], coincidental with the three hydrophobic regions commented above. It is also known that NS4A, in concert with other viral and host proteins, promotes significant intracellular membrane changes essential for viral replication [9,20,21]. It would be possible that the tightly membrane associated domain described by Bartensschlager et al. could behave similarly to other comparable domains of other non-structural viral proteins, such as the AH2 domain of NS4B protein from hepatitis C virus [47,48]. These domains would have the potential to traverse the phospholipid bilayer as a transmembrane segment, would be engaged in oligomerization, and have the capability of modifying the membrane phase. For NS4B, leakage data defined four segments, 50–80, 94–127, 163–190 and 210–240, which coincided with four hydrophobic regions detected

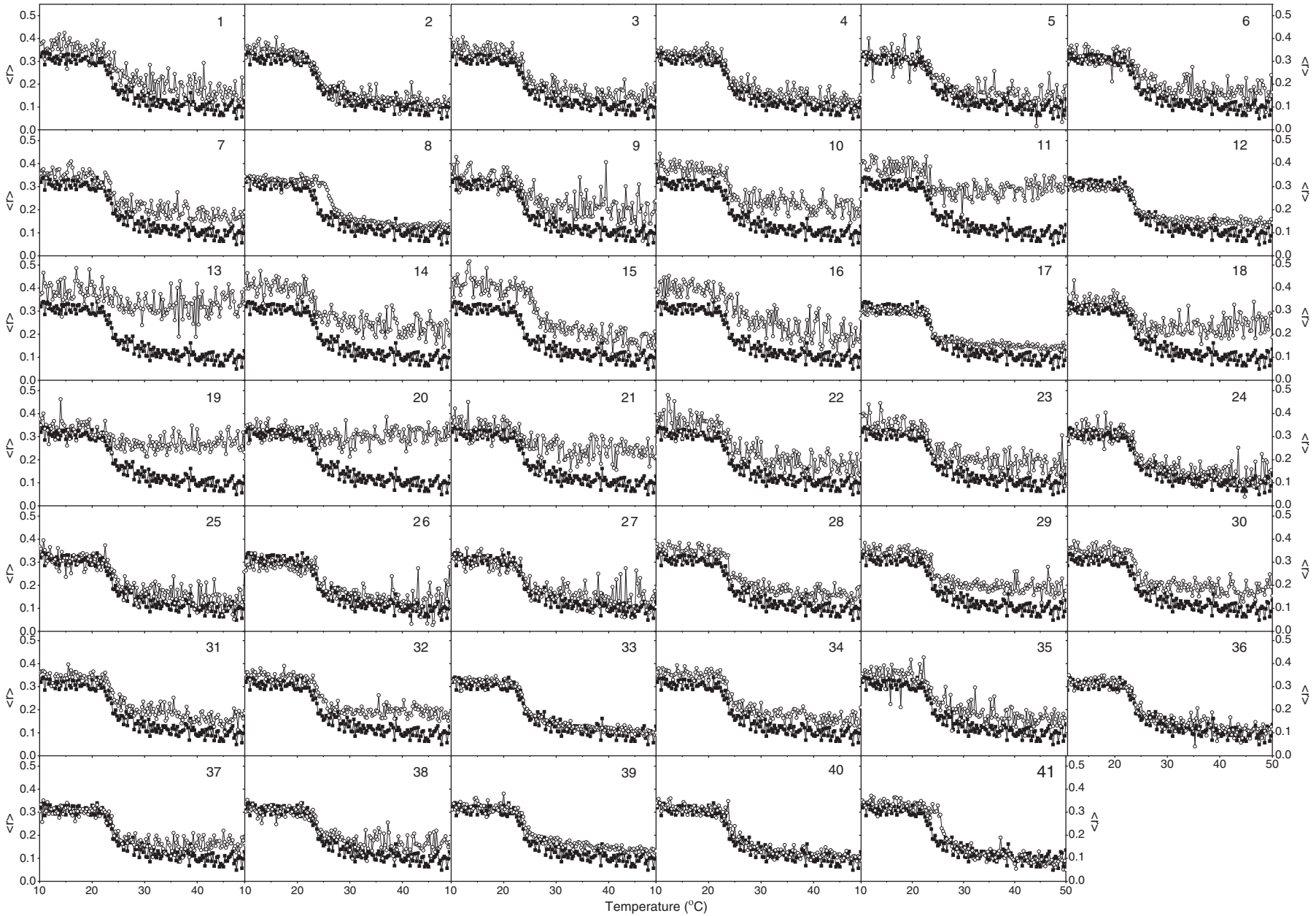

Fig. 6. Steady-state anisotropy, <r>, of DPH incorporated into DMPC model membranes as a function of temperature in the presence of the peptide library corresponding to NS4B. Each peptide is identified by its corresponding number. Data correspond to vesicles containing pure phospholipids (●) and phospholipids plus peptides (○).The peptide to phospholipid molar ratio was 1:15.

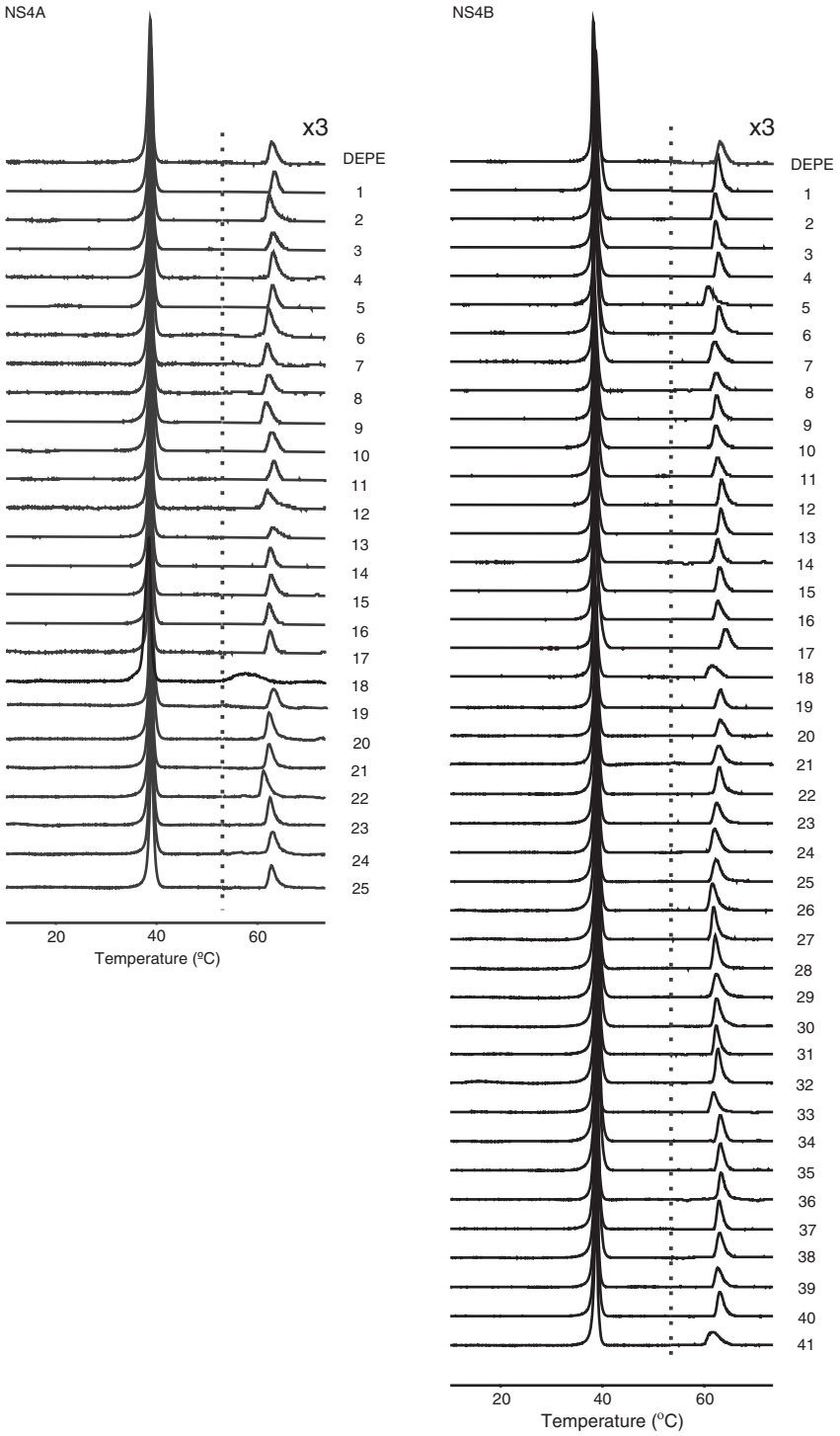

Fig. 7. Differential scanning calorimetry heating-scan thermograms of DEPE in the presence of peptides from NS4A (left) and NS4B (right) DENV protein libraries at a phospholipid/peptide molar ratio of 15:1. The thermogram of pure DEPE is shown on top of each column for comparison. Numbers represent the peptide number in the library. All the thermograms were normalized to the same amount of lipid.

he two dimensional plots. Again, no specificity on liposome composition was observed. These data would imply that these regions could represent membrane-traversing regions, whereas the other NS4B detected regions could represent membrane surface interacting regions. The identified membrane-traversing regions would include the membrane spanning domains, essential for NS4B function [18] and the membrane interacting regions would include a region needed for IFN antagonism, essential for the viral life cycle [24]. These characteristics would imply that NS4B should be engaged in both membrane arrangement and protein/protein and/or lipid/protein interactions. These proteins would have the ability to fluctuate between different conformational states and that would be one of the main differences with fusion proteins; for example, DENV E protein, a class II fusion protein, possesses several membrane interacting domains apart from two proposed transmembrane ones [32]. DENV E protein would have the capability to change from a pre-fusion metastable conformation to a fusion stable one, but not to fluctuate between them [49].

The existence of a large number of hydrophobic and interfacial regions in both DENV NS4A and NS4B proteins would suggest that they could oscillate between metastable and stable conformations defining therefore the mechanism of formation of the replication complex. As it has been commented above and similarly to other enveloped viruses, DENV rearranges cell internal membranes to establish specific sites of replication, critical for the virus life cycle [9–11]. DENV NS4A and NS4B proteins are the main proteins, if solely, engaged in this task. Their function, and therefore their properties, should be similar to other non–structural proteins from other enveloped viruses engaged in similar functions, such as NS4B from hepatitis C virus [41,42]. These proteins might be multifunctional but at least they should have the capacity of disrupting the bilayer structure by modulating the biophysical properties of the membrane phospholipids as it has been shown here. This perturbation should be strong enough to make possible the special rearrangement of the host membranes that gives place to the formation of the replication complex. The required structure inter-conversions might be part of the structural transitions that transform them from the inactive to the active state; they are probably driven by the interaction of different membranotropic segments, such as those described in this work. The inhibition of membrane interaction by direct action on both proteins would be an additional approach to fight against DENV infection. An understanding of the structural features of these processes, directly related to membrane interaction, is essential because they are attractive drug targets. In summary, membrane inducing leakage peptides from both NS4A and NS4B did not have any specific interaction with any specific lipid, and peptides eliciting leakage rupture all types of membrane model systems independently of phospholipid head group, charge and structure. The coincidental results obtained through both the theoretical and experimental data, would point out that these sequences should be important regions of this protein and would be engaged in membrane interaction.

Acknowledgements

This work was partially supported by grant BFU2008-02617-BMC (Ministerio de Ciencia y Tecnología, Spain) to J.V. We are especially grateful to BEI Resources, National Institute of Allergy and Infectious Diseases, Manassas, VA, USA, for the peptides used in this work. H.N. is supported by a “Santiago Grisolía” fellowship from Generalitat Valenciana.

References

[1] M.G. Guzman, G. Kouri, Dengue: an update, Lancet Infect. Dis. 2 (2002) 33–42.
[2] S.B. Halstead, Dengue, Lancet 370 (2007) 1644–1652.
[3] S. Urcuqui-Inchima, C. Patino, S. Torres, A.L. Haenni, F.J. Diaz, Recent developments in understanding dengue virus replication, Adv. Virus Res. 77 (2010) 1–39.
[4] B. Pastorino, A. Nougairede, N. Wurtz, E. Gould, X. de Lamballerie, Role of host cell factors in flavivirus infection: implications for pathogenesis and development of antiviral drugs, Antiviral. Res. 87 (2010) 281–294.
[5] R. Perera, R.J. Kuhn, Structural proteomics of dengue virus, Curr. Opin. Microbiol. 11 (2008) 369–377.
[6] S. Bressanelli, K. Stiasny, S.L. Allison, E.A. Stura, S. Duquerroy, J. Lescar, F.X. Heinz, F.A. Rey, Structure of a flavivirus envelope glycoprotein in its low-pH-induced membrane fusion conformation, EMBO J. 23 (2004) 728–738.
[7] M. Kielian, F.A. Rey, Virus membrane-fusion proteins: more than one way to make a hairpin, Nat. Rev. Microbiol. 4 (2006) 67–76.
[8] S. Mukhopadhyay, R.J. Kuhn, M.G. Rossmann, A structural perspective of the flavivirus life cycle, Nat. Rev. Microbiol. 3 (2005) 13–22.
[9] S. Miller, S. Kastner, J. Krijnse-Locker, S. Buhler, R. Bartenschlager, The non-structural protein 4A of dengue virus is an integral membrane protein inducing membrane alterations in a 2K-regulated manner, J. Biol. Chem. 282 (2007) 8873–8882.
[10] S. Miller, J. Krijnse-Locker, Modification of intracellular membrane structures for virus replication, Nat. Rev. Microbiol. 6 (2008) 363–374.
[11] S. Welsch, S. Miller, I. Romero-Brey, A. Merz, C.K. Bleck, P. Walther, S.D. Fuller, C. Antony, J. Krijnse-Locker, R. Bartenschlager, Composition and three-dimensional architecture of the dengue virus replication and assembly sites, Cell Host Microbe 5 (2009) 365–375.
[12] M.M. Samsa, J.A. Mondotte, N.G. Iglesias, I. Assuncao-Miranda, G. Barbosa-Lima, A.T. Da Poian, P.T. Bozza, A.V. Gamarnik, Dengue virus capsid protein usurps lipid droplets for viral particle formation, PLoS Pathog. 5 (2009) e1000632.
[13] J.M. Mackenzie, A.A. Khromykh, M.K. Jones, E.G. Westaway, Subcellular localization and some biochemical properties of the flavivirus Kunjin nonstructural proteins NS2A and NS4A, Virology 245 (1998) 203–215.
[14] B.D. Lindenbach, C.M. Rice, Trans-complementation of yellow fever virus NS1 reveals a role in early RNA replication, J. Virol. 71 (1997) 9608–9617.
[15] B.D. Lindenbach, C.M. Rice, Genetic interaction of flavivirus nonstructural proteins NS1 and NS4A as a determinant of replicase function, J. Virol. 73 (1999) 4611–4621.
[16] A.E. Gorbalenya, A.P. Donchenko, E.V. Koonin, V.M. Blinov, N-terminal domains of putative helicases of flavi- and pestiviruses may be serine proteases, Nucleic Acids Res. 17 (1989) 3889–3897.
[17] E.V. Koonin, Computer-assisted identification of a putative methyltransferase domain in NS5 protein of flaviviruses and lambda 2 protein of reovirus, J. Gen. Virol. 74 (Pt 4) (1993) 733–740.
[18] S. Miller, S. Sparacio, R. Bartenschlager, Subcellular localization and membrane topology of the dengue virus type 2 non-structural protein 4B, J. Biol. Chem. 281 (2006) 8854–8863.
[19] S.A. Shiryaev, A.V. Chernov, A.E. Aleshin, T.N. Shiryaeva, A.Y. Strongin, NS4A regulates the ATPase activity of the NS3 helicase: a novel cofactor role of the non-structural protein NS4A from West Nile virus, J. Gen. Virol. 90 (2009) 2081–2085.
[20] J. Roosendaal, E.G. Westaway, A. Khromykh, J.M. Mackenzie, Regulated cleavages at the West Nile virus NS4A-2K-NS4B junctions play a major role in rearranging cytoplasmic membranes and Golgi trafficking of the NS4A protein, J. Virol. 80 (2006) 4623–4632.
[21] J.E. McLean, A. Wudzinska, E. Datan, D. Quaglino, Z. Zakeri, Flavivirus NS4A-induced autophagy protects cells against death and enhances virus replication, J. Biol. Chem. 286 (2011) 22147–22159.
[22] M.L. Ng, S.S. Hong, Flavivirus infection: essential ultrastructural changes and association of Kunjin virus NS3 protein with microtubules, Arch. Virol. 106 (1989) 103–120.
[23] E.G. Westaway, J.M. Mackenzie, M.T. Kenney, M.K. Jones, A.A. Khromykh, Ultrastructure of Kunjin virus-infected cells: colocalization of NS1 and NS3 with double-stranded RNA, and of NS2B with NS3, in virus-induced membrane structures, J. Virol. 71 (1997) 6650–6661.
[24] J.L. Munoz-Jordan, G.G. Sanchez-Burgos, M. Laurent-Rolle, A. Garcia-Sastre, Inhibition of interferon signaling by dengue virus, Proc. Natl. Acad. Sci. U. S. A. 100 (2003) 14333–14338.
[25] I. Umareddy, A. Chao, A. Sampath, F. Gu, S.G. Vasudevan, Dengue virus NS4B interacts with NS3 and dissociates it from single-stranded RNA, J. Gen. Virol. 87 (2006) 2605–2614.
[26] S. Tajima, T. Takasaki, I. Kurane, Restoration of replication-defective dengue type 1 virus bearing mutations in the N-terminal cytoplasmic portion of NS4A by additional mutations in NS4B, Arch. Virol. 156 (2011) 63–69.
[27] A.J. Perez-Berna, A.S. Veiga, M.A. Castanho, J. Villalain, Hepatitis C virus core protein binding to lipid membranes: the role of domains 1 and 2, J. Viral Hepat. 15 (2008) 346–356.
[28] J. Guillen, A.J. Perez-Berna, M.R. Moreno, J. Villalain, Identification of the membrane-active regions of the severe acute respiratory syndrome coronavirus spike membrane glycoprotein using a 16/18-mer peptide scan: implications for the viral fusion mechanism, J. Virol. 79 (2005) 1743–1752.
[29] A.J. Perez-Berna, M.R. Moreno, J. Guillen, A. Bernabeu, J. Villalain, The membrane-active regions of the hepatitis C virus E1 and E2 envelope glycoproteins, Biochemistry 45 (2006) 3755–3768.
[30] M.R. Moreno, M. Giudici, J. Villalain, The membranotropic regions of the endo and ecto domains of HIV gp41 envelope glycoprotein, Biochim. Biophys. Acta 1758 (2006) 111–123.
[31] A.J. Perez-Berna, J. Guillen, M.R. Moreno, A. Bernabeu, G. Pabst, P. Laggner, J. Villalain, Identification of the membrane-active regions of hepatitis C virus p7 protein: biophysical characterization of the loop region, J. Biol. Chem. 283 (2008) 8089–8101.
[32] H. Nemesio, F. Palomares-Jerez, J. Villalain, The membrane-active regions of the dengue virus proteins C and E, Biochim. Biophys. Acta 1808 (2011) 2390–2402.
[33] T.W. Keenan, D.J. Morre, Phospholipid class and fatty acid composition of Golgi apparatus isolated from rat liver and comparison with other cell fractions, Biochemistry 9 (1970) 19–25.
[34] A.G. Krainev, D.A. Ferrington, T.D. Williams, T.C. Squier, D.J. Bigelow, Adaptive changes in lipid composition of skeletal sarcoplasmic reticulum membranes associated with aging, Biochim. Biophys. Acta 1235 (1995) 406–418.
[35] L.D. Mayer, M.J. Hope, P.R. Cullis, Vesicles of variable sizes produced by a rapid extrusion procedure, Biochim. Biophys. Acta 858 (1986) 161–168.
[36] C.S.F. Böttcher, C.M. Van Gent, C. Fries, A rapid and sensitive sub-micro phosphorus determination, Anal. Chim. Acta 1061 (1961) 203–204.
[37] H. Edelhoch, Spectroscopic determination of tryptophan and tyrosine in proteins, Biochemistry 6 (1967) 1948–1954.
[38] A. Bernabeu, J. Guillen, A.J. Perez-Berna, M.R. Moreno, J. Villalain, Structure of the C-terminal domain of the pro-apoptotic protein Hrk and its interaction with model membranes, Biochim. Biophys. Acta 1768 (2007) 1659–1670.
[39] M.R. Moreno, J. Guillen, A.J. Perez-Berna, D. Amoros, A.I. Gomez, A. Bernabeu, J. Villalain, Characterization of the interaction of two peptides from the N terminus of the NHR domain of HIV-1 gp41 with phospholipid membranes, Biochemistry 46 (2007) 10572–10584.
[40] B.R. Lentz, Use of fluorescent probes to monitor molecular order and motions within liposome bilayers, Chem. Phys. Lipids 64 (1993) 99–116.

[41] J. Guillen, A. Gonzalez-Alvarez, J. Villalain, A membranotropic region in the C-terminal domain of hepatitis C virus protein NS4B Interaction with membranes, Biochim. Biophys. Acta 1798 (2010) 327–337.
[42] M.F. Palomares-Jerez, J. Villalain, Membrane interaction of segment H1 (NS4B(H1)) from hepatitis C virus non-structural protein 4B, Biochim. Biophys. Acta 1808 (2011) 1219–1229.
[43] R.A. Gadkari, N. Srinivasan, Prediction of protein–protein interactions in dengue virus coat proteins guided by low resolution cryoEM structures, BMC Struct. Biol. 10 (2010) 17.
[44] L.M. Contreras, F.J. Aranda, F. Gavilanes, J.M. Gonzalez-Ros, J. Villalain, Structure and interaction with membrane model systems of a peptide derived from the major epitope region of HIV protein gp41: implications on viral fusion mechanism, Biochemistry 40 (2001) 3196–3207.
[45] R.M. Epand, Lipid polymorphism and protein–lipid interactions, Biochim. Biophys. Acta 1376 (1998) 353–368.
[46] A.J. Perez-Berna, G. Pabst, P. Laggner, J. Villalain, Biophysical characterization of the fusogenic region of HCV envelope glycoprotein E1, Biochim. Biophys. Acta 1788 (2009) 2183–2193.
[47] J. Gouttenoire, V. Castet, R. Montserret, N. Arora, V. Raussens, J.M. Ruysschaert, E. Diesis, H.E. Blum, F. Penin, D. Moradpour, Identification of a novel determinant for membrane association in hepatitis C virus nonstructural protein 4B, J. Virol. 83 (2009) 6257–6268.
[48] J. Gouttenoire, P. Roingeard, F. Penin, D. Moradpour, Amphipathic alpha-helix AH2 is a major determinant for the oligomerization of hepatitis C virus nonstructural protein 4B, J. Virol. 84 (2010) 12529–12537.
[49] J.M. Smit, B. Moesker, I. Rodenhuis-Zybert, J. Wilschut, Flavivirus cell entry and membrane fusion, Viruses 3 (2011) 160–171.
[50] S.H. White, W.C. Wimley, Membrane protein folding and stability: physical principles, Annu. Rev. Biophys. Biomol. Struct. 28 (1999) 319–365.
[51] D.M. Engelman, T.A. Steitz, A. Goldman, Identifying nonpolar transbilayer helices in amino acid sequences of membrane proteins, Annu. Rev. Biophys. Biophys. Chem. 15 (1986) 321–353.
[52] T. Hessa, N.M. Meindl-Beinker, A. Bernsel, H. Kim, Y. Sato, M. Lerch-Bader, I. Nilsson, S.H. White, G. von Heijne, Molecular code for transmembrane-helix recognition by the Sec61 translocon, Nature 450 (2007) 1026–1030.
[53] C.P. Moon, K.G. Fleming, Side-chain hydrophobicity scale derived from transmembrane protein folding into lipid bilayers, Proc. Natl. Acad. Sci. U. S. A. 108 (2011) 10174–10177.
[54] J. Koehler, N. Woetzel, R. Staritzbichler, C.R. Sanders, J. Meiler, A unified hydrophobicity scale for multispan membrane proteins, Proteins 76 (2009) 13–29.
[55] D. Eisenberg, R.M. Weiss, T.C. Terwilliger, The helical hydrophobic moment: a measure of the amphiphilicity of a helix, Nature 299 (1982) 371–374.

Membranotropic regions of Dengue virus prM protein.

Henrique Nemésio, José Villalaín

Instituto de Biología Molecular y Celular, Universidad Miguel Hernández, E-03202 Elche (Alicante), Spain

Sent to **Biochemistry**

MEMBRANOTROPIC REGIONS OF DENGUE VIRUS prM PROTEIN

Henrique Nemésio, and José Villalaín *

Instituto de Biología Molecular y Celular, Universidad “Miguel Hernández”

E-03202 Elche-Alicante, Spain,

RUNNING TITLE: Membranotropic regions of DENGUE virus protein prM

WORD COUNT ABSTRACT: 188

WORD COUNT MAIN TEXT: 4653

KEYWORDS: Dengue virus; prM; viral fusion; viral entry

FUNDING: This work was partially supported by grant BFU2008-02617-BMC (Ministerio de Ciencia y Tecnología, Spain) to J.V.

*Address correspondence to:
José Villalaín
Instituto de Biología Molecular y Celular
Universidad "Miguel Hernández"
E-03202 Alicante (Spain).
Tel: +34 966 658 762;
Fax +34 966 658 758;
E-mail: jvillalain@umh.es

ABBREVIATIONS

BPI	Bovine liver L-α-phosphatidylinositol
BPS	Bovine brain L-α-phosphatidylserine
CF	5-Carboxyfluorescein
CHOL	Cholesterol
CL	Bovine heart cardiolipin
DENV	Dengue virus
DMPC	1,2-Dimyristoyl-*sn*-glycero-3-phosphatidylcholine
DMPG	1,2-Dimyristoyl-*sn*-glycero-3-[phospho-rac-glycerol]
DPH	1,6-Diphenyl-1,3,5-hexatriene
DSC	Differential Scanning Calorimetry
EPA	Egg L-α-phosphatidic acid
EPC	Egg L-α-phosphatidylcholine
ER	Endoplasmic reticulum
ESM	Egg sphingomyelin
LUV	Large unilamellar vesicles
MLV	Multilamellar vesicles
T_m	Temperature of the gel-to–liquid crystalline phase transition
TM	Transmembrane domain
TPE	Egg transphosphatidylated L-α-phosphatidylethanolamine

ABSTRACT

The Dengue virus (DENV) prM protein consists of two moieties, the pr and M domains. Apart from preventing the premature fusion activity of the DENV E protein, prM has several other unknown biological roles, displaying both protein/protein and membrane/protein interactions. Although prM protein is an essential component of the DENV viral cycle, little is known about its biological functions and what regions of this protein are responsible for said functions. By performing an exhaustive study of membrane rupture induced by a prM peptide library on simple and complex model membranes as well as their ability to modulate the phospholipid phase transitions of DMPC and DMPG, six membranotropic regions on the prM protein have been identified. Apart from the previously identified two transmembrane segments of the protein, one of these regions probably interacts with the fusion E protein and another one, the stem segment, would interact with the membrane modulating its structure. These data will help us understand the molecular mechanism of viral entry and morphogenesis, allow the identification of new targets for the treatment of Dengue virus infection and make possible the future development of DENV entry inhibitors.

Dengue virus (DENV) is a constituent of the genus *Flavivirus*, which along with *Hepacivirus* and *Pestivirus* composes the *Flaviviridae* family [1]. Dengue disease is becoming a great public health concern since DENV is the arthropod borne virus with the highest incidence in the human population, with over 390 million estimated infections per year [2]. Patients infected can show a wide range of symptoms, from less to most severe: asymptomatic, mild fever (Dengue fever), Dengue haemorrhagic fever and Dengue shock syndrome [3]. The two latter life-threatening serious conditions are often but not always developed in individuals secondarily affected by heterologous subtypes. There is actually no clinical treatment for DENV infection and no antivirals or vaccines against DENV virus are currently available, so that more than 2 billion people, mainly in poor countries, are at risk in the world [4]. The main strategy to thwart the spread of the infection is based on the control of the mosquito vector (Aedes spp.) itself but the ever increasing global temperature and travelling frequency introduces a real risk of vector spreading to previously unaffected zones.

DENV is a positive-sense, single-stranded RNA virus with approximately 10.7 kb. It contains un-translated regions both at the 5' and 3' ends, flanking a single open reading frame encoding a polyprotein of over 3000 amino acids, which after infection is subsequently cleaved by cellular and viral proteases into three structural proteins (C, prM and E), and seven non-structural proteins [5]. The surface of the virion is composed of a lipid bilayer where 180 copies of E and M protein (a derivative of the prM protein) heterodimers are embedded. The nucleocapsid (composed of C protein and viral RNA) is inside this lipid bilayer [5]. Similarly to other enveloped viruses, the DENV virus enters the cells through receptor mediated endocytosis in a rather complicated process [1c, 5-6] and rearranges cell internal membranes to establish the

replication complex (membranous web) [7]. Details about DENV replication process remain largely unclear, but most, if not all of the DENV proteins, are involved and function in a complex web of protein-protein interactions [1c, 5]. DENV replicates its genome in a membrane-associated replication complex, and morphogenesis and virion budding have been suggested to take place in the endoplasmic reticulum (ER) or ER derived membranes. Considering the structural proteins, the C protein plays a role in the specific encapsidation of the genome and it is essential for the viral assembly [8]. The E protein is a class II fusion protein, essential for attachment, membrane fusion, and assembly. A series of conformational changes occurring in the DENV E protein, driven by the endosomal low-pH, give place to the fusion of the viral and endosomal membranes [1c, 5]. The stem region of the E protein has been proposed to be engaged in the fusion process but the critical regions of the stem region are not known with certainty [5-6, 9].

The prM protein consists of an N-terminal pr domain followed by the M protein and separated by a furin cleavage site [10]. The pr part of the protein consists mainly of β-strands whereas M consists of a linear structure followed by a mainly α-helical stem region and two transmembrane helices [10]. During maturation of the viral particle in the host cell, after traversing the trans Golgi network, the decreasing pH inside the vesicle containing the viral particle(s) (with E and prM proteins embedded in its lipid bilayer) induces a conformational change in this complex that is reversible as long as prM remains intact [10]. As soon as furin cleaves the bond between pr and M, the former is released and the conformational change is no longer reversible, rendering the virus fully mature, thus infectious [5, 10]. The M protein remains in the mature particle as a transmembrane protein covered by the E protein layer. Some non-

structural functions have been also assigned to prM, including a role in apoptosis, since a region of the M protein triggered apoptosis in mouse neuroblastoma and human hepatoma cells [11]. It has also been shown that prM/M interacts with host proteins such as human dynein, vacuolar ATPase and claudin 1, facts that support its importance in the entry and assembly stages of the viral cycle [12]. It has been reported that the expression of M protein alone was sufficient for it to adopt the predicted topology and localise to the ER membrane and that the pr peptide might contain an ER retention signal, possibly important for the correct formation of the prM-E complexes [13]. Interestingly, Zhang et al. have described protein M as a membrane-anchored, pH-sensing, multistep chaperone of protein E [14]. Despite these very important results, the full impact of prM/M in the viral cycle is far from defined.

We have recently identified the membrane-active regions of a number of viral proteins by observing the effect of protein-derived peptide libraries on model membrane integrity [15]. These results allowed us to propose the location of different protein segments implicated in either protein-lipid or protein-protein interactions and help us to understand the mechanisms underlying the interaction between viral proteins and membranes. Motivated by the need to understand the interaction of prM with membranes, considering that it is essential in the viral RNA replication process, and additionally, that DENV protein/membrane and protein/protein interactions are an attractive target for antiviral drug development, we have characterized the membranotropic regions of DENV prM protein. By using a peptide library encompassing the full length of prM and assessing their effect on membrane integrity using model biomembranes, we have identified several prM regions with different interacting capabilities. These data will help us understand the molecular mechanism

of viral fusion and morphogenesis, identify new targets for the treatment of Dengue virus infection as well as render the future development of DENV entry inhibitors which may lead to new vaccine strategies possible.

MATERIALS AND METHODS

Materials and reagents. The peptide library derived from DENV Type 2 NGC prM protein, consisting of 21 peptides (Table 1), was obtained from BEI Resources, National Institute of Allergy and Infectious Diseases, Manassas, VA, USA. All peptides had a purity of about 80% and they were not capped. Peptides were solubilized in water/2,2,2-trifluoroethanol at 70:30 ratios (v/v). Bovine brain phosphatidylserine (BPS), bovine liver L-α-phosphatidylinositol (BPI), cholesterol (Chol), egg L-α-phosphatidic acid (EPA), egg L-α-phosphatidylcholine (EPC), egg sphingomyelin (ESM), egg transphosphatidylated L-α-phosphatidylethanolamine (TPE), bovine heart cardiolipin (CL), 1,2-dimyristoyl-sn-glycero-3-phosphatidylcholine (DMPC), 1,2-dimyristoylphosphatidylglycerol (DMPG), 1,2-dielaidoyl-sn-glycero-3-phosphatidylethanolamine (DEPE) and liver lipid extract were obtained from Avanti Polar Lipids (Alabaster, AL, USA). The lipid composition of the synthetic endoplasmic reticulum (ER) mixture was EPC/CL/BPI/TPE/BPS/EPA/ESM/Chol at a molar ratio of 59:0.37:7.7:18:3.1:1.2:3.4:7.8 [16] whereas the liver lipid extract contained 42%, phosphatidylcholine, 22% phosphatidylethanolamine, 7% Chol, 8% phosphatidylinositol, 1% lysophosphatidylinositol, and 21% miscellaneous lipids including neutral ones, as stated by the manufacturer. 1,6-Diphenyl-1,3,5-hexatriene (DPH) was obtained from Molecular Probes (Eugene, OR). 5-Carboxyfluorescein (CF, >95% by HPLC), Triton X-100, EDTA and HEPES were purchased from Sigma-Aldrich (Madrid, ES). All other chemicals were commercial samples of the highest purity available (Sigma-Aldrich, Madrid, ES). Water was deionized, twice-distilled and passed through a Milli-Q equipment (Millipore Ibérica, Madrid, ES) to a resistivity higher than 18 MΩ cm.

Approximate location of Table 1

Vesicle preparation. Aliquots containing the appropriate amount of lipid in chloroform-methanol (2:1 v/v) were placed in a test tube, the solvents were removed by evaporation under a stream of O_2-free nitrogen, and finally, traces of solvents were eliminated under vacuum in the dark for >3 h. The lipid films were resuspended in an appropriate buffer and incubated either at 25ºC or 10ºC above the phase transition temperature (T_m) with intermittent vortexing for 30 min to hydrate the samples and obtain multilamellar vesicles (MLV). The samples were frozen and thawed five times to ensure complete homogenization and maximization of peptide/lipid contacts with occasional vortexing. Phospholipid and peptide concentration were measured by methods described previously [17].

Membrane leakage measurement. Large unilamellar vesicles (LUV) with a mean diameter of 0.1 μm were prepared from MLV by the extrusion method [18] using polycarbonate filters with a pore size of 0.1 μm (Nuclepore Corp., Cambridge, CA, USA) in buffer containing 10 mM Tris, 20 mM NaCl, pH 7.4 (at 25ºC), and CF at a concentration of 40 mM. Breakdown of the vesicle membrane leads to contents leakage, i.e., CF fluorescence. Non-encapsulated CF was separated from the vesicle suspension through a Sephadex G-75 filtration column (Pharmacia, Uppsala, SW, EU) eluted with buffer containing either 10 mM Tris, 100 mM NaCl, 0.1 mM EDTA, pH 7.4. Leakage of intraliposomal CF was assayed by treating the probe-loaded liposomes (final lipid concentration, 0.125 mM) with the appropriate amounts of peptides on microtiter plates stabilized at 25ºC using a microplate reader (FLUOstar,

BMG Labtech, GER, EU), each well containing a final volume of 170 μl. The medium in the microtiter plates was continuously stirred to allow the rapid mixing of peptide and vesicles. Leakage was measured at an approximate peptide-to-lipid molar ratio of 1:25. Changes in fluorescence intensity were recorded with excitation and emission wavelengths set at 492 and 517 nm, respectively. One hundred percent release was achieved by adding Triton X-100 to a final concentration of 0.5% (w/w) to the microtiter plates. Fluorescence measurements were made initially with probe-loaded liposomes, afterwards by adding peptide solution and finally adding Triton X-100 to obtain 100% leakage. Leakage was quantified on a percentage basis according to the equation, % Release = $[(F_f-F_0)/(F_{100}-F_0)]*100$, F_f being the equilibrium value of fluorescence after peptide addition, F_0 the initial fluorescence of the vesicle suspension and F_{100} the fluorescence value after addition of Triton X-100. For details see refs. [19]

Differential scanning calorimetry. MLVs were formed as stated above in 20 mM HEPES, 100 mM NaCl, 0.1 mM EDTA, pH 7.4. The peptide was added to obtain a peptide/lipid molar ratio of 1:15. The final volume was 0.8 mL (0.6 mM lipid concentration), and incubated 10 ºC above the T_m of each phospholipid for 1 h with occasional vortexing. Differential scanning calorimetry (DSC) experiments were performed in a VP-DSC differential scanning calorimeter (MicroCal LLC, MA) under a constant external pressure of 30 psi in order to avoid bubble formation and samples were heated at a constant scan rate of 60 ºC/h. Experimental data were corrected from small mismatches between the two cells by subtracting a buffer baseline prior to data analysis. The excess heat capacity functions were analysed using Origin 7.0 (Microcal Software). The thermograms were defined by the onset and completion

temperatures of the transition peaks obtained from heating scans. In order to avoid artefacts due to the thermal history of the sample, the first scan was never considered; second and further scans were carried out until a reproducible and reversible pattern was obtained.

Steady-state Fluorescence Anisotropy. MLVs were formed in a buffer composed of 100 mM NaCl, 0.1 mM EDTA, 20 mM HEPES at either pH 7.4 or pH 6.0 (at 25ºC). Aliquots of DPH in N,N'-dimethylformamide (0.2 mM) were directly added to the lipid suspension to obtain a probe/lipid molar ratio of 1:500. DPH, a widespread membrane fluorescent probe for monitoring the organization and dynamics of membranes, is known to partition mainly into the hydrophobic core of the membrane [20]. Samples were incubated for 60 min at 10ºC above the gel to liquid-crystalline phase transition temperature T_m of the phospholipid mixture. Afterwards, the peptides were added to obtain a peptide/lipid molar ratio of 1:15 and incubated 10ºC above the T_m of each lipid for one hour, with occasional vortexing. All fluorescence studies were carried using 5 mm x 5 mm quartz cuvettes in a final volume of 400 µl (315 µM lipid concentration). The steady state fluorescence anisotropy was measured with an automated polarization accessory using a Varian Cary Eclipse fluorescence spectrometer, coupled to a Peltier for automatic temperature change. The vertically and horizontally polarized emission intensities, elicited by vertically polarized excitation, were corrected for background scattering by subtracting the corresponding polarized intensities of a phospholipid preparation lacking probes. The G-factor, accounting for differential polarization sensitivity, was determined by measuring the polarized components of the fluorescence of the probe with horizontally polarized excitation ($G=I_{HV}/I_{HH}$). Samples were excited at 360 nm and emission was recorded

at 430 nm, with excitation and emission slits of 5 nm. Anisotropy values were calculated using the formula $<r> = (I_{VV}-GI_{VH})/(I_{VV}+2GI_{VH})$, where I_{VV} and I_{VH} are the measured fluorescence intensities (after appropriate background subtraction) with the excitation polarizer vertically oriented and the emission polarizer vertically and horizontally oriented, respectively.

RESULTS AND DISCUSSION

We have carried an exhaustive analysis of the different regions of DENV prM protein which might interact either with phospholipid membranes or with other proteins using a similar approach to that used before [15e, f], i.e., using a peptide library derived from the prM protein (Table 1). Although we have studied the effect of a prM peptide library derived from DENV2 strain, the information gathered should be similar for the other three DENV strains since there is a remarkable identity at the primary structure level of the protein for the four known DENV strains (Figure 1). Figure 1 shows the sequences of the prM protein for four representative different DENV serotypes and the alignment of forty-one different strains pertaining to the four serotypes. If we only consider fully conserved residues, sequence identity is 53%, but considering conserved and strongly similar residues the identity increases to 78%. The peptide library we have used in this work is composed of 21 different peptides (Table 1) and their correlation with the prM sequence is shown in Figure 1. Because the peptide library includes the whole sequence of the protein and each individual peptide, i, overlaps with two and three consecutive peptides, i+1 and i+2, by approximately 11 and 4 residues respectively, the obtained data can be extrapolated to protein segments rather than on the effect of isolated peptides. Apart from its availability and peptide solubility, this is the main reason to choose this peptide library.

Approximate location of Figure 1

Two-dimensional plots of hydrophobicity and interfaciality for the whole prM protein, depicted in Figure 2, were obtained taking into consideration the arrangement of the amino acids in the space assuming it adopts an α-helical structure along the whole sequence; they were used in order to detect surfaces along the prM protein which might be identified as membrane and/or protein interacting zones [15b, 21]. As observed in Figure 2, it can be recognized the presence of different regions with large hydrophobic moment values along the surface of the protein. Using these two-dimensional plots it is possible to distinguish two types of patches, those which do not comprise the perimeter of the helix and those which embrace the full perimeter [21]. The first type could favour the interaction with other similar patches along the same or other proteins as well as with the membrane surface whereas the second one could represent transmembrane domains or membrane interacting domains [15a, 15c, 21-22]. As shown in Figure 2, two patches corresponding to the first type and two patches corresponding to the second type are clearly observed; the first two would correspond approximately to residues 66-80 and 122-131 whereas the other two would correspond approximately to residues 133-144 and 152-162. Residues 66-80 pertain to the pr moiety whereas residues 122-131, 133-144 and 152-162 pertain to the M moiety [10]. The patch located between residues 66 and 80 of pr, which is more intense on the water-to-interface than on the water-to-bilayer map, is close to the electrostatic patch of the pr protein comprising residues Asp^{63} and Asp^{65} which specifically interacts with another DENV E protein electrostatic patch (residues His^{244} and Lys^{247}) [10]. The existence of an interfacial/hydrophobic patch near to an electrostatic one would imply that both of them would interact with complementary patches located on the DENV E protein surface [10, 23]. With respect to the M protein, residues 122-131, 133-144 and 152-162 pertain to the stem/interfacial

and transmembrane regions of the M protein. This is in accordance with previous data where the stem region was defined from residues 111 to 131 and the two mainly α-helical transmembrane helices went from residues 131 to 166 [10]. This description of interfacial and hydrophobic rich surfaces fits very well with previous data from the prM protein and adds interesting information highlighting the great utility of these two-dimensional maps in identifying specific regions in proteins [15b, 21].

Approximate location of Figure 2

We have studied the effect of the prM peptide library on membrane rupture by monitoring CF leakage from different liposome compositions and the results are presented in Figure 3 [22]. We have tested five different lipid compositions, simple and complex (Figure 3). The simple compositions contained EPC/Chol at a phospholipid molar ratio of 5:1 (Figure 3A), EPC/SM at a phospholipid molar ratio of 5:1 (Figure 3B) and EPC/SM/Chol at a phospholipid molar ratio of 5:1:1 (Figure 3C), whereas the complex ones consisted of an ER synthetic lipid mixture resembling the ER membrane (Figure 3D) and a lipid extract of liver membranes (Figure 3E). It should be recalled that DENV virus is associated with membranes of the ER or an ER-derived modified compartment. The leakage data (Figures 3A to 3E) shows that some peptides exerted a significant leakage effect, most probably by giving place to local defects in the membrane. Although there were some differences depending on liposome composition, they were not significant to infer any specific relationship between lipid composition and leakage. The leakage effects were mainly focused on two specific regions delimited by peptides 4-6 (residues 22 to 52) and 18-21 (residues 124 to 164), the first group pertaining to the pr moiety and the second one

to the M moiety. Leakage values elicited by peptides 18-21 were significant, since they oscillated between 30 and 50%. Lower, but significant, leakage values were found for peptides 4-6, since 10-15% leakage values were found (Figure 3).

Approximate location of Figure 3

The average leakage of all membrane compositions tested for the prM protein is presented in Figure 3F and it can be compared to the water-to-interfacial (Figure 3G, data obtained from Figure 2A) and water-to-bilayer data (Figure 3H, data obtained from Figure 2B). It can be observed that the leakage data fits perfectly well with the hydrophobic and interfacial regions, overall defining 6 different and characteristic regions (Figure 3F). Region 1 would be a broad region and comprise residues 20 to 50; this region would be defined by relatively low leakage and hydrophobic values. Region 2 would be defined by residues 70 to 80 and would be characterized by a relatively high interfacial and hydrophobic character but no leakage. In principle this region would define a protein-protein interaction domain. Region 3, comprised by residues 95 and 115, would be defined by no leakage and low interfacial and hydrophobic character, which might suggest a weak protein-protein interacting region. Region 4 would be defined by significant and dramatic leakage values concurrent with high interfaciality and low hydrophobicity. This region would outline the stem/pre-transmembrane region of the prM protein. The existence of pre-transmembrane domains in viral proteins with a strong propensity for partitioning into membrane interfaces is well-known [24]. These domains are characterized by having high water-to-interface transfer free energies immediately followed by high water-to-bilayer transfer free energies, usually with some overlapping. These characteristics

are presented by the prM region 4 (see Figures 3G and 3H) so that it would be reasonable to suppose that the stem region of the prM protein could behave as a pre-transmembrane interacting domain. Regions 5 and 6 would be defined by residues 130 to 142 and residues 149 to 162 and present high leakage and significant interfacial and hydrophobic values, delineating the extension of the two transmembrane domains of the prM protein. In summary, peptides from DENV2 prM protein, capable of inducing membrane leakage, did not have any specific interaction with any specific lipid, as they elicited similar membrane rupture on all types of membrane model systems independently of phospholipid head group, charge and structure. The coincidental results obtained through both the theoretical and experimental data, would point out that these sequences should be important regions of this protein and would be engaged in membrane interaction either with its surface or its interior.

Approximate location of Figure 4

Phospholipids can undergo a cooperative melting reaction linked to the loss of conformational order of the lipid chains; this melting process can be influenced by many types of molecules including peptides and proteins. The effect of the prM peptide library on the thermotropic phase behaviour of phospholipid multilamellar vesicles was studied using differential scanning calorimetry, DSC, (Figure 4). Aqueous dispersions of the pure phospholipids DMPC and DMPG undergo a gel to liquid-crystalline phase transition ($P_{\beta'}$-L_{α}) T_m in the lamellar phase at about 23-24 ºC and in addition a pre-transition at about 12-13ºC ($L_{\beta'}$-$P_{\beta'}$). As observed in Figure 4A, when DMPC was studied in the presence of each of the peptides corresponding to

the prM derived peptide library, both pre and main transitions were present in all samples, displaying similar enthalpies, independently of the peptide tested. There were minor changes in the T_m temperatures for several samples (peptides 12 and 14 induced the greatest effect since they decreased T_m from 23.4ºC in the pure phospholipid to 22ºC in the presence of the peptides). There was also some decrease in the cooperativity of DMPC upon peptide addition but, similarly to what has been commented above, the increase in width was a slight one. Contrarily to what was seen in DMPC in the case of the negatively charged phospholipid DMPG some peptides elicited a significant effect both on the pre and the main transition temperatures (Figure 4B). The most significant effect was observed for peptides 16 (net charge of 0, see Table 1) and 17 (net charge of +2), since they abolished the pretransition and significantly decreased the cooperativity of the main transition (see Figure 4). These peptides increased the T_m temperature of DMPC from 22.8ºC in the pure phospholipid to 25.6ºC in the presence of the peptides. Peptides 8 and 11, having net charges of -1 and +1 respectively, also elicited a significant effect on DMPG, since they induced the appearance of more than one peak and an increase of about 4-5ºC in the width of the T_m transition (Figure 4). Besides peptides 8 and 11, peptides 1, 18,19, 20 and 21 (net charges of +1, +1, 0, +1 and +1, respectively) also induced significant effects on the T_m transition of DMPG, since they were responsible for the appearance of two peaks in the main transition (Figure 4B). The presence of different peaks in the thermograms indicate that the peptides were capable of affecting DMPG model membranes inducing the formation of mixed lipid phases, enriched and impoverished in peptide. By comparing Figures 3 and 4 it can be observed that there is a coincidence of the high-effect peptides with high leakage zones, demonstrating their specific interaction with the membrane as well as their

modulatory effect. The specific effect that some peptides have on DMPG do not seem to be exclusively electrostatic, since the net charge of those peptides affecting more dramatically the phospholipid (see above) range from -1 to +2, including the intermediate values.

Approximate location of Figure 5

The effect of the prM peptide library on the structural and thermotropic properties of phospholipid membranes was also investigated by measuring the steady-state fluorescence anisotropy of the fluorescent probe DPH incorporated into model membranes as a function of temperature. The phospholipids which have been studied are DMPC at pH 7.4 and pH 6.0 (Supplemental Figures 1 and 2, respectively) and DMPG at pH 7.4 (Figure 5). DMPC, in the presence of several of the peptides and at both pH values, presented a slight decrease in the cooperativity of the thermal transition, but no significant change in the T_m when compared to the pure lipid (Supplemental Figures 1 and 2). However, there were several peptides which increased the anisotropy of DMPC above the T_m of the phospholipid, specifically peptides 4-5 and peptides 18-21 (Supplemental Figures 1 and 2). The increase in anisotropy elicited by peptides 18-21 was significantly higher than that observed for peptides 4-5. It should be recalled that peptides 4-5 pertain to region 1 and peptides 18-21 to regions 4-6 as defined previously (Figure 3). A relatively similar pattern was found for DMPG, since some peptides decreased slightly the cooperativity of the thermal transition without altering the T_m itself (Figure 5). Similarly to what has been commented above, peptides 4-5 and peptides 18-21 increased the anisotropy of the mixture above but not below the T_m of the phospholipid, significantly

higher for the later than the former (Figure 5). Interestingly, these data would suggest that peptides 4-5 interact with the membrane interface and peptides 18-21, which interestingly coincide with the two transmembrane regions of the prM protein, with the deep part of the membrane (the DPH probe is known to be located inside the palisade structure of the membrane).

In conclusion, using both theoretical and experimental data we have been able to identify different protein/protein and protein/membrane interacting regions on the DENV prM protein highlighting that not only the pr moiety could interact with the fusion E protein but also the M moiety. Apart from the two transmembrane regions of prM (regions 5 and 6, Figure 3), the most relevant interacting regions should be regions 1 (protein-protein, pr domain) and 4 (membrane-protein, M domain). It should be recalled that the E protein also possesses several membrane interacting domains apart from two proposed transmembrane ones [15f]. Our data would imply that the prM protein could be engaged in both protein/protein and/or lipid/protein interactions thorough the diferent regions described in this work which might help us to understand its specific role in the DENV viral cycle. Apart from that, the M moiety could interact with the membrane interface through the stem/interfacial segment of the protein modifying the capability of the E protein to interact with it. From the general picture shown above, it can be gathered that the distribution of interfaciality and hydrophobicity on the protein surface would relate to its biological function, i.e., membrane traversing segments, membrane surface interaction, protein-protein oligomerization and/or protein-protein interaction. Furthermore, it is known that viral proteins can interconvert between different structures with different biological properties (active/inactive, mature/immature states). These structural transitions are

driven by a plethora of molecular interactions, including interactions between membranotropic protein segments such as those described here. An understanding of the structural features of these processes, directly related to membrane interaction, is essential because they are attractive drug targets since the inhibition of membrane and/or protein-protein interaction by a direct action would be an additional approach to fight against DENV infection.

CONCLUSION

We have identified different regions on the DENV prM protein highlighting that not only the pr moiety could interact with the fusion E protein but also the M moiety. The pr moiety would comprise two segments, a membrane and a protein interacting domains, whereas the M moiety would comprise four segments, a membrane and a protein interacting domains as well as two transmembrane domains. Apart from that, the M moiety could interact with the membrane interface through the stem/interfacial segment of the protein modifying the capability of the E protein to interact with it. These zones should be involved in a complex web of interactions with both the fusion E protein and the membrane and should be considered interesting therapeutic targets.

ACKNOWLEDGEMENTS

This work was partially supported by grant BFU2008-02617-BMC (Ministerio de Ciencia y Tecnología, Spain) to J.V. We are especially grateful to BEI Resources, National Institute of Allergy and Infectious Diseases, Manassas, VA, USA, for the peptides used in this work. H.N. is supported by a FPU fellowship from MECD (Ministerio de Educación, Cultura y Deporte), Spain.

LEGENDS TO FIGURES

FIGURE 1. Sequences of the prM protein for four representative different DENVserotypes. The sequences were split for better visualization. A global Clustalw2 alignment was computed using forty-one strains derived from DENV1 (02_20, 05K4147DK1, 297arg00, BIDV1323, BIDV1800, BIDV1841, BIDV1926VN2008, BIDV2143, BIDV2243VE2007 and ThD1004901), DENV2 (NGC, BIDV633, BIDV687, CSF381, CSF63, DakArD20761, DF707, DF755, MD1504, MD903 and MD917), DENV3 (05K797DK1, 07CHLS001, 98, 98TWmosq, BIDV1831VN2007, BIDV1874VN2007, BR29002, C036094, TB55i and ThD31283_98) and DENV4 (2A, BIDV2165VE1998, BIDV2170VE1999, H241, rDEN4del30, Sin897695, ThD4047697, ThD4048501, Vp4 and Yama). Below each table there is a graphic line showing the relative location and length of each peptide in the peptide library. Maximum overlap between adjacent peptides is 11 amino acids.

FIGURE 2. Calculated **t**wo-dimensional plot of the average normalized (A) water-to-membrane and (B) water-to-interface transfer free energy scales in kcal/mol for prM protein [25]. Transfer free energies (kcal/mol) were obtained from Wimley and White [26], Engelman et al. [27], Hessa et al. [28], Moon and Fleming [29], Meiler et al. [30] and Eisenberg et al. [31]. Positive values represent positive transfer free energy values and therefore the higher (darker) the value, the greater the probability to interact with the membrane surface and/or hydrophobic core. The sequence of the DENV2 NGC prM protein overlaps the two-dimensional plots to easily follow the text. The sequence

number of the rightmost residue and a schematic diagram of the different domains of the prM protein according to literature is shown in (C).

FIGURE 3. Effect of the peptide library derived from the DENV2 prM protein on the release of LUV CF contents for different lipid compositions. Leakage data (membrane rupture) for LUVs composed for LUVs composed of (A) EPC/Chol at a phospholipid molar ratio of 5:1, (B) EPC/SM at a phospholipid molar ratio of 5:1,(C) EPC/SM/Chol at a phospholipid molar ratio of 5:1:1,(D) ER complex synthetic lipid mixture and (E) lipid extract of liver membranes. Vertical bars indicate standard deviations of the mean of quintuplicate samples.

Figure 4. Differential scanning calorimetry heating thermograms corresponding to model membranes composed of (A) DMPC and (B) DMPG in the absence and in the presence of the peptides belonging to the prM protein library at a phospholipid/peptide molar ratio of 10:1. All the thermograms were normalized to the same amount of lipid.

FIGURE 5. Steady-state anisotropy, <r>, of the DPH probe incorporated into DMPG model membranes as a function of temperature in the presence of the peptide library corresponding to prM and at pH 7.4. Each peptide is identified by its corresponding number. Data correspond to vesicles containing pure phospholipid (●) and phospholipid plus peptide (○).The peptide to phospholipid molar ratio was 1:15.

TABLE 1

Sequence and residue position of all peptides contained in the DENV2 NGC prM derived library.

PEPTIDE NUMBER	*NO. OF AMINO ACIDS*	*SEQUENCE*	*AMINO ACID POSITION*	*NET CHARGE*
1	16	FHLTTRNGEPHMIVSR	1-16	+1
2	18	NGEPHMIVSRQEKGKSLL	7-24	+1
3	17	SRQEKGKSLLFKTEDGV	15-31	+1
4	18	SLLFKTEDGVNMCTLMAM	22-39	-1
5	15	GVNMCTLMAMDLGEL	30-44	-2
6	18	TLMAMDLGELCEDTITYK	35-52	-3
7	15	ELCEDTITYKCPFLK	43-57	-1
8	17	TITYKCPFLKQNEPEDI	48-64	-1
9	20	FLKQNEPEDIDCWCNSTSTW	55-74	-3
10	18	DCWCNSTSTWVTYGTCTT	63-80	-1
11	18	TWVTYGTCTTTGEHRREK	71-88	+1
12	18	TTTGEHRREKRSVALVPH	79-96	+2
13	18	EKRSVALVPHVGMGLETR	87-104	+1
14	15	PHVGMGLETRTETWM	95-109	-1
15	18	GLETRTETWMSSEGAWKH	100-117	-1
16	18	WMSSEGAWKHAQRIETWI	108-125	0
17	18	KHAQRIETWILRHPGFTI	116-133	+2
18	17	WILRHPGFTIMAAILAY	124-140	+1
19	17	FTIMAAILAYTIGTTHF	131-147	0
20	18	LAYTIGTTHFQRALIFIL	138-155	+1
21	19	HFQRALIFILLTAVAPSMT	146-164	1

REFERENCES

1. (a) Guzman, M. G.; Kouri, G., Dengue: an update. *Lancet Infect Dis* **2002,** *2* (1), 33-42; (b) Halstead, S. B., Dengue. *Lancet* **2007,** *370* (9599), 1644-52; (c) Mukhopadhyay, S.; Kuhn, R. J.; Rossmann, M. G., A structural perspective of the flavivirus life cycle. *Nat Rev Microbiol* **2005,** *3* (1), 13-22.

2. Bhatt, S.; Gething, P. W.; Brady, O. J.; Messina, J. P.; Farlow, A. W.; Moyes, C. L.; Drake, J. M.; Brownstein, J. S.; Hoen, A. G.; Sankoh, O.; Myers, M. F.; George, D. B.; Jaenisch, T.; Wint, G. R.; Simmons, C. P.; Scott, T. W.; Farrar, J. J.; Hay, S. I., The global distribution and burden of dengue. *Nature* **2013,** *496* (7446), 504-7.

3. WHO *Dengue: Guidelines for Diagnosis, Treatment, Prevention and Control*; World Health Organization: 2009.

4. Pastorino, B.; Nougairede, A.; Wurtz, N.; Gould, E.; de Lamballerie, X., Role of host cell factors in flavivirus infection: Implications for pathogenesis and development of antiviral drugs. *Antiviral Res* **2010,** *87* (3), 281-94.

5. Perera, R.; Kuhn, R. J., Structural proteomics of dengue virus. *Curr Opin Microbiol* **2008,** *11* (4), 369-77.

6. (a) Bressanelli, S.; Stiasny, K.; Allison, S. L.; Stura, E. A.; Duquerroy, S.; Lescar, J.; Heinz, F. X.; Rey, F. A., Structure of a flavivirus envelope glycoprotein in its low-pH-induced membrane fusion conformation. *Embo J* **2004,** *23* (4), 728-38; (b) Kielian, M.; Rey, F. A., Virus membrane-fusion proteins: more than one way to make a hairpin. *Nat Rev Microbiol* **2006,** *4* (1), 67-76.

7. (a) Miller, S.; Kastner, S.; Krijnse-Locker, J.; Buhler, S.; Bartenschlager, R., The non-structural protein 4A of dengue virus is an integral membrane protein inducing membrane alterations in a 2K-regulated manner. *J Biol Chem* **2007,** *282*

(12), 8873-82; (b) Miller, S.; Krijnse-Locker, J., Modification of intracellular membrane structures for virus replication. *Nat Rev Microbiol* **2008,** *6* (5), 363-74; (c) Welsch, S.; Miller, S.; Romero-Brey, I.; Merz, A.; Bleck, C. K.; Walther, P.; Fuller, S. D.; Antony, C.; Krijnse-Locker, J.; Bartenschlager, R., Composition and three-dimensional architecture of the dengue virus replication and assembly sites. *Cell Host Microbe* **2009,** *5* (4), 365-75.

8. Qi, R. F.; Zhang, L.; Chi, C. W., Biological characteristics of dengue virus and potential targets for drug design. *Acta Biochim Biophys Sin (Shanghai)* **2008,** *40* (2), 91-101.

9. Hsieh, S. C.; Zou, G.; Tsai, W. Y.; Qing, M.; Chang, G. J.; Shi, P. Y.; Wang, W. K., The C-terminal helical domain of dengue virus precursor membrane protein is involved in virus assembly and entry. *Virology* **2011,** *410* (1), 170-80.

10. Li, L.; Lok, S. M.; Yu, I. M.; Zhang, Y.; Kuhn, R. J.; Chen, J.; Rossmann, M. G., The flavivirus precursor membrane-envelope protein complex: structure and maturation. *Science* **2008,** *319* (5871), 1830-4.

11. Catteau, A.; Kalinina, O.; Wagner, M. C.; Deubel, V.; Courageot, M. P.; Despres, P., Dengue virus M protein contains a proapoptotic sequence referred to as ApoptoM. *J Gen Virol* **2003,** *84* (Pt 10), 2781-93.

12. (a) Brault, J. B.; Kudelko, M.; Vidalain, P. O.; Tangy, F.; Despres, P.; Pardigon, N., The interaction of flavivirus M protein with light chain Tctex-1 of human dynein plays a role in late stages of virus replication. *Virology* **2011,** *417* (2), 369-78; (b) Duan, X.; Lu, X.; Li, J.; Liu, Y., Novel binding between pre-membrane protein and vacuolar ATPase is required for efficient dengue virus secretion. *Biochem Biophys Res Commun* **2008,** *373* (2), 319-24; (c) Gao, F.; Duan, X.; Lu, X.; Liu, Y.; Zheng, L.; Ding, Z.; Li, J., Novel binding between pre-membrane protein and claudin-1 is

required for efficient dengue virus entry. *Biochem Biophys Res Commun* **2010,** *391* (1), 952-7; (d) Che, P.; Tang, H.; Li, Q., The interaction between claudin-1 and dengue viral prM/M protein for its entry. *Virology* **2013,** *446* (1-2), 303-13.

13. Wong, S. S.; Haqshenas, G.; Gowans, E. J.; Mackenzie, J., The dengue virus M protein localises to the endoplasmic reticulum and forms oligomers. *FEBS Lett* **2012,** *586* (7), 1032-7.

14. Halstead, S. B., Identifying protective dengue vaccines: guide to mastering an empirical process. *Vaccine* **2013,** *31* (41), 4501-7.

15. (a) Perez-Berna, A. J.; Veiga, A. S.; Castanho, M. A.; Villalain, J., Hepatitis C virus core protein binding to lipid membranes: the role of domains 1 and 2. *J Viral Hepat* **2008,** *15* (5), 346-56; (b) Guillen, J.; Perez-Berna, A. J.; Moreno, M. R.; Villalain, J., Identification of the membrane-active regions of the severe acute respiratory syndrome coronavirus spike membrane glycoprotein using a 16/18-mer peptide scan: implications for the viral fusion mechanism. *J Virol* **2005,** *79* (3), 1743-52; (c) Perez-Berna, A. J.; Moreno, M. R.; Guillen, J.; Bernabeu, A.; Villalain, J., The membrane-active regions of the hepatitis C virus E1 and E2 envelope glycoproteins. *Biochemistry* **2006,** *45* (11), 3755-68; (d) Moreno, M. R.; Giudici, M.; Villalain, J., The membranotropic regions of the endo and ecto domains of HIV gp41 envelope glycoprotein. *Biochim Biophys Acta* **2006,** *1758* (1), 111-23; (e) Perez-Berna, A. J.; Guillen, J.; Moreno, M. R.; Bernabeu, A.; Pabst, G.; Laggner, P.; Villalain, J., Identification of the Membrane-active Regions of Hepatitis C Virus p7 Protein: BIOPHYSICAL CHARACTERIZATION OF THE LOOP REGION. *J Biol Chem* **2008,** *283* (13), 8089-101; (f) Nemesio, H.; Palomares-Jerez, F.; Villalain, J., The membrane-active regions of the dengue virus proteins C and E. *Biochim Biophys Acta* **2011,** *1808* (10), 2390-402.

16. (a) Keenan, T. W.; Morre, D. J., Phospholipid class and fatty acid composition of golgi apparatus isolated from rat liver and comparison with other cell fractions. *Biochemistry* **1970,** *9* (1), 19-25; (b) Krainev, A. G.; Ferrington, D. A.; Williams, T. D.; Squier, T. C.; Bigelow, D. J., Adaptive changes in lipid composition of skeletal sarcoplasmic reticulum membranes associated with aging. *Biochim Biophys Acta* **1995,** *1235* (2), 406-18.

17. (a) Böttcher, C. S. F.; Van Gent, C. M.; Fries, C., A rapid and sensitive sub-micro phosphorus determination. *Anal Chim Acta* **1961,** *1061*, 203-204; (b) Edelhoch, H., Spectroscopic determination of tryptophan and tyrosine in proteins. *Biochemistry* **1967,** *6* (7), 1948-54.

18. Mayer, L. D.; Hope, M. J.; Cullis, P. R., Vesicles of variable sizes produced by a rapid extrusion procedure. *Biochim Biophys Acta* **1986,** *858* (1), 161-8.

19. (a) Bernabeu, A.; Guillen, J.; Perez-Berna, A. J.; Moreno, M. R.; Villalain, J., Structure of the C-terminal domain of the pro-apoptotic protein Hrk and its interaction with model membranes. *Biochim Biophys Acta* **2007,** *1768* (6), 1659-70; (b) Moreno, M. R.; Guillen, J.; Perez-Berna, A. J.; Amoros, D.; Gomez, A. I.; Bernabeu, A.; Villalain, J., Characterization of the Interaction of Two Peptides from the N Terminus of the NHR Domain of HIV-1 gp41 with Phospholipid Membranes. *Biochemistry* **2007,** *46* (37), 10572-84.

20. Lentz, B. R., Use of fluorescent probes to monitor molecular order and motions within liposome bilayers. *Chem Phys Lipids* **1993,** *64* (1-3), 99-116.

21. Guillen, J.; Gonzalez-Alvarez, A.; Villalain, J., A membranotropic region in the C-terminal domain of Hepatitis C virus protein NS4B Interaction with membranes. *Biochim Biophys Acta* **2010,** *1798* (3), 327-337.

22. Palomares-Jerez, M. F.; Villalain, J., Membrane interaction of segment H1 (NS4B(H1)) from hepatitis C virus non-structural protein 4B. *Biochim Biophys Acta* **2011,** *1808*, 1219-1229.

23. Gadkari, R. A.; Srinivasan, N., Prediction of protein-protein interactions in dengue virus coat proteins guided by low resolution cryoEM structures. *BMC Struct Biol* **2010,** *10*, 17.

24. Palomares-Jerez, F.; Nemesio, H.; Villalain, J., The membrane spanning domains of protein NS4B from hepatitis C virus. *Biochim Biophys Acta* **2012,** *1818* (12), 2958-66.

25. Nemesio, H.; Palomares-Jerez, F.; Villalain, J., NS4A and NS4B proteins from dengue virus: membranotropic regions. *Biochim Biophys Acta* **2012,** *1818* (11), 2818-30.

26. White, S. H.; Wimley, W. C., Membrane protein folding and stability: physical principles. *Annu Rev Biophys Biomol Struct* **1999,** *28*, 319-65.

27. Engelman, D. M.; Steitz, T. A.; Goldman, A., Identifying nonpolar transbilayer helices in amino acid sequences of membrane proteins. *Annu Rev Biophys Biophys Chem* **1986,** *15*, 321-53.

28. Hessa, T.; Meindl-Beinker, N. M.; Bernsel, A.; Kim, H.; Sato, Y.; Lerch-Bader, M.; Nilsson, I.; White, S. H.; von Heijne, G., Molecular code for transmembrane-helix recognition by the Sec61 translocon. *Nature* **2007,** *450* (7172), 1026-30.

29. Moon, C. P.; Fleming, K. G., Side-chain hydrophobicity scale derived from transmembrane protein folding into lipid bilayers. *Proc Natl Acad Sci U S A* **2011,** *108* (25), 10174-7.

30. Koehler, J.; Woetzel, N.; Staritzbichler, R.; Sanders, C. R.; Meiler, J., A unified hydrophobicity scale for multispan membrane proteins. *Proteins* **2009,** *76* (1), 13-29.

31. Eisenberg, D.; Weiss, R. M.; Terwilliger, T. C., The helical hydrophobic moment: a measure of the amphiphilicity of a helix. *Nature* **1982,** *299* (5881), 371-4.

SUPPORTING INFORMATION AVAILABLE

Full description of the material. This material is available free of charge via the Internet at http://pubs.acs.org .

SUPPLEMENTAL FIGURE 1. Steady-state anisotropy, <r>, of the DPH probe incorporated into DMPC model membranes as a function of temperature in the presence of the peptide library corresponding to prM at pH 7.4. Each peptide is identified by its corresponding number. Data correspond to vesicles containing pure phospholipid (●) and phospholipid plus peptide (○).The peptide to phospholipid molar ratio was 1:15.

SUPPLEMENTAL FIGURE 1. Steady-state anisotropy, <r>, of the DPH probe incorporated into DMPC model membranes as a function of temperature in the presence of the peptide library corresponding to prM at pH 6.0. Each peptide is identified by its corresponding number. Data correspond to vesicles containing pure phospholipid (●) and phospholipid plus peptide (○).The peptide to phospholipid molar ratio was 1:15.

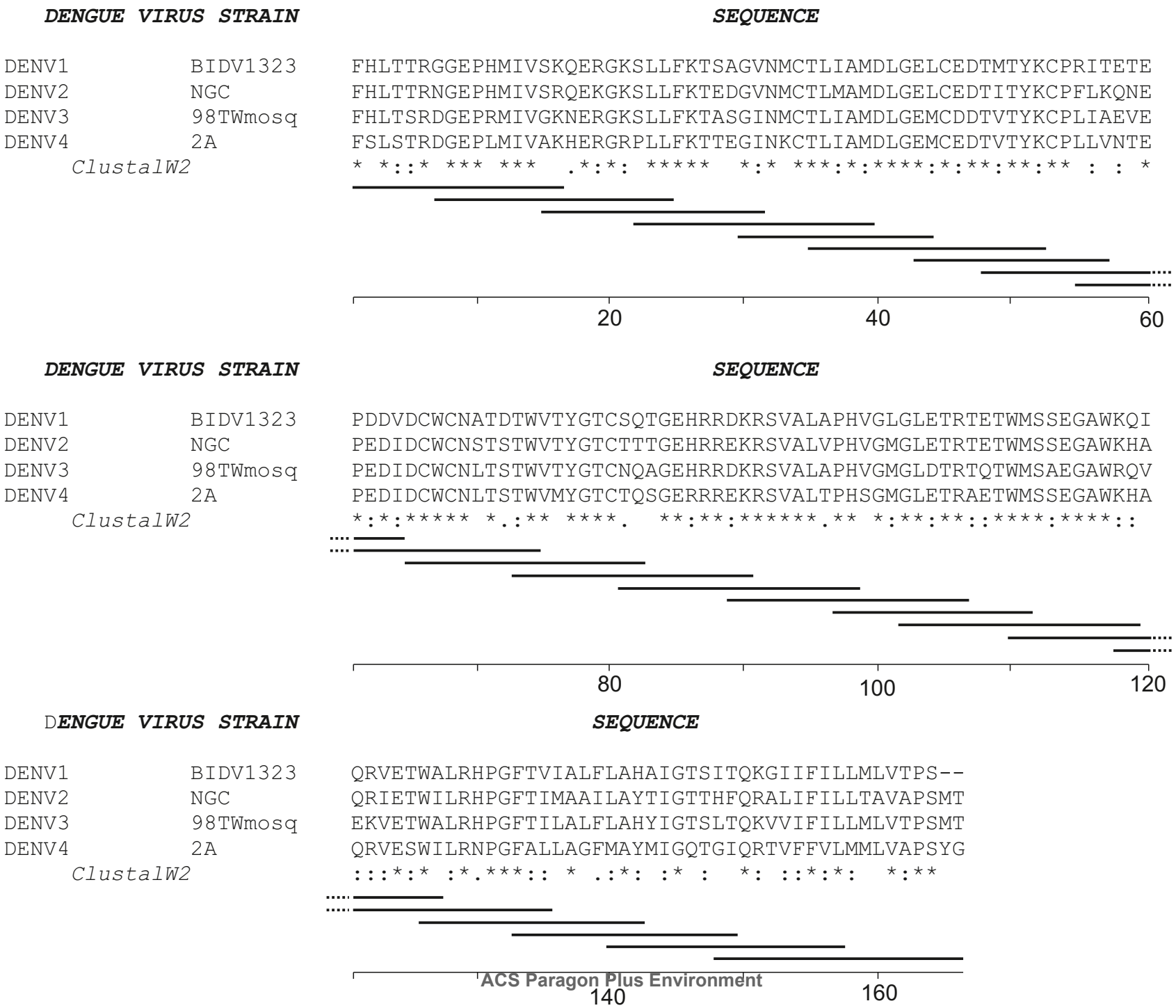

FIGURE 1

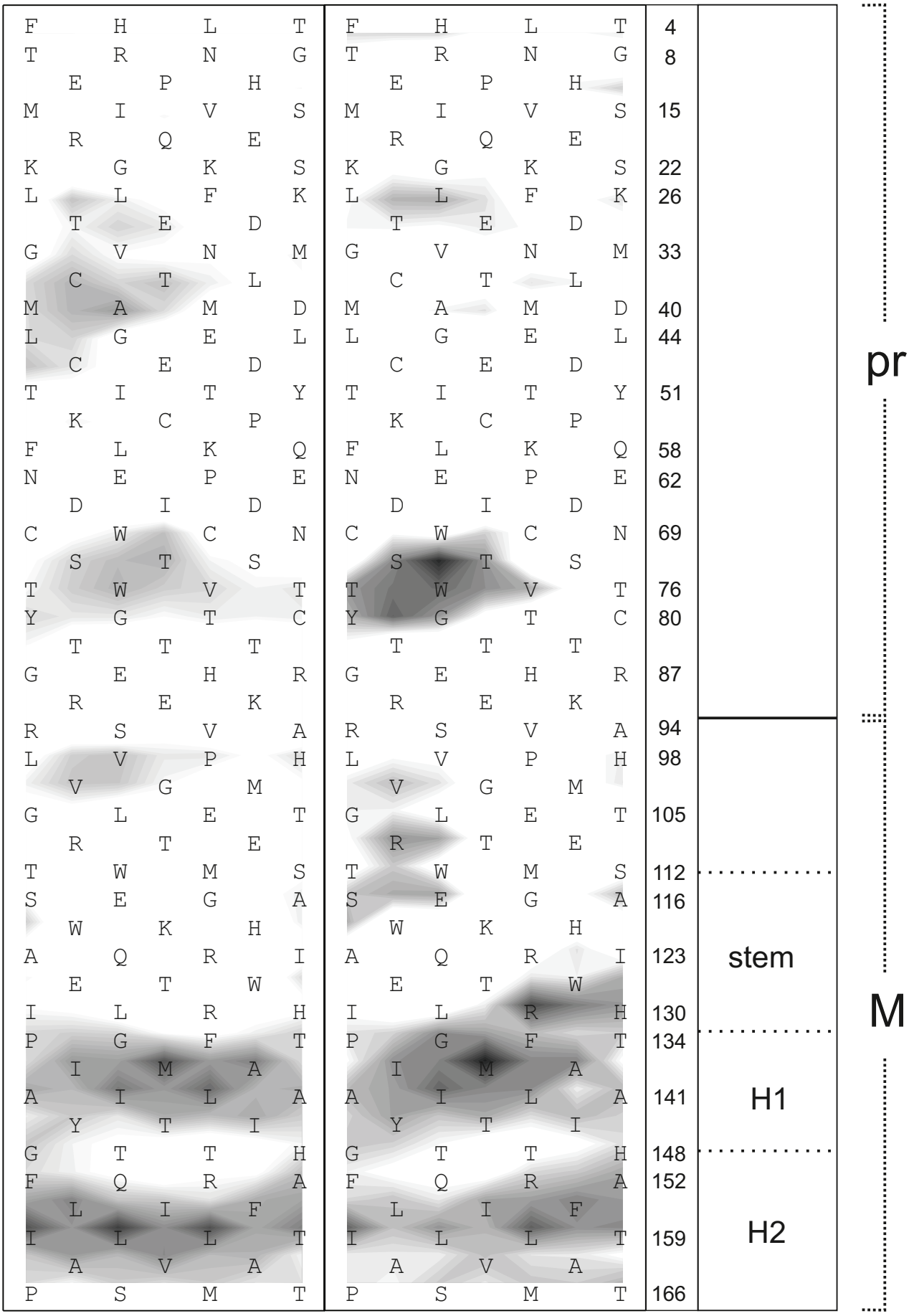
A
B
C
4
8
15
22
26
33
40
44
51
58
62
69
76
80
87
94
98
105
112
116
123
130
134
141
148
152
159
166
pr
M
stem
H1
H2

FIGURE 2

FIGURE 3

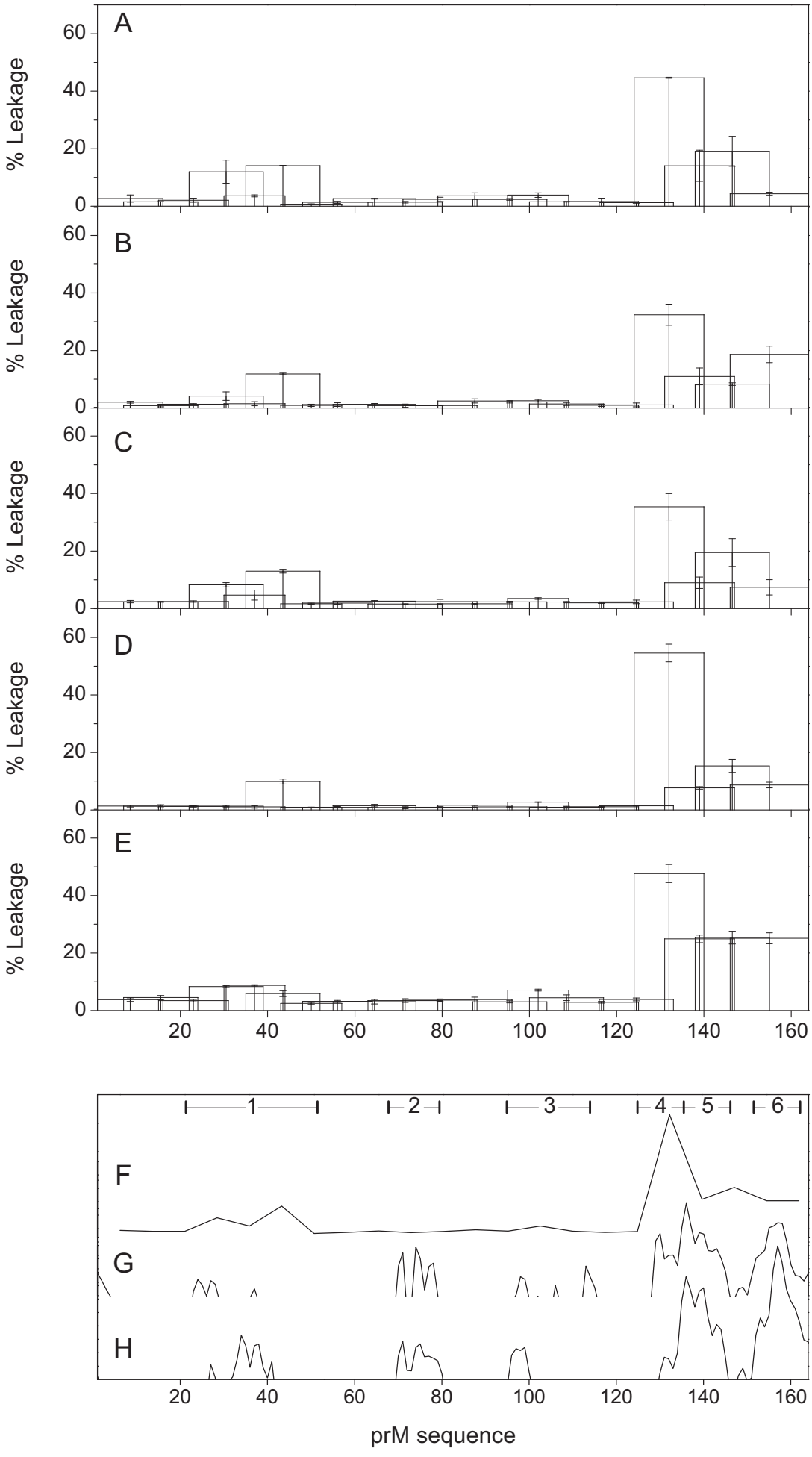

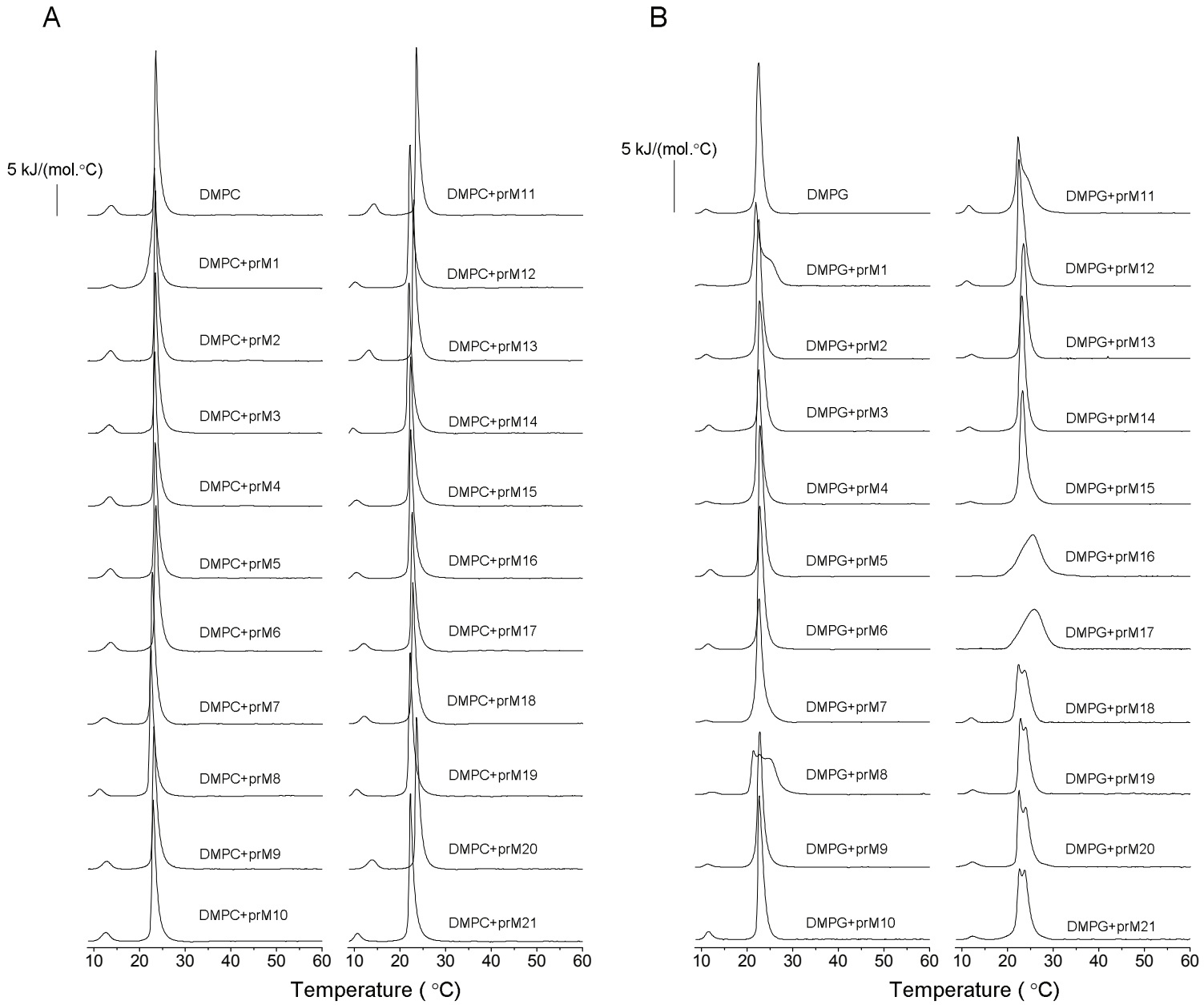
A
5 kJ/(mol.°C)
DMPC
DMPC+prM1
DMPC+prM2
DMPC+prM3
DMPC+prM4
DMPC+prM5
DMPC+prM6
DMPC+prM7
DMPC+prM8
DMPC+prM9
DMPC+prM10
DMPC+prM11
DMPC+prM12
DMPC+prM13
DMPC+prM14
DMPC+prM15
DMPC+prM16
DMPC+prM17
DMPC+prM18
DMPC+prM19
DMPC+prM20
DMPC+prM21
10 20 30 40 50 60
Temperature (°C)
B
5 kJ/(mol.°C)
DMPG
DMPG+prM1
DMPG+prM2
DMPG+prM3
DMPG+prM4
DMPG+prM5
DMPG+prM6
DMPG+prM7
DMPG+prM8
DMPG+prM9
DMPG+prM10
DMPG+prM11
DMPG+prM12
DMPG+prM13
DMPG+prM14
DMPG+prM15
DMPG+prM16
DMPG+prM17
DMPG+prM18
DMPG+prM19
DMPG+prM20
DMPG+prM21
10 20 30 40 50 60
Temperature (°C)

FIGURE 5

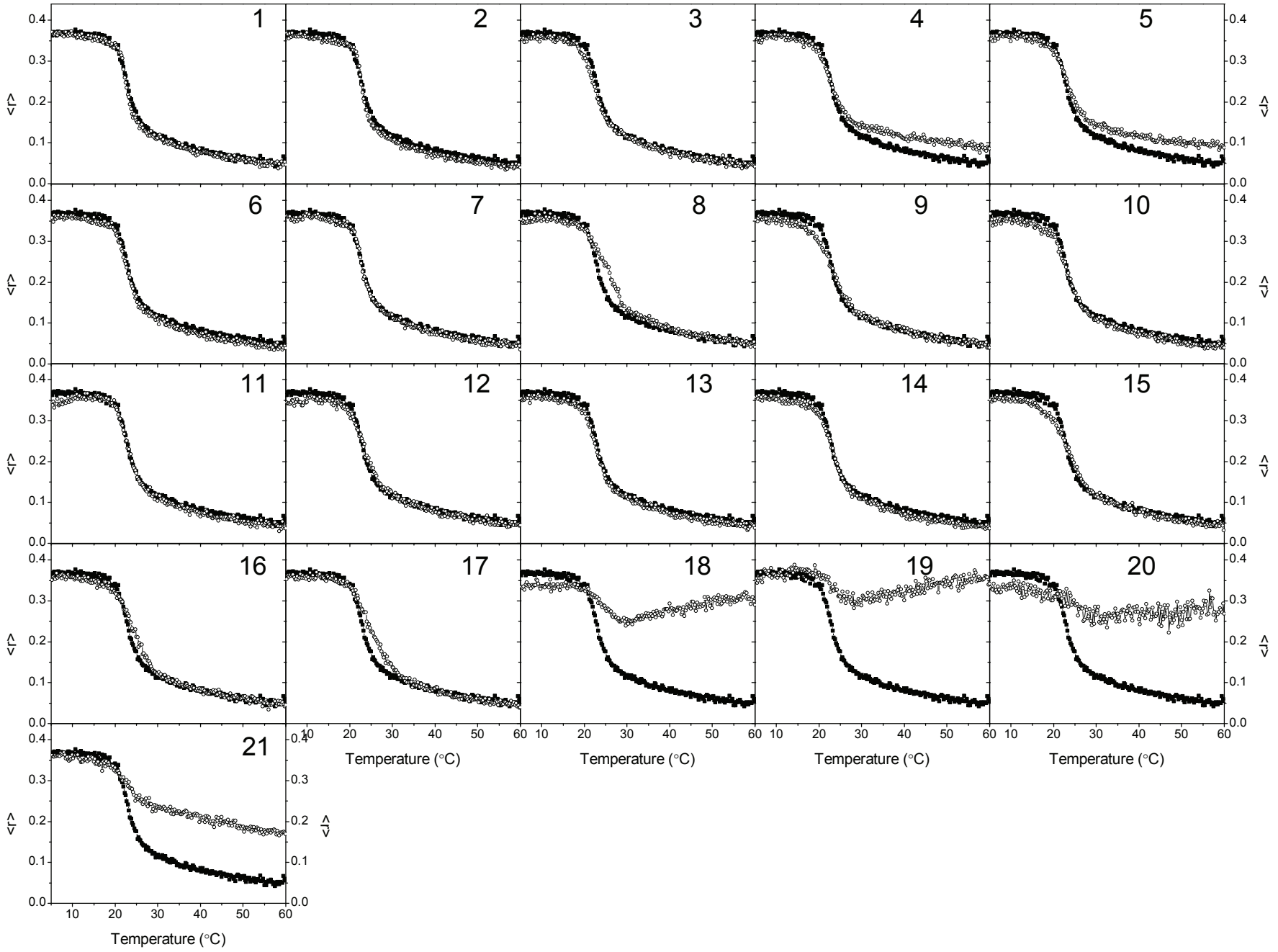

Membrane interacting regions of Dengue virus NS2A protein.

Henrique Nemésio, José Villalaín

Instituto de Biología Molecular y Celular, Universidad Miguel Hernández, E-03202 Elche (Alicante), Spain

Sent to **Journal of Biophysical Chemistry B**

MEMBRANE INTERACTING REGIONS OF DENGUE VIRUS NS2A PROTEIN

Henrique Nemésio, and José Villalaín *

Molecular and Cellular Biology Institute, Universitas “Miguel Hernández”,

E-03202 Elche-Alicante, Spain

RUNNING TITLE: Membranotropic regions of DENVC NS2A

WORD COUNT ABSTRACT: 164

WORD COUNT MAIN TEXT: 7133

KEYWORDS

Dengue, NS2A, membrane, topology

*Address correspondence to:

José Villalaín
Instituto de Biología Molecular y Celular
Universidad "Miguel Hernández"
E-03202 Alicante (Spain).
Tel: +34 966 658 762;
Fax +34 966 658 758;
E-mail: jvillalain@umh.es

ABBREVIATIONS

BMP	Bis(monomyristoylglycero)phosphate
BPI	Bovine brain L-α-phosphadidylinositol
BPS	Bovine brain L-α-phosphatidylserine
CF	5-Carboxyfluorescein
Chol	Cholesterol
CL	Bovine heart cardiolipin
DENV	Dengue virus
DEPE	1,2-Dielaidoyl-sn-glycero-3-phosphatidylethanolamine
DMPA	1,2-Dimyristoyl-sn-glycero-3-phosphatidic acid
DMPC	1,2-Dimyristoyl-sn-glycero-3-phosphatidylcholine
DMPG	1,2-Dimyristoyl-sn-glycero-3-[phospho-rac-glycerol]
DMPS	1,2-Dimyristoyl-sn-glycero-3-phosphatidylserine
DPH	1,6-Diphenyl-1,3,5-hexatriene
DSC	Differential Scanning Calorimetry
EPA	Egg L-α-phosphatidic acid
EPC	Egg L-α-phosphatidylcholine
EPG	Egg L-α-phosphatidylglycerol
ER	Endoplasmic reticulum
ESM	Egg sphingomyelin
FPE	N-(fluorescein-5-thiocarbamoyl)-1,2-dihexadecanoyl-sn-glycero-3-phosphoethanolamine
FTIR	Fourier transform infrared spectroscopy
LUV	Large unilamellar vesicles,
MLV	Multilamellar vesicles
TFE	2,2,2-Trifluoroethanol
T_m	Temperature of the gel-to–liquid crystalline phase transition
TM	Transmembrane domain
TPE	Egg transphosphatidylated L-α-phosphatidylethanolamine

ABSTRACT

The Dengue virus (DENV) NS2A protein, essential for viral replication, is a poorly characterized membrane protein. NS2A displays both protein/protein and membrane/protein interactions but little is known about its biological functions and what regions of this protein are responsible for them. By performing an exhaustive study of membrane rupture induced by a NS2A peptide library on simple and complex model membranes and ability to modulate the phospholipid phase transition, we have identified different membranotropic regions of NS2A protein. Moreover, we have carried out a study of the interaction of a peptide corresponding to one of these regions, peptide dens25, with model biomembranes. This peptide presents an interfacial/hydrophobic pattern characteristic of a membrane-proximal segment. We show that dens25 interacts with membranes containing negatively-charged phospholipids, is capable of rupturing membranes, and its membrane-activity is modulated by membrane superficial charge. These results identify an important region in the DENV NS2A protein which might be directly implicated in the DENV life cycle through the modulation of membrane structure.

INTRODUCTION

The *Flaviviridae* family is composed of three genera, *Flavivirus, Hepacivirus and Pestivirus* [1]. Dengue virus and several other highly pathogenic viruses such as West Nile virus (WNV) and Japanese encephalitis virus (JEV) are part of the Flavivirus genus. For the best part of the last century, Dengue virus (DENV) has been the most prevalent arbovirus affecting the human population. Once restricted to the tropics and sub-tropics, it is now spreading to previously unaffected zones, owing to the dispersion of its vectors, *Aedes* spp., driven by several factors, among them an ever-increasing global temperature and widespread travelling. Apart from that, the fact that the last year there were over 390 million estimated cases [2], DENV is becoming a serious threat to public health. Although the most common clinical manifestations are asymptomatic or mild fevers that can be tackled with well-equipped hospitals, there are two other serious life threatening situations with mortality rates surpassing 20% if left unattended [3]: Dengue haemorrhagic fever and Dengue shock syndrome. It should not be left out the fact that more than 40 % of the world population lives in regions where Dengue vectors thrive, leaving close to 3 billion people at risk in the world [4]. Although several compounds have been identified to inhibit DENV replication [5], there is actually no clinical treatment for its infection.

There are four serologically and genetically related Dengue viruses possessing 69-78% identity at the amino acid level [6]. DENV is a positive-sense, single-stranded RNA virus. It contains un-translated regions at the 5' and 3' ends, flanking a single open reading frame that encodes a single polyprotein of over 3000 amino acids, which is cleaved by cellular and viral proteases into three structural

proteins, C, prM and E, and seven non-structural (NS) proteins, NS1, NS2A, NS2B, NS3, NS4A, NS4B and NS5 [7]. Similarly to other enveloped viruses, the DENV virus enters the cells via receptor mediated endocytosis [7-10] and rearranges cell internal membranes to establish specific sites of replication [11-13]. Details about DENV replication process remain largely unclear, but most if not all of the DENV proteins, are involved and function in a complex web of protein-protein and lipid-protein interactions [7,10]. DENV replicates its genome in a membrane-associated replication complex, and morphogenesis and virion budding have been suggested to take place in the endoplasmic reticulum (ER) or ER derived membranes. Although the specific genome encapsulation, virion formation and fusion processes are widely accepted to be almost exclusively carried through by the structural proteins C, prM and class II fusion protein E, much is still being debated about the exclusivity of those proteins in those processes [14-16]

All the polyprotein processing and viral RNA replication steps are generally assigned to the non-structural proteins, including the formation of replication complexes of the virus [17]. The accumulated knowledge on the functions of NS1, NS2A, NS4A and NS4B on the viral cycle is very sparse, mainly due to their considerable hydrophobicity and the difficulty of discerning their exact roles [18]. NS4A and NS4B seem to be involved in the host's immune system evasion and immune response, affecting several pathways [19,20]. Protein NS1 is found mainly in the cytosol of the cell, rendering it an ideal antigen for DENV infection detection, and seems to play a role in autophagy as well [21]. One of the proteins found in the replication complex of flaviviruses is NS2A [17], what would certify its role in the viral replication. This protein is required for the proper processing of NS1, possesses specific

recognition sites for certain proteases, is also involved in the interferon inhibition by NS4A and NS4B and is mainly found in ER membranes [19,22,23]. Recently, a topology model was proposed where NS2A is described as having one N-terminal segment from residues 1 to 31 that does not seem to interact with ER membranes, followed by a segment, residues 32 to 68, that despite lacking the ability to traverse the membrane is proposed to be in close association with it [24]. Two transmembrane segments ensue from residues 69 to 119, followed by a non-transmembrane segment from residues 120 to 142, and ending with three transmembrane segments from residues 143 to 209.

We have resorted to a set of biophysical methods used extensively in our laboratory [25-32] that allow the screening of membrane interacting regions from viral proteins. Using peptide libraries encompassing the protein full length and thorough characterization of those lipid protein interactions we sought to highlight regions that could be important for proper NS2A function. It is known that NS2A is a poorly characterized highly hydrophobic protein that requires the membrane to perform its functions. Considering that NS2A is essential in the viral RNA replication process, and that DENV protein/membrane and protein/protein interactions are an attractive target for antiviral drug development, we have characterized the membranotropic regions of DENV NS2A protein, identifying several regions with different interacting capabilities. Besides, we characterize a NS2A peptide, peptide dens25, with interesting properties in the presence of different membrane model systems. We have used fluorescence spectroscopy techniques to assess membrane rupture, alteration of the fluorescence signal of FPE-labelled membranes in the presence of this peptide as well as steady state-fluorescence anisotropy. Calorimetric studies

using differential scanning calorimetry (DSC) and Fourier transform infrared spectroscopy (FTIR) were also performed, using several model membrane systems. These data will help us to understand the molecular mechanism of viral morphogenesis, identify new targets for the treatment of Dengue virus infection as well as render the future development of DENV entry inhibitors which may lead to new vaccine strategies possible.

MATERIALS AND METHODS

Materials and reagents.

A set of 35 peptides derived from Dengue Virus Type 2 NGC NS2A protein (Table 1) was obtained through BEI Resources, National Institute of Allergy and Infectious Diseases, Manassas, VA, USA. Peptides were solubilized in water/2,2,2-trifluoroethanol at a 70:30 ratio (v/v). The peptides had a purity of about 80%. The peptide dens25 corresponding to the sequence ^{30}KHAILLVAVSFVTLITGNMSFRDLGR^{55} from Dengue Virus Type 2 NGC NS2A protein (with N-terminal acetylation and C-terminal acetylation) was obtained from Genemed Synthesis, San Antonio, TX. This peptide was purified by reverse-phase HPLC (Kromasil C18, 250 x 4.6 mm, with a flow rate of 1 mL/min, solvent A, 0.1% trifluoroacetic acid, solvent B, 99.9% acetonitrile and 0.1% trifluoroacetic acid) to > 95% purity and its composition and molecular mass were confirmed by amino acid analysis and mass spectroscopy. Considering that trifluoroacetate has a strong infrared absorbance at approximately 1673 cm^{-1}, that can interfere significantly with the peptide Amide I band [33], residual trifluoroacetic acid, used both in peptide synthesis and in the HPLC mobile phase, was removed after several lyophilisation/solubilisation cycles in 10 mM HCl [34]. Bovine brain phosphatidylserine (BPS), bovine liver L-α-phosphatidylinositol (BPI), cholesterol (Chol), egg phosphatidic acid (EPA), egg L-α-phosphatidylcholine (EPC), egg sphingomyelin (ESM), egg trans-sterified L-α-phosphatidylethanolamine (TPE), tetramyristoyl cardiolipin (CL), liver lipid extract, bis(monomyristoylglycero)phosphate (BMP), 1,2-dimyristoilphosphatidylcholine (DMPC), 1,2-dimyristoylphosphatidylglycerol (DMPG),

1,2-dimyristoylphosphatidylserine (DMPS), 1,2-dimyristoylphosphatidic acid (DMPA), 1,2-dielaidoyl-sn-glycero-3-phosphatidylethanolamine (DEPE) were obtained from Avanti Polar Lipids (Alabaster, AL, USA). The lipid composition of the synthetic endoplasmic reticulum was EPC/CL/BPI/TPE/BPS/EPA/SM/Chol at a molar ratio of 59:0.37:7.7:18:3.1:1.2:3.4:7.8 [35,36] whereas the liver lipid extract contained 42%, phosphatidylcholine, 22% phosphatidylethanolamine, 7% Chol, 8% phosphatidylinositol, 1% lysophosphatidylinositol, and 21% miscellaneous lipids including neutral ones, as stated by the manufacturer.. 5-Carboxyfluorescein (CF, >95% by HPLC), deuterium oxide (99.9% by atom), Triton X-100, EDTA and HEPES were purchased from Sigma-Aldrich (Madrid, ES). 1,6-diphenyl-1,3,5-hexatriene (DPH) and N-(fluorescein-5-thiocarbamoyl)-1,2-dihexadecanoyl-sn-glycero-3-phosphoethanolamine (fluorescein DHPE or FPE) were obtained from Molecular Probes (Eugene, OR). All other chemicals were commercial samples of the highest purity available (Sigma-Aldrich, Madrid, ES). Water was deionized, twice-distilled and passed through a Milli-Q equipment (Millipore Ibérica, Madrid, ES) to a resistivity higher than 18 MΩ·cm.

Vesicle preparation.

Aliquots containing the appropriate amount of lipid in chloroform-methanol (2:1 vol/vol) were placed in a test tube, the solvents were removed by evaporation under a stream of O_2-free N_2, and finally, traces of solvents were eliminated under vacuum in the dark for >3 h. The lipid films were resuspended in an appropriate buffer and incubated either at 25ºC or 10ºC above the phase transition temperature (Tm) with intermittent vortexing for 30 min to hydrate the samples and obtain multilamellar

vesicles (MLV). The samples were frozen and thawed five times to ensure complete homogenization and maximization of peptide/lipid contacts with occasional vortexing. Large unilamellar vesicles (LUV) with a mean diameter of 0.1 μm were prepared from MLV by the extrusion method [37] using polycarbonate filters with a pore size of 0.1 μm (Nuclepore Corp., Cambridge, CA, USA). For infrared spectroscopy, 200 μg of peptide were added to the appropriate amount of dried lipid and lyophilized. The samples were hydrated in 100 μl of D_2O buffer containing 20 mM HEPES, 1 mM EDTA, either 25 or 100mM NaCl, at pH 7.4 and incubated at 10ºC above the T_m of the phospholipid mixture with intermittent vortexing for 45 min to hydrate the samples and obtain MLV. The samples were frozen and thawed as above. Finally the suspensions were centrifuged at 14000 rpm at 25ºC for 10 min to remove the peptide unbound to the membranes. The pellet was re-suspended in 25 μl of D_2O buffer and incubated for 45 min at 10ºC above the T_m of the lipid mixture, unless stated otherwise. The phospholipid and peptide concentration were measured by methods described elsewhere [38,39].

Membrane leakage measurement.

LUVs with a mean diameter of 0.1 μm were prepared as indicated above in buffer containing 10 mM Tris, 20 mM NaCl, pH 7.4 (at 25ºC), and CF at a concentration of 40 mM. Non-encapsulated CF was separated from the vesicle suspension through a filtration column containing Sephadex G-50 (GE Healthcare), eluted with buffer containing 10 mM Tris, 100 mM NaCl (except in the case of one single experiment with liver lipid extract where 40 mM NaCl was used) and 0.1 mM EDTA at pH 7.4. Membrane rupture (leakage) of intralipossomal CF was assayed by treating the

probe-loaded liposomes (final lipid concentration, 0.125 mM) with the appropriate amounts of peptide (peptide-to-lipid molar ratio of 1:25) on microtiter plates using a microplate reader (FLUOstar; BMG Labtech, Offenburg, Germany), stabilized at 25ºC, each well containing 170 µL. The medium in the microtiter plates was continuously stirred to allow the rapid mixing of peptide and vesicles. Changes in fluorescence intensity were recorded with excitation and emission wavelengths set at 492 and 517 nm, respectively. One hundred percent release was achieved by adding Triton X-100 to the microtiter plate to a final concentration of 0.5% (w/w). Fluorescence measurements were made initially with probe-loaded liposomes, followed by peptide addition and finally adding Triton X-100 to obtain maximum leakage. Membrane leakage was quantified on a percentage basis according to the equation, $\%Release = 100(F_f-F_0)/(F_{100}-F_0)$, F_f being the equilibrium value of fluorescence after peptide addition, F_0 the initial fluorescence of the vesicle suspension and F_{100} the fluorescence value after addition of Triton X-100. For details see refs. [40,41].

Steady-state Fluorescence Anisotropy.

MLVs were formed in buffers composed of 20 mM HEPES either alone or containing different concentrations of NaCl or KCl at pH 7.4 and 25ºC. Aliquots of DPH in N,N'-dimethylformamide (0.2 mM) were directly added to the lipid suspension to obtain a probe/lipid molar ratio of 1:500. DPH and its derivatives are popular membrane fluorescent probes for the monitoring of the organization and dynamics of membranes. DPH is known to partition mainly into the hydrophobic core of the membrane [42]. Samples were incubated for 60 min at 10ºC above the gel to liquid-

crystalline phase transition temperature T_m of the phospholipid mixture. Afterwards, the peptides were added to obtain a peptide/lipid molar ratio of 1:15 and incubated 10ºC above the T_m of each lipid for one hour, with occasional vortexing. All fluorescence studies were carried using 5 mm x 5 mm quartz cuvettes in a final volume of 400 µl (315 µM lipid concentration). The steady state fluorescence anisotropy was measured with an automated polarization accessory using a Varian Cary Eclipse fluorescence spectrometer, coupled to a Peltier for automatic temperature change. The vertically and horizontally polarized emission intensities, elicited by vertically polarized excitation, were corrected for background scattering by subtracting the corresponding polarized intensities of a phospholipid preparation lacking probes. The G-factor, accounting for differential polarization sensitivity, was determined by measuring the polarized components of the fluorescence of the probe with horizontally polarized excitation ($G=I_{HV}/I_{HH}$). Samples were excited at 360 nm and emission was recorded at 430 nm, with excitation and emission slits of 5 nm. Anisotropy values were calculated using the formula $\langle r \rangle = (I_{VV}-GI_{VH})/(I_{VV}+2GI_{VH})$, where I_{VV} and I_{VH} are the measured fluorescence intensities (after appropriate background subtraction) with the excitation polarizer vertically oriented and the emission polarizer vertically and horizontally oriented, respectively.

Fluorescence measurements using FPE-labelled membranes.

LUVs with a mean diameter of 0.1 µM were prepared in buffer containing 10 mM Tris-HCl at pH 7.4 (at 25ºC). The vesicles were labelled exclusively in the outer bilayer leaflet with FPE as described previously [43]**.** LUVs were incubated with 0.1 mol % FPE dissolved in ethanol (never more than 0.1 % of the total aqueous volume) at

37 ºC for one hour in the dark. Any remaining unincorporated FPE was removed by gel filtration on Sephadex G-25 column equilibrated with the appropriate buffer. FPE-vesicles were stored at 4 ºC until use in an O_2-free atmosphere. Fluorescence time courses of FPE-labelled vesicles were measured after the desired amount of peptide was added into 400 µL of lipid suspension (200 µM lipid) using a Varian Cary Eclipse fluorescence spectrometer. Excitation and emission wavelengths were set at 490 and 520 nm, respectively, using excitation and emission slits set at 5 nm. Temperature was controlled with a thermostatic bath at 25 ºC. The contribution of light scattering to the fluorescence signals was measured in experiments without the dye and was subtracted from the fluorescence traces. Data were fitted to a hyperbolic binding model [44] using the equations $F = F_{max}[P]/(K_d+[P])$ or $F = F_{max}[P]^n/(K_d+[P]^n)$, where F is the fluorescence variation, F_{max} the maximum fluorescence variation, $[P]$ the peptide concentration, K_d the dissociation constant of the membrane binding process and n, the Hill coefficient.

Differential Scanning Calorimetry.

MLVs were formed as stated above in 20 mM HEPES and different concentrations of NaCl at pH 7.4. The peptides were added to obtain a peptide/lipid molar ratio of 1:10. The final lipid concentration was 600 µM and the samples were incubated 10 ºC above the T_m of each lipid for 1 hour with occasional vortexing. Samples were degassed under vacuum for 10-15 minutes with gentle stirring, prior to being loaded into the calorimetric cell. DSC experiments were performed in a VP-DSC differential scanning calorimeter (MicroCal LLC, MA) under a constant external pressure of 30 psi in order to avoid bubble formation, and samples were heated at a constant scan

rate of 60ºC/h. Experimental data were corrected from small mismatches between the two cells by subtracting a buffer baseline prior to data analysis. The excess heat capacity functions were analysed using Origin 7.0 (MicroCal software). The error in determination of T_c was 0.2ºC. The thermograms were defined by the onset and completion temperatures of the transition peaks obtained from heating scans. The phase transition temperature was defined as the temperature at the peak maximum. In order to avoid artefacts due to the thermal history of the sample, the first scan was never considered; second and further scans were carried out until a reproducible and reversible pattern was obtained.

Infrared spectroscopy.

Approximately 25 µL of a pelleted sample in D_2O prepared as stated above were placed between CaF_2 windows separated by 50 µm thick Teflon spacers in a liquid demountable cell (Harrick, Ossining, NY). The spectra were obtained in a Bruker IF66S spectrometer using a deuterated triglycine sulfate detector. Each spectrum was obtained by collecting 300 interferograms with a nominal resolution of 2 cm^{-1}, transformed using triangular apodization; a sample shuttle accessory was used to obtain sample and background spectra in order to average background spectra between sample spectra over the same time period. The spectrometer was continuously purged with dry air at a dew point of -40 ºC. All samples were equilibrated at the lowest temperature for 20 min before acquisition. An external bath circulator, connected to the infrared spectrometer, controlled the sample temperature. For temperature studies, samples were scanned using 2 ºC intervals and a 2 min delay between each consecutive scan. Subtraction of buffer spectra

taken at the same temperature as the samples, center of gravity frequencies, band-narrowing methods and band fitting were performed interactively using either GRAMS/32 or Spectra-Calc (Galactic Industriesm Salem, MA) as described previously [40,45].

RESULTS

NS2A is a membrane protein with possibly five transmembrane domains and at least two membrane interacting regions [24]. NS2A, essential in the viral RNA replication, is one of the least characterized DENV proteins due to its highly hydrophobic character. Therefore a multitude of questions remain unanswered about its structure, function and lipid-protein interacting regions. We have carried an exhaustive analysis of the different regions of DENV NS2A protein which might interact with membranes, using a peptide library derived from the NS2A protein composed of 35 different overlapping peptides (Table 1). Because the peptide library includes the whole sequence of the protein and each individual peptide, i, overlaps with two and three consecutive peptides, i+1 and i+2, by approximately 11 and 5 residues respectively, the obtained data should be analysed considering the effect of protein segments rather than that of isolated peptides. Furthermore, we have characterized the effect of a peptide derived from protein NS2A, peptide dens25, on different membrane model systems with interesting results. These data will help us understand the molecular mechanism of viral morphogenesis, and identify new targets for the treatment of Dengue virus infection which may lead to alternative therapeutic targets.

Approximate location of Table 1

Taking into consideration the spatial arrangement of amino acids in an α-helical structure and applying it to the whole sequence [32], we have obtained the

average normalized water-to-membrane and water-to-interface transfer free energy scales for thirty-five DENV NS2A sequences (Figure 1A). Ten different regions having large hydrophobic and interfacial values along the protein sequence are distinguisable: region *a* encompassing residues from 6 to 19, region *b* from 30 to 54, region *c* from 55 to 62, region *d* from 70 to 83, region *e* from 83 to 93, region *f* from 101 to 115, region *g* from 124 to 136, region *h* from 145 to 164, region *i* from 165 to 182 and region *j* from 192 to 211. Xie et al. [24] suggested the existence of eight different regions for the NS2B topology: regions 1 (residues 3-24), 2 (residues 32-51) and 5 (residues 120-140) as peripheral segments and regions 3 (residues 69-93), 4 (residues 100-118), 6 (residues 143-163), 7 (residues 165-186) and 8 (residues 189-209) as transmembrane segments (see Figure 1A). Interestingly regions *a*, *b* and *g* coincide with regions 1, 2 and 5, whereas regions *d-e, f, h, i,* and *j* coincide with regions 3, 4, 6, 7 and 8. Region *c* has both a lower intensity and a smaller length than expected to be considered as either a membrane interacting domain or a transmembrane segment [32]. The existence of pre-transmembrane domains with a strong propensity for partitioning into membrane interfaces in different viral proteins is well-known [32]. These domains show characteristic high water-to-interface transfer free energies overlapping with high water-to-bilayer transfer free energies. Figure 1B shows the normalized water-to-bilayer and water-to-interface transfer free energies for NS2A region *b* encompassing amino acids 30 to 55 (the sequence is also shown). As observed, a segment of high water-to-bilayer transfer free energy is immediately followed by a region of high water-to-interface transfer free energy, a characteristic pattern of pre-transmembrane domains (also called stem or membrane-proximal domains). This pattern is characterized by a strong propensity to partition into and interact with membrane interfaces [26,46-53], suggesting that this segment might interact

significantly with membranes. Region 2 is coincidental with region *b*, and has already been proposed to associate with the membrane [24]. Therefore, this region could interact with membranes in an analogous way to other similar viral pre-transmembrane domains (see below).

Approximate location of Figure 1

We have studied the effect of the NS2A peptide library on membrane rupture by monitoring CF leakage from different liposome compositions and the results are presented in Figure 2. We have tested seven different lipid compositions, simple and complex. The simple compositions contained EPC (Figure 2A), EPC/Chol at a phospholipid molar ratio of 5:1 (Figure 2B), EPC/BMP at a phospholipid molar ratio of 5:1 (Figure 2C), EPC/BPI at a phospholipid molar ratio of 5:1 (figure 2D) and EPC/SM/Chol at a phospholipid molar ratio of 5:2:1 (Figure 2E), whereas the complex ones consisted of an ER synthetic lipid mixture resembling the ER membrane (Figure 2F) and a lipid extract of liver membranes (Figure 2G). It should be recalled that DENV virus is associated with ER or ER-derived membranes [54]. The leakage data showed that some peptides exerted a significant leakage effect and that there were some differences depending on liposome composition. The leakage effects were focused on two segments, one segment delimited by residues 25 to 41 corresponding to peptide 5, and a long segment delimited by residues 103 to 183 (peptides 18-29). Leakage elicited by peptide 5 was remarkable in the presence of liver liposomes, since about a leakage value of 45% was observed (Figure 2G). Lower but significant values were found for liposomes containing BMP (about 18%, Figure 2C) and ER-like membranes (about 10%, Figure 2F). Leakage values elicited

by peptides 18-29 were lower than that observed with peptide 5, oscillating between 10 and 20%. Apart from these differences, leakage induction was consistent throughout all liposome compositions used (Figure 2). It is interesting to note that peptide 5 overlaps region *b* and peptides 18 to 29 overlap regions *f, g, h* and *i*. Peptide 5 would be defined by a significant leakage value concurrent with high hydrophobicity and interfaciality (see above) and therefore would have a high propensity for partitioning into the membrane interface [32].

Approximate location of Figure 2

Phospholipids can undergo a cooperative melting reaction linked to the loss of conformational order of the lipid acyl chains; this melting process can be influenced by many types of molecules including peptides and proteins. The effect of the NS2A peptide library on the structural and thermotropic properties of phospholipid membranes was investigated by measuring the steady-state fluorescence anisotropy of the fluorescent probe DPH incorporated into model membranes as a function of temperature (DMPC, Supplemental Figure 1, and DMPG, Supplemental Figure 2). There were no significant changes in the T_m of DMPC in the presence of the NS2A derived peptides, but some of them, namely peptides 2, 5 and 12, elicited a significant effect on anisotropy and cooperativity (Supplemental Figure 1). In the case of DMPG, there were more peptides affecting the thermotropic behaviour of the phospholipid (Supplemental Figure 2). However, peptides 2, 5, 10 and 12 were the ones that elicited a significant effect on the cooperativity, T_m and/or the anisotropy of DMPG. These data would suggest that these peptides should interact with membranes at a relative deep location, considering that DPH is known to locate

inside the palisade structure of the membrane. The specific effect that these peptides have on DMPG does not seem to be exclusively electrostatic, since the net charge of peptides having a remarkable effect, i.e., peptides 2, 5, 10 and 12, are -2, +2, -1 and 0, respectively (Table 1).

As shown above, peptide 5 presents a distinctive pattern characteristic of a membrane-proximal domain (Figure 1B), elicits a significant leakage value (Figure 2) and affects the thermotropic behaviour of both DMPC (supplemental Figure 1) and DMPG (supplemental Figure 2). Furthermore, the region where peptide 5 resides has been proposed to bind to the membrane surface [24]. Therefore we have carried a thorough characterization of peptide dens25, corresponding to the NS2A segment comprised by residues 30 to 55 and its membrane interactions in order to determine the membranotropic characteristics of this region of the protein. Since peptide dens25 lacks a Trp residue and therefore intrinsic fluorescence, we have used the electrostatic surface potential probe FPE [41] to monitor its ability to bind to model membranes composed of different lipid compositions at different lipid/peptide ratios (Figure 3A). As observed in the Figure, peptide dens25 had a higher affinity for model membranes composed of negatively charged phospholipids, as well as the complex ER and liver lipid membranes. The dependence of peptide binding on membrane surface total charge is demonstrated by the linear dependence of FPE fluorescence and EPG content for membranes containing different lipid molar ratios of EPC and EPG (Figure 3A, insert). A similar linear relationship is observed for EPC/BPS membranes (not shown). Interestingly, lower affinity was observed for zwitterionic liposomes, i.e., those composed of EPC, EPC/Chol and EPC/SM/Chol (Figure 3A). All FPE binding data could be adjusted to a binding profile having either

a sigmoidal (Hill coefficient of approximately 1) or a hyperbolic dependence, which might suggest that the interaction of the peptide with the membrane was monomeric.

Approximate location of Figure 3

The effect of the dens25 peptide on the release of encapsulated fluorophores trapped inside model membranes was also studied. dens25 was able to induce the release of encapsulated CF in a dose-dependent manner and the effect was significantly different for different lipid compositions (Figure 3B). Liposomes composed of EPC/EPG and EPC/BPS presented respective leakage values of 91 and 90% at peptide/lipid ratios of 0.066. Significant leakage values were observed for liposomes composed of the ER-like complex mixture and the liver lipid extract, since at the same peptide/lipid ratios, leakage values of 84 and 78% were found. Liposomes composed of EPC and EPC/ESM at a molar ratio of 5:1 presented similar leakage values of 68 and 71%, respectively. However, addition of Chol to these last lipid compositions, i.e., EPC/Chol at a molar ratio of 5:1 and EPC/ESM/Chol at a molar ratio of 5:1:1, significantly reduced the leakage values to 53 and 56 %, respectively. From all these data it could be concluded that Peptide dens25 exerts a highr leakage on liposomes composed of negatively-charged phospholipids and a lower one when Chol is present.

Approximate location of Figure 4

As noted above, peptide dens25 seems to interact more significantly with negatively-charged phospholipids; however, this interaction could be specifically with

either the phospholipid head-group or with the negative charge or both. In order to discriminate between these two possibilities, we have studied the contribution of ionic strength to the thermotropic phase behaviour of the negatively-charged phospholipid DMPG in the absence and in the presence of peptide dens25 by steady-state fluorescence anisotropy of the fluorescent probe DPH (Figure 4). In the absence of salts, the transition of pure DMPG was a broad one (Figure 4A), as it has been noted before [55]. In the presence of peptide dens25 at a lipid/peptide molar ratio of 10 to 1, the anisotropy of DMPG increased significantly above the T_m (Figure 4A), but the cooperativity of the transition was similar to that found in pure DMPG (Figure 4M). When increasing concentrations of either NaCl (Figures 4C, E, G, I and K) or KCl (Figures 4D, F, H, J, and L) were added to pure DMPG, the cooperativity of the phospholipid increased. However, in the presence of the peptide, the cooperativity of DMPG steadily increased, although slightly, at increasing concentrations of either NaCl or KCl (Figure 4M). As observed in the figure, even at a concentration of 300mM of either NaCl or KCl, the cooperativity was lower than that found for the pure phospholipid, but higher than the cooperativity found at lower salt concentrations. These data would suggest that the interaction of the peptide with negatively-charged phospholipids would be mainly of an electrostatic nature. The difference of anisotropy in the absence and in the presence of peptide is shown in Figure 4N. It can be observed that the difference is inversely proportional to the salt concentration, being lower for NaCl than for KCl, which would indicate that, not only an increase in ionic strength reduces the effect of the peptide on the membrane, but also that there are subtle differences between the sodium and potassium ions.

The effect of peptide dens25 on the thermotropic phase behaviour of phospholipid multilamellar vesicles was also studied using differential scanning calorimetry, DSC (Figure 5). When properly hydrated and in the presence of salt, DMPC and DMPG display two endothermic peaks on heating, corresponding to the pre-transition (appearing at about 12-14ºC, $L_{\beta'}$-$P_{\beta'}$) and the main transition (appearing at about 23-24ºC, $P_{\beta'}$-L_{α}). Incorporation of dens25 into DMPC at a lipid/peptide ratio of 10:1 did not significantly alter the thermotropic behaviour of the pure phospholipid, neither at low nor at high ionic strength (Figures 5A and B, respectively). In contrast, the main transition of pure DMPG at 25mM NaCl was apparently composed of two different peaks, which should be due to mixed phases (Figure 5C). Incorporation of peptide dens25 induced a significant lowering of the cooperativity of the transition but no change in the number of peaks was observed (Figure 5C). In the presence of 100 mM NaCl the main transition of pure DMPG was composed of only one peak as expected, showing a large cooperativity (Figure 5D). When dens25 was incorporated to the membrane, a broad main transition peak was observed, indicating a significant lowering in cooperativity (Figure 5D). The pattern observed at 300 mM NaCl for pure DMPG was similar to the one found at 100 mM NaCl, since only one very cooperative peak was observed (Figures 5E and 5D, respectively). The addition of peptide dens25 lowered the cooperativity of the main transition, but the width at 300 mM NaCl was narrower than at 100 mM, indicating that an increase of NaCl concentration induced an increase in the cooperativity of the main transition (Figures 5D and E). In the case of DMPS, a similar pattern was observed. In the presence of 25 mM NaCl, peptide dens25 induced a significant decrease in cooperativity in DMPS when compared to the pure phospholipid (Figure 5F), whereas in the presence of 100 mM NaCl the peptide hardly exerted any effect on the main

transition of the phospholipid (Figure 5G). In the presence of 25 mM NaCl, 14BMP, a negatively-charged phospholipid, presented two low-enthalpy peaks and one high-enthalpy peak (Figure 5H). In the presence of dens25, two peaks were observed, a low-enthalpy peak and a high-enthalpy one, the latterº displaced to lower temperatures when compared to the pure phospholipid. In the presence of 100 mM NaCl, 14BMP presented a normal pattern, i.e., a low-enthalpy and a high-enthalpy peaks corresponding to the L_{c1}-L_{c2} and L_{c2}-L_{α} transitions (Figure 5I). Apart from abolishing the low-enthalpy peak, peptide dens25 did not exert any other significant effect on the high-enthalpy high-temperature peak (Figure 5I). These DSC data would suggest that peptide dens25 affects more significantly the phase transition of negatively-charged phospholipids in the absence of salt, effect that is significantly reduced when ionic strength is reduced, i.e., the less salt concentration, the bigger the effect dens25 has on negatively-charged phospholipids.

Approximate location of Figure 5

To further explore the effects of peptide dens25 on different types of model membranes, we have studied the ester C=O stretching band of DMPC and DMPC, which appears between 1745 and 1720 cm^{-1} in infrared spectroscopy (Figure 6). The frequency maximum of the ester C=O band of pure DMPC in the presence of 25 mM NaCl displayed two transitions at about 17ºC and 23ºC, coincident with the pre-transition and main gel to liquid crystalline phase transition of the pure phospholipid (Figure 6A). In the presence of the peptide, the frequency of the ester C=O band of DMPC displayed only one transition at about 24ºC (Figure 6A). However, its absolute frequency was higher in the presence of the peptide than in its absence, suggesting

that the peptide increased the intensity of the 1743 cm^{-1} component relative to the 1727 cm^{-1} one, i.e., the amount of non-hydrogen bonded C=O ester bands increased in the presence of the peptide [56,57]. In the presence of 100 mM NaCl a relatively similar pattern was found for DMPC (Figure 6B). The frequency maximum of the ester C=O band of the pure phospholipid displayed two transitions at about 16ºC and 24ºC, i.e., the pre-transition and the main phase transition (Figure 6A). In the presence of the peptide, the frequency of the ester C=O band displayed two transitions, a broad one at about 16ºC and a narrow one at 24ºC. As before, its absolute frequency was higher in the presence of the peptide than in its absence; however, it was not as high as it was found in the presence of 25 mM NaCl (compare Figures 6A and 6B). The frequency maximum of the ester C=O band of pure DMPG in the presence of 25 mM NaCl displayed two transitions, a broad one at about 14ºC and a narrow one at 23ºC, coincident with the pre-transition and main phase transition of the pure phospholipid in accordance with the DSC data (Figure 6C). In the presence of the peptide, it is noteworthy that the frequency of the ester C=O band of DMPC displayed no transition at all in the temperature range studied (Figure 6C). In the presence of 100 mM NaCl the frequency maximum of the ester C=O band of pure DMPG displayed two transitions, a broad one at about 14ºC and a relatively cooperative one at 22ºC, coincident with the pre- and main transition of the pure phospholipid (Figure 6C). In the presence of the dens25 peptide, the frequency of the ester C=O band displayed only a broad transition at about 24ºC, in accordance with DSC (Figure 6D). Its absolute frequency was higher in the presence of the peptide than in its absence but at temperatures higher than the main transition (Figure 6D). In accordance with the data described above, these data would suggest that peptide dens25 affects the phase transition of DMPG, a negatively-charged phospholipid, but

not that of DMPC, a zwitterionic one, in the presence of relatively low concentrations of NaCl. Conversely, the interaction of peptide dens25 with DMPG is abolished at relatively high salt concentrations.

Approximate location of Figure 6

We have also studied the secondary structure of the dens25 peptide in the presence of DMPC and DMPG at different salt concentrations by analysing the infrared Amide I' band located between 1700 and 1600 cm^{-1} (Figure 6). The infrared Amide I' spectra of fully hydrated dens25 in the presence of DMPC and 25 mM NaCl below and above the main phase transition of the phospholipid are shown in Figure 6A. At both temperatures, the Amide I' band presented two bands appearing at about 1648 and 1623 cm^{-1}, the former with relative lower intensity that the later. The band at about 1623 cm^{-1} would indicate the existence of aggregated β structures, whereas the broad band with the intensity maxima at about 1648 cm^{-1} would correspond to a mixture of mainly unordered and helical structures [58,59]. Upon data fitting, the relative intensity of the 1648 cm^{-1} band was about 73% and about 27% for the 1623 cm^{-1} band. In the presence of 100 mM NaCl and below and above the main transition of the phospholipid, the Amide I' band of dens25 presented a similar pattern, i.e., two bands at about 1648 and 1623 cm^{-1}, with relative intensities of 68% and 32%, respectively (Figure 6B). The infrared Amide I' spectra of fully hydrated dens25 in the presence of DMPG and 25 mM NaCl below and above the main phase transition of the phospholipid are shown in Figure 6C. In this case and in contrast to the DMPC sample, the Amide I' band of dens25 presented two bands with slightly different frequencies. These two bands have a maximum at about 1653 cm^{-1} and 1626 cm^{-1},

and their relative intensities were about 85% and about 15%, respectively (Figure 6C). In the presence of 100 mM NaCl and below and above the main transition of the phospholipid, the Amide I' band of dens25 presented two bands but their frequencies were slightly different than in the presence of 25 mM NaCl, about 1648 cm^{-1} and 1622 cm^{-1} (Figure 6D). In this case, the relative intensities of these two bands were also different, since it was found that they were 68% and 32%, respectively. From this picture it is clear that in the presence of DMPG and at low NaCl concentration, the secondary structure of dens25 is different from that at high NaCl concentration, and this one presents a similar pattern to that found in the presence of DMPC at both low and high salt concentration. Although aggregated structures and helical and disordered structures are present in all samples, the quantity of aggregated β structures diminished dramatically, i.e., the relative amount of either helical or disordered or both increased, in the presence of negatively-charged phospholipids at low salt concentration.

DISCUSSION

DENV NS2A protein is essential in the viral RNA replication process, it is a poorly characterized highly hydrophobic protein and requires the membrane to perform its functions. In this work we have characterized its membrane active regions by using a NS2A derived peptide library and have identified several regions with different interacting capabilities. Additionally, we have characterized a NS2A peptide, peptide dens25, with interesting properties in the presence of different membrane model systems. We have carried out an in-depth biophysical study aimed at the elucidation of the capacity of this region to interact and disrupt membranes, by studying the structural and dynamic features which might be relevant for that disruption.

We have been able to distinguish ten different regions with large hydrophobic and interfacial values in NS2A. One of these regions, region b, was characterized by having high water-to-interface transfer free energies overlapping high water-to-bilayer transfer free energies. We have also studied the effect of a NS2A peptide library on membrane rupture and observed two segments with significant rupture capabilities, one segment delimited by residues 25 to 41 corresponding to peptide 5, and a long segment delimited by residues 103 to 183 corresponding to peptides 18-29. Interestingly peptide 5 overlapped with region b and peptides 18 to 29 encompass a broad region where the supposed transmembrane segments of NS2A reside. We also studied the effect of the NS2A derived peptide library on the structural and thermotropic properties of phospholipid membranes and found several peptides (peptides 2, 5, 10 and 12) which induced a significant effect on the cooperativity and

the anisotropy of the phospholipids studied. Since peptide 5 presents a distinctive pattern, elicits a significant leakage value, affects the thermotropic behaviour of both DMPC and DMPG and has been proposed to bind to the membrane surface [24], we have selected the NS2A segment comprised by residues 30 to 55, peptide dens25, to characterize its effect on model membranes.

Peptide dens25 had a higher affinity for model membranes composed of negatively charged phospholipids, and its binding was apparently dependent on membrane surface total charge, i.e., the more negative, the greater the binding. The dens25 peptide was capable of altering membrane stability causing the release of fluorescent probes, this effect being dependent on the lipid/peptide molar ratio and lipid composition. Remarkably, the highest CF release was observed for liposomes containing negatively-charged phospholipids whereas Chol induced lower leakage values. We have also shown that the dens25 peptide was capable of affecting the steady state fluorescence anisotropy of fluorescent probes located in the palisade structure of the membrane, especially those composed of negatively-charged phospholipids. Significantly, the interaction of dens25 seemed to be of an electrostatic nature, the obtained data indicating that the effect was inversely proportional to the salt concentration in the medium. Calorimetry experiments further corroborated these results, with peptide dens25 affecting more significantly the phase transition of negatively-charged phospholipids in the absence of salt, effect that was significantly reduced when the ionic strength was increased, i.e., the less salt concentration, the bigger the effect dens25 has on negatively-charged phospholipids. These results were also confirmed by the infrared analysis of the ester C=O stretching carbonyl band of the phospholipids. In the presence of low salt

concentrations dens25 affected the phase transition of the negatively-charged molecule DMPG but not the zwitterionic one, DMPC. This interaction was abolished when the peptide was in the presence of relatively high concentrations of salt.

The infrared spectra of the Amide I' region of the fully hydrated dens25 peptide in the presence of different phospholipids and at different temperatures, displayed a coexistence of unordered, aggregated and helical structures. However, the relative proportion of secondary structure varied depending on phospholipid type and salt concentration. In the presence of DMPG and at low NaCl concentration, the secondary structure of dens25 was different from that at high NaCl concentration, and this one was similar to that found in the presence of DMPC at both low and high salt concentration. Although aggregated structures and helical and disordered structures are present in all samples, the quantity of aggregated β structures diminished dramatically, i.e., the relative amount of either helical or disordered or both increased, in the presence of negatively-charged phospholipids at low salt concentration. These results imply that the secondary structure of the dens25 peptide was affected by its binding to the membrane, so that membrane binding modulates the secondary structure of the peptide as it has been suggested for other peptides [60,61]. At the same time, differences in the frequency of the carbonyl band of the phospholipids were observed, showing that peptide binding also modulated phospholipid conformation.

Taken together all these results, it is clear that this NS2A segment interacts electrostatically with the membrane when negatively-charged phospholipids are present. The specific disrupting effect elicited by peptide dens25 should be primarily

due the electrostatic nature of the phospholipids, i.e., charge, with a slight contribution of hydrophobic interactions. Interestingly, peptide dens25 is able to affect the lipid milieu from the membrane surface down to the hydrophobic core. Its location should be at or near the membrane interface, influencing the fluidity of the phospholipids, most probably with an in-plane orientation rather than in a transmembrane position [62]. Moreover, its interfacial properties suggest that this segment could behave similarly to a pre-transmembrane domain partitioning into and interacting with the membrane depending on the membrane composition and/or other proteins [36, 64, 65], being the responsible of the fluctuation of the protein between different topologies and therefore possible locations [8, 9, 66]. The results described in this work identify an important region in the DENV NS2A protein, which might be of critical importance in the Dengue virus life cycle. Moreover, an understanding of NS2A membrane molecular interactions during the DENV replication cycle might allow the identification of new targets for the treatment of Dengue virus infection and a novel approach to anti-Dengue therapy.

ACKNOWLEDGEMENTS

This work was partially supported by grant BFU2008-02617-BMC (Ministerio de Ciencia y Tecnología, Spain) to J.V. We owe a debt of gratitude to BEI Resources, National Institute of Allergy and Infectious Diseases, Manassas, VA, USA, for the peptides used in this work. H.N. is supported by a FPU fellowship from MECD (Ministerio de Educación, Cultura y Deporte), Spain.

DECLARATIONS OF INTEREST

None to declare

LEGENDS TO FIGURES

FIGURE 1. (A) Averaged normalized water-to-membrane (——) and water-to-interface (−−−−) transfer free energy scales for forty-one DENV NS2A sequences. The NS2A sequences pertained to *DENV1* (02_20, 05K4147DK1, 297arg00, BIDV1323, BIDV1800, BIDV1841, BIDV1926VN2008, BIDV2143, BIDV2243VE2007 and ThD1004901), *DENV2* (NGC, BIDV633, BIDV687, CSF381, CSF63, DakArD20761, DF707, DF755, MD1504, MD903 and MD917), *DENV3* (05K797DK1, 07CHLS001, 98, 98TWmosq, BIDV1831VN2007, BIDV1874VN2007, BR29002, C036094, TB55i and ThD31283_98) and *DENV4* (2A, BIDV2165VE1998, BIDV2170VE1999, H241, rDEN4del30, Sin897695, ThD4047697, ThD4048501, Vp4 and Yama) strains [25,61]. Transfer free energies (kcal/mol) were obtained from Wimley and White [62], Engelman et al. [63], Hessa et al. [64], Moon and Fleming [65], Meiler et al. [66] and Eisenberg et al. [67]. Regions 1-8 [24] and *a-j* (this work) are depicted. (B) Enlargement of the 30-55 segment, showing the sequence of the dens25 peptide.

FIGURE 2. Membrane rupture (CF leakage) induced by the peptide library derived from DENV2 NS2A protein on LUVs composed of (A) EPC, (B) EPC/Chol at a molar proportion of 5:1, (C) EPC/BMP at a molar proportion of 5:1, (D) EPC/BPI at a molar proportion of 5:1, (E) EPC/ESM/Chol at a molar proportion of 5:2:1, (F) ER complex synthetic lipid mixture and (G) liver lipid extract. Vertical bars indicate standard deviations of the mean of quadruplicate samples.

FIGURE 3. (A) Fluorescence signal amplitude of FPE versus dens25 peptide concentration to determine peptide binding to membrane model systems and (B)

effect of dens25 peptide on the release (membrane rupture) of CF using different lipid compositions. The lipid compositions used were EPC (■), EPC/BPI at a molar proportion of 1:1 (●), EPC/CL at a molar proportion of 1:1 (▲), EPC/BPS at a molar proportion of 5:1 (▼), EPC/BPS at a molar proportion of 5:3 (◆), EPC/Chol at a molar proportion of 5:1 (◄), EPC/EPG at a molar proportion of 1:1 (►), EPC/EPG at a molar proportion of 5:1 (⬢), EPC/EPG at a molar proportion of 5:3 (□), EPC/ESM at a molar proportion of 5:1 (⬟), EPC/ESM/Chol at a molar proportion of 5:1:1 (Δ), ER complex synthetic lipid mixture (+), and liver lipid extract (×).The buffer contained no NaCl in (A) but 100mM NaCl in (B). The insert shows the dependence of FPE fluorescence on EPC/EPG ratio for liposome compositions containing EPC and EPG and 36 μM of peptide. See text for details.

FIGURE 4. Steady-state anisotropy <r> of the DPH probe incorporated into DMPG membranes as a function of temperature at pH 7.4 in the absence (■,▲) and in the presence (□,Δ) of peptide dens25 at a peptide/lipid molar ratio of 1:10 and in the presence of different concentrations of NaCl (■,□) or KCl (▲,Δ). Buffers contained 20 mM HEPES, 0.1 mM EDTA and (A) 0 mM of NaCl, (B) 0 mM KCl, (C) 50 mM NaCl, (D) 50 mM KCl, (E) 100 mM NaCl, (F) 100 mM KCl, (G) 150 mM NaCl, (H) 150 mM KCl, (I) 200 mM Na Cl, (J) 200 mM KCl, (K) 300 mM NaCl and (L) 300 mM KCl. The value of the first derivative of <r> with respect to temperature for each sample at its absolute minimum ($T=T_m$) is shown in (M), whereas the difference in <r> at 40ºC in the absence and in the presence of peptide is shown in (N).

Figure 5. Differential scanning calorimetry heating thermograms corresponding to model membranes composed of DMPC (A and B), DMPG (C, D and E), DMPS (F

and G), and BMP (H and I) in the absence (top curves) and in the presence of peptide dens25 (bottom curves) at a phospholipid/peptide molar ratio of 10:1. Buffer contained 20 mM HEPES, 0.1 mM EDTA, pH 7.4 and one of the following NaCl concentrations: 25 mM NaCl (A, C, F and H), 100 mM NaCl (B, D, G and I) or 300 mM NaCl (E). All thermograms were normalized to the same amount of lipid.

FIGURE 6. Temperature dependence of the frequencies of the C=O carbonyl stretching band of in the absence (■) and in the presence (○) of peptide dens25 as a function of temperature for different membrane model systems. The model membranes were composed of DMPC (A and B) and DMPG (C and D) in buffer containing 20 mM HEPES, 0.1 mM EDTA and either 25 mM NaCl (A, C) or 100 mM NaCl (B, D) at pH 7.4. Representative spectra of the membrane model systems in the absence (——) and in the presence (−−−−) of peptide dens25 are also shown. The phospholipid/peptide molar ratio was 15:1.

SUPPLEMENTAL FIGURE 1. Steady-state anisotropy, <r>, of the DPH probe incorporated into DMPC model membranes as a function of temperature in the presence of the peptide library corresponding to DENV2 NS2A protein. Each peptide is identified by its corresponding number. Data correspond to vesicles containing pure phospholipid (●) and phospholipid plus peptide (○).The peptide to phospholipid molar ratio was 1:15.

SUPPLEMENTAL FIGURE 2. Steady-state anisotropy, <r>, of the DPH probe incorporated into DMPG model membranes as a function of temperature in the presence of the peptide library corresponding to DENV2 NS2A protein. Each peptide is identified by its corresponding number. Data correspond to vesicles containing pure phospholipid (●) and phospholipid plus peptide (○).The peptide to phospholipid molar ratio was 1:15.

TABLE 1

Sequence and residue position of the peptides contained in the DENV2 NS2A derived peptide library. The sequence of peptide dens25, **KHAILLVAVSFVTLITGNMSFRDLGR**, is underlined. See text for details.

Peptide	Amino acid sequence	Sequence	Length	Net charge
1	GHGQIDNFSLGVLGMAL	1 - 17	17	-1
2	NFSLGVLGMALFLEEML	7 - 23	17	-2
3	LGMALFLEEMLRTRVGT	13 - 29	17	0
4	LEEMLRTRVGTKHAILL	19 - 35	17	+1
5	TRVGTKHAILLVAVSFV	25 - 41	17	+2
6	HAILLVAVSFVTLITGN	31 - 47	17	0
7	AVSFVTLITGNMSFRDL	37 - 53	17	0
8	LITGNMSFRDLGRVMVM	43 - 59	17	+1
9	SFRDLGRVMVMVGATMT	49 - 65	17	+1
10	RVMVMVGATMTDDIGMG	55 - 71	17	-1
11	GATMTDDIGMGVTYLAL	61 - 77	17	-2
12	DIGMGVTYLALLAAFKV	67 - 83	17	0
13	TYLALLAAFKVRPTFAA	73 - 89	17	+2
14	AAFKVRPTFAAGLLLRK	79 - 95	17	+4
15	PTFAAGLLLRKLTSKEL	85 - 101	17	+2
16	LLLRKLTSKELMMTTIG	91 - 107	17	+2
17	TSKELMMTTIGIVLLSQ	97 - 113	17	0
18	MTTIGIVLLSQSTIPET	103 - 119	17	-1
19	VLLSQSTIPETILELTD	109 - 125	17	-3
20	TIPETILELTDALALGM	115 - 131	17	-3
21	LELTDALALGMMVLKMV	121 - 137	17	-1
22	LALGMMVLKMVRKMEKY	127 - 143	17	+3
23	VLKMVRKMEKYQLAVTI	133 - 149	17	+3
24	KMEKYQLAVTIMAILCV	139 - 155	17	+1
25	LAVTIMAILCVPNAVIL	145 - 161	17	0
26	AILCVPNAVILQNAWKV	151 - 167	17	+1
27	NAVILQNAWKVSCTILA	157 - 173	17	+1
28	NAWKVSCTILAVVSV	163 - 177	15	+1
29	VSCTILAVVSVSPLFLT	167 - 183	17	0
30	AVVSVSPLFLTSSQQKA	173 - 189	17	+1
31	PLFLTSSQQKADWIPLA	179 - 195	17	0
32	SQQKADWIPLALTIKGL	185 - 201	17	+1
33	WIPLALTIKGLNPTAIF	191 - 207	17	+1
34	TIKGLNPTAIFLTTLSR	197 - 213	17	+2
35	PTAIFLTTLSRTNKKR	203 - 218	16	+4

REFERENCES

(1) *Molecular Virology and Control of Flaviviruses*; Caister Academic Press, 2012.

(2) Bhatt, S.; Gething, P. W.; Brady, O. J.; Messina, J. P.; Farlow, A. W.; Moyes, C. L.; Drake, J. M.; Brownstein, J. S.; Hoen, A. G.; Sankoh, O.; Myers, M. F.; George, D. B.; Jaenisch, T.; Wint, G. R.; Simmons, C. P.; Scott, T. W.; Farrar, J. J.; Hay, S. I. *Nature* **2013**, *496*, 504.

(3) WHO "Dengue: Guidelines for Diagnosis, Treatment, Prevention and Control," World Health Organization, 2009.

(4) Pastorino, B.; Nougairede, A.; Wurtz, N.; Gould, E.; de Lamballerie, X. *Antiviral Res* **2010**, *87*, 281.

(5) Noble, C. G.; Chen, Y. L.; Dong, H.; Gu, F.; Lim, S. P.; Schul, W.; Wang, Q. Y.; Shi, P. Y. *Antiviral Res* **2010**, *85*, 450.

(6) Urcuqui-Inchima, S.; Patino, C.; Torres, S.; Haenni, A. L.; Diaz, F. J. *Adv Virus Res* **2010**, *77*, 1.

(7) Perera, R.; Kuhn, R. J. *Curr Opin Microbiol* **2008**, *11*, 369.

(8) Bressanelli, S.; Stiasny, K.; Allison, S. L.; Stura, E. A.; Duquerroy, S.; Lescar, J.; Heinz, F. X.; Rey, F. A. *Embo J* **2004**, *23*, 728.

(9) Kielian, M.; Rey, F. A. *Nat Rev Microbiol* **2006**, *4*, 67.

(10) Mukhopadhyay, S.; Kuhn, R. J.; Rossmann, M. G. *Nat Rev Microbiol* **2005**, *3*, 13.

(11) Miller, S.; Kastner, S.; Krijnse-Locker, J.; Buhler, S.; Bartenschlager, R. *J Biol Chem* **2007**, *282*, 8873.

(12) Miller, S.; Krijnse-Locker, J. *Nat Rev Microbiol* **2008**, *6*, 363.

(13) Welsch, S.; Miller, S.; Romero-Brey, I.; Merz, A.; Bleck, C. K.; Walther, P.; Fuller, S. D.; Antony, C.; Krijnse-Locker, J.; Bartenschlager, R. *Cell Host Microbe* **2009**, *5*, 365.

(14) Brault, J. B.; Kudelko, M.; Vidalain, P. O.; Tangy, F.; Despres, P.; Pardigon, N. *Virology* **2011**, *417*, 369.

(15) Catteau, A.; Kalinina, O.; Wagner, M. C.; Deubel, V.; Courageot, M. P.; Despres, P. *J Gen Virol* **2003**, *84*, 2781.

(16) Catteau, A.; Roue, G.; Yuste, V. J.; Susin, S. A.; Despres, P. *Biochimie* **2003**, *85*, 789.

(17) Mackenzie, J. M.; Khromykh, A. A.; Jones, M. K.; Westaway, E. G. *Virology* **1998**, *245*, 203.

(18) Miller, S.; Sparacio, S.; Bartenschlager, R. *J Biol Chem* **2006**, *281*, 8854.

(19) Munoz-Jordan, J. L.; Sanchez-Burgos, G. G.; Laurent-Rolle, M.; Garcia-Sastre, A. *Proc Natl Acad Sci U S A* **2003**, *100*, 14333.

(20) Rodenhuis-Zybert, I. A.; Wilschut, J.; Smit, J. M. *Cell Mol Life Sci* **2010**, *67*, 2773.

(21) Muller, D. A.; Young, P. R. *Antiviral Res* **2013**, *98*, 192.

(22) Falgout, B.; Chanock, R.; Lai, C. J. *J Virol* **1989**, *63*, 1852.

(23) Hori, H.; Lai, C. J. *J Virol* **1990**, *64*, 4573.

(24) Yeagle, P. L.; Young, J.; Hui, S. W.; Epand, R. M. *Biochemistry* **1992**, *31*, 3177.

(25) Guillen, J.; Perez-Berna, A. J.; Moreno, M. R.; Villalain, J. *J Virol* **2005**, *79*, 1743.

(26) Moreno, M. R.; Giudici, M.; Villalain, J. *Biochim Biophys Acta* **2006**, *1758*, 111.

(27) Nemesio, H.; Palomares-Jerez, F.; Villalain, J. *Biochim Biophys Acta* **2011**, *1808*, 2390.

(28) Nemesio, H.; Palomares-Jerez, F.; Villalain, J. *Biochim Biophys Acta* **2012**, *1818*, 2818.

(29) Perez-Berna, A. J.; Moreno, M. R.; Guillen, J.; Bernabeu, A.; Villalain, J. *Biochemistry* **2006**, *45*, 3755.

(30) Perez-Berna, A. J.; Veiga, A. S.; Castanho, M. A.; Villalain, J. *J Viral Hepat* **2008**, *15*, 346.

(31) Perez-Berna, A. J.; Guillen, J.; Moreno, M. R.; Bernabeu, A.; Pabst, G.; Laggner, P.; Villalain, J. *J Biol Chem* **2008**, *283*, 8089.

(32) Palomares-Jerez, F.; Nemesio, H.; Villalain, J. *Biochim Biophys Acta* **2012**, *1818*, 2958.

(33) Surewicz, W. K.; Mantsch, H. H.; Chapman, D. *Biochemistry* **1993**, *32*, 389.

(34) Zhang, Y. P.; Lewis, R. N.; Hodges, R. S.; McElhaney, R. N. *Biochemistry* **1992**, *31*, 11572.

(35) Krainev, A. G.; Ferrington, D. A.; Williams, T. D.; Squier, T. C.; Bigelow, D. J. *Biochim Biophys Acta* **1995**, *1235*, 406.

(36) Keenan, T. W.; Morre, D. J. *Biochemistry* **1970**, *9*, 19.

(37) Mayer, L. D.; Hope, M. J.; Cullis, P. R. *Biochim Biophys Acta* **1986**, *858*, 161.

(38) Böttcher, C. S. F.; Van Gent, C. M.; Fries, C. *Anal Chim Acta* **1961**, *1061*, 203.

(39) Edelhoch, H. *Biochemistry* **1967**, *6*, 1948.

(40) Bernabeu, A.; Guillen, J.; Perez-Berna, A. J.; Moreno, M. R.; Villalain, J. *Biochim Biophys Acta* **2007**, *1768*, 1659.

(41) Moreno, M. R.; Guillen, J.; Perez-Berna, A. J.; Amoros, D.; Gomez, A. I.; Bernabeu, A.; Villalain, J. *Biochemistry* **2007**, *46*, 10572.

(42) Lentz, B. R. *Chem Phys Lipids* **1993**, *64*, 99.

(43) Wall, J.; Ayoub, F.; O'Shea, P. *J Cell Sci* **1995**, *108 (Pt 7)*, 2673.

(44) Golding, C.; Senior, S.; Wilson, M. T.; O'Shea, P. *Biochemistry* **1996**, *35*, 10931.

(45) Giudici, M.; Poveda, J. A.; Molina, M. L.; de la Canal, L.; Gonzalez-Ros, J. M.; Pfuller, K.; Pfuller, U.; Villalain, J. *FEBS J* **2006**, *273*, 72.

(46) Guillen, J.; Perez-Berna, A. J.; Moreno, M. R.; Villalain, J. *Biochemistry* **2008**, *47*, 8214.

(47) Shnaper, S.; Sackett, K.; Gallo, S. A.; Blumenthal, R.; Shai, Y. *J Biol Chem* **2004**, *279*, 18526.

(48) Salzwedel, K.; West, J. T.; Hunter, E. *J Virol* **1999**, *73*, 2469.

(49) Perez-Berna, A. J.; Bernabeu, A.; Moreno, M. R.; Guillen, J.; Villalain, J. *Biochim Biophys Acta* **2008**, *1778*, 2069.

(50) Lorizate, M.; Huarte, N.; Saez-Cirion, A.; Nieva, J. L. *Biochim Biophys Acta* **2008**, *1778*, 1624.

(51) Lorizate, M.; de la Arada, I.; Huarte, N.; Sanchez-Martinez, S.; de la Torre, B. G.; Andreu, D.; Arrondo, J. L.; Nieva, J. L. *Biochemistry* **2006**, *45*, 14337.

(52) Gouttenoire, J.; Castet, V.; Montserret, R.; Arora, N.; Raussens, V.; Ruysschaert, J. M.; Diesis, E.; Blum, H. E.; Penin, F.; Moradpour, D. *J Virol* **2009**, *83*, 6257.

(53) Gouttenoire, J.; Roingeard, P.; Penin, F.; Moradpour, D. *J Virol* **2010**, *84*, 12529.

(54) Heaton, N. S.; Randall, G. *Viruses* **2011**, *3*, 1332.

(55) Epand, R. M.; Hui, S. W. *FEBS Lett* **1986**, *209*, 257.

(56) Lewis, R. N.; McElhaney, R. N.; Pohle, W.; Mantsch, H. H. *Biophys J* **1994**, *67*, 2367.

(57) Blume, A.; Hubner, W.; Messner, G. *Biochemistry* **1988**, *27*, 8239.

(58) Arrondo, J. L.; Goni, F. M. *Prog Biophys Mol Biol* **1999**, *72*, 367.

(59) Byler, D. M.; Susi, H. *Biopolymers* **1986**, *25*, 469.

(60) Palomares-Jerez, M. F.; Guillen, J.; Villalain, J. *Biochim Biophys Acta* **2010**, *1798*, 1212.

(61) Guillen, J.; Gonzalez-Alvarez, A.; Villalain, J. *Biochim Biophys Acta* **2010**, *1798*, 327.

(62) White, S. H.; Wimley, W. C. *Annu Rev Biophys Biomol Struct* **1999**, *28*, 319.

(63) Engelman, D. M.; Steitz, T. A.; Goldman, A. *Annu Rev Biophys Biophys Chem* **1986**, *15*, 321.

(64) Hessa, T.; Meindl-Beinker, N. M.; Bernsel, A.; Kim, H.; Sato, Y.; Lerch-Bader, M.; Nilsson, I.; White, S. H.; von Heijne, G. *Nature* **2007**, *450*, 1026.

(65) Moon, C. P.; Fleming, K. G. *Proc Natl Acad Sci U S A* **2011**, *108*, 10174.

(66) Koehler, J.; Woetzel, N.; Staritzbichler, R.; Sanders, C. R.; Meiler, J. *Proteins* **2009**, *76*, 13.

(67) Eisenberg, D.; Weiss, R. M.; Terwilliger, T. C. *Nature* **1982**, *299*, 371.

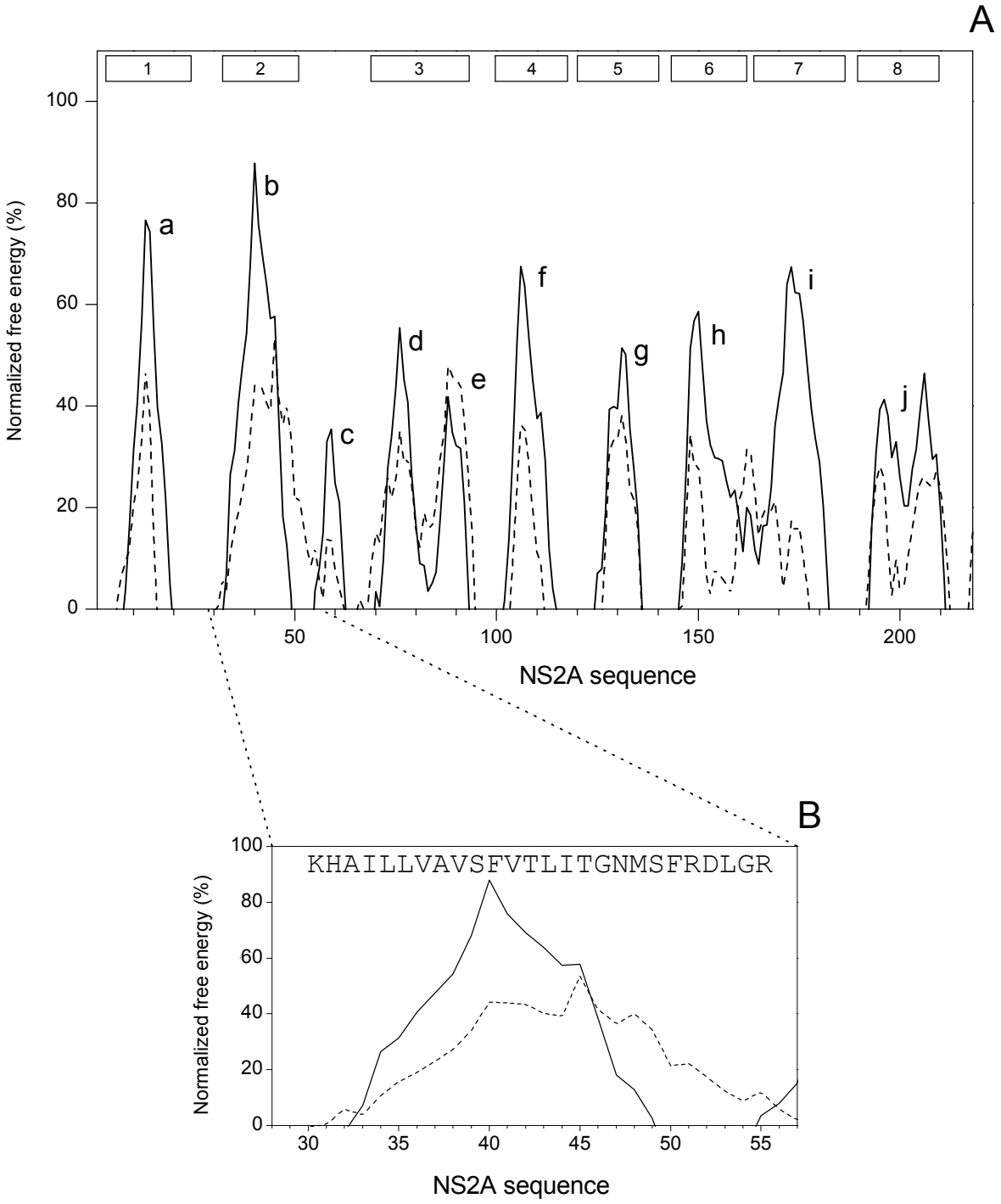
A
1
2
3
4
5
6
7
8
a
b
c
d
e
f
g
h
i
j
Normalized free energy (%)
NS2A sequence
B
KHAILLVAVSFVTLITGNMSFRDLGR
Normalized free energy (%)
NS2A sequence

FIGURE 2

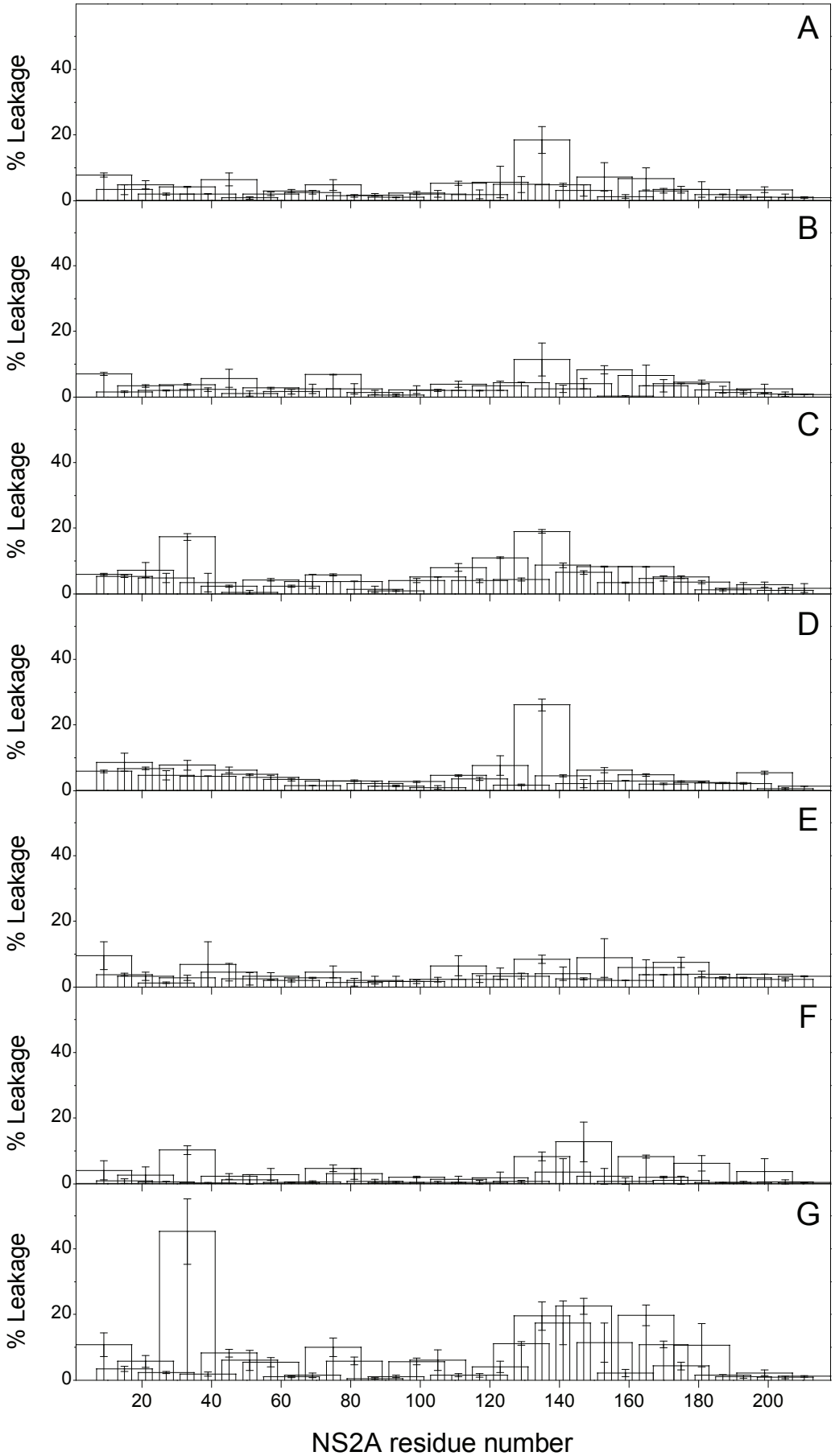
A
B
C
D
E
F
G
% Leakage
0
20
40
20
40
60
80
100
120
140
160
180
200
NS2A residue number

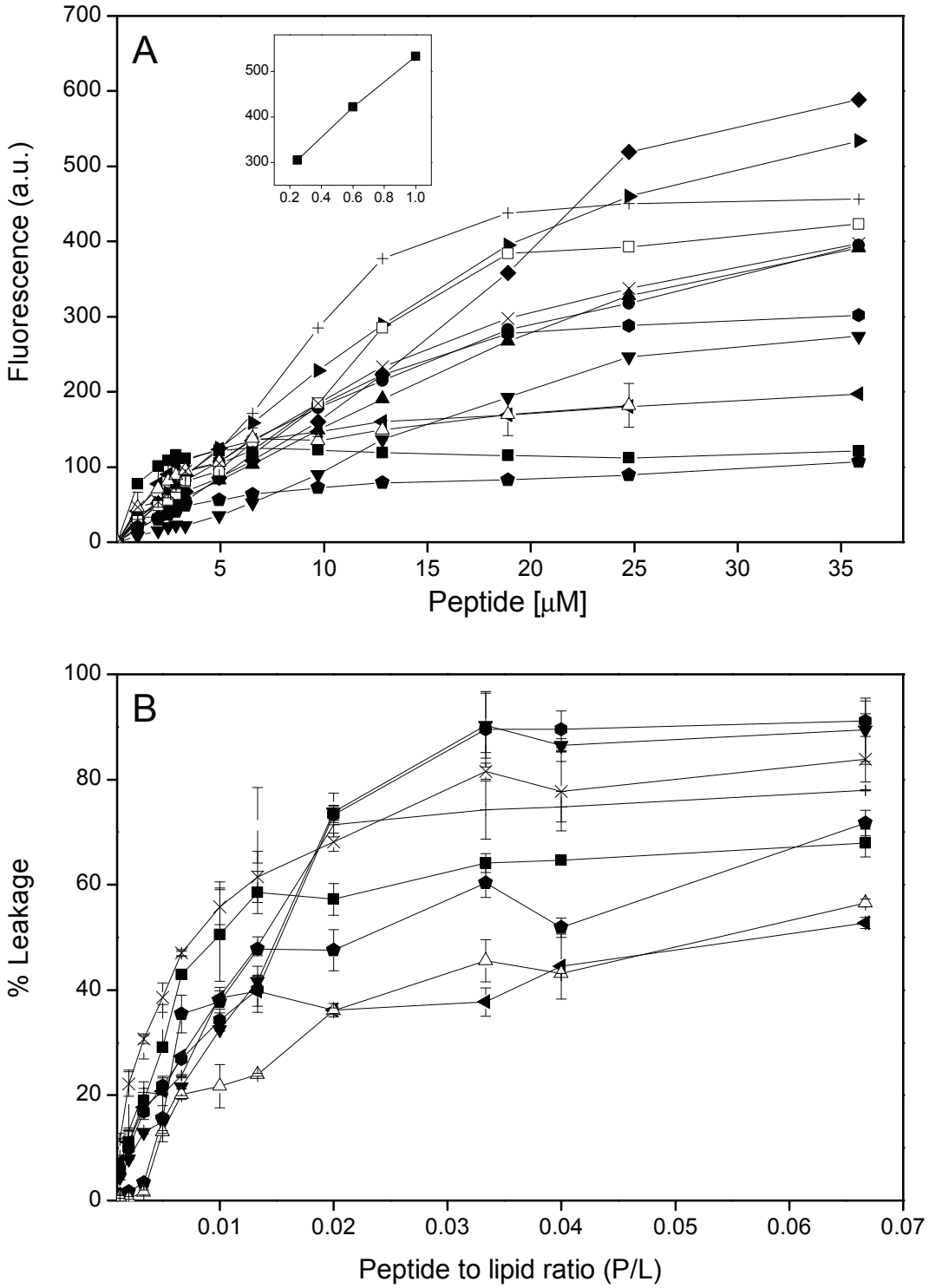
A
Fluorescence (a.u.)
Peptide [μM]
B
% Leakage
Peptide to lipid ratio (P/L)

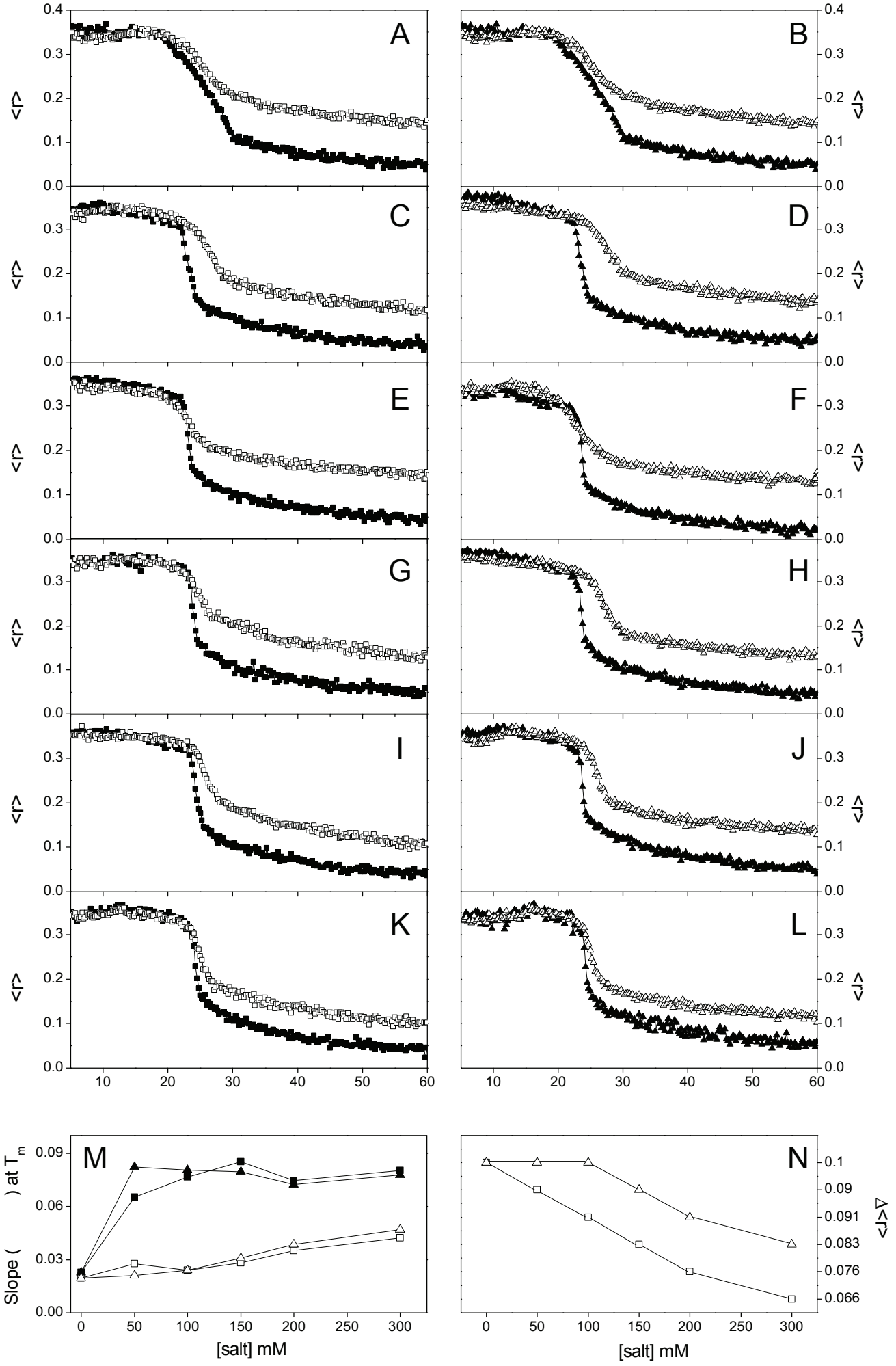
A
B
C
D
E
F
G
H
I
J
K
L
<r>
<r>
0.0
0.1
0.2
0.3
0.4
10
20
30
40
50
60
M
N
Slope ( ) at T_m
0.00
0.03
0.06
0.09
0.066
0.076
0.083
0.091
0.1
0
50
100
150
200
250
300
[salt] mM
[salt] mM
Δ<r>

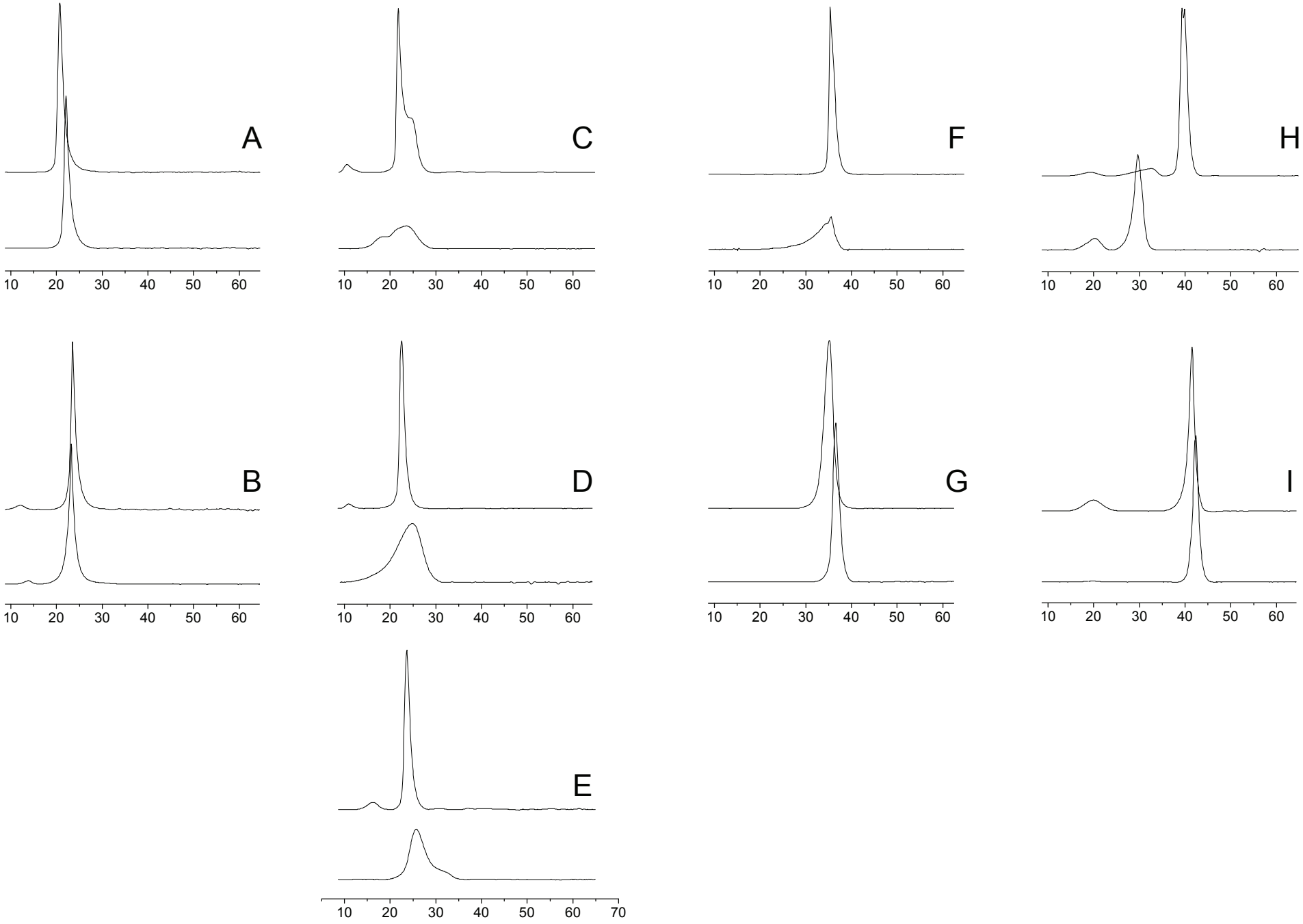

FIGURE 5

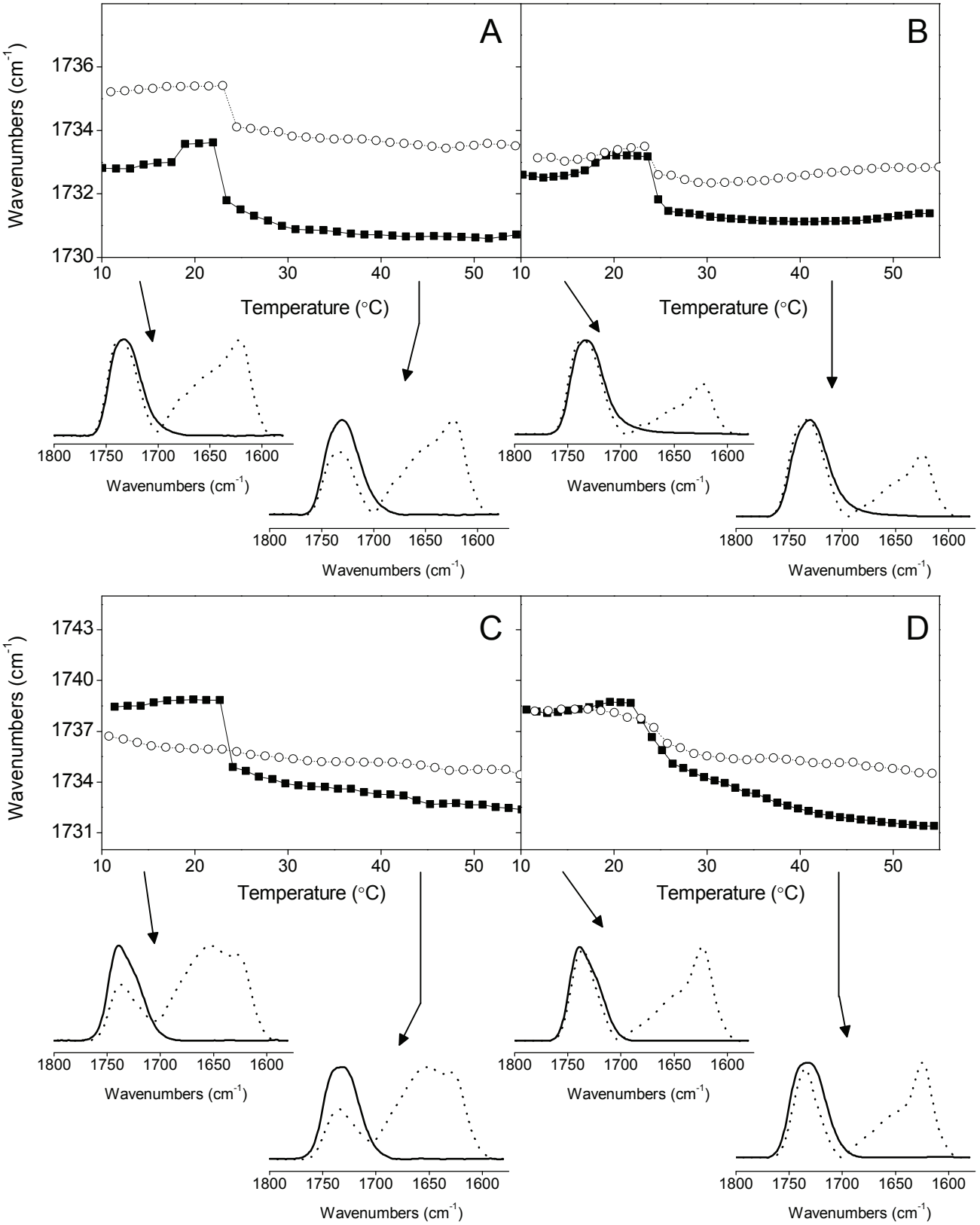

FIGURE 6

CHAPTER 5. OVERALL RESULTS AND DISCUSSION

CHAPTER 5. OVERALL RESULTS AND DISCUSSION

Dengue virus (DENV) is part of the family *Flaviviridae* and its genus is Flavivirus along with JEV and WNV for example. It is the most prevalent arthropod-borne virus (arbovirus) in the human population, affecting about 400 million people every year according to recent estimates [109]. People infected by this virus present different clinical manifestations ranging from asymptomatic illness to dengue fever ("break-bone fever") and two more serious and life-threatening features, Dengue Haemorrhagic fever (DHF) and Dengue shock syndrome (DSS). There is currently no safe and effective vaccines nor antiviral drugs to counter this pathogen, being this partially attributable to the need to address the tetravalent nature of this virus and a phenomenon called antibody dependent enhancement (ADE) of Dengue which increases the severity of a second heterologous infection. DENV comprises four distinct serotypes that share 69-78 % identity at the primary sequence level [356]. The mature virion is composed of a nucleocapsid, which itself consists of multiple copies of C protein associated with the viral RNA genome (vRNA), enclosed by a host derived lipid bilayer where 180 copies of M and E proteins lie flat against the surface. DENV has a plethora of receptors at the surface of cells and it enters cells by receptor-mediated endocytosis through clathrin-coated pits [54, 119, 182]. A decrease in pH inside the endosome triggers a conformational change of E class II fusion protein that results in the fusion of viral and host membranes. The energy required for the fusion process to occur is thought to come from both these conformational changes and lipid membrane restructuring [40, 54, 75]. Following fusion, the nucleocapsid is released into the cytoplasm where it dissociates into C proteins and vRNA. The positive single stranded RNA molecule is then translated into a single polyprotein with some 3000 amino acids that is targeted to the ER membrane close to the nucleus by signal sequences. Here, both viral and host proteases cleave this polyprotein into three structural proteins C, prM, E and seven non-structural proteins NS1, NS2A, NS2B, NS3, NS4A, NS4B and NS5. All the structural proteins seem to remain anchored in the ER and ER-derived membranes, while non-structural proteins form replication complexes in membrane structures like double-membrane vesicles (DMV) and paracrystalline arrays [170, 171, 264] where the viral replication occurs, safely hidden from host RNAses and proteases. It is in these membranes that the viral budding process occurs with the formation of immature and

subviral particles. These particles then begin their transit through the trans-Golgi network (TGN). During this transit the decrease in pH in vesicles favours the cleavage of the pr peptide (part of prM) a segment that prevents the early exposure of the fusion loop at the tip of E protein's domain II, which would result in membrane fusion. Following exocytosis, the pr peptide is released and the fully mature particle is thus ready to start the whole process anew [79, 119].

Both C and E proteins have mainly structural functions such as fusion (E), specific encapsidation of the genome (C) or the viral budding process (C and E). C protein has two distinct structural features in its dimer conformation: one highly charged region (+46) that is thought to interact with vRNA molecules and a hydrophobic region inside a concave groove that could bind to membranes [219]. Apart from its C-terminal signal sequence, no other membrane binding sequence has been proven to bind to membranes. As for E, apart from its fusion loop with affinity for membranes located at the tip of its domain II (central region in the primary sequence and at one extreme of the tertiary structure), only the membrane anchoring domain III, the stem region and at least two transmembrane helices have any ascribed membrane interactions [223].

To highlight all of the membrane interacting regions of both of these proteins and whether they have membrane modulating capabilities, we undertook a biophysical study resorting to a series of previously described techniques, peptide libraries encompassing the full length of those proteins and membrane model systems with a variety of compositions [357-359]. At first we represented the water-to-bilayer and water-to-interface transfer free energies of each residue in a bidimensional chart that assumes an α-helix secondary structure. Although this is not necessarily the structure of these proteins (the E protein is mainly β sheet), this representation has been shown to efficiently predict possible membrane interacting domains in previous works [357-359] and as it will be seen further ahead, the regions defined by this methodology coincide with those defined by experimental data. In this kind of representation two types of regions or patches can be assigned, one covering the full horizontal length (perimeter of the α-helix arrangement), representing either membrane interacting domains (if it has less than 15 amino acids) or transmembrane domains (if it has more than 15 amino acids), and another less extensive and that does not encompass the full length of the structure, associated with protein-protein interactions. One hydrophobic patch (C1)

covering the full horizontal length of the map has been found for protein C from residues 40 to 59 (Figure 2 A-C, P1), coincident with a previously described region postulated to interact with membranes [219], surrounded by two highly charged regions from residues 3 to 32 and 67 to 100, coincident with two predicted highly charged regions.

The same methodology was applied to protein E and eleven patches have been defined. Seven of them are either membrane interacting regions or involved in protein-protein interactions: E1 from residues 20 to 31, located in domain I (correspondence between peptides and domains is found in Figure 1, P1), E2 from residues 101 to 118 encompassing parts of domains I and II, E3 from residues 213 to 222 located in domain II, E4 from residues 255 to 266 in domain II, E5 from residues 277 to 287 in domain II, E6 from residues 376 to 382 between domains I and III and E7 from residues 397 to 409 between domains III and the EH1 α-helix domain of the stem region [360]. The remaining five encompass the full horizontal length of the structure, possibly transmembrane regions, E8 from residues 101 to 118, in domain II and coincident with the fusion loop, E9 from residues 420 to 436 and E10 from residues 439 to 453 which compose the EH2 α-helix domain of the stem region and finally E11 and E12 from residues 457 to 469 and 476 to 493 respectively, coincident with previously described transmembrane domains TM1 and TM2 of E [75, 119, 223]. Using peptide libraries derived from both full-length proteins (Figure 1, P1) and membrane model systems we completed this study with membrane leakage measurements (Figures 4 and 5, P1) and differential scanning calorimetry experiments (Figure 6, P1).

For protein C, a leakage region CL1 coincident with the C1 region induced virtually complete rupture of membranes regardless of lipid composition (Table 3 and Figure 4, P1), from ER-mimicking formulations (Figure 4 G-O, P1) to membranes containing BMP, a lipid found in late endosomes (Figure 4 E, P1), a liver extract (Figure 4 F, P1) and to membranes composed of EPC/ESM/Chol that mimic the composition of certain lipid rafts (Figure 4 D, P1). On another level, these peptides did not affect the thermotropic behaviour of DEPE, a lipid molecule known to form type II phases and thus influence membrane curvature (Figure 6 A and 6 C, P1). As for protein E, at least five distinct regions induced significant membrane leakage, some to a larger extent than others (Table 3, P1). Each of those can be mapped to at least one of the eleven regions found previously, EL1 from residues 88 to 107, coincident with the E8 region and the

fusion loop, EL2 from residues 198 to 221, between E2 and E3, containing a proline rich motif related to protein-protein interactions [361], EL3 from residues 270 to 309 coincident with E5, EL4 from residues 406 to 422 between E7 and E9-10, the two helical domains of the stem regions of E and EL5 from residues 428 to 479, coincident with the EH2 α-helical domain of the stem and the first transmembrane domain (TM1). EL5 elicits the strongest effect on membrane rupture by far, independent of composition, confirming its membrane effect. Considering that peptides derived from the region inhibit viral infectivity [288] and a peptide derived from the EL4 region and the N-terminal of EL5 induced the release of genome deficient virions [290], these two regions might be important for membrane fusion and the specific encapsidation of the genome (this in concert with C). EL3/E5 elicited a more modest leakage with no apparent dependence of composition. As for EL2 (between E2 and E3) its effect was more or less conserved except for membranes mimicking lipid raft compositions like EPC/ESM/Chol 5:2:1 (Figure 5 D, P1) where this membrane leakage was increased and two other where it was reduced, one containing BMP (found in late endosomes, Figure 5 E, P1) and another made of a liver extract (Figure 5 F, P1). The fusion loop EL1 region had a small yet discernible effect in all assayed compositions except liver membranes (Figure 5 F, P1). Interestingly, the previously described TM2 region exerted no effect. Similar to protein C, peptides derived from this protein had little to no effect on the thermotropic behaviour of DEPE except its C-terminal EL4 and EL5 regions from residues 406 to 479 that increased the temperature of its sensitive Lα to H_{II} phase transition. In light of recent discoveries and these data, it is not too bold to suggest that EL4 might be involved in membrane fusion and rearrangement, possibly an interesting target to develop antiviral drugs.

Following the line of evidence from the first paper (P1) we proceeded to characterize the C1/CL1 highly hydrophobic, membrane-active and conserved (Table I, P2) region from residues 39 to 56 of protein C with sequence GRGPLKLFMALVAFLRFL henceforth named $DENV2_{C6}$. Noting that it lacks tryptophan residues, its membrane binding extent was assessed indirectly through the use of a PE derived fluorophore (FPE) that is sensitive to surface potential changes, as done in previous works [362]. This peptide shows high affinity to negatively charged membranes like EPC/EPA, EPC/BPS or ER (Figure 1, P2) and lower affinity for zwitterionic membranes (except EPC) composed of EPC and either Chol or both Chol and ESM, lipid mixtures found in

lipids rafts. Interestingly, assuming either a sigmoidal or hyperbolic binding model, ER had a Hill coefficient of 3 while all the others had a unitary Hill coefficient, suggesting that $DENV2_{C6}$ might interact with membranes in trimeric and monomeric conformations respectively. $DENV2_{C6}$ completely ruptures liposomes regardless of composition in a dose-dependent manner (Figure 2). Firstly, membranes composed of zwitterionic lipids Chol, ESM or EPC are completely ruptured (over 80 % of membrane leakage) even at a lipid to peptide ratio of 800 to 1 (0.16 μM peptide) (Figure 2 C, P2). It is clear (Figure 5 A, P2) that if membranes contain negative lipids this leakage effect is dose-dependent with values as low as 5 % at 800 to 1 lipid to peptide in liver membranes and higher than 80% at 5 to 1. Chol seems to slightly reduce membrane leakage in negatively charged membranes (Figures 2 A and 2 B, P2). To assess if there is any interaction with a specific lipid, the same composition of ER (ER 58:6) was used with all lipids except EPC (58) at equal proportions (6) and removing one by one (Figure 2 D, P2). The only discernible effect was a reduction in membrane rupture when either BPI or TPE were removed, but only at high lipid to peptide ratios (over 300 to 1). Experiments performed with FD20 and FD70 dextrans, fluorescent molecules with Stokes radii of 33 Å and 60 Å respectively, significantly larger than CF's 6 Å have shown that this peptide might induce very large pores on the membrane because it could still induce the release of those dextrans, regardless of lipid composition. To assess the influence of $DENV2_{C6}$ on the thermotropic behaviour of lipids and the relative location of the peptide-lipid interaction, the steady-state fluorescence anisotropy of DPH was measured in the presence and absence of the peptide (Figure 3, P2). For DMPC, DMPG and DMPS the presence of $DENV2_{C6}$ decreased the cooperativity of the main transition without affecting its temperature. It also increased the post-transition anisotropy of DPH but not that of TMA-DPH. DPPC and DSPC are respectively 2 and 4 carbons longer than DMPC and the effect of this peptide on their thermal behaviour confirming an interaction at a deep level. In the case of DMPA, $DENV2_{C6}$ increased the T_m, decreased the cooperativity of its transition and the post-transition anisotropy of DPH. As for BMP, this peptide decreased its transition cooperativity while increasing the post-transition anisotropy of DPH. All in all, $DENV2_{C6}$ affected the anisotropy of DPH to a greater extent than that of TMA-DPH what would mean this peptide interacts with the membrane at a deeper location, affecting the membrane fluidity. These results have been complemented with differential scanning calorimetry (Figure 4, P2) When incorporated into DMPC, $DENV2_{C6}$ abolished its pre-transition from L_β' to P_β',

decreased both the temperature (T_m) and cooperativity (broadened peak) of its main transition (P_β' to L_α) and induced the formation of mixed phases as represented by the overlapping bands seen on the thermogram. All in all, because $DENV2_{C6}$ affected the steady state anistotropy of DPH to a larger extent than that of TMA-DPH, it is safe to assume that this peptide affects the membrane at deeper location, affecting its fluidity [363]. These results have been complemented by differential scanning calorimetry where the thermotropic behaviour of several lipids in the presence of $DENV2_{C6}$ (15 to 1 lipid to peptide ratio) was compared to that of pure lipid (Figure 4, P2). When incorporated into DMPC (Figure 4 A, P2), $DENV2_{C6}$ abolished the pre-transition from L_β' to P_β' of that lipid, decreased its T_m, broadened its main transition peak, what points to a reduced cooperativity and because it shows at least two overlapping peaks, mixed phases might be present. It slightly reduced the T_m of DEPE and the cooperativity of DMPS and PSM. DMPG had its cooperativity decreased by the presence of $DENV2_{C6,}$ yet its pre-transition was not affected. BMP, a PG analogue maintained its first transition while its high enthalpy main transition had its cooperativity and transition temperature decreased, concomitant with the appearance of mixed phases. To ascertain whether $DENV2_{C6}$ affects the polar head of lipids or their acyl chains and if its secondary structure is modified in the presence of lipids we used FTIR spectroscopy (Figure 5, P2). The amide I' band of the fully hydrated $DENV2_{C6}$ consists mainly of aggregated b structures with characteristic bands at 1693 cm^{-1} and 1624 cm^{-1} with a contribution of α–helical and unordered structures represented by the band at 1651 cm^{-1}. The intensity of the 1693 cm^{-1} band reduced with increasing temperature, while that of the 1683 cm^{-1} (β turns) increased. These bands were all present in the amide I' band of $DENV2_{C6}$ mixed with either DMPG or BMP, yet there was a clear decrease of the 1651 cm^{-1} band area. When added to DMPC, $DENV2_{C6}$'s main secondary structure changed to mainly α-helical and unordered structures (1651 cm^{-1}). Relying on the C=O and CH_2 stretching bands of lipids in the absence and presence of peptide, the influence of peptides on the thermotropic behaviour of lipids can also be assessed. $DENV2_{C6}$ decreased the T_m of DMPC (Figures 6 A and 6 D, P2) and the absolute maxima of both bands. This last result is indicative of two phenomena, on the one hand the increase of the maximum of the C=O band is related to an increase of the 1743 cm^{-1} band, C=O groups involved in non-hydrogen bonds, with respect to the 1723 cm^{-1} band, C=O groups involved in hydrogen bonds while on the other hand, higher maxima of the CH_2

suggest an increase of acyl chain mobility. The transition temperature of DMPG is not affected in the presence of this peptide, yet its presence induces the formation of a quasi-crystalline phase (detected by the two peaks seen in Figure 6 B, P2) [364]. As for BMP, this peptide only elicits a decrease in transition cooperativity. To conclude, $DENV2_{C6}$ binds strongly to membranes, primarily due to hydrophobic effects, although its stronger effect in the presence of negative lipids hints at an electrostatic contribution. Because it affects more strongly the anisotropy of DPH rather than that of TMA-DPH, it is not unreasonable to suppose it affects membranes at a deeper location. Furthermore, it interacts strongly with membranes containing BMP, a lipid found in late endosome membranes [161], therefore it might have a role in the fusion process, along with E. All of these data undoubtedly point to a modulatory binding effect of $DENV2_{C6}$ on membranes, providing important clues to develop strategies to target this interaction.

Of all non-structural proteins, NS2A, NS4A and NS4B are the less characterized, possibly owing to their high hydrophobicity. It has been previously described that NS4A might be involved in the membrane rearrangements necessary for the establishment of the viral replication complex, in the translocation of the NS4B into the ER lumen, in the induction of autophagy which results in cell protection against death, in viral replication due to its co-localization with replication complexes and in IFN antagonism with NS2A and NS4B [245, 263-265, 271]. A recent topology model [264] predicts an initial N-terminal region from residues 1 to 49 that does not interact with membranes, followed by three transmembrane segments from residues 50 to 73, 76 to 89 and 101 to 127, a small loop with the NS4A-2k cleavage site and a 2k fragment that acts as the signal sequence for NS4B translocation. As for NS4B, it appears to play roles in the modulation of NS3's helicase function, it forms a complex with NS3 and NS5 that holds the separated strands apart while the helicase moves along the duplex and it is also involved in the IFN α/β antagonism by blocking the phosphorylation of STAT1 [267, 272, 273, 275, 276]. A recent topology model of NS4B [272] predicts two N-terminal segments from residues 1 to 56 and 56 to 93 that do not traverse membranes but remain associated with it, followed by three transmembrane segments from residues 101 to 129 (pTMD3), 165 to 190 (pTMD4) and from residues 217 to 244 (pTMD5). Monomers of NS4B are bound by the cytosolic loop (residues 129 to 165) between pTMD3 and pTMD4 forming dimers [276]. To understand which regions of both these proteins interact and modulate lipid membranes, a biophysical study was conducted

much like in P1, using peptide libraries derived from both NS4A and NS4B (Figure 2, P3) and membrane models of different lipid compositions. At first, a bidimensional representation of hydrophobicity and interfaciality of every residue was produced (Figure 1 and Table 1, P3) to detect possible transmembrane domains, membrane-interacting or protein-protein interaction regions. In NS4A and in accordance with previous data, three hydrophobic segments encompassing the full horizontal length and with over 15 amino acids (characteristics of a putative transmembrane domain) were found, 4A1 from residues 51 to 72, 4A2 from residues 78 to 98 and 4A3 from residues 103 to 120. A similar result was found for fragment 2k (from residues 128 o 150 of protein NS4A). In the case of NS4B, the distinction between transmembrane domains and membrane-interacting domains is murky, although nine hydrophobic patches can be resolved, 4B1 from residues 35 to 52, 4B2 from residues 60 to 78, 4B3 from residues 89 to 100, 4B4 from residues 103 to 122, 4B5 from residues 137 to 155, 4B6 from residues 168 to 188, 4B7 from residues 190 to 205, 4B8 from residues 212 to 225 and 4B9 from residues 229 to 240. When assessing membrane rupture on several membranes (Figures 3 and 4, P3), two broad segments from residues 52 to 90 (4AL1) and from residues 90 to 125 (4AL2) elicited noteworthy leakage, surpassing 60 % in some cases. These two bands match with 4A1-3 hydrophobic patches. Interestingly the 2k fragment did not induce significant membrane leakage to any of the ER-derived membranes, suggesting it might not interact strongly with these membranes, essential in the viral cycle during the replication phase. As for NS4B, four different leakage inducing regions were detected, 4BL1 from residues 50 to 80 (roughly coincident with 4B2), 4BL2 from residues 94 to 127 (coincident with 4B4), 4BL3 from residues 163 to 190 (coincident with 4B6) and 4BL4 (coincident with both 4B8 and 4B9). The influence of these peptides in the thermotropic behaviour of lipids and the depth of interaction were assessed by measuring the steady-state fluorescence anisotropy of DPH inserted into membranes. For NS4A, an initial 4AR1 region from residues 1 to 23 changed the T_m temperature of DMPC, a second broad region 4AR2 from 63 to 126 affected both the T_m and the post-transition anisotropy of DPH and the 2k fragment region from residues 128 to 150 affected the post-transition anisotropy. In the case of NS4B five regions were discerned, 4BR1 including part of the 2k fragment and from residues 1 to 10 of NS4B affected both the steady state anisotropy of DPH and the T_m of DMPC, 4BR2 from residues 28 to 45 barely affected the anisotropy of the probe, 4BR3 from residues 64 to 136 induced changes to both the anisotropy and T_m, 4BR4 from residues 159 to

176 and 4BR5 from residues 194 to 217 elicited anisotropy changes and 4BR6 from residues 236 to 248 increased T_m by 3 ºC. Only NS4A's peptide 18 (from residues 98 to 114) affected the thermotropic behaviour of DEPE, decreasing its L_α to H_{II} phase transition by 5 ºC. Considering the strong line of evidence provided by literature, theoretical predictions and experimental observations, several of these regions might be directly involved in some of their respective protein's functions. Starting with NS4A, its region from residues 50 to 73, described as a possible transmembrane segment in literature, elicited significant leakage to all studied membranes (4AL1), had high hydrophobicity (4A1) and affected the steady-state fluorescence anisotropy of DMPC-inserted DPH (4AR2), making it a strong candidate to take part in membrane interaction and modulation during the viral cycle. The region between residues 63 to 126, described in literature as the putative C-terminal transmembrane domains of NS4A, had high positive hydrophobicity (4A2-3), elicited significant leakage (4AL1-2), affected the anisotropy of DMPC-inserted DPH (4AR2) and a section of it (from residues 98 to 114) affected the L_α to H_{II} phase transition of DEPE, suggesting it might be involved in modulation of membrane structure, essential for the establishment of viral replication complexes. Interestingly, the 2k fragment had a high hydrophobicity and affected the anisotropy of DMPC-inserted DPH yet did not induce leakage in ER membranes, a clear selective membrane interaction that would point to a conformational change during the viral replication. The degree of consistency between literature, theoretical and experimental data is also astonishing for NS4B. Segment pTMD2 from literature matches a leakage-inducing region (4BL1) with high hydrophobicity (4B2) and membrane thermal modulating capabilities (4BR3), segments pTMD3 from residues 101 to 129, pTMD4 from residues 165 to 190 and pTMD5 from residues 217 to 244 also match experimental evidence detected in hydrophobicity patches (4B3-4, 4B6 and 4B8-9 respectively), leakage experiments (4BL2, 4BL3 and 4BL4 respectively) and anisotropy experiments (4BR3, 4BR4 and 4BR6 respectively). Interestingly, the cytosolic loop from residues 129 to 165 was detected as a possible protein-protein interacting region (less than 15 amino acids in length and not encompassing the full horizontal length of the bidimensional representation of hydrophobicity and interfaciality) and did not affect membranes in any experiment designed to detect membrane-active regions.

Of the three structural proteins, prM/M was thought to merely act as an anchoring aid to E and as a cover for the fusion loop to prevent premature membrane fusion. Nevertheless, its interactions with dynein, vATPase and claudin [226-228], suggest it might play a role in the transportation inside the cell and the regulation of the endosomal pH. It also triggers apoptosis in mouse neuroblastoma and human hepatoma cells [224, 225]. This protein is composed of an N-terminal mainly β-strand pr moiety (from residues 1 to 94), followed by a furin cleavage site and a mainly α-helical M protein with a stem region (from residues 112 to 130) and two transmembrane helices (from residues 130 to 148 and 148 to 166) [208]. Both the underlying mechanisms behind these functions and the regions of prM involved still remain elusive. Applying the methodology described above (P1, P3) and a prM peptide library (Table 1 and Figure 1, P4) the putative transmembrane, membrane-interacting and protein-protein interacting regions were highlighted (Figure 2, P4). Two patches with the characteristics of protein-protein interacting regions were defined from residues 66 to 80 (in the pr moiety) and 122 to 131 (in the M stem region) and two patches characteristic of membrane-interacting domains from residues 133 to 144 and 152 to 162 (coincident with the H1 and H2 transmembrane domains of M [208]) were found. From membrane leakage experiments (Figure 3, P4) two different regions were pinpointed encompassing residues 20 through 50 and 124 through 164. From differential scanning calorimetry experiments with DMPC and DMPG (Figure 4, P4) some peptides affected (although barely) the main transition temperature of DMPC but the most significant effect was seen on DMPG membranes. Peptides 1 (residues 1 to 16), 8 (residues 48 to 64), 11 (residues 71 to 88) and 16 through 21 (residues 108 164) induced the formation of mixed phases around the main transition, enriched and impoverished in peptide. Furthermore, peptides 16 and 17 (residues 108 to 133) completely abolished the pre-transition (L_β' to L_α). The effect of these peptides on the structural and thermotropic properties of DMPC and DMPG membranes were also assessed (Figure S1 and Figures S2 and 5 respectively). The most significant effect exerted on all membranes was an increase in the post-transition anisotropy of DPH induced by peptides 4-5 (residues 22 to 44) and peptides 18 to 21 (residues 124 to 164), with an emphasis on the latter's effect. This suggests a more superficial interaction of peptides 4 and 5 with the membrane and a deeper one between peptides 18-21 and the membrane. Taken all together, these results suggest that prM is composed of seven regions with membrane-

interacting capabilities. Region 1 from residues 20 to 50 had significant hydrophobicity (Figure 3 H, P4), which along with superimposed high interfaciality values (Figure 3 G, P4), rupture induction (Figure 3 F) and a mild effect on the steady state anisotropy of DPH points to an interaction with the membrane, albeit at a superficial location. Region 2 from residues 50 to 80 would be characterized by low leakage values, moderate to high hydrophobicity/interfaciality and, interestingly, moderate modulation of the thermotropic behaviour of lipids, possibly owing to its hydrophobicity. This region could be considered a protein-protein interacting domain. Region 3 from residues 95 to 115 would be characterized by low leakage and interfacial/hydrophobicity values and no effect on the thermotropic behaviour of lipids what would render it a weak protein-protein interacting region. Region 4 (encompassing the region between residues 120 to 130), coincident with the stem region of M protein, would be characterized by high leakage, high hydrophobicity and an induction of mixed phase formation in assayed membrane models, suggesting it would be a pre-transmembrane interacting domain. The last regions (5 and 6 from Figure 3, P4) would encompass the two transmembrane domains of M and, as shown in these results, they induce rupture of all assayed membranes, display high hydrophobicity/interfaciality values, drastically increase the post-transition steady state anisotropy of DPH and also induce the formation of lipid phases with varying peptide content. These regions probably interact with membranes and modulate their structure.

NS2A, a highly hydrophobic small protein has a handful of known functions. It co-localizes with dsRNA and the viral replication complex, suggesting a possible role in viral replication, it is required in IFN α/β antagonism and it is found in ER membranes [166, 262, 263]. A recent topology model [260] proposes an N-terminal segment from residues 1 to 31 that does not interact with membranes followed by a membrane-interacting domain from residues 32 to 68, two transmembrane segments from residues 69 to 119, a non-transmembrane segment from residues 120 to 142 and three C-terminal transmembrane domains from residues 143 to 209. Due to its hydrophobicity and a multitude of unanswered questions regarding its functionality, we sought to apply the methodology used in other studies (P1, P3 and P4) to highlight possible transmembrane segments, membrane-interacting domains and protein-protein interacting regions. (Figure 1, P5). From this first study, ten different regions were identified as hydrophobic patches: region a from residues 6 to 19, region b from residues 30 to 54,

region c from residues 55 to 62, region d from residues 70 to 83, region e from residues 83 to 93, region f from residues 101 to 115, region g from residues 124 to 136, region h from residues 145 to 164, region i from residues 165 to 182 and region j from residues 192 to 211. Each region from the described topological model has their equivalent in this list: the N-terminal region that would not interact with membranes is coincident with region a, the first membrane interacting domain with region b, the first transmembrane segment with regions d and e, the second transmembrane segment with region f, the second membrane interacting domain with g and the three C-terminal transmembrane domains with the last three regions h, i and j. Two regions elicited membrane leakage (Figure 2, P5) in all assayed membrane compositions, one from residues 25 to 41 and another broad region from residues 103 to 183. Two noteworthy observations require further description: the first transmembrane region from residues 69 to 118 had little to no effect on membrane rupture, possibly attributable to insertion without rupture and peptide 5 (residues 25 to 41) induced a composition-dependent rupture of membranes, ranging from 5% in zwitterionic membranes to 45% in liver membranes. This same region affected the thermotropic behaviour of both DMPC and DMPG membranes, measured by a decrease in cooperativity, variation of T_m and modification of the steady-state fluorescence anisotropy of DPH. Taking into account these results, peptide dens25, coincident with residues 30 to 55 of NS2A, matching both the hydrophobic region b and peptide 5, was subjected to a more thorough biophysical characterization. The lack of tryptophan residues in dens25's sequence required the indirect assessment of membrane binding using FPE as commented previously in P2. This peptide binds strongly to negative membranes yet not so intensely to zwitterionic membranes (Figure 3 A, P5). This charge dependence is supported by the linear relationship between FPE fluorescence intensity upon peptide addition and molar fraction of EPG in membranes (inset of Figure 3 A, P5). These data adjusted to a hyperbolic model with unitary Hill coefficient, suggesting a monomeric interaction. Its dose-dependent effect on membrane rupture was readily evident and the addition of Chol to EPC and EPC/ESM seemingly reduces the leakage induced by dens25 (from 68 and 71% to 53 and 56 % respectively) (Figure 3 B, P5). Peptide dens25 affects the thermotropic behaviour of negatively charged DMPG in a charge dependent manner (Figure 4, P5), being the effect extension inversely proportional to the ionic strength of the buffer. As seen by differential scanning calorimetry (Figure 5, P5), dens25 affected the transition of all negative lipids at a lower salt concentration (25 mM NaCl). In

DMPG and DMPS, dens25 decreases the cooperativity of the main lipid phase transition and induced the formation of mixed phases represented by overlapping bands in the thermograms. The main transition of BMP at 41 ºC decreases to 29 ºC in the presence of this peptide at low salt concentrations (a dramatic shift of 12 ºC) and if three peaks were observed on the pure lipid thermogram, only two were visible upon dens25 addition. These effects were minimized at a higher salt concentration as seen in all membranes, suggesting an electrostatic peptide-lipid interaction. Even so, at high salt concentrations, dens25 still affected the thermotropic behaviour of DMPG (Figures 5 C-E). FTIR experiments (Figure 6, P5) confirmed the electrostatic nature of dens25's interaction with membranes. Analysing the maxima of the C=O stretching band of DMPC and DMPG in the absence or presence of dens25 at low (25 mM) and high (100 mM) NaCl concentrations, pure lipids at high salt concentrations present both their L_{β}' at P_{β}' and P_{β}' to L_{α} characteristic transitions (Figures 6 A and 6B) while in the presence of peptide, the maxima of DMPG's C=O band were higher than those of the pure lipid. This is a result of an increase of the 1743 cm^{-1} (those C=O that do not partake in hydrogen-bonds) band with respect to the 1727 cm^{-1} band (those C=O that form hydrogen bonds). In accordance with previous data, at low salt concentrations dens25 affects the thermotropic behaviour of lipids (clearly seen in Figure 6 C, P5), where dens25 completely abolishes the main transition of DMPG and decreases the cooperativity of DMPC's main transition. It is interesting to note that dens25 in the presence of DMPC and DMPC at high NaCl concentration has a similar secondary structure with a predominance of β-aggregated structures. When the salt concentration was reduced, dens25's secondary structure changed from mainly aggregated structures to mainly α-helical and unordered ones in DMPG. In summary, peptide dens25, derived from a previously highlighted NS2A's highly hydrophobic region (which also affected membranes), had a dramatic effect on the thermotropic behaviour and structural integrity of negatively charged membranes with a lower effect on zwitterionic membranes. Adding to that, because this effect is inversely proportional to the ionic strength of the buffers, dens25's interaction with membranes should be electrostatic in nature. This region presented high interfaciality values what would suggest that, depending on the membrane composition, this region could alternate between membrane bound and membrane-free conformations, an important phenomenon in membrane modulation.

CHAPTER 6. RESUMEN/ABSTRACT

CHAPTER 6. RESUMEN/ABSTRACT

RESUMEN

El virus del Dengue perteneciente a la familia *Flaviviridae,* es el arbovírus (transmitido por un artrópodo, en este caso mosquitos del género *Aedes*) causante de las mayores tasas de mortalidad y morbilidad en todo el Mundo, con aproximadamente 400 millones de infecciones estimadas anualmente en los trópicos y sub-trópicos [109]. La infección por este virus se caracteriza por cuatro cuadros clínicos distintos, con creciente grado de severidad: infección sin síntomas, fiebre del Dengue (DF en inglés), fiebre hemorrágica del Dengue (DHF en inglés) y sindroma de choque del Dengue (DSS en inglés). A pesar de su alta prevalencia, en la actualidad no existen ni vacunas ni fármacos antivirales para contrarrestar esta enfermedad, siendo el control de las poblaciones de vectores la única medida utilizada a gran escala [55, 107, 117]. Este virus se clasifica en cuatro serotipos distintos que comparten un 69-78% de identidad a nivel de secuencia primaria [356] y se compone de una nucleocapsida, formada por múltiples copias de la proteína C asociada al genoma vírico, envuelta por una capa lipídica derivada del huésped donde se encuentran 180 copias de las proteínas M y E asociadas en heterodimeros. El genoma vírico es una molécula de ARN de cadena sencilla y polaridad positiva y tiene aproximadamente 11 kb con un único marco abierto de lectura (ORF en inglés) que codifica una única poli proteína que, tras su procesamiento por proteasas virales y del huésped, da lugar a tres proteínas estructurales C, prM y E y siete proteínas no-estructurales NS1, NS2A, NS2B, NS3, NS4A, NS4B, NS5 [79, 119]. Este virus entra en las células por endocitosis mediada por receptores y el pH ácido en el interior del endosoma induce un cambio conformacional que hace que el péptido de fusión, localizado en la proteína E (una proteína de fusión de clase II) se acerque a la membrana del endosoma y se dé el proceso de fusión con consecuente liberación de la nucleocapsida en el citoplasma [365]. Los procesos de replicación del genoma vírico y ensamblaje de las partículas virales ocurren en membranas derivadas del retículo endoplásmico, criadas y reorganizadas por proteínas del virus. Tras su ensamblaje, las partículas víricas inmaduras inician su tránsito por el complejo trans-Golgi donde una disminución del pH intravesicular promueve la acción de la enzima furina que rompe el enlace peptídico entre el péptido pr (cubre el péptido de fusión y

previene una fusión prematura antes de la salida del virus) y la proteína M en la proteína prM. Tras exocitosis, la liberación del péptido pr representa el paso final de maduración. Tanto en procesos de entrada y salida del virus como en los pasos de replicación y ensamblaje, todas las proteínas del virus necesitan y utilizan membranas lipídicas para ejecutar sus funciones, ya que inducen cambios estructurales en aquellas para formar sus complejos de replicación, para llevar a cabo el proceso de fusión y asegurar ensamblaje viral. Los efectos de las proteínas estructurales y no estructurales del virus del Dengue en membranas son conocidos, pero los mecanismos por los cuales estas alteraciones se producen no están definidos, aún menos las proteínas implicadas y las regiones membrano-activas de estas proteínas son casi desconocidas. Como tal, nos propusimos definir las regiones membrano-activas de las proteínas de este virus, tanto las estructurales (C, prM y E) como las no-estructurales de cuyas funciones se sabe muy poco.

La proteína C forma dímeros formados mayoritariamente por hélices α, en los cuales se encuentran dos regiones con características interesantes a nivel de interacciones moleculares, una región altamente hidrofóbica que sugiere una interacción con membranas [215] y otra región con una gran concentración de carga positiva que podría interaccionar con el genoma vírico [219]. Se sabe que esta proteína es responsable de la encapsidación especifica del genoma [79, 219] y que se acumula en vesículas lipídicas derivadas del retículo endoplásmico [218]. En esta proteína hemos identificado dos regiones membrano-activas correspondientes a la región altamente hidrofóbica de los residuos 39 al 56 y a la secuencia señal en la región C-terminal. La proteína E es una proteína de fusión de clase II, cuya región N-terminal (residuos 1 al 395) se divide en tres dominios formados por estructuras beta [54, 119], dominio I N-terminal, flanqueado en un lado por el dominio II que contiene el péptido de fusión (residuos 98 a 112) y por otro el dominio III que es la región de anclaje a membrana y donde se encuentran los sitios de unión a receptores. La región C-terminal de esta proteína estaría formada por una región tallo y dos dominios transmembrana con estructura helicoidal. Estas regiones contribuyen en los cambios conformacionales necesarios en el proceso de fusión y las regiones transmembrana estarían involucradas en interacciones proteína-proteína o lípido-proteína [75, 164, 285, 360]. Encontramos cinco regiones membrano-activas en esta proteína que coinciden con el péptido de fusión (residuos 88 a 122), una región rica en prolina, de interacción con proteínas (residuos 198 a 221), otra región

coincidente con una zona hidrofóbica previamente descrita (residuos 270 a 309), una región correspondiente una parte de la zona tallo (residuos 406 a 422) y finalmente una región de los residuos 428-479 que contiene parte de la región tallo y uno de los dos dominios transmembrana descritos. Estos resultados definen las regiones de esta proteína que interaccionan con membranas y demuestran la importancia de las mismas en las interacciones en las cuales la proteína nativa tiene un papel activo.

Un péptido procedente de la proteína C de los residuos 39 al 56, $DENV2_{C6}$, localizado en una región altamente hidrofóbica del dímero de aquella proteína, el cual es necesario en los procesos de maduración vírica, unión a vesículas lipídicas y ensamblaje viral [215, 218] induce efectos significativos en membranas modelo. Se une con alta afinidad a variadas membranas modelo, sin una distinción clara entre membranas de diferente composición lipídica e induce una rotura casi completa de membranas lipídicas de variada composición. También es capaz de modificar el comportamiento termo trópico de variadas biomembranas, induciendo la formación de fases con diferente distribución peptídica y afectando la anisotropía de fluorescencia de una sonda localizada en el interior de la bicapa lipídica. Este péptido afecta extensivamente a membranas con BMP, un lípido encontrado principalmente en endosomas [161], lo que indicaría una posible función en la fusión del virus con membranas durante la infección. Además, como se puede observar en los experimentos de espectroscopia infrarroja (Figura 5, P2), la estructura secundaria de este péptido sufre cambios en presencia de membranas, especialmente en membranas de DMPC, donde su estructura cambia significativamente en comparación con el péptido en disolución.

Las proteínas NS4A y NS4B son proteínas altamente hidrofóbicas involucradas en diversas funciones en el ciclo viral. Se sabe que la proteína NS4A modula la ATPasa de NS3 [265], se localiza en el complejo de replicación con otras proteínas estructurales y que se encuentra en membranas del retículo endoplásmico pudiendo modular la curvatura de membranas [264, 267]. Además, esta proteína parece ser importante en la inhibición de la respuesta por interferón [263], aparte de contribuir para reducir la apoptosis celular a través de la activación de autofagia, alargando la vida celular [271]. Un modelo topológico recientemente descrito define dos segmentos transmembrana separados por un segmento que estaría en contacto con la membrana y un fragmento 2k en su región C-terminal, fundamental para la translocación de la proteína NS4B hacia el lumen del retículo endoplásmico [264]. Pudimos definir dos regiones capaces de

afectar a la estructura e integridad de membranas lipídicas de los residuos 52 al 90 y de los residuos 90 al 125, coincidente con los segmentos transmembrana definidos en el modelo topológico referido arriba. El segmento 2k en la zona C-terminal de esta proteína parece no afectar a la integridad de membranas derivadas del retículo endoplásmico lo que sugiere un posible cambio conformacional dependiente de la composición lipídica, un fenómeno muy común en procesos de modulación de membranas de muchos ciclos virales. En cuanto a la proteína NS4B, esta parece ser la proteína de mayor importancia en la inhibición de la respuesta por interferón de las células infectadas, inhibiendo la fosforilación de STAT1 [273]. Su co-localización con ARN de cadena doble y las proteínas NS3 y NS5 sugiere que podrá participar en la replicación viral [275]. Además, esta proteína forma dímeros a través de una región denominada bucle citosólico. Esto demuestra su papel doble en interacciones proteína-lípido y lípido-lípido [276]. En su modelo topológico más reciente, esta proteína se compone de al menos tres regiones transmembrana precedidas por dos dominios que podrían interaccionar con membranas [272]. Definimos cuatro segmentos membrano-activos en esta proteína, de los residuos 50 al 80, 94 al 127, 163 al 190 y 210 al 240 y al menos uno de posible interacción con membranas coincidente con la región de dimerización. De estos resultados se puede concluir que esta proteína participa activamente en la modulación y reorganización de membranas así como en la interacción con otras proteínas.

La proteína prM se compone de dos regiones distintas, el péptido pr de los residuos 1 al 91 y la proteína M de los residuos 91 al 166, formada a su vez por una región tallo de los residuos 112 al 132, seguida de dos regiones transmembrana [125, 208, 209, 223]. A parte su función de prevención de una fusión prematura, protegiendo al péptido de fusión, esta proteína parece jugar un papel en el transporte intracelular y en la regulación de apoptosis [224-228]. Se descubrió recientemente que esta proteína forma oligomeros en membranas derivadas del retículo endoplásmico al mismo tiempo que reorganiza estas membranas [102]. Aplicando la metodología supra citada pudimos definir al menos una región de interacción con proteínas en la región del péptido pr, que sería la región de contacto con la proteína E, y una región no-transmembrana de interacción con membranas. En la proteína M se detectaron las regiones transmembrana de esta proteína y la región tallo que parece modular el comportamiento termo trópico

de las membranas estudiadas. Estos resultados parecen confirmar la interacción de esta proteína con membranas y definen las regiones involucradas en esa función.

La proteína NS2A es la proteína menos estudiada y caracterizada de todas las proteínas de este virus pero los estudios realizados hasta el momento parecen indicar un papel muy importante de esta proteína en todo el ciclo. Se integra en el complejo de replicación [261], es necesaria para el ensamblaje viral, ya que mutaciones en esta reducen significativamente la carga viral [260], es necesaria para el procesamiento de la proteína NS1 [260] y, en concierto con las proteínas NS4A y NS4B, inhibe la respuesta por interferón [263]. Es una proteína altamente hidrofóbica y está formada por al menos cinco regiones transmembrana y dos regiones de interacción con membranas [260]. Su localización en membranas y fuerte carácter hidrofóbico sugieren que esta proteína es capaz de reorganizar membranas lipídicas y con eso contribuir a la formación de los complejos de replicación viral. Definimos dos regiones de interacción con membranas en esta proteína de sus residuos 25 al 41 y de los residuos 103 al 183. La primera región coincide con una de las regiones de interacción con membranas sugerida en el modelo topológico y su efecto parece depender de la composición lipídica. Esta región fue estudiada en mayor detalle y comprobamos que su efecto en membranas es dependiente tanto de la composición lipídica como de la fuerza iónica de su entorno. El componente electrostático de esta interacción es predominante y su efecto selectivo nos permite sugerir que esta región podría adoptar diferentes conformaciones en membranas y alternar entre una orientación en contacto directo o no con aquellas y así afectar a la conformación y función de la proteína nativa.

Estos resultados motivaron la elaboración de esta tesis doctoral, la publicación de tres artículos científicos, el envío de otros dos para su publicación y variadas comunicaciones a congresos nacionales e internacionales.

ABSTRACT

Dengue virus, part of the *Flaviviridae* family is the most prevalent virus in the human population and is responsible for the highest morbidity and mortality rates worldwide, with about 400 million infections estimated yearly in tropics and subtropics [109]. People infected by DENV present symptomatology with varying severity degrees: asymptomatic, Dengue fever (DF), Dengue haemorrhagic fever (DHF) and Dengue Shock syndrome (DSS). Despite its prevalence, there are currently neither effective antivirals nor antiviral drugs against DENV, being the sole eradication strategies based on the control of mosquito populations [55, 107, 117]. This virus is classified into three distinct serotypes with 69-78 % primary sequence identity [356] and it is composed of a nucleocapsid, formed by several molecules of protein C bound to the viral RNA genome, enclosed by a host derived lipid bilayer where 180 copies of proteins M and E are embedded as heterodimers. Its positive single-stranded RNA genome of some 11 kb possesses a single ORF that encodes a single polyprotein of about 3000 amino acids. After appropriate processing by viral and host proteases, this polyprotein gives rise to three structural proteins C, prM and E and seven non-structural proteins NS1, NS2A, NS2B, NS3, NS4A, NS4B and NS5 [79, 119]. DENV enters cells by receptor mediated endocytosis and the decrease in pH inside endosomes triggers a conformational change that results in the insertion of the fusion peptide (located in protein E, a class II fusion protein) into the endosomal membrane, resulting in the release of the nucleocapsid into the cytoplasm [365]. Viral replication and assembly processes occur in ER-derived membranes, sequestered and reorganized by the virus. Following its assembly, the immature virions start their transit through the trans-Golgi network, where a decrease in pH triggers the furin cleavage of the peptide bond between the pr peptide and the M protein. When the virion is exocyted, the pr peptide is released and the viral particle is rendered fully mature. Both in entry and exit steps, all viral proteins require and use membranes to exert their functions, e.g. by modulating their structure to form replication complexes, to execute their fusion process or even to carry out viral assembly. The effects DENV proteins have on membranes are known, yet the mechanisms by which those occur are elusive, the proteins involved are even less known and the exact regions in those proteins that interact with membranes are virtually

unknown. Therefore, we sought to highlight the membrane-active regions of DENV's structural proteins and the lesser known and most hydrophobic non-structural proteins.

Protein C forms mainly α-helical dimers in solutions, where two regions possess interesting biophysical characteristics: one is highly hydrophobic, suggesting possible membrane interactions [215] while the other has a high positive charge concentration, what would point to a possible interaction with the negatively charged viral RNA genome [219]. It is known that this protein is responsible for the specific encapsidation of the genome [79, 219] and that it accumulates around ER-derived lipid droplets [218]. We have identified two membrane-active regions in this protein, corresponding to the highly hydrophobic region from residues 39 to 56 and its C-terminal signal sequence. Protein E is a class II fusion protein with its N-terminal region (residues 1 to 395) divided into three domains formed by beta structures [54, 119], an N-terminal domain I, flanked on one side by domain II (where the fusion peptide is located between residues 98 to 112) and on the other by domain III, the putative location of the receptor binding sites. Its C-terminal region would be composed of a stem region followed by two helical transmembrane domains. These regions contribute to the conformational changes required for membrane fusion and the transmembrane regions would be involved in protein-lipid and lipid-lipid interactions [75, 164, 285, 360]. We have found at least five membrane-active regions in this protein, coincident with the fusion peptide (residues 88 to 122), a proline-rich region involved in protein-protein interaction (residues 198 to 221), another previously described hydrophobic region (residues 270 to 309), a region coincident with the stem region (residues 406 to 422) and finally a region from residues 428 to 479 that contains part of the stem region and one of the previously described transmembrane domains. These results define the membrane interacting regions of these proteins and corroborate the importance of these in the interactions of native proteins.

A peptide derived from protein C from residues 39 to 56, $DENV2_{C6}$, located in a highly hydrophobic region in the C protein dimer, required for appropriate viral maturation, vesicle binding and viral assembly [215, 218] induces significant effects to membrane model systems. It binds with high affinity to several membrane models and ruptures them with no clear distinction between membranes with different composition, It can also modulate the thermotropic behaviour of membranes, inducing the formation of lipid phases with different peptide concentrations and altering the steady-state fluorescence anisotropy of probes inserted into the lipid palisade. This peptide

significantly affects BMP (a lipid found predominantly in endosomes [161]) containing membranes, what suggests a possible function in viral fusion during infection. Moreover, FTIR experiments have shown that this peptide has different secondary structure in solution and in DMPC membranes, meaning that it is a two way protein-lipid interaction.

Proteins NS4A and NS4B are highly hydrophobic proteins involved in several functions in the viral cycle. It is known that NS4A modulates the ATPase function of NS3 [265], co-localizes with other viral proteins in the replication complex and it can be found in ER membranes, modulating its curvature [264, 267]. Furthermore, this protein seems to play a role in the interferon response [263], inhibition of apoptosis through autophagy induction what increases the cellular lifespan [271]. A recently described topology model suggests two transmembrane segments separated by a membrane interacting domain and its C-terminal region is a 2k fragment, responsible for the translocation of NS4B into the ER lumen [264]. We could delineate two regions that affect the structure and integrity of the lipid membrane from residues 52 to 90 and 90 to 125, matching the transmembrane segments of the topological model. The 2k fragment does not seem to affect ER membranes, what would suggest conformational changes dependent on lipid composition, a fairly common process of membrane modulation in viral cycles. As for protein NS4B, it seems to be the most important protein in interferon response inhibition by inhibiting the STAT1 phosphorylation [273]. Its co-localization with dsRNA and proteins NS3 and NS5 suggests it might play a role in the viral replication [275]. Adding to that, this protein forms dimers through a cytosolic loop. These findings provide a clear indication of its hybrid lipid-lipid and protein-lipid interacting capabilities [276]. In its most recent topology model, this protein is composed of at least three transmembrane domains preceded by two membrane-interacting domains [272]. We highlighted four membrane-active segments in this protein from residues 50 to 80, 94 to 127, 163 to 190 and 210 to 240 and at least one segment coincident with the dimerization region that could interact with membranes. We conclude that this protein actively modulates and reorganizes membranes and also possibly interacts with other proteins.

The prM protein is composed of two different regions, peptide pr from residues 1 to 91 and the M protein from residues 91 to 166, that is in turn composed of a stem region from residues 112 to 132 followed by two transmembrane segments [125, 208, 209, 223]. Apart from tis fusion preventive function, by protecting the fusion peptide, this protein plays a role in intracellular transport and apoptosis regulation [224-228]. It has been recently found that this protein forms oligomers in ER-derived membranes while reorganizing them [102]. We could determine at least on protein interacting region in the pr peptide that would match the region of contact with protein E and a membrane interacting region in the same moiety. As for protein M, the transmembrane segments were detected and the stem region modulates the thermotropic behaviour of membranes. These results provide the confirmation that this protein interacts with membranes and define the regions involved in this phenomenon

Protein NS2A is the less characterized of all DENV proteins yet the literature points to its roles in important processes of the viral cycle. It is part of the replication complex [261], it is required in the viral assembly, shown by the fact that mutations in this protein significantly reduce the viral load [260], it is needed for proper NS1 processing [260] and , in concert with NS4A and NS4B, inhibits the interferon response [263]. It is a highly hydrophobic protein composed of at least five transmembrane and two membrane interacting regions [260]. Its location in membranes and hydrophobic affinity suggest that this protein might also reorganize membranes thus aiding the formation of the replication complexes. Using the above stated methodology, we defined at least two membrane interacting domains from residues 25 to 41 and 103 to 183. The first region matches one of the membrane interacting regions defined in the topology model and its effect is dependent on the lipid composition. This region was characterized in detail and its interaction with membranes depends not only on the lipid composition but also on the ionic strength of its environment. Its interaction with membranes is mainly electrostatic and its selective effect hints at a possible conformational change switching between membrane bound and membrane-free states, thus modulating membrane structure.

These results yielded three published scientific papers, two already sent for their publication, several congress abstracts and this PhD. Thesis.

CHAPTER 7. CONCLUSIONES/CONCLUSIONS

CHAPTER 7. CONCLUSIONES/CONCLUSIONS

CONCLUSIONES

De todos los resultados presentados con anterioridad se pueden extraer algunas conclusiones:

1. Utilizando un conjunto de técnicas biofísicas pudimos identificar las regiones membrano-activas de todas las proteínas estructurales del virus del Dengue (C, prM y E) y de las proteínas no-estructurales menos caracterizadas NS2A, NS4A y NS4B.

2. Se definieron 5 regiones en las proteínas C (1) y E (4) coincidentes con regiones fundamentales para el ciclo viral en procesos de fusión y ensamblaje vírico.

3. Una de esas regiones, de los residuos 39 al 56 de la proteína C, descrito anteriormente como una posible región de interacción con membranas, se une fuertemente a membranas con preferencia por membranas con lípidos aniónicos, provoca la rotura completa de todo tipo de membranas y modula el comportamiento termotrópico de lípidos. Se sugiere que esta región está involucrada en procesos de fusión de membranas conjuntamente con la proteína E.

4. Encontramos al menos cinco regiones de interacción con membranas en la proteína NS4A, tres de las cuales se corresponden con segmentos transmembrana previamente descritos y dos interaccionan con la membrana a nivel superficial. Curiosamente, el fragmento 2k no fue capaz de producir rotura de membranas derivadas del retículo endoplásmico (ER), lo que nos sugiere que este fragmento interacciona de manera menos fuerte con membranas o que se inserta en ellas en el complejo de replicación.

5. Se encontraron tanto regiones transmembrana como regiones de interacción con membrana en la proteína NS4B, lo que sugiere un papel de esta proteína tanto en reorganización de membranas como en interacciones proteína-lípido.

6. Aparte de las regiones transmembrana, en la proteína precursora de membrana (prM) encontramos una región de interacción con proteínas (posiblemente la región de interacción con la proteína E), un segmento de transmembrana que coincide con la región tallo de esta proteína y que por su marcado efecto en membranas podría alternar entre una conformación en contacto con la membrana o sin interaccionar con esta, modulando su comportamiento.

7. Identificamos un segmento relativamente largo en NS2A con capacidad de romper membranas de todo tipo así como una región de interacción con membranas con efectos dependientes de composición.

8. Una de las regiones encontradas en la proteína NS2A, de los residuos 30 al 55 y denominada dens25, se une con alta afinidad a y modula el comportamiento termotrópico de membranas con lípidos aniónicos. Este efecto tiene un fuerte componente de tipo electrostático y se ve reducido en presencia de Chol. Proponemos que esta región sufre cambios conformacionales dependientes de la proporción de lípidos negativos en la membrana, pudiendo interaccionar de forma selectiva en varios pasos del ciclo viral.

From all results obtained in this thesis, some conclusions can be drawn:

1. Relying on an array of several biophysical techniques we highlighted different membrane-active regions in all structural proteins of DENV (C, prM and E) and its less characterized non-structural proteins NS2A, NS4A and NS4B.

2. At least five highly hydrophobic regions between proteins C (one) and E (four) could induce the rupture of membrane model systems to a large extension and coincided with regions deemed essential for some of those proteins' functions.

3. One of those highly hydrophobic regions, from residues 39 to 56 of protein C, matching a putative membrane interacting domain, binds strongly to membranes, with a slight preference for membranes with anionic lipids, induces a virtually complete membrane rupture independent of composition and modulates thermotropic lipid phase behaviour. We suggest this region might be involved directly in the membrane fusion process with the E protein.

4. We have found at least five membrane-active regions in NS4A, three of which were the transmembrane segments and other two in close association with it. The fragment 2k did not induce rupture of ER-derived membranes, suggesting that it either does not interact strongly with said membranes during the viral cycle or it is inserted into them in the replication complex.

5. Both membrane traversing regions and membrane interacting regions were defined in NS4B, suggesting that this protein is involved in membrane rearrangements, protein-lipid and protein-protein interactions.

6. Other than the two transmembrane regions, the prM protein presented one protein-interacting region (possibly the region of interaction with E), a pre-transmembrane segment, matching the stem region, with significant effects on membranes that could switch between membrane bound and unbound conformations, altering the membrane structure and polymorphism.

7. We have identified a broad region in NS2A with membrane rupture capabilities independent of membrane composition and a membrane-interacting region with composition dependent effects.

8. A region encompassing residues 30 to 55 of NS2A called dens25, with composition dependent effects on membranes, binds strongly to membranes with anionic lipids and exerts modifications to the membrane structure of anionic membranes with a large electrostatic contribution, effect reduced in the presence of Chol. We propose this region undergoes conformational changes dependent on the local concentration of anionic lipids that render it membrane active or membrane inactive, contributing to the viral replication.

REFERENCES

1. Doherty, G.J. and H.T. McMahon, *Mediation, modulation, and consequences of membrane-cytoskeleton interactions.* Annu Rev Biophys, 2008. **37**: p. 65-95.
2. Luckey, M., *Membrane Structural Biology with biochemical and biophysical foundations* First ed. 2008, New York: Cambridge University Press. 332.
3. Fricke, H., *The electrical capacity of suspensions with special reference to blood.* Journal of General Physiology, 1925.
4. Langmuir, I., *The constitution and fundamental properties of solids and liquids. II. Liquids.* Journal of the American Chemical Society, 1917. **39**(9): p. 1848-1906.
5. Adam, N.K., *The properties and molecular structure of thin films of palmitic acid on water. Part I.* Proceedings of the Royal Society: A, 1921. **99**: p. 336-351.
6. Gorter, E., Grendel, F., *On bimolecular layers of lipoids on the chromocytes of the blood.* Journal of Experimental Medicine, 1924: p. 439-443.
7. Danielli, J.F., Davson, H., *A contribution to the theory of permeability of thin films.* Journal of Cellular Physiology, 1935. **5**(4): p. 495-508.
8. Bangham, A.D., Horne, R.W., *Negative staining of phospholipids and their structural modification by surface-active agents as observed in the electron microscope.* Journal of Molecular Biology, 1964. **8**(5): p. 660-668.
9. Singer, S.J. and G.L. Nicolson, *The fluid mosaic model of the structure of cell membranes.* Science, 1972. **175**(4023): p. 720-31.
10. Frye, L.D. and M. Edidin, *The rapid intermixing of cell surface antigens after formation of mouse-human heterokaryons.* J Cell Sci, 1970. **7**(2): p. 319-35.
11. Ohvo-Rekila, H., et al., *Cholesterol interactions with phospholipids in membranes.* Prog Lipid Res, 2002. **41**(1): p. 66-97.
12. Simons, K. and W.L. Vaz, *Model systems, lipid rafts, and cell membranes.* Annu Rev Biophys Biomol Struct, 2004. **33**: p. 269-95.
13. Engelman, D.M., *Membranes are more mosaic than fluid.* Nature, 2005. **438**(7068): p. 578-80.
14. Leventis, P.A. and S. Grinstein, *The distribution and function of phosphatidylserine in cellular membranes.* Annu Rev Biophys, 2010. **39**: p. 407-27.
15. Cox, D.L.N.a.M.M., *Lehninger Principles of Biochemistry*. 4th ed, ed. D.L.N.a.M.M. Cox. 2004: W. H. Freeman.
16. Ramstedt, B. and J.P. Slotte, *Membrane properties of sphingomyelins.* FEBS Lett, 2002. **531**(1): p. 33-7.
17. Brown, D.A. and E. London, *Structure and function of sphingolipid- and cholesterol-rich membrane rafts.* J Biol Chem, 2000. **275**(23): p. 17221-4.
18. Elson, E.L., et al., *Phase separation in biological membranes: integration of theory and experiment.* Annu Rev Biophys, 2010. **39**: p. 207-26.
19. Fahy, E., et al., *A comprehensive classification system for lipids.* J Lipid Res, 2005. **46**(5): p. 839-61.
20. Chen, H.W., *Role of cholesterol metabolism in cell growth.* Fed Proc, 1984. **43**(1): p. 126-30.
21. Villalain, J., *Location of cholesterol in model membranes by magic-angle-sample-spinning NMR.* Eur J Biochem, 1996. **241**(2): p. 586-93.
22. Cronan, J.E., *Bacterial membrane lipids: where do we stand?* Annu Rev Microbiol, 2003. **57**: p. 203-24.
23. Alberts B., J.A., Lewis J., Raff M., Roberts K., Walter P. , *Molecular Biology of the Cell*. 5th ed, ed. G.S. Anderson M. 2008: Garland Science Taylor and Francis Group.

24. Wiener, M.C. and S.H. White, *Structure of a fluid dioleoylphosphatidylcholine bilayer determined by joint refinement of x-ray and neutron diffraction data. II. Distribution and packing of terminal methyl groups.* Biophys J, 1992. **61**(2): p. 428-33.
25. Wiener, M.C. and S.H. White, *Structure of a fluid dioleoylphosphatidylcholine bilayer determined by joint refinement of x-ray and neutron diffraction data. III. Complete structure.* Biophys J, 1992. **61**(2): p. 434-47.
26. Chiu, S.W., et al., *Incorporation of surface tension into molecular dynamics simulation of an interface: a fluid phase lipid bilayer membrane.* Biophys J, 1995. **69**(4): p. 1230-45.
27. White, S.H. and W.C. Wimley, *Hydrophobic interactions of peptides with membrane interfaces.* Biochim Biophys Acta, 1998. **1376**(3): p. 339-52.
28. Siegel, D.P., *Energetics of intermediates in membrane fusion: comparison of stalk and inverted micellar intermediate mechanisms.* Biophys J, 1993. **65**(5): p. 2124-40.
29. Mayer, L.D., M.J. Hope, and P.R. Cullis, *Vesicles of variable sizes produced by a rapid extrusion procedure.* Biochim Biophys Acta, 1986. **858**(1): p. 161-8.
30. Epand, R., *Membrane Lipid Polymorphism*, in *Methods in Membrane Lipids*, D. A., Editor. 2007, Humana Press: Totowa, New Jersey.
31. Israelachvili, J.N., S. Marcelja, and R.G. Horn, *Physical principles of membrane organization.* Q Rev Biophys, 1980. **13**(2): p. 121-200.
32. Luzzati, V., A. Tardieu, and T. Gulik-Krzywicki, *Polymorphism of lipids.* Nature, 1968. **217**(5133): p. 1028-30.
33. Luzzati, V., et al., *Structure of the cubic phases of lipid-water systems.* Nature, 1968. **220**(5166): p. 485-8.
34. Luzzati, V., *Biological significance of lipid polymorphism: the cubic phases.* Curr Opin Struct Biol, 1997. **7**(5): p. 661-8.
35. Brunger, A.T., *Structure and function of SNARE and SNARE-interacting proteins.* Q Rev Biophys, 2005. **38**(1): p. 1-47.
36. Chen, E.H. and E.N. Olson, *Unveiling the mechanisms of cell-cell fusion.* Science, 2005. **308**(5720): p. 369-73.
37. Eckert, D.M. and P.S. Kim, *Mechanisms of viral membrane fusion and its inhibition.* Annu Rev Biochem, 2001. **70**: p. 777-810.
38. Hernandez, L.D., et al., *Virus-cell and cell-cell fusion.* Annu Rev Cell Dev Biol, 1996. **12**: p. 627-61.
39. Primakoff, P. and D.G. Myles, *Cell-cell membrane fusion during mammalian fertilization.* FEBS Lett, 2007. **581**(11): p. 2174-80.
40. Wessels, L. and K. Weninger, *Physical aspects of viral membrane fusion.* ScientificWorldJournal, 2009. **9**: p. 764-80.
41. Burger, K.N., *Greasing membrane fusion and fission machineries.* Traffic, 2000. **1**(8): p. 605-13.
42. Basanez, G., *Membrane fusion: the process and its energy suppliers.* Cell Mol Life Sci, 2002. **59**(9): p. 1478-90.
43. Chernomordik, L.V. and M.M. Kozlov, *Membrane hemifusion: crossing a chasm in two leaps.* Cell, 2005. **123**(3): p. 375-82.
44. Harrison, S.C., *Viral membrane fusion.* Nat Struct Mol Biol, 2008. **15**(7): p. 690-8.
45. Zimmerberg, J. and L.V. Chernomordik, *Membrane fusion.* Adv Drug Deliv Rev, 1999. **38**(3): p. 197-205.
46. Bezrukov, S., *Functional consequences of lipid packing stress.* Current Opinion in Colloid & Interface Science, 2000. **5**(3-4): p. 237-243.
47. Kozlov, M.M., et al., *Stalk mechanism of vesicle fusion. Intermixing of aqueous contents.* Eur Biophys J, 1989. **17**(3): p. 121-9.
48. Kozlovsky, Y. and M.M. Kozlov, *Stalk model of membrane fusion: solution of energy crisis.* Biophys J, 2002. **82**(2): p. 882-95.

49. Kuzmin, P.I., et al., *A quantitative model for membrane fusion based on low-energy intermediates.* Proc Natl Acad Sci U S A, 2001. **98**(13): p. 7235-40.
50. Markin, V.S. and J.P. Albanesi, *Membrane fusion: stalk model revisited.* Biophys J, 2002. **82**(2): p. 693-712.
51. Siegel, D.P., *The modified stalk mechanism of lamellar/inverted phase transitions and its implications for membrane fusion.* Biophys J, 1999. **76**(1 Pt 1): p. 291-313.
52. Chernomordik, L.V., G.B. Melikyan, and Y.A. Chizmadzhev, *Biomembrane fusion: a new concept derived from model studies using two interacting planar lipid bilayers.* Biochim Biophys Acta, 1987. **906**(3): p. 309-52.
53. Zampighi, G.A., et al., *Conical electron tomography of a chemical synapse: vesicles docked to the active zone are hemi-fused.* Biophys J, 2006. **91**(8): p. 2910-8.
54. Bressanelli, S., et al., *Structure of a flavivirus envelope glycoprotein in its low-pH-induced membrane fusion conformation.* EMBO J, 2004. **23**(4): p. 728-38.
55. Halstead, S.B., *Dengue.* Lancet, 2007. **370**(9599): p. 1644-52.
56. Kielian, M., *Class II virus membrane fusion proteins.* Virology, 2006. **344**(1): p. 38-47.
57. Kielian, M. and F.A. Rey, *Virus membrane-fusion proteins: more than one way to make a hairpin.* Nat Rev Microbiol, 2006. **4**(1): p. 67-76.
58. Weissenhorn, W., A. Hinz, and Y. Gaudin, *Virus membrane fusion.* FEBS Lett, 2007. **581**(11): p. 2150-5.
59. Lee, C.J., et al., *Cholesterol effectively blocks entry of flavivirus.* J Virol, 2008. **82**(13): p. 6470-80.
60. Noisakran, S., et al., *Association of dengue virus NS1 protein with lipid rafts.* J Gen Virol, 2008. **89**(Pt 10): p. 2492-500.
61. Garcia Cordero, J., et al., *Caveolin-1 in lipid rafts interacts with dengue virus NS3 during polyprotein processing and replication in HMEC-1 cells.* PLoS One, 2014. **9**(3): p. e90704.
62. Bavari, S., et al., *Lipid raft microdomains: a gateway for compartmentalized trafficking of Ebola and Marburg viruses.* J Exp Med, 2002. **195**(5): p. 593-602.
63. Aman, M.J., et al., *Molecular mechanisms of filovirus cellular trafficking.* Microbes Infect, 2003. **5**(7): p. 639-49.
64. Bender, F.C., et al., *Specific association of glycoprotein B with lipid rafts during herpes simplex virus entry.* J Virol, 2003. **77**(17): p. 9542-52.
65. Chung, C.S., C.Y. Huang, and W. Chang, *Vaccinia virus penetration requires cholesterol and results in specific viral envelope proteins associated with lipid rafts.* J Virol, 2005. **79**(3): p. 1623-34.
66. Thorp, E.B. and T.M. Gallagher, *Requirements for CEACAMs and cholesterol during murine coronavirus cell entry.* J Virol, 2004. **78**(6): p. 2682-92.
67. Yonezawa, A., M. Cavrois, and W.C. Greene, *Studies of ebola virus glycoprotein-mediated entry and fusion by using pseudotyped human immunodeficiency virus type 1 virions: involvement of cytoskeletal proteins and enhancement by tumor necrosis factor alpha.* J Virol, 2005. **79**(2): p. 918-26.
68. Martens, S. and H.T. McMahon, *Mechanisms of membrane fusion: disparate players and common principles.* Nat Rev Mol Cell Biol, 2008. **9**(7): p. 543-56.
69. Skehel, J.J. and D.C. Wiley, *Receptor binding and membrane fusion in virus entry: the influenza hemagglutinin.* Annu Rev Biochem, 2000. **69**: p. 531-69.
70. Freed, E.O., D.J. Myers, and R. Risser, *Characterization of the fusion domain of the human immunodeficiency virus type 1 envelope glycoprotein gp41.* Proc Natl Acad Sci U S A, 1990. **87**(12): p. 4650-4.
71. Yang, Z.N., et al., *The crystal structure of the SIV gp41 ectodomain at 1.47 A resolution.* J Struct Biol, 1999. **126**(2): p. 131-44.
72. Weissenhorn, W., et al., *Crystal structure of the Ebola virus membrane fusion subunit, GP2, from the envelope glycoprotein ectodomain.* Mol Cell, 1998. **2**(5): p. 605-16.

73. White, J.M., et al., *Structures and mechanisms of viral membrane fusion proteins: multiple variations on a common theme.* Crit Rev Biochem Mol Biol, 2008. **43**(3): p. 189-219.
74. Lescar, J., et al., *The Fusion glycoprotein shell of Semliki Forest virus: an icosahedral assembly primed for fusogenic activation at endosomal pH.* Cell, 2001. **105**(1): p. 137-48.
75. Modis, Y., et al., *Structure of the dengue virus envelope protein after membrane fusion.* Nature, 2004. **427**(6972): p. 313-9.
76. Nybakken, G.E., et al., *Crystal structure of the West Nile virus envelope glycoprotein.* J Virol, 2006. **80**(23): p. 11467-74.
77. Op De Beeck, A., et al., *Characterization of functional hepatitis C virus envelope glycoproteins.* J Virol, 2004. **78**(6): p. 2994-3002.
78. Schibli, D.J. and W. Weissenhorn, *Class I and class II viral fusion protein structures reveal similar principles in membrane fusion.* Mol Membr Biol, 2004. **21**(6): p. 361-71.
79. Perera, R. and R.J. Kuhn, *Structural proteomics of dengue virus.* Curr Opin Microbiol, 2008. **11**(4): p. 369-77.
80. Qi, R.F., L. Zhang, and C.W. Chi, *Biological characteristics of dengue virus and potential targets for drug design.* Acta Biochim Biophys Sin (Shanghai), 2008. **40**(2): p. 91-101.
81. Zaitseva, E., et al., *Class II fusion protein of alphaviruses drives membrane fusion through the same pathway as class I proteins.* J Cell Biol, 2005. **169**(1): p. 167-77.
82. Kadlec, J., et al., *The postfusion structure of baculovirus gp64 supports a unified view of viral fusion machines.* Nat Struct Mol Biol, 2008. **15**(10): p. 1024-30.
83. Roche, S., et al., *Crystal structure of the low-pH form of the vesicular stomatitis virus glycoprotein G.* Science, 2006. **313**(5784): p. 187-91.
84. Roche, S., et al., *Structure of the prefusion form of the vesicular stomatitis virus glycoprotein G.* Science, 2007. **315**(5813): p. 843-8.
85. Heldwein, E.E., et al., *Crystal structure of glycoprotein B from herpes simplex virus 1.* Science, 2006. **313**(5784): p. 217-20.
86. F. X. Heinz, C.M., R. H. Purcell, E. A. Gould, C. R. Howard, M. Houghton, R. J. M. Moormann, C. M. Rice, H. J. Thiel, *Family flaviviridae*, in *Virus Taxonomy: 7th International Committee for the Taxonomy of Viruses*, C.M.F. M. H. V. Regenmortel, D. H. L. Bishop, E. Carstens, M. K. Estes, S. Lemon, J. Maniloff, M. A. Mayo, D. McGeoh, C. R. Pringle, R. B. Wickner, Editor. 2000: San Diego.
87. Reed, W., *Recent Researches concerning the Etiology, Propagation, and Prevention of Yellow Fever, by the United States Army Commission.* J Hyg (Lond), 1902. **2**(2): p. 101-19.
88. Ashburn, P.M. and C.F. Craig, *Experimental investigations regarding the etiology of dengue fever. 1907.* J Infect Dis, 2004. **189**(9): p. 1747-83; discussion 1744-6.
89. Calisher, C.H., et al., *Antigenic relationships between flaviviruses as determined by cross-neutralization tests with polyclonal antisera.* J Gen Virol, 1989. **70 (Pt 1)**: p. 37-43.
90. Repik, P.M., et al., *RNA fingerprinting as a method for distinguishing dengue 1 virus strains.* Am J Trop Med Hyg, 1983. **32**(3): p. 577-89.
91. Trent, D., et al., *WHO Working Group on technical specifications for manufacture and evaluation of dengue vaccines, Geneva, Switzerland, 11-12 May 2009.* Vaccine, 2010. **28**(52): p. 8246-55.
92. Trent, D.W., et al., *Genetic variation and microevolution of dengue 2 virus in Southeast Asia.* Virology, 1989. **172**(2): p. 523-35.
93. Trent, D.W., et al., *Genetic variation among dengue 2 viruses of different geographic origin.* Virology, 1983. **128**(2): p. 271-84.
94. Rico-Hesse, R., *Molecular evolution and distribution of dengue viruses type 1 and 2 in nature.* Virology, 1990. **174**(2): p. 479-93.

95. Goncalvez, A.P., et al., *Diversity and evolution of the envelope gene of dengue virus type 1.* Virology, 2002. **303**(1): p. 110-9.
96. Vasilakis, N. and S.C. Weaver, *The history and evolution of human dengue emergence.* Adv Virus Res, 2008. **72**: p. 1-76.
97. Lewis, J.A., et al., *Phylogenetic relationships of dengue-2 viruses.* Virology, 1993. **197**(1): p. 216-24.
98. Rico-Hesse, R., et al., *Origins of dengue type 2 viruses associated with increased pathogenicity in the Americas.* Virology, 1997. **230**(2): p. 244-51.
99. Twiddy, S.S., et al., *Phylogenetic relationships and differential selection pressures among genotypes of dengue-2 virus.* Virology, 2002. **298**(1): p. 63-72.
100. Twiddy, S.S., C.H. Woelk, and E.C. Holmes, *Phylogenetic evidence for adaptive evolution of dengue viruses in nature.* J Gen Virol, 2002. **83**(Pt 7): p. 1679-89.
101. Vasilakis, N., R.B. Tesh, and S.C. Weaver, *Sylvatic dengue virus type 2 activity in humans, Nigeria, 1966.* Emerg Infect Dis, 2008. **14**(3): p. 502-4.
102. Wang, E., et al., *Evolutionary relationships of endemic/epidemic and sylvatic dengue viruses.* J Virol, 2000. **74**(7): p. 3227-34.
103. Rudnick, A. *Proceedings of the International Conference on Dengue/DHF*. in *International Conference on Dengue/DHF*. 1984. Kuala Lumpur.
104. Ratnam, I., et al., *Dengue fever and international travel.* J Travel Med, 2013. **20**(6): p. 384-93.
105. Kyle, J.L. and E. Harris, *Global spread and persistence of dengue.* Annu Rev Microbiol, 2008. **62**: p. 71-92.
106. Meltzer, E. and E. Schwartz, *A travel medicine view of dengue and dengue hemorrhagic fever.* Travel Med Infect Dis, 2009. **7**(5): p. 278-83.
107. WHO, *WHO: Dengue haemorrhagic fever: Diagnosis, treatment, prevention and control*. 2nd Edition ed. 1997, Geneva.
108. WHO, *Global Surveillance of epidemic prone infectious diseases*. 2005, WHO: Geneva.
109. Bhatt, S., et al., *The global distribution and burden of dengue.* Nature, 2013. **496**(7446): p. 504-7.
110. Effler, P.V., et al., *Dengue fever, Hawaii, 2001-2002.* Emerg Infect Dis, 2005. **11**(5): p. 742-9.
111. Imrie, A., et al., *Molecular epidemiology of dengue in the Pacific: introduction of two distinct strains of dengue virus type-1 [corrected] into Hawaii.* Ann Trop Med Parasitol, 2006. **100**(4): p. 327-36.
112. Kouri, G., M.G. Guzman, and J. Bravo, *Hemorrhagic dengue in Cuba: history of an epidemic.* Bull Pan Am Health Organ, 1986. **20**(1): p. 24-30.
113. Sousa, C.A., et al., *Ongoing outbreak of dengue type 1 in the Autonomous Region of Madeira, Portugal: preliminary report.* Euro Surveill, 2012. **17**(49).
114. Gjenero-Margan, I., et al., *Autochthonous Dengue Fever in Croatia, August–September 2010.* Euro Surveill, 2011. **16**(9).
115. Gould, E.A., et al., *First cases of autochthonous dengue fever and chikungunya fever in France: from bad dream to reality!* Clin Microbiol Infect, 2010. **16**(12): p. 1702-4.
116. McFee, R.B., *Viral hemorrhagic fever viruses.* Dis Mon, 2013. **59**(12): p. 410-25.
117. WHO, *Dengue: Guidelines for Diagnosis, Treatment, Prevention*

and Control. 2009, World Health Organization.
118. Yu, I.M., et al., *Association of the pr peptides with dengue virus at acidic pH blocks membrane fusion.* J Virol, 2009. **83**(23): p. 12101-7.
119. Mukhopadhyay, S., R.J. Kuhn, and M.G. Rossmann, *A structural perspective of the flavivirus life cycle.* Nat Rev Microbiol, 2005. **3**(1): p. 13-22.
120. Kuhn, R.J., et al., *Structure of dengue virus: implications for flavivirus organization, maturation, and fusion.* Cell, 2002. **108**(5): p. 717-25.

121. Zhang, Y., et al., *Structures of immature flavivirus particles.* EMBO J, 2003. **22**(11): p. 2604-13.
122. Zhang, X., et al., *Dengue structure differs at the temperatures of its human and mosquito hosts.* Proc Natl Acad Sci U S A, 2013. **110**(17): p. 6795-9.
123. Cleaves, G.R. and D.T. Dubin, *Methylation status of intracellular dengue type 2 40 S RNA.* Virology, 1979. **96**(1): p. 159-65.
124. Markoff, L., *5'- and 3'-noncoding regions in flavivirus RNA.* Adv Virus Res, 2003. **59**: p. 177-228.
125. Lindenbach, B.D., H.-J. Thiel, and C.M. Rice, *Flaviviridae: The Viruses and Their Replication*, in *Fields Virology*, D.M. Knipe and P.M. Howley, Editors. 2007, Lippincott-Raven: Philadelphia.
126. Jessie, K., et al., *Localization of dengue virus in naturally infected human tissues, by immunohistochemistry and in situ hybridization.* J Infect Dis, 2004. **189**(8): p. 1411-8.
127. Wu, S.J., et al., *Human skin Langerhans cells are targets of dengue virus infection.* Nat Med, 2000. **6**(7): p. 816-20.
128. Halstead, S.B., J.S. Porterfield, and E.J. O'Rourke, *Enhancement of dengue virus infection in monocytes by flavivirus antisera.* Am J Trop Med Hyg, 1980. **29**(4): p. 638-42.
129. Miller, J.L., et al., *The mannose receptor mediates dengue virus infection of macrophages.* PLoS Pathog, 2008. **4**(2): p. e17.
130. Cabrera-Hernandez, A., et al., *Dengue virus entry into liver (HepG2) cells is independent of hsp90 and hsp70.* J Med Virol, 2007. **79**(4): p. 386-92.
131. Kangwanpong, D., N. Bhamarapravati, and H.L. Lucia, *Diagnosing dengue virus infection in archived autopsy tissues by means of the in situ PCR method: a case report.* Clin Diagn Virol, 1995. **3**(2): p. 165-72.
132. Suksanpaisan, L., A. Cabrera-Hernandez, and D.R. Smith, *Infection of human primary hepatocytes with dengue virus serotype 2.* J Med Virol, 2007. **79**(3): p. 300-7.
133. Avirutnan, P., et al., *Dengue virus infection of human endothelial cells leads to chemokine production, complement activation, and apoptosis.* J Immunol, 1998. **161**(11): p. 6338-46.
134. Chareonsirisuthigul, T., S. Kalayanarooj, and S. Ubol, *Dengue virus (DENV) antibody-dependent enhancement of infection upregulates the production of anti-inflammatory cytokines, but suppresses anti-DENV free radical and pro-inflammatory cytokine production, in THP-1 cells.* J Gen Virol, 2007. **88**(Pt 2): p. 365-75.
135. Chen, S.T., et al., *CLEC5A is critical for dengue-virus-induced lethal disease.* Nature, 2008. **453**(7195): p. 672-6.
136. Edgil, D., et al., *Translation efficiency determines differences in cellular infection among dengue virus type 2 strains.* Virology, 2003. **317**(2): p. 275-90.
137. Gromowski, G.D. and A.D. Barrett, *Characterization of an antigenic site that contains a dominant, type-specific neutralization determinant on the envelope protein domain III (ED3) of dengue 2 virus.* Virology, 2007. **366**(2): p. 349-60.
138. Halstead, S.B., *Neutralization and antibody-dependent enhancement of dengue viruses.* Adv Virus Res, 2003. **60**: p. 421-67.
139. Huang, K.J., et al., *The dual-specific binding of dengue virus and target cells for the antibody-dependent enhancement of dengue virus infection.* J Immunol, 2006. **176**(5): p. 2825-32.
140. King, C.A., et al., *Release of vasoactive cytokines by antibody-enhanced dengue virus infection of a human mast cell/basophil line.* J Virol, 2000. **74**(15): p. 7146-50.
141. Kurane, I., A. Meager, and F.A. Ennis, *Dengue virus-specific human T cell clones. Serotype crossreactive proliferation, interferon gamma production, and cytotoxic activity.* J Exp Med, 1989. **170**(3): p. 763-75.

142. Lin, Y.L., et al., *Involvement of oxidative stress, NF-IL-6, and RANTES expression in dengue-2-virus-infected human liver cells.* Virology, 2000. **276**(1): p. 114-26.
143. Littaua, R., I. Kurane, and F.A. Ennis, *Human IgG Fc receptor II mediates antibody-dependent enhancement of dengue virus infection.* J Immunol, 1990. **144**(8): p. 3183-6.
144. Moreno-Altamirano, M.M., et al., *Susceptibility of mouse macrophage J774 to dengue virus infection.* Intervirology, 2007. **50**(3): p. 237-9.
145. van der Schaar, H.M., et al., *Characterization of the early events in dengue virus cell entry by biochemical assays and single-virus tracking.* J Virol, 2007. **81**(21): p. 12019-28.
146. Thepparit, C., et al., *Internalization and propagation of the dengue virus in human hepatoma (HepG2) cells.* Intervirology, 2004. **47**(2): p. 78-86.
147. Chen, Y., et al., *Dengue virus infectivity depends on envelope protein binding to target cell heparan sulfate.* Nat Med, 1997. **3**(8): p. 866-71.
148. Germi, R., et al., *Heparan sulfate-mediated binding of infectious dengue virus type 2 and yellow fever virus.* Virology, 2002. **292**(1): p. 162-8.
149. Hilgard, P. and R. Stockert, *Heparan sulfate proteoglycans initiate dengue virus infection of hepatocytes.* Hepatology, 2000. **32**(5): p. 1069-77.
150. Chen, Y.C., S.Y. Wang, and C.C. King, *Bacterial lipopolysaccharide inhibits dengue virus infection of primary human monocytes/macrophages by blockade of virus entry via a CD14-dependent mechanism.* J Virol, 1999. **73**(4): p. 2650-7.
151. Reyes-Del Valle, J., et al., *Heat shock protein 90 and heat shock protein 70 are components of dengue virus receptor complex in human cells.* J Virol, 2005. **79**(8): p. 4557-67.
152. Jindadamrongwech, S., C. Thepparit, and D.R. Smith, *Identification of GRP 78 (BiP) as a liver cell expressed receptor element for dengue virus serotype 2.* Arch Virol, 2004. **149**(5): p. 915-27.
153. Thepparit, C. and D.R. Smith, *Serotype-specific entry of dengue virus into liver cells: identification of the 37-kilodalton/67-kilodalton high-affinity laminin receptor as a dengue virus serotype 1 receptor.* J Virol, 2004. **78**(22): p. 12647-56.
154. Lozach, P.Y., et al., *Dendritic cell-specific intercellular adhesion molecule 3-grabbing non-integrin (DC-SIGN)-mediated enhancement of dengue virus infection is independent of DC-SIGN internalization signals.* J Biol Chem, 2005. **280**(25): p. 23698-708.
155. Dejnirattisai, W., et al., *Lectin switching during dengue virus infection.* J Infect Dis, 2011. **203**(12): p. 1775-83.
156. van der Schaar, H.M., et al., *Dissecting the cell entry pathway of dengue virus by single-particle tracking in living cells.* PLoS Pathog, 2008. **4**(12): p. e1000244.
157. Coil, D.A. and A.D. Miller, *Phosphatidylserine is not the cell surface receptor for vesicular stomatitis virus.* J Virol, 2004. **78**(20): p. 10920-6.
158. Kobayashi, T., et al., *Separation and characterization of late endosomal membrane domains.* J Biol Chem, 2002. **277**(35): p. 32157-64.
159. Krishnan, M.N., et al., *Rab 5 is required for the cellular entry of dengue and West Nile viruses.* J Virol, 2007. **81**(9): p. 4881-5.
160. Modriansky, M. and Z. Dvorak, *Microtubule disruptors and their interaction with biotransformation enzymes.* Biomed Pap Med Fac Univ Palacky Olomouc Czech Repub, 2005. **149**(2): p. 213-5.
161. Zaitseva, E., et al., *Dengue virus ensures its fusion in late endosomes using compartment-specific lipids.* PLoS Pathog, 2010. **6**(10): p. e1001131.
162. Allison, S.L., et al., *Oligomeric rearrangement of tick-borne encephalitis virus envelope proteins induced by an acidic pH.* J Virol, 1995. **69**(2): p. 695-700.
163. Stiasny, K., et al., *Structural requirements for low-pH-induced rearrangements in the envelope glycoprotein of tick-borne encephalitis virus.* J Virol, 1996. **70**(11): p. 8142-7.

164. Allison, S.L., et al., *Synthesis and secretion of recombinant tick-borne encephalitis virus protein E in soluble and particulate form.* J Virol, 1995. **69**(9): p. 5816-20.
165. Lorenz, I.C., et al., *Folding and dimerization of tick-borne encephalitis virus envelope proteins prM and E in the endoplasmic reticulum.* J Virol, 2002. **76**(11): p. 5480-91.
166. Kummerer, B.M. and C.M. Rice, *Mutations in the yellow fever virus nonstructural protein NS2A selectively block production of infectious particles.* J Virol, 2002. **76**(10): p. 4773-84.
167. Liu, W.J., et al., *Complementation analysis of the flavivirus Kunjin NS3 and NS5 proteins defines the minimal regions essential for formation of a replication complex and shows a requirement of NS3 in cis for virus assembly.* J Virol, 2002. **76**(21): p. 10766-75.
168. Mackenzie, J., *Wrapping things up about virus RNA replication.* Traffic, 2005. **6**(11): p. 967-77.
169. Chu, P.W. and E.G. Westaway, *Molecular and ultrastructural analysis of heavy membrane fractions associated with the replication of Kunjin virus RNA.* Arch Virol, 1992. **125**(1-4): p. 177-91.
170. Miller, S. and J. Krijnse-Locker, *Modification of intracellular membrane structures for virus replication.* Nat Rev Microbiol, 2008. **6**(5): p. 363-74.
171. Welsch, S., et al., *Composition and three-dimensional architecture of the dengue virus replication and assembly sites.* Cell Host Microbe, 2009. **5**(4): p. 365-75.
172. Mackenzie, J.M., A.A. Khromykh, and E.G. Westaway, *Stable expression of noncytopathic Kunjin replicons simulates both ultrastructural and biochemical characteristics observed during replication of Kunjin virus.* Virology, 2001. **279**(1): p. 161-72.
173. Pena, J. and E. Harris, *Early dengue virus protein synthesis induces extensive rearrangement of the endoplasmic reticulum independent of the UPR and SREBP-2 pathway.* PLoS One, 2012. **7**(6): p. e38202.
174. Heaton, N.S., et al., *Dengue virus nonstructural protein 3 redistributes fatty acid synthase to sites of viral replication and increases cellular fatty acid synthesis.* Proc Natl Acad Sci U S A, 2010. **107**(40): p. 17345-50.
175. Mackenzie, J.M., A.A. Khromykh, and R.G. Parton, *Cholesterol manipulation by West Nile virus perturbs the cellular immune response.* Cell Host Microbe, 2007. **2**(4): p. 229-39.
176. Perera, R., et al., *Dengue virus infection perturbs lipid homeostasis in infected mosquito cells.* PLoS Pathog, 2012. **8**(3): p. e1002584.
177. Shrivastava, S., et al., *Hepatitis C virus upregulates Beclin1 for induction of autophagy and activates mTOR signaling.* J Virol, 2012. **86**(16): p. 8705-12.
178. Singh, R., et al., *Autophagy regulates lipid metabolism.* Nature, 2009. **458**(7242): p. 1131-5.
179. Fischl, W. and R. Bartenschlager, *Exploitation of cellular pathways by Dengue virus.* Curr Opin Microbiol, 2011. **14**(4): p. 470-5.
180. Allison, S.L., et al., *Two distinct size classes of immature and mature subviral particles from tick-borne encephalitis virus.* J Virol, 2003. **77**(21): p. 11357-66.
181. Ferlenghi, I., et al., *Molecular organization of a recombinant subviral particle from tick-borne encephalitis virus.* Mol Cell, 2001. **7**(3): p. 593-602.
182. Flipse, J., J. Wilschut, and J.M. Smit, *Molecular mechanisms involved in antibody-dependent enhancement of dengue virus infection in humans.* Traffic, 2013. **14**(1): p. 25-35.
183. Diamond, M.S., et al., *Infection of human cells by dengue virus is modulated by different cell types and viral strains.* J Virol, 2000. **74**(17): p. 7814-23.
184. Diamond, M.S., et al., *Modulation of Dengue virus infection in human cells by alpha, beta, and gamma interferons.* J Virol, 2000. **74**(11): p. 4957-66.

185. Ho, L.J., et al., *Dengue virus type 2 antagonizes IFN-alpha but not IFN-gamma antiviral effect via down-regulating Tyk2-STAT signaling in the human dendritic cell.* J Immunol, 2005. **174**(12): p. 8163-72.
186. Shresta, S., et al., *Interferon-dependent immunity is essential for resistance to primary dengue virus infection in mice, whereas T- and B-cell-dependent immunity are less critical.* J Virol, 2004. **78**(6): p. 2701-10.
187. de Kruif, M.D., et al., *Differential gene expression changes in children with severe dengue virus infections.* PLoS Negl Trop Dis, 2008. **2**(4): p. e215.
188. Tsai, Y.T., et al., *Human TLR3 recognizes dengue virus and modulates viral replication in vitro.* Cell Microbiol, 2009. **11**(4): p. 604-15.
189. Loo, Y.M., et al., *Distinct RIG-I and MDA5 signaling by RNA viruses in innate immunity.* J Virol, 2008. **82**(1): p. 335-45.
190. Diamond, M.S., T.C. Pierson, and D.H. Fremont, *The structural immunology of antibody protection against West Nile virus.* Immunol Rev, 2008. **225**: p. 212-25.
191. Klasse, P.J. and Q.J. Sattentau, *Occupancy and mechanism in antibody-mediated neutralization of animal viruses.* J Gen Virol, 2002. **83**(Pt 9): p. 2091-108.
192. Lisova, O., et al., *Mapping to completeness and transplantation of a group-specific, discontinuous, neutralizing epitope in the envelope protein of dengue virus.* J Gen Virol, 2007. **88**(Pt 9): p. 2387-97.
193. Oliphant, T., et al., *Antibody recognition and neutralization determinants on domains I and II of West Nile Virus envelope protein.* J Virol, 2006. **80**(24): p. 12149-59.
194. Rajamanonmani, R., et al., *On a mouse monoclonal antibody that neutralizes all four dengue virus serotypes.* J Gen Virol, 2009. **90**(Pt 4): p. 799-809.
195. Thompson, B.S., et al., *A therapeutic antibody against west nile virus neutralizes infection by blocking fusion within endosomes.* PLoS Pathog, 2009. **5**(5): p. e1000453.
196. Lai, C.Y., et al., *Antibodies to envelope glycoprotein of dengue virus during the natural course of infection are predominantly cross-reactive and recognize epitopes containing highly conserved residues at the fusion loop of domain II.* J Virol, 2008. **82**(13): p. 6631-43.
197. Cardosa, M.J., et al., *Antibodies against prM protein distinguish between previous infection with dengue and Japanese encephalitis viruses.* BMC Microbiol, 2002. **2**: p. 9.
198. Flamand, M., et al., *Dengue virus type 1 nonstructural glycoprotein NS1 is secreted from mammalian cells as a soluble hexamer in a glycosylation-dependent fashion.* J Virol, 1999. **73**(7): p. 6104-10.
199. Beltramello, M., et al., *The human immune response to Dengue virus is dominated by highly cross-reactive antibodies endowed with neutralizing and enhancing activity.* Cell Host Microbe, 2010. **8**(3): p. 271-83.
200. Schieffelin, J.S., et al., *Neutralizing and non-neutralizing monoclonal antibodies against dengue virus E protein derived from a naturally infected patient.* Virol J, 2010. **7**: p. 28.
201. Midgley, C.M., et al., *An in-depth analysis of original antigenic sin in dengue virus infection.* J Virol, 2011. **85**(1): p. 410-21.
202. Boonnak, K., et al., *Cell type specificity and host genetic polymorphisms influence antibody-dependent enhancement of dengue virus infection.* J Virol, 2011. **85**(4): p. 1671-83.
203. Moi, M.L., et al., *Involvement of the Fc gamma receptor IIA cytoplasmic domain in antibody-dependent enhancement of dengue virus infection.* J Gen Virol, 2010. **91**(Pt 1): p. 103-11.
204. Rodrigo, W.W., et al., *Differential enhancement of dengue virus immune complex infectivity mediated by signaling-competent and signaling-incompetent human Fcgamma RIA (CD64) or FcgammaRIIA (CD32).* J Virol, 2006. **80**(20): p. 10128-38.

205. Halstead, S.B. and E.J. O'Rourke, *Dengue viruses and mononuclear phagocytes. I. Infection enhancement by non-neutralizing antibody.* J Exp Med, 1977. **146**(1): p. 201-17.
206. Dejnirattisai, W., et al., *Cross-reacting antibodies enhance dengue virus infection in humans.* Science, 2010. **328**(5979): p. 745-8.
207. Rodenhuis-Zybert, I.A., et al., *Immature dengue virus: a veiled pathogen?* PLoS Pathog, 2010. **6**(1): p. e1000718.
208. Li, L., et al., *The flavivirus precursor membrane-envelope protein complex: structure and maturation.* Science, 2008. **319**(5871): p. 1830-4.
209. Yu, I.M., et al., *Structure of the immature dengue virus at low pH primes proteolytic maturation.* Science, 2008. **319**(5871): p. 1834-7.
210. Rolph, M.S., et al., *Downregulation of interferon-beta in antibody-dependent enhancement of dengue viral infections of human macrophages is dependent on interleukin-6.* J Infect Dis, 2011. **204**(3): p. 489-91.
211. Ubol, S., et al., *Mechanisms of immune evasion induced by a complex of dengue virus and preexisting enhancing antibodies.* J Infect Dis, 2010. **201**(6): p. 923-35.
212. Kou, Z., et al., *Human antibodies against dengue enhance dengue viral infectivity without suppressing type I interferon secretion in primary human monocytes.* Virology, 2011. **410**(1): p. 240-7.
213. Ubol, S. and S.B. Halstead, *How innate immune mechanisms contribute to antibody-enhanced viral infections.* Clin Vaccine Immunol, 2010. **17**(12): p. 1829-35.
214. Kofler, R.M., F.X. Heinz, and C.W. Mandl, *Capsid protein C of tick-borne encephalitis virus tolerates large internal deletions and is a favorable target for attenuation of virulence.* J Virol, 2002. **76**(7): p. 3534-43.
215. Markoff, L., B. Falgout, and A. Chang, *A conserved internal hydrophobic domain mediates the stable membrane integration of the dengue virus capsid protein.* Virology, 1997. **233**(1): p. 105-17.
216. Sangiambut, S., et al., *Multiple regions in dengue virus capsid protein contribute to nuclear localization during virus infection.* J Gen Virol, 2008. **89**(Pt 5): p. 1254-64.
217. Colpitts, T.M., et al., *Dengue virus capsid protein binds core histones and inhibits nucleosome formation in human liver cells.* PLoS One, 2011. **6**(9): p. e24365.
218. Samsa, M.M., et al., *Dengue virus capsid protein usurps lipid droplets for viral particle formation.* PLoS Pathog, 2009. **5**(10): p. e1000632.
219. Ma, L., et al., *Solution structure of dengue virus capsid protein reveals another fold.* Proc Natl Acad Sci U S A, 2004. **101**(10): p. 3414-9.
220. Hallenberger, S., et al., *Inhibition of furin-mediated cleavage activation of HIV-1 glycoprotein gp160.* Nature, 1992. **360**(6402): p. 358-61.
221. Shiryaev, S.A., et al., *Targeting host cell furin proprotein convertases as a therapeutic strategy against bacterial toxins and viral pathogens.* J Biol Chem, 2007. **282**(29): p. 20847-53.
222. Thomas, G., *Furin at the cutting edge: from protein traffic to embryogenesis and disease.* Nat Rev Mol Cell Biol, 2002. **3**(10): p. 753-66.
223. Zhang, W., et al., *Visualization of membrane protein domains by cryo-electron microscopy of dengue virus.* Nat Struct Biol, 2003. **10**(11): p. 907-12.
224. Catteau, A., et al., *Dengue virus M protein contains a proapoptotic sequence referred to as ApoptoM.* J Gen Virol, 2003. **84**(Pt 10): p. 2781-93.
225. Catteau, A., et al., *Expression of dengue ApoptoM sequence results in disruption of mitochondrial potential and caspase activation.* Biochimie, 2003. **85**(8): p. 789-93.
226. Brault, J.B., et al., *The interaction of flavivirus M protein with light chain Tctex-1 of human dynein plays a role in late stages of virus replication.* Virology, 2011. **417**(2): p. 369-78.

227. Duan, X., et al., *Novel binding between pre-membrane protein and vacuolar ATPase is required for efficient dengue virus secretion.* Biochem Biophys Res Commun, 2008. **373**(2): p. 319-24.
228. Gao, F., et al., *Novel binding between pre-membrane protein and claudin-1 is required for efficient dengue virus entry.* Biochem Biophys Res Commun, 2010. **391**(1): p. 952-7.
229. Wong, S.S., et al., *The dengue virus M protein localises to the endoplasmic reticulum and forms oligomers.* FEBS Lett, 2012. **586**(7): p. 1032-7.
230. Zhang, Y., et al., *Conformational changes of the flavivirus E glycoprotein.* Structure, 2004. **12**(9): p. 1607-18.
231. Perera, R., M. Khaliq, and R.J. Kuhn, *Closing the door on flaviviruses: entry as a target for antiviral drug design.* Antiviral Res, 2008. **80**(1): p. 11-22.
232. Melo, M.N., et al., *Interaction of the Dengue virus fusion peptide with membranes assessed by NMR: The essential role of the envelope protein Trp101 for membrane fusion.* J Mol Biol, 2009. **392**(3): p. 736-46.
233. Fritz, R., et al., *The unique transmembrane hairpin of flavivirus fusion protein E is essential for membrane fusion.* J Virol, 2011. **85**(9): p. 4377-85.
234. Lin, S.R., et al., *The helical domains of the stem region of dengue virus envelope protein are involved in both virus assembly and entry.* J Virol, 2011. **85**(10): p. 5159-71.
235. Gutsche, I., et al., *Secreted dengue virus nonstructural protein NS1 is an atypical barrel-shaped high-density lipoprotein.* Proc Natl Acad Sci U S A, 2011. **108**(19): p. 8003-8.
236. Avirutnan, P., et al., *Vascular leakage in severe dengue virus infections: a potential role for the nonstructural viral protein NS1 and complement.* J Infect Dis, 2006. **193**(8): p. 1078-88.
237. Falgout, B., et al., *Immunization of mice with recombinant vaccinia virus expressing authentic dengue virus nonstructural protein NS1 protects against lethal dengue virus encephalitis.* J Virol, 1990. **64**(9): p. 4356-63.
238. Schlesinger, J.J., M.W. Brandriss, and E.E. Walsh, *Protection of mice against dengue 2 virus encephalitis by immunization with the dengue 2 virus non-structural glycoprotein NS1.* J Gen Virol, 1987. **68 (Pt 3)**: p. 853-7.
239. Muller, D.A. and P.R. Young, *The flavivirus NS1 protein: molecular and structural biology, immunology, role in pathogenesis and application as a diagnostic biomarker.* Antiviral Res, 2013. **98**(2): p. 192-208.
240. Mackenzie, J.M., M.K. Jones, and P.R. Young, *Immunolocalization of the dengue virus nonstructural glycoprotein NS1 suggests a role in viral RNA replication.* Virology, 1996. **220**(1): p. 232-40.
241. Westaway, E.G., et al., *Ultrastructure of Kunjin virus-infected cells: colocalization of NS1 and NS3 with double-stranded RNA, and of NS2B with NS3, in virus-induced membrane structures.* J Virol, 1997. **71**(9): p. 6650-61.
242. D'Arcy, A., et al., *Purification and crystallization of dengue and West Nile virus NS2B-NS3 complexes.* Acta Crystallogr Sect F Struct Biol Cryst Commun, 2006. **62**(Pt 2): p. 157-62.
243. Erbel, P., et al., *Structural basis for the activation of flaviviral NS3 proteases from dengue and West Nile virus.* Nat Struct Mol Biol, 2006. **13**(4): p. 372-3.
244. Amberg, S.M., et al., *NS2B-3 proteinase-mediated processing in the yellow fever virus structural region: in vitro and in vivo studies.* J Virol, 1994. **68**(6): p. 3794-802.
245. Lin, C., et al., *Cleavage at a novel site in the NS4A region by the yellow fever virus NS2B-3 proteinase is a prerequisite for processing at the downstream 4A/4B signalase site.* J Virol, 1993. **67**(4): p. 2327-35.
246. Bartelma, G. and R. Padmanabhan, *Expression, purification, and characterization of the RNA 5'-triphosphatase activity of dengue virus type 2 nonstructural protein 3.* Virology, 2002. **299**(1): p. 122-32.

247. Benarroch, D., et al., *The RNA helicase, nucleotide 5'-triphosphatase, and RNA 5'-triphosphatase activities of Dengue virus protein NS3 are Mg2+-dependent and require a functional Walker B motif in the helicase catalytic core.* Virology, 2004. **328**(2): p. 208-18.
248. Li, H., et al., *The serine protease and RNA-stimulated nucleoside triphosphatase and RNA helicase functional domains of dengue virus type 2 NS3 converge within a region of 20 amino acids.* J Virol, 1999. **73**(4): p. 3108-16.
249. Wengler, G., *The NS 3 nonstructural protein of flaviviruses contains an RNA triphosphatase activity.* Virology, 1993. **197**(1): p. 265-73.
250. Hanley, K.A., et al., *Paired charge-to-alanine mutagenesis of dengue virus type 4 NS5 generates mutants with temperature-sensitive, host range, and mouse attenuation phenotypes.* J Virol, 2002. **76**(2): p. 525-31.
251. Khromykh, A.A., M.T. Kenney, and E.G. Westaway, *trans-Complementation of flavivirus RNA polymerase gene NS5 by using Kunjin virus replicon-expressing BHK cells.* J Virol, 1998. **72**(9): p. 7270-9.
252. Egloff, M.P., et al., *An RNA cap (nucleoside-2'-O-)-methyltransferase in the flavivirus RNA polymerase NS5: crystal structure and functional characterization.* EMBO J, 2002. **21**(11): p. 2757-68.
253. Bartholomeusz, A. and P. Thompson, *Flaviviridae polymerase and RNA replication.* J Viral Hepat, 1999. **6**(4): p. 261-70.
254. Nomaguchi, M., et al., *De novo synthesis of negative-strand RNA by Dengue virus RNA-dependent RNA polymerase in vitro: nucleotide, primer, and template parameters.* J Virol, 2003. **77**(16): p. 8831-42.
255. Cui, T., et al., *Recombinant dengue virus type 1 NS3 protein exhibits specific viral RNA binding and NTPase activity regulated by the NS5 protein.* Virology, 1998. **246**(2): p. 409-17.
256. Johansson, M., et al., *A small region of the dengue virus-encoded RNA-dependent RNA polymerase, NS5, confers interaction with both the nuclear transport receptor importin-beta and the viral helicase, NS3.* J Gen Virol, 2001. **82**(Pt 4): p. 735-45.
257. Kapoor, M., et al., *Association between NS3 and NS5 proteins of dengue virus type 2 in the putative RNA replicase is linked to differential phosphorylation of NS5.* J Biol Chem, 1995. **270**(32): p. 19100-6.
258. Best, S.M., et al., *Inhibition of interferon-stimulated JAK-STAT signaling by a tick-borne flavivirus and identification of NS5 as an interferon antagonist.* J Virol, 2005. **79**(20): p. 12828-39.
259. Medin, C.L., K.A. Fitzgerald, and A.L. Rothman, *Dengue virus nonstructural protein NS5 induces interleukin-8 transcription and secretion.* J Virol, 2005. **79**(17): p. 11053-61.
260. Xie, X., et al., *Membrane topology and function of dengue virus NS2A protein.* J Virol, 2013. **87**(8): p. 4609-22.
261. Mackenzie, J.M., et al., *Subcellular localization and some biochemical properties of the flavivirus Kunjin nonstructural proteins NS2A and NS4A.* Virology, 1998. **245**(2): p. 203-15.
262. Leung, J.Y., et al., *Role of nonstructural protein NS2A in flavivirus assembly.* J Virol, 2008. **82**(10): p. 4731-41.
263. Munoz-Jordan, J.L., et al., *Inhibition of interferon signaling by dengue virus.* Proc Natl Acad Sci U S A, 2003. **100**(24): p. 14333-8.
264. Miller, S., et al., *The non-structural protein 4A of dengue virus is an integral membrane protein inducing membrane alterations in a 2K-regulated manner.* J Biol Chem, 2007. **282**(12): p. 8873-82.
265. Shiryaev, S.A., et al., *NS4A regulates the ATPase activity of the NS3 helicase: a novel cofactor role of the non-structural protein NS4A from West Nile virus.* J Gen Virol, 2009. **90**(Pt 9): p. 2081-5.

266. Lindenbach, B.D. and C.M. Rice, *Genetic interaction of flavivirus nonstructural proteins NS1 and NS4A as a determinant of replicase function.* J Virol, 1999. **73**(6): p. 4611-21.
267. Roosendaal, J., et al., *Regulated cleavages at the West Nile virus NS4A-2K-NS4B junctions play a major role in rearranging cytoplasmic membranes and Golgi trafficking of the NS4A protein.* J Virol, 2006. **80**(9): p. 4623-32.
268. Broker, L.E., F.A. Kruyt, and G. Giaccone, *Cell death independent of caspases: a review.* Clin Cancer Res, 2005. **11**(9): p. 3155-62.
269. Kroemer, G. and M. Jaattela, *Lysosomes and autophagy in cell death control.* Nat Rev Cancer, 2005. **5**(11): p. 886-97.
270. Ogata, M., et al., *Autophagy is activated for cell survival after endoplasmic reticulum stress.* Mol Cell Biol, 2006. **26**(24): p. 9220-31.
271. McLean, J.E., et al., *Flavivirus NS4A-induced autophagy protects cells against death and enhances virus replication.* J Biol Chem, 2011. **286**(25): p. 22147-59.
272. Miller, S., S. Sparacio, and R. Bartenschlager, *Subcellular localization and membrane topology of the Dengue virus type 2 Non-structural protein 4B.* J Biol Chem, 2006. **281**(13): p. 8854-63.
273. Munoz-Jordan, J.L., et al., *Inhibition of alpha/beta interferon signaling by the NS4B protein of flaviviruses.* J Virol, 2005. **79**(13): p. 8004-13.
274. Kakumani, P.K., et al., *Role of RNA interference (RNAi) in dengue virus replication and identification of NS4B as an RNAi suppressor.* J Virol, 2013. **87**(16): p. 8870-83.
275. Umareddy, I., et al., *Dengue virus NS4B interacts with NS3 and dissociates it from single-stranded RNA.* J Gen Virol, 2006. **87**(Pt 9): p. 2605-14.
276. Zou, J., et al., *Dimerization of flavivirus NS4B protein.* J Virol, 2014. **88**(6): p. 3379-91.
277. Rodrigues, H.S., M.T. Monteiro, and D.F. Torres, *Vaccination models and optimal control strategies to dengue.* Math Biosci, 2014. **247**: p. 1-12.
278. Halstead, S.B., *Dengue.* Curr Opin Infect Dis, 2002. **15**(5): p. 471-6.
279. Pooja, C., Y Amrita, and C. Viney, *Clinical implications and treatment of dengue.* Asian Pacific Journal of Tropical Medicine, 2014: p. 169-178.
280. Fu, G., et al., *Female-specific flightless phenotype for mosquito control.* Proc Natl Acad Sci U S A, 2010. **107**(10): p. 4550-4.
281. Gilbert, N. (2010) *GM mosquitoes wipe out dengue fever in trial*.
282. McMeniman, C.J., et al., *Stable introduction of a life-shortening Wolbachia infection into the mosquito Aedes aegypti.* Science, 2009. **323**(5910): p. 141-4.
283. Back, A.T. and A. Lundkvist, *Dengue viruses - an overview.* Infect Ecol Epidemiol, 2013. **3**.
284. Kampmann, T., et al., *In silico screening of small molecule libraries using the dengue virus envelope E protein has identified compounds with antiviral activity against multiple flaviviruses.* Antiviral Res, 2009. **84**(3): p. 234-41.
285. Modis, Y., et al., *A ligand-binding pocket in the dengue virus envelope glycoprotein.* Proc Natl Acad Sci U S A, 2003. **100**(12): p. 6986-91.
286. Teoh, E.P., et al., *The structural basis for serotype-specific neutralization of dengue virus by a human antibody.* Sci Transl Med, 2012. **4**(139): p. 139ra83.
287. Liao, M. and M. Kielian, *Domain III from class II fusion proteins functions as a dominant-negative inhibitor of virus membrane fusion.* J Cell Biol, 2005. **171**(1): p. 111-20.
288. Schmidt, A.G., P.L. Yang, and S.C. Harrison, *Peptide inhibitors of dengue-virus entry target a late-stage fusion intermediate.* PLoS Pathog, 2010. **6**(4): p. e1000851.
289. Costin, J.M., et al., *Structural optimization and de novo design of dengue virus entry inhibitory peptides.* PLoS Negl Trop Dis, 2010. **4**(6): p. e721.
290. Lok, S.M., et al., *Release of dengue virus genome induced by a peptide inhibitor.* PLoS One, 2012. **7**(11): p. e50995.

291. Nemesio, H., F. Palomares-Jerez, and J. Villalain, *The membrane-active regions of the dengue virus proteins C and E.* Biochim Biophys Acta, 2011. **1808**(10): p. 2390-402.
292. Menendez-Arias, L., *Molecular basis of human immunodeficiency virus drug resistance: an update.* Antiviral Res, 2010. **85**(1): p. 210-31.
293. Soriano, V., et al., *Emerging drugs for hepatitis C.* Expert Opin Emerg Drugs, 2008. **13**(1): p. 1-19.
294. Leung, D., et al., *Activity of recombinant dengue 2 virus NS3 protease in the presence of a truncated NS2B co-factor, small peptide substrates, and inhibitors.* J Biol Chem, 2001. **276**(49): p. 45762-71.
295. Mueller, N.H., et al., *Identification and biochemical characterization of small-molecule inhibitors of west nile virus serine protease by a high-throughput screen.* Antimicrob Agents Chemother, 2008. **52**(9): p. 3385-93.
296. Yin, Z., et al., *An adenosine nucleoside inhibitor of dengue virus.* Proc Natl Acad Sci U S A, 2009. **106**(48): p. 20435-9.
297. Malet, H., et al., *The flavivirus polymerase as a target for drug discovery.* Antiviral Res, 2008. **80**(1): p. 23-35.
298. Deas, T.S., et al., *Inhibition of flavivirus infections by antisense oligomers specifically suppressing viral translation and RNA replication.* J Virol, 2005. **79**(8): p. 4599-609.
299. Holden, K.L., et al., *Inhibition of dengue virus translation and RNA synthesis by a morpholino oligomer targeted to the top of the terminal 3' stem-loop structure.* Virology, 2006. **344**(2): p. 439-52.
300. Kinney, R.M., et al., *Inhibition of dengue virus serotypes 1 to 4 in vero cell cultures with morpholino oligomers.* J Virol, 2005. **79**(8): p. 5116-28.
301. Somnuke, P., et al., *N-linked glycosylation of dengue virus NS1 protein modulates secretion, cell-surface expression, hexamer stability, and interactions with human complement.* Virology, 2011. **413**(2): p. 253-64.
302. Rathore, A.P., et al., *Celgosivir treatment misfolds dengue virus NS1 protein, induces cellular pro-survival genes and protects against lethal challenge mouse model.* Antiviral Res, 2011. **92**(3): p. 453-60.
303. Botting, C. and R.J. Kuhn, *Novel approaches to flavivirus drug discovery.* Expert Opin Drug Discov, 2012. **7**(5): p. 417-28.
304. Hombach, J., et al., *Scientific consultation on immunological correlates of protection induced by dengue vaccines report from a meeting held at the World Health Organization 17-18 November 2005.* Vaccine, 2007. **25**(21): p. 4130-9.
305. Sabchareon, A., et al., *Safety and immunogenicity of tetravalent live-attenuated dengue vaccines in Thai adult volunteers: role of serotype concentration, ratio, and multiple doses.* Am J Trop Med Hyg, 2002. **66**(3): p. 264-72.
306. Sun, W., et al., *Vaccination of human volunteers with monovalent and tetravalent live-attenuated dengue vaccine candidates.* Am J Trop Med Hyg, 2003. **69**(6 Suppl): p. 24-31.
307. Guy, B., et al., *Preclinical and clinical development of YFV 17D-based chimeric vaccines against dengue, West Nile and Japanese encephalitis viruses.* Vaccine, 2010. **28**(3): p. 632-49.
308. Osorio, J.E., et al., *Development of DENVax: a chimeric dengue-2 PDK-53-based tetravalent vaccine for protection against dengue fever.* Vaccine, 2011. **29**(42): p. 7251-60.
309. Durbin, A.P., et al., *Development and clinical evaluation of multiple investigational monovalent DENV vaccines to identify components for inclusion in a live attenuated tetravalent DENV vaccine.* Vaccine, 2011. **29**(42): p. 7242-50.
310. Coller, B.A., et al., *The development of recombinant subunit envelope-based vaccines to protect against dengue virus induced disease.* Vaccine, 2011. **29**(42): p. 7267-75.

311. Beckett, C.G., et al., *Evaluation of a prototype dengue-1 DNA vaccine in a Phase 1 clinical trial.* Vaccine, 2011. **29**(5): p. 960-8.
312. Bangham, A.D., M.M. Standish, and J.C. Watkins, *Diffusion of univalent ions across the lamellae of swollen phospholipids.* J Mol Biol, 1965. **13**(1): p. 238-52.
313. Bangham, A.D., M.M. Standish, and G. Weissmann, *The action of steroids and streptolysin S on the permeability of phospholipid structures to cations.* J Mol Biol, 1965. **13**(1): p. 253-9.
314. Jones, M.N., *The surface properties of phospholipid liposome systems and their characterisation.* Adv Colloid Interface Sci, 1995. **54**: p. 93-128.
315. Usher, J.R., R.M. Epand, and D. Papahadjopoulos, *The effect of free fatty acids on the thermotropic phase transition of dimyristoyl glycerophosphocholine.* Chem Phys Lipids, 1978. **22**(3): p. 245-53.
316. Lasic, D.D., *Liposomes in gene delivery*. 1997, Boca Raton, FL: CRC Press. 295 p.
317. Jesorka, A. and O. Orwar, *Liposomes: technologies and analytical applications.* Annu Rev Anal Chem (Palo Alto Calif), 2008. **1**: p. 801-32.
318. Butko, P., et al., *Membrane permeabilization induced by cytolytic delta-endotoxin CytA from Bacillus thurigiensis var. israelensis.* Biochemistry, 1996. **35**: p. 11355-11360.
319. Szoka, F.J. and D. Papahadjopoulos, *Comparative properties and methods of preparation of lipid vesicles (liposomes).* Annual Review of Biophysics and Bioengineering, 1980. **9**: p. 467-508.
320. New, R., *Liposomes, a practical approach*, ed. Oxford. 1990: IRL Press.
321. Guillén, J., et al., *Identification of the Membrane-Active Regions of the Severe Acute Respiratory Syndrome Coronavirus Spike Membrane Glycoprotein Using a 16/18-Mer Peptide Scan: Implications for the Viral Fusion Mechanism.* Journal of Virology, 2005. **79**(3): p. 1743-1752.
322. Eisenberg, D., R.M. Weiss, and T.C. Terwilliger, *The helical hydrophobic moment: a measure of the amphiphilicity of a helix.* Nature, 1982. **299**: p. 371-374.
323. Eisenberg, D., et al., *Analysis of membrane and surface protein sequences with the hydrophobic moment plot.* Journal of Molecular Biology, 1984. **179**: p. 125-142.
324. White, S.H. and W.C. Wimley, *Membrane protein folding and stability: physical principles.* Annu Rev Biophys Biomol Struct, 1999. **28**: p. 319-65.
325. Moreno, M.R., M. Giudici, and J. Villalaín, *The membranotropic regions of the endo and ecto domains of HIV gp41 envelope glycoprotein.* Biochimica et Biophysica Acta, 2006. **1758**(1): p. 111-123.
326. Pérez-Berná, A.J., et al., *The membrane-active regions of the hepatitis C virus E1 and E2 envelope glycoproteins.* Biochemistry, 2006. **45**(11): p. 3755-3768.
327. Wimley, W.C. and S.H. White, *Experimentally determined hydrophobicity scale for proteins at membrane interfaces.* Nature Structural Biology, 1996. **3**(10): p. 842-848.
328. White, S.H. and W.C. Wimley, *Membrane protein folding and stability: physical principles.* Annual Review of Biophysics and Biomolecular Structure, 1999. **28**: p. 319-365.
329. Kaiser, R.D. and E. London, *Location of diphenylhexatriene (DPH) and its derivatives within membranes: comparison of different fluorescence quenching analyses of membrane depth.* Biochemistry, 1998. **37**(22): p. 8180-90.
330. Kaiser, R.D. and E. London, *Location of diphenylhexatriene (DPH) and its derivatives within membranes: comparison of different fluorescence quenching analyses of membrane depth.* Biochemistry, 1999. **38**(8): p. 2610.
331. Cevc, G., *Membrane electrostatics.* Biochim Biophys Acta, 1990. **1031**(3): p. 311-82.
332. Cafiso, D., et al., *Measuring electrostatic potentials adjacent to membranes.* Methods Enzymol, 1989. **171**: p. 342-64.
333. McLaughlin, S., *The electrostatic properties of membranes.* Annu Rev Biophys Biophys Chem, 1989. **18**: p. 113-36.

334. Wall, J., F. Ayoub, and P. O'Shea, *Interactions of macromolecules with the mammalian cell surface.* J Cell Sci, 1995. **108 (Pt 7)**: p. 2673-82.
335. Wall, J., et al., *The use of fluoresceinphosphatidylethanolamine (FPE) as a real-time probe for peptide-membrane interactions.* Mol Membr Biol, 1995. **12**(2): p. 183-92.
336. Gross, E., R.S. Bedlack, Jr., and L.M. Loew, *Dual-wavelength ratiometric fluorescence measurement of the membrane dipole potential.* Biophys J, 1994. **67**(1): p. 208-16.
337. Gomez-Fernandez, J.C., et al., *Protein-lipid interaction. Biophysical studies of (Ca2+ + Mg2+)-ATPase reconstituted systems.* Biochim Biophys Acta, 1980. **598**(3): p. 502-16.
338. Mabrey, S., P.L. Mateo, and J.M. Sturtevant, *High-sensitivity scanning calorimetric study of mixtures of cholesterol with dimyristoyl- and dipalmitoylphosphatidylcholines.* Biochemistry, 1978. **17**(12): p. 2464-8.
339. Privalov, P.L. and V.V. Filimonov, *Thermodynamic analysis of transfer RNA unfolding.* J Mol Biol, 1978. **122**(4): p. 447-64.
340. Privalov, P.L. and N.N. Khechinashvili, *A thermodynamic approach to the problem of stabilization of globular protein structure: a calorimetric study.* J Mol Biol, 1974. **86**(3): p. 665-84.
341. Privalov, P.L. and S.A. Potekhin, *Scanning microcalorimetry in studying temperature-induced changes in proteins.* Methods Enzymol, 1986. **131**: p. 4-51.
342. Jelesarov, I. and H.R. Bosshard, *Isothermal titration calorimetry and differential scanning calorimetry as complementary tools to investigate the energetics of biomolecular recognition.* J Mol Recognit, 1999. **12**(1): p. 3-18.
343. Huang, C. and S. Li, *Calorimetric and molecular mechanics studies of the thermotropic phase behavior of membrane phospholipids.* Biochim Biophys Acta, 1999. **1422**(3): p. 273-307.
344. Barth, A., *The infrared absorption of amino acid side chains.* Prog Biophys Mol Biol, 2000. **74**(3-5): p. 141-73.
345. Mantsch, H.H. and R.N. McElhaney, *Phospholipid phase transitions in model and biological membranes as studied by infrared spectroscopy.* Chem Phys Lipids, 1991. **57**(2-3): p. 213-26.
346. Sutherland, G.B., *Infrared analysis of the structure of amino acids, polypeptides and proteins.* Adv Protein Chem, 1952. **7**: p. 291-318.
347. Cameron, D., Moffatt, G., Douglas, J., *A generalized approach to derivative spectroscopy.* Applied Spectroscopy, 1987. **41**: p. 539-544.
348. Mantsch, H.H., Casal, H. L., Jones, R. N., *Resolution enhancement of infrared spectra of biological systems.* Advanced infrared Raman spectroscopy, 1986. **13**: p. 1-46.
349. Moffatt, D.J., Mantsch, H. H., *Fourier resolution enhancement of infrared spectral data.* Methods Enzymol, 1992. **210**: p. 192-200.
350. Arrondo, J.L. and F.M. Goni, *Structure and dynamics of membrane proteins as studied by infrared spectroscopy.* Prog Biophys Mol Biol, 1999. **72**(4): p. 367-405.
351. Surewicz, W.K., H.H. Mantsch, and D. Chapman, *Determination of protein secondary structure by Fourier transform infrared spectroscopy: a critical assessment.* Biochemistry, 1993. **32**(2): p. 389-94.
352. Arrondo, J.L., et al., *Quantitative studies of the structure of proteins in solution by Fourier-transform infrared spectroscopy.* Prog Biophys Mol Biol, 1993. **59**(1): p. 23-56.
353. Krimm, S. and J. Bandekar, *Vibrational spectroscopy and conformation of peptides, polypeptides, and proteins.* Adv Protein Chem, 1986. **38**: p. 181-364.
354. Lee, D.C. and D. Chapman, *Infrared spectroscopic studies of biomembranes and model membranes.* Biosci Rep, 1986. **6**(3): p. 235-56.
355. Lee, D.C., I.R. Miller, and D. Chapman, *An infrared spectroscopic study of metastable and stable forms of hydrated cerebroside bilayers.* Biochim Biophys Acta, 1986. **859**(2): p. 266-70.

356. Urcuqui-Inchima, S., et al., *Recent developments in understanding dengue virus replication.* Adv Virus Res, 2010. **77**: p. 1-39.
357. Guillen, J., et al., *Identification of the membrane-active regions of the severe acute respiratory syndrome coronavirus spike membrane glycoprotein using a 16/18-mer peptide scan: implications for the viral fusion mechanism.* J Virol, 2005. **79**(3): p. 1743-52.
358. Moreno, M.R., M. Giudici, and J. Villalain, *The membranotropic regions of the endo and ecto domains of HIV gp41 envelope glycoprotein.* Biochim Biophys Acta, 2006. **1758**(1): p. 111-23.
359. Perez-Berna, A.J., et al., *The membrane-active regions of the hepatitis C virus E1 and E2 envelope glycoproteins.* Biochemistry, 2006. **45**(11): p. 3755-68.
360. Allison, S.L., et al., *Mapping of functional elements in the stem-anchor region of tick-borne encephalitis virus envelope protein E.* J Virol, 1999. **73**(7): p. 5605-12.
361. Gadkari, R.A. and N. Srinivasan, *Prediction of protein-protein interactions in dengue virus coat proteins guided by low resolution cryoEM structures.* BMC Struct Biol, 2010. **10**: p. 17.
362. Moreno, M.R., et al., *Characterization of the interaction of two peptides from the N terminus of the NHR domain of HIV-1 gp41 with phospholipid membranes.* Biochemistry, 2007. **46**(37): p. 10572-84.
363. Contreras, L.M., et al., *Structure and interaction with membrane model systems of a peptide derived from the major epitope region of HIV protein gp41: implications on viral fusion mechanism.* Biochemistry, 2001. **40**(10): p. 3196-207.
364. Epand, R.M., et al., *Formation of a new stable phase of phosphatidylglycerols.* Biophys J, 1992. **63**(2): p. 327-32.
365. Rodenhuis-Zybert, I.A., J. Wilschut, and J.M. Smit, *Dengue virus life cycle: viral and host factors modulating infectivity.* Cell Mol Life Sci, 2010. **67**(16): p. 2773-86.